SKB

TECHNICAL REPORT 89-12

Hydraulic interference tests and tracer tests within the Brändan area, Finnsjön study site
The Fracture Zone Project – Phase 3

Jan-Erik Andersson, Lennart Ekman, Erik Gustafsson,
Rune Nordqvist, Sven Tirén

Swedish Geological Co, Uppsala

June 1988

SVENSK KÄRNBRÄNSLEHANTERING AB
SWEDISH NUCLEAR FUEL AND WASTE MANAGEMENT CO

BOX 5864 S-102 48 STOCKHOLM
TEL 08-665 28 00 TELEX 13108-SKB

HYDRAULIC INTERFERENCE TESTS AND TRACER TESTS WITHIN THE BRÄNDAN AREA, FINNSJÖN STUDY SITE
The Fracture Zone Project - Phase 3

Jan-Erik Andersson, Lennart Ekman, Erik Gustafsson, Rune Nordqvist, Sven Tirén

Swedish Geological Co, Uppsala

June 1988

SWEDISH GEOLOGICAL CO
Division of Engineering Geology
Client: SKB

REPORT
ID-no: IRAP 88250
Date: 1988-06-17
Revised: 1989-04-14

HYDRAULIC INTERFERENCE TESTS AND TRACER TESTS WITHIN THE BRÄNDAN AREA, FINNSJÖN STUDY SITE

The Fracture Zone Project - Phase 3

Jan-Erik Andersson
Lennart Ekman
Erik Gustafsson
Rune Nordqvist
Sven Tirén

Uppsala June 1988

Keywords: Nuclear waste,Sweden, Finnsjön, hydrogeology, fracture zones, tracer test, interference tests, crystalline rock

ABSTRACT

The report covers the perfomance and interpretation of a series of hydraulic interference tests and a tracer test in fracture Zone 2 within the Brändan area, Finnsjön. The interference tests were performed by pumping from isolated sections of one borehole and recording the resulting pressure changes in multiple-observation sections (generally five) in adjacent boreholes as well as in the pumping borehole. The tracer test was performed by pulse injection of tracers in isolated sections of the near-region observation boreholes and monitoring the break-through of tracers in the pumping borehole.

The interference tests showed that different response patterns were generated in the near-region and in the more distant region from the pumping borehole. In the near-region, primary responses in high-conductive, low-porosity flow paths between the boreholes generally dominate. The tracer test also indicates that the primary responses may be strongly influenced by local heterogeneities. At longer distances more averaged responses generally occurred with similar responses in the multiple-sections in the boreholes.

The hydraulic interference test as well as the tracer test documented a very high transmissivity of Zone 2, particularily in its upper part.

The interference tests indicated hydraulic interaction between Zone 2 and the over- and underlying rock. Zone 2 was found to be bounded and may be represented by a triangular-shaped area. Inflow to Zone 2 occured during pumping, possibly via other fracture zones. Responses due to the pumping occurred at long distances (up to about 1.5 km) from the pumping borehole.

A numerical model was used to simulate the responses of the interference tests. Good agreement was achieved between simulated and observed responses from the most distant boreholes but decreased agreement in the near-region boreholes. This fact was attributed to local heterogeneities in the near-region.

FOREWORD

The planning of the interference tests presented in this report started during the late autumn 1987 and the instrumentation of the boreholes was performed during the winter. The first interference test started on February 16, 1988. All field activities were terminated by the end of March 1988. Lennart Ekman had the overall responsibility for the planning and field investigations.

In the present report Jan-Erik Andersson is responsible for the interpretation of the interference tests and for the conclusions (Chapter 5, 6 and 9). Sven Tirén worked out an updated geological overview of the Brändan area (Chapter 2) and Lennart Ekman gave an overview of the hydrogeological conditions (Chapter 3) as well a description of the design and performance of the interference tests (Chapter 4). Erik Gustafsson is responsible for Chapter 7 (tracer tests) and Rune Nordqvist for Chapter 8 (numerical simulations) and for Section 4.3.5 (data acquisition) in Chapter 4. Finally, Jan-Erik Andersson, with valuable assistance from Tapsa Tammela, was the editor of the report, and Mr. Andersson also wrote the introduction (Chapter 1).

CONTENTS

1. INTRODUCTION

The purpose of the Fracture Zone Project managed by the Swedish Nuclear Fuel and Waste Management Company (SKB) is to study the barrier function of fracture zones in crystalline rock with respect to radionuclide migration. The project comprises three phases of geoscientific investigations within the Brändan area, Finnsjön study site (Figures 1.1 and 1.2). The field activities of the first two phases, respectively preliminary and detailed investigations of fracture zones, are now concluded. The first phase included surface studies as well as borehole investigations in old and newly drilled boreholes and covered several geoscientific disciplines. Phase one was performed at two separate investigation campaigns, phase 1a and 1b, and is reported in Ahlbom et al. (1986) (phase 1a) and Ahlbom et al. (1987) (phase 1b).

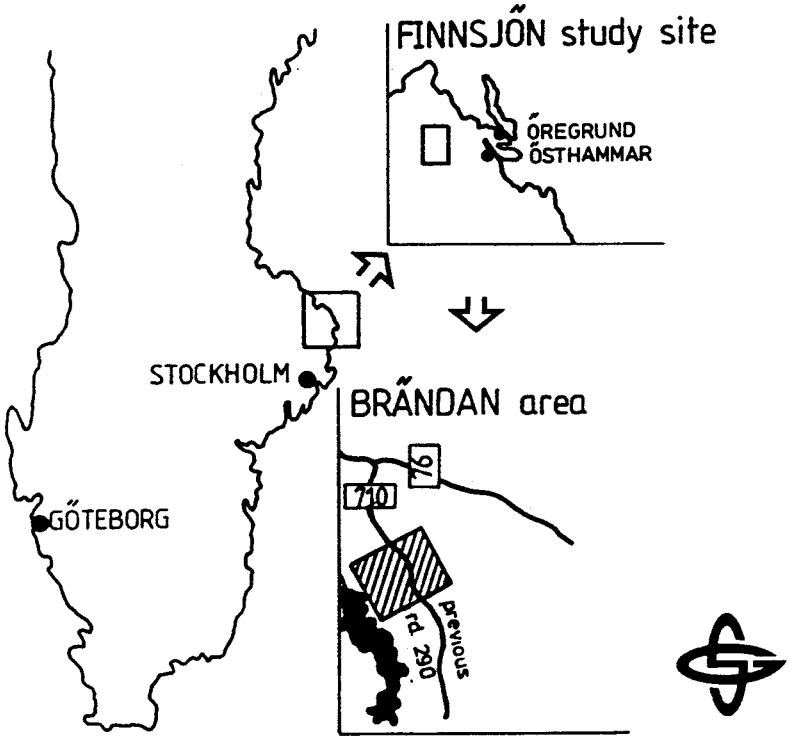

Figure 1.1 Location of the Brändan area at the Finnsjön study site.

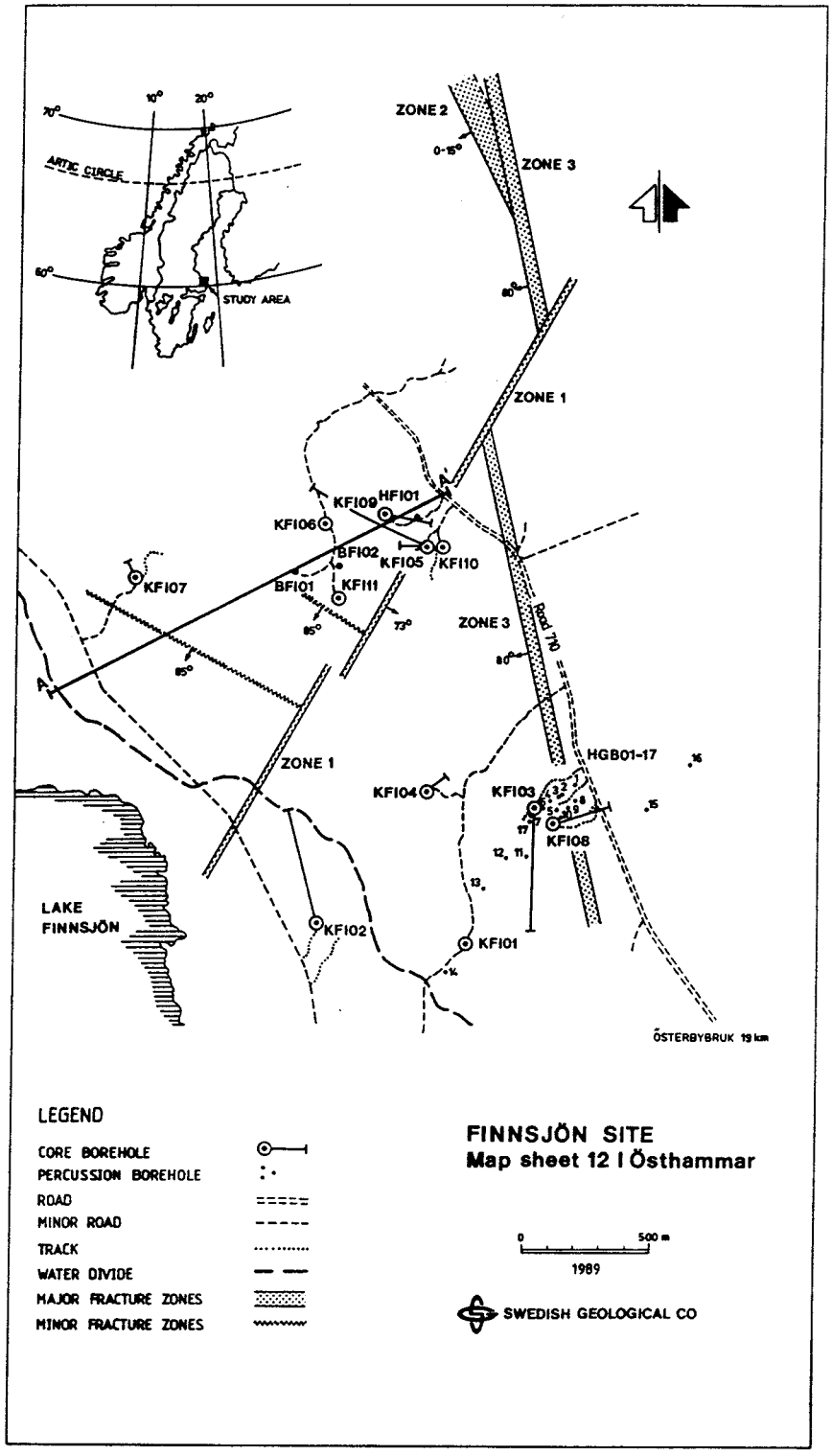

Figure 1.2 Map of the Brändan area (NW of Zone 1) and adjacent parts of the Finnsjön site showing borehole locations and fracture zones. The location of profile A - A´ shown in Figure 1.3 is also marked.

Phase 2 included detailed hydrogeological, hydrochemical and geophysical investigations as well as model simulations. Results from Phase 2 are reported by Niva (1987) (borehole radar measurements), Stenberg (1987) (tubewave measurements), Smellie et al. (1987) (hydrochemical investigations), Andersson and Andersson (1987) (model simulations), Nordqvist and Andersson (1987) (model predictions), Andersson et al. (1988) (single-hole hydraulic tests) and Gustafsson and Eriksson (1988) (point dilution investigations).

During Phase 1 and 2, a major subhorizontal fracture zone, denominated Zone 2, was selected for detailed investigations. Zone 2 is inclined c. 16 degrees from the horizontal, and the upper boundary of the fracture zone is encountered at depths ranging from less than 100 m to about 300 m and is penetrated by all boreholes drilled within the Brändan area (Figure 1.3). Most boreholes penetrate the total thickness of Zone 2. The first two investigation phases were focused on the geological/ tectonical and geohydrological character of Zone 2.

For the planned investigations during Phase 3 an additional large-diameter borehole, BFI02, was drilled in October 1987. A documentation of the geoinvestigations carried out in borehole BFI02 was made by Ekman et al. (1988).

Phase 3, which is now ongoing, involves comprehensive hydraulic interference testing between boreholes and extensive tracer tests within Zone 2 of the Brändan area. In this report the hydraulic interference tests together with an updated geological overview of Zone 2 and adjacent parts, preliminary tracer tests and numerical model simulations of the responses of the interference tests are presented.

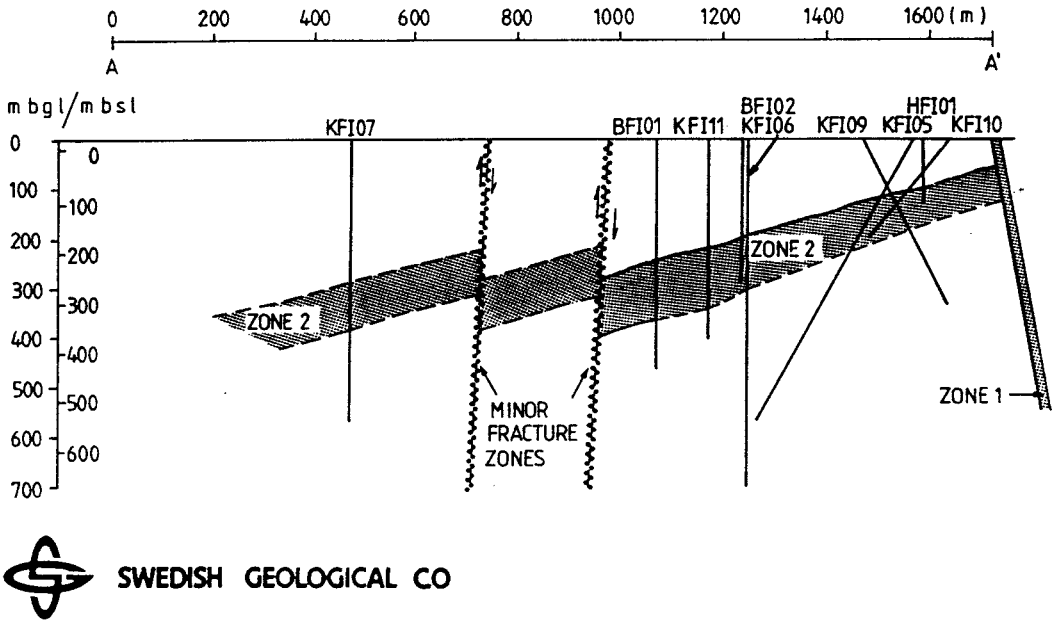

Figure 1.3 Schematic structural profile through the Brändan area. The boreholes are projected onto the profile.

The primary goals of the hydraulic interference tests were to:

- determine the hydraulic properties of Zone 2 and parts thereof
- investigate the flow pattern within Zone 2
- investigate the outer boundary conditions of Zone 2 and the hydraulic interaction with adjacent rock at longer distances
- identify deviating responses, e.g. heterogeneities within Zone 2
- assist in the design and performance of the planned tracer tests
- appraise the combined use of tracer tests and interference tests as discussed by Andersson and Hansson (1986).

2. GEOLOGIC OVERVIEW OF THE BRÄNDAN AREA

2.1 Introduction

The gently inclined, SSW dipping, Zone 2 in a foliated granodiorite of Svecokarelian age (c 1.8 Ga) within the Precambrian peneplain of northeastern Uppland has been investigated by extensive drilling. The initial ductile deformation, resulting in the formation of the zone, started more than 1.7 Ga ago. It was followed by shearing during ductile-brittle transitional conditions later followed by brittle deformation. Zone 2 was formed in a thrust regime (Munier and Tirén, in prep) with the maximum compression axis trending nearly northeast-southwest. The zone is c 100 m wide with an anastomosing shear pattern. Late reactivation occurred preferentially in the upper part of the zone. The fracture zone is displaced by subvertical faults.

In the sections below the following geological topics are treated:

- Previous works
- Structural framework of the rock mass (fracture systems, fracture zones and rock blocks)
- Character of the gently inclined fracture zone, Zone 2.

2.2 Previous works

The geologic investigations of the Finnsjön study site, which include the Brändan area, were performed during 1976-1979. The SKB Fracture Zone Project started in 1984 with complementary drillings and ground geophysic measurements. Ahlbom et al. (1986) presented a summary of the previous works and the results of the initial phase of the Fracture Zone Project. Tirén (in Ahlbom et al. 1988) gave a detailed description of

Table 2.1 Fracture zones in the Brändan area (Figure 2.1)

Zone No	Orient	Width (m)	Trace length (m)	Fracture frequency range (fr/m)	Remote sensing	Surface mapping	Ground geophysics	Borehole	Borehole radar	Block boundary
1	N30E/75SE	20-30	>2 500	20-50	x	x	x	KFI05,10	KFI10	Brändan Block Gåvastbo Block Zone 2 Unit
2	N28W/16SW	100-150		<32				KFI05-07,09-11 BFI01-02,HFI01	KFI05-07,10-11 BFI01-02	Brändan Block Zone 2 Unit
3	N26W/80SW	>25	>3 000		x	x		KFI08	KFI08	Gåvastbo Block
4	N50W/80SW	<20	1 000		x					Brändan Block Zone 2 Unit
5	N60W/80SW	<10	800		x					
6	N60W/80SW	5	700	0,5-5		x	x	HFI01	HFI01	
7	N60W/90		450		x				BFI01-02	
8	N60W	<10	>900		x	x				
9	N60W	<10	350		x	x				
10	N60W		>1 000		x	x				Brändan Block Gåvastbo Block Zone 2 Unit
11	N60W		300		x					
12	N30E/85NW		400		x	x			BFI02	
13	N23W/19SW	<5	1 000	<5	x		x	KFI06,11		
14	NS/15W	<65	>1 600	<5	x	x		KFI07		Brändan Block
15	NS/15W		>1 600		x	x		KFI07		

wide, traceable for more than 2.5 km, and terminates westwards in the lake Finnsjön. Local N30E zones are few and shorter than 500 m. The trace length of other N30E striking zones are in the order of some hundred metres. The trace lengths of N60W- and N20W-fracture zones are relatively long, more than 300 m.

In a previous report (Ahlbom et al. 1986) the extensive N-S trending zones in between boreholes BFI01 and KFI07 were given a dip of 85° to SW. This was argued by an indication of a steep dip of the Gåvastbo Zone, Zone 3, (Figure 2.1), according to the borehole radar log of borehole KFI08. The dip of minor N20W zones in the Brändan area indicate gentle dips towards SW, i.e. they parallel Zone 2. The fracture frequency of these zones is

low, in general less than 5 fractures/m. However, according to the fracture model of the area, Figure 2.4, inclinations of 15°, 50° and 85° are all possible for the N20W-trending zones. A dip of 15° fits in this case the fracture configuration in borehole KFI07.

Zone 2 (N28W/16SW), not exposed in the Brändan area, is described in a separate section below (2.6). Zone 2 continues westwards (down dip) for more than 1 km.

2.5 Local rock blocks

In this paper a local block is defined as a rock volume outlined by fracture zones persistent for more than 500 m and having a width of more than 10 m, Figure 2.2. Orientations of block boundaries are given in Table 2.1.

The most obvious rock block boundary is the Brändan Zone (N30E/75SE, c.20-30 m wide), a higher order discontinuity along which late displacement (oblique slip) has occurred (zone number 1, Figure 2.1 and Table 2.1). The rock block west of the Brändan zone is the Brändan Block and to the east is the Gåvastbo Block.

The northern block boundary of the Brändan Block is outside the detailed investigated area and parallels a gabbro (zone number 4, Figure 2.1 and Table 2.1). The western boundary of the Brändan Block is partly defined by a N20W trending zone dipping c 15° to the southwest. The ground surface expression of this zone is relatively wide, c 200 m, Figure 2.1. The southern part of this zone is offset by a N60W fault with a downthrough to the south. The N60W fault constitutes the southern border of the Brändan Block. As the N20W zone parallels Zone 2, an additional fracture zone situated just outside the Brändan area (a N30E/75SE zone), morphologically expressed but not verified

in the field, must be engaged to define the complete western boundary. The lower limit of the Brändan Block is the gently inclined Zone 2.

The Brändan Block is a polyhedron with three sets of subparallel surfaces, Figure 2.2, and it has a low density of internal fractures (c. 1 fracture/m of core KFI11).

Below the Brändan Block the Zone 2 Unit is situated. The N60W and N30E rock block boundaries are faults truncating and displacing Zone 2. Zone 2 itself is a wedge shaped unit which is distorted by reactivation of minor N60W faults, Figure 2.1. The upper and lower boundaries of Zone 2 are described in section 2.6.

The rock block below the Zone 2 Unit has a fracture density (c. 3.2 fractures/m of core KFI11) equal to the fracture density of Zone 2 (c. 3.5 fractures/m of core KFI11).

The local rock block southeast of the Brändan Block, the Gåvastbo Block, has a triangular ground surface expression outlined by N30E, N60W and N20W trending faults. Its configuration of fractures, fracture density, and types of fracture infilling minerals differ compared to the Brändan Block and resemble the Zone 2 Unit. The lower limit of this rock block is defined by a surface dipping gently westward. This surface (dipping 10-20^{o}W) outcrops along the Gåvastbo Zone and intersects the Brändan Zone. The Gåvastbo Block is composed of a low resistive rock (Ahlbom et al. 1986) indicating that it is highly fractured.

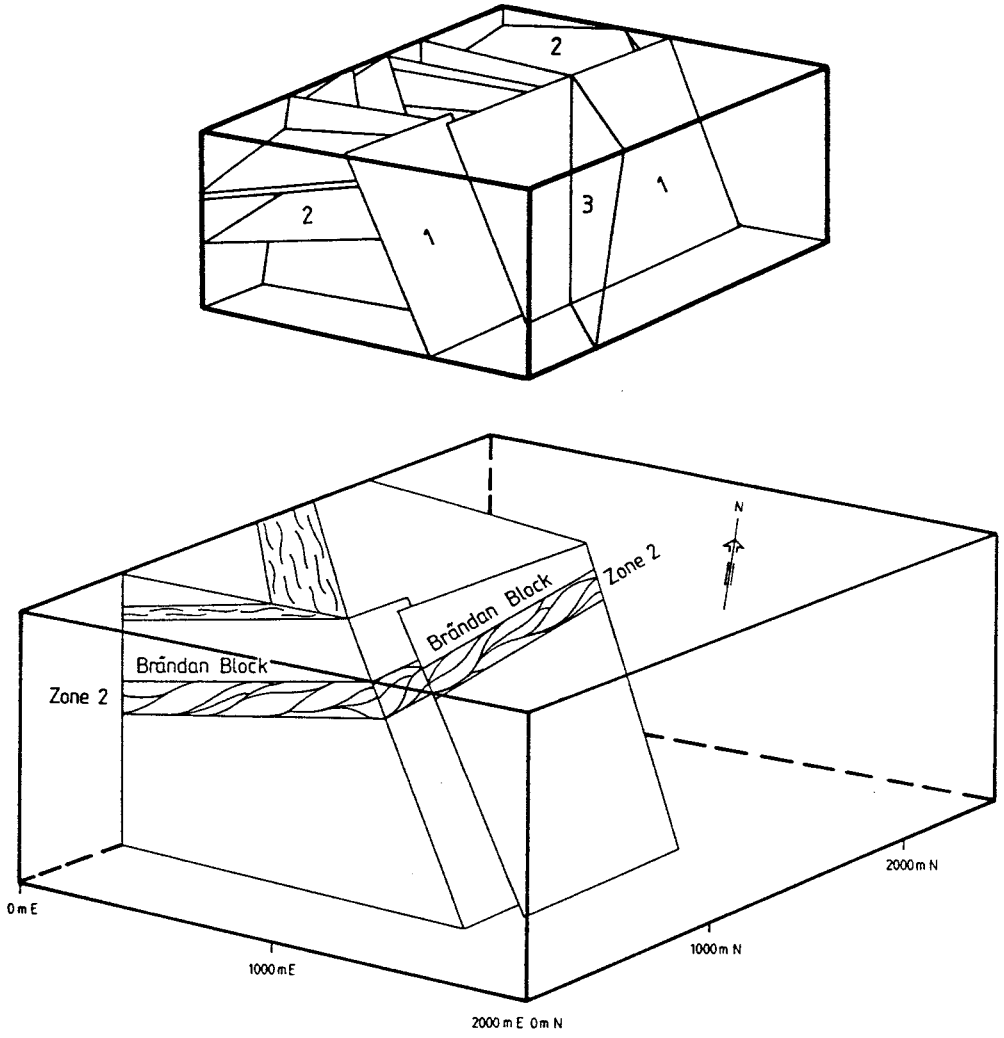

Figure 2.2 Brändan Block and Zone 2 Unit, Brändan area, northeastern Uppland.

2.6 Character of fracturing within Zone 2 and adjacent parts

Fractures logged on drillcores from the Brändan area are all unorientated. The results of the fracture survey performed on outcrops were the basis of a semiquantitative analysis of the fracture populations in the three vertical boreholes (KFI06, 07 and 11); the fractures were grouped into three classes according to their dips (0-19°, 20-69° and 70-90°, Figure 2.3). Vertical-subvertical fractures as well as gently-subhorizontal fractures are represented in the outcrops in the Brändan Block. Fractures inclined 20°-69° are scarce why these fractures logged on cores are considered as genetically related to Zone 2.

Small scale structures displayed on outcrops are used as indicators of the mesoscopic deformation pattern in Zone 2.

The general appearance of deformed sections within Zone 2 is an early ductile deformation, locally with mylonites, overprinted by reddening of the rock, brecciation, and formation of sealed fractures, and late formation of water conductive fracture zones.

In Figure 2.4 a model of Zone 2 is presented as an anastomosing network of minor shear and fracture zones enveloping lozenges (oblique-angled paralellogram) of mildly deformed rock. Zone 2 is a planar shear zone from which minor, moderately inclined zones (splays) cut upwards into the above lying rock block.

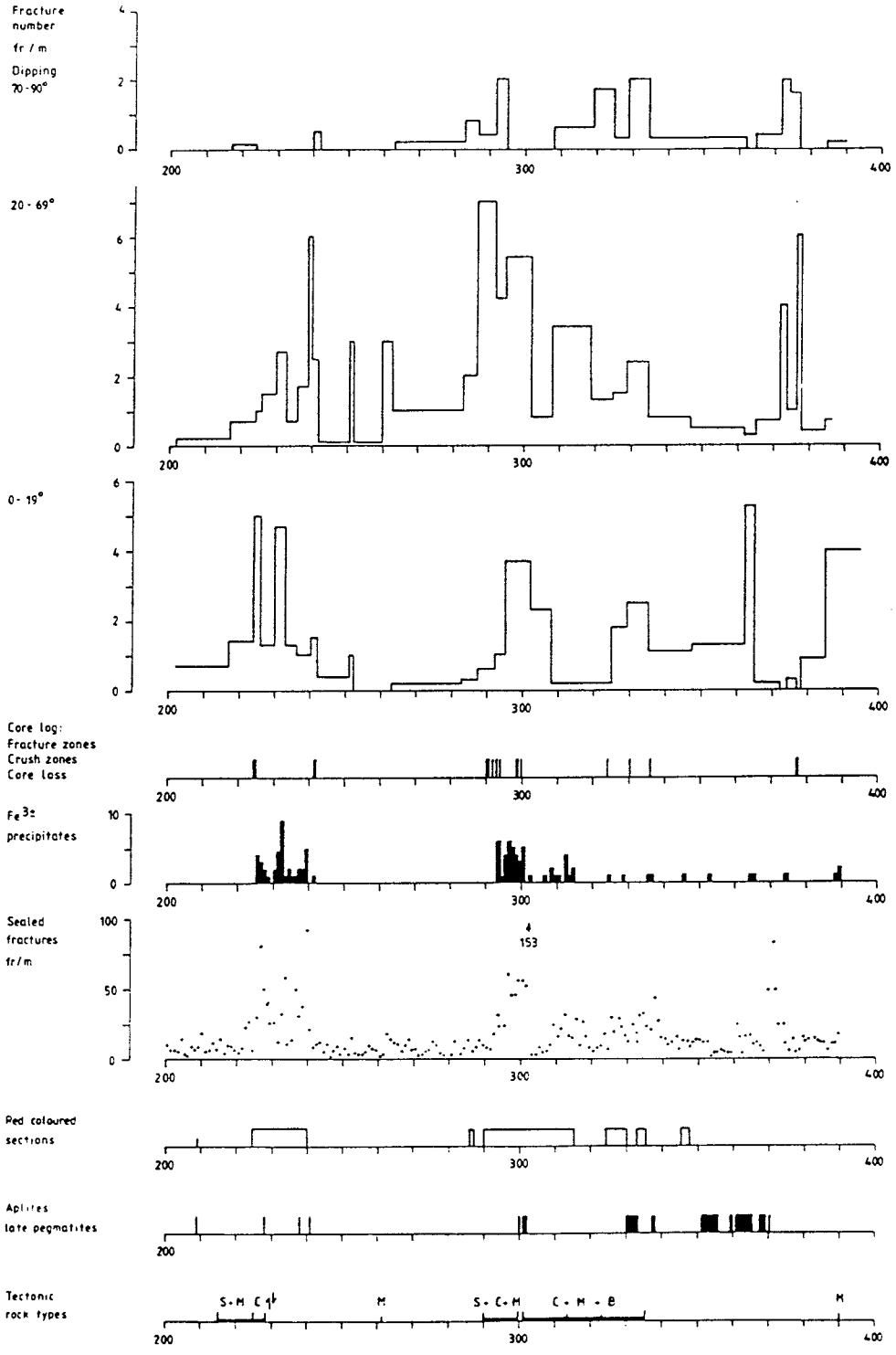

Figure 2.3 Composite geologic log of borehole KFI11 across Zone 2, section 200-390 m. S = ductile shear, M = mylonite, C = cataclasite and B = breccia. Arrows = slickenside striation. Foliation: 0^{o} = horizontal, 90^{o} = vertical.

The fracturing in Zone 2 is inhomogeneous and has an average of less than 5 fractures/m. The fracturing in the Brändan Block above Zone 2 is much less, average of c. 1 fracture/m, while there is no contrast of fracturing between Zone 2 and the rock below Zone 2.

The boundary between the Brändan Block and Zone 2 is distinct or transitional. It is distinct where the border is defined by gently dipping fractures and it is transitional where it is defined by splays cutting upwards from Zone 2 into the Brändan Block. Locally the lowermost parts of the Brändan Block have also an increase of vertical, often open rough fractures.

The fracturing in Zone 2 displays some regularities. Vertical fractures are scarce in section with high frequency of gently dipping fractures. The frequency of moderately dipping fractures increase together with gently dipping fractures. They are also often increased in sections inbetween zones of gently dipping fractures. The moderately dipping fractures together with the vertical fractures contribute to the vertical transport of water into and in Zone 2 while the gently dipping fractures rule the lateral transport of water along Zone 2. The rock just below Zone 2 has a high component of fractures and fracture zones with moderate to subvertical dips.

Style of deformation, wall rock alteration and fracture infillings indicate that the water flow system in the rock mass in time has become more and more restricted to discrete zones. The most water conductive sections coincide with a high population of gently inclined open fractures (dipping 10-20^{o}). The sections are narrow, in most cases some decimetres or centimetres wide, and only one of these zones is conspicuous.

The highest hydraulic conductivity measured in the cored boreholes coincides with a shear breccia, less than 1 dm wide, situated in a c. 1 m wide section with a fracture density less

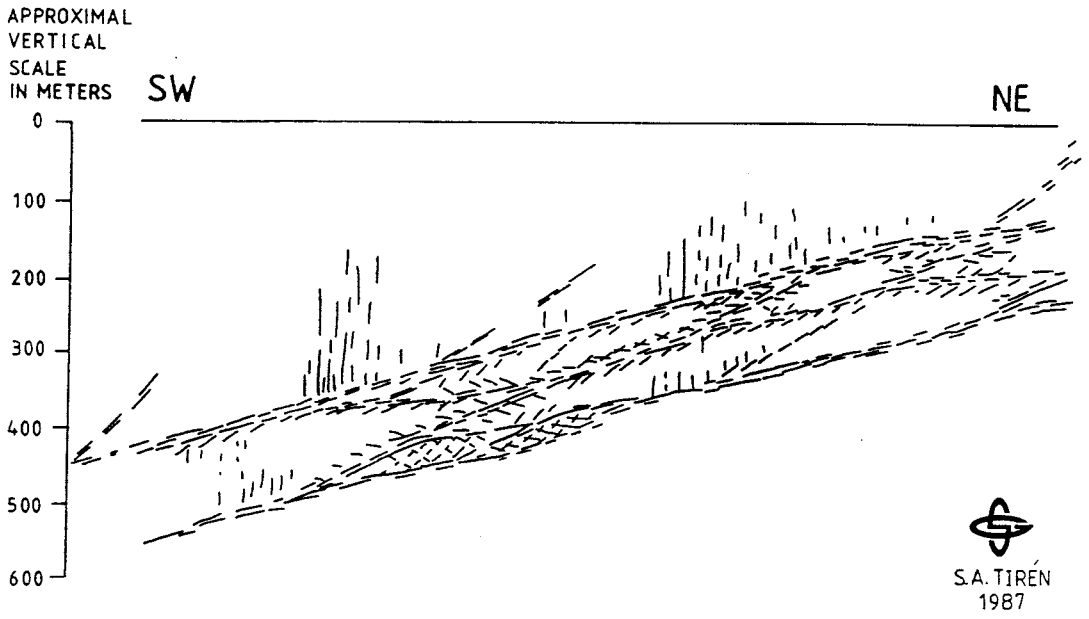

Figure 2.4 Fracture model of Zone 2.

than 8 fractures per metres of the core. This structure, dominated by gently dipping fractures, is situated in the uppermost part of Zone 2 in a 30 m reddened section with several minor units (up to 5 m wide) with a high density of sealed fractures.

Notable is that the increased densities of "open" fractures often occur along the rims of zones with a high density of sealed fractures in the upper part of Zone 2, while in the lower parts of Zone 2 the highest density of open fractures are situated within zones of sealed fractures, cf. Figure 4.3.

Configuration of fracture sets in the Brändan area, and in Zone 2 especially, gives intersection liniations, channels, in an approx. NW-SE direction, ie parallel to the intermediate principal axis of stress (σ_2 oriented NW) during the formation of Zone 2 and the late reactivation of Zone 2 (σ_2 oriented WNW) (Munier and Tirén, in prep).

3. HYDROGEOLOGICAL OVERVIEW OF THE BRÄNDAN AREA

3.1 Background

The groundwater hydrology of the Brändan area has been investigated during several campaigns since 1977. The investigations have comprised single hole water injection tests in core and percussion boreholes (Carlsson et al. 1980, Ahlbom et al. 1986, Ahlbom et al. 1987, Andersson et al. 1988, Ekman et al. 1988), groundwater head measurements (Larsson and Jacobsson 1982, Ahlbom et al. 1987), pressure registration during drilling of new boreholes (Ahlbom et al. 1986 and Ahlbom et al. 1987), preliminary tracer tests (Ahlbom et al. 1986, Ahlbom et al. 1987), groundwater flow determinations by the point dilution method (Gustafsson and Eriksson 1988) and groundwater chemical investigations (Ahlbom et al. 1987, Ekman et al. 1988).

3.2 Hydraulic conductivity

The single hole injection tests, performed down to c. 700 m below the ground surface, have revealed a generally decreasing hydraulic conductivity with depth (Figure 3.1). (All figures in this chapter origin from the reports referred to in Section 3.1). However, in the decreasing trend, there are sudden conductivity high peaks which become evened out when measuring with long test sections, but which are very obvious for results from short-section tests (see e.g. boreholes KFI05, KFI06 and KFI09, Figures 3.1 and 3.2). The most prominent conductivity increase is caused by Zone 2 and in some boreholes by superficial fracture zones. In several boreholes, especially KFI11 and BFI02, Figure 3.3, the rock section between the ground surface and Zone 2 consists of rather long intervals of low-conductive rock, which causes a large conductivity contrast between Zone 2 and the abovelying rock. This fact indicates, that Zone 2 hydraulically may act as a perfectly confined

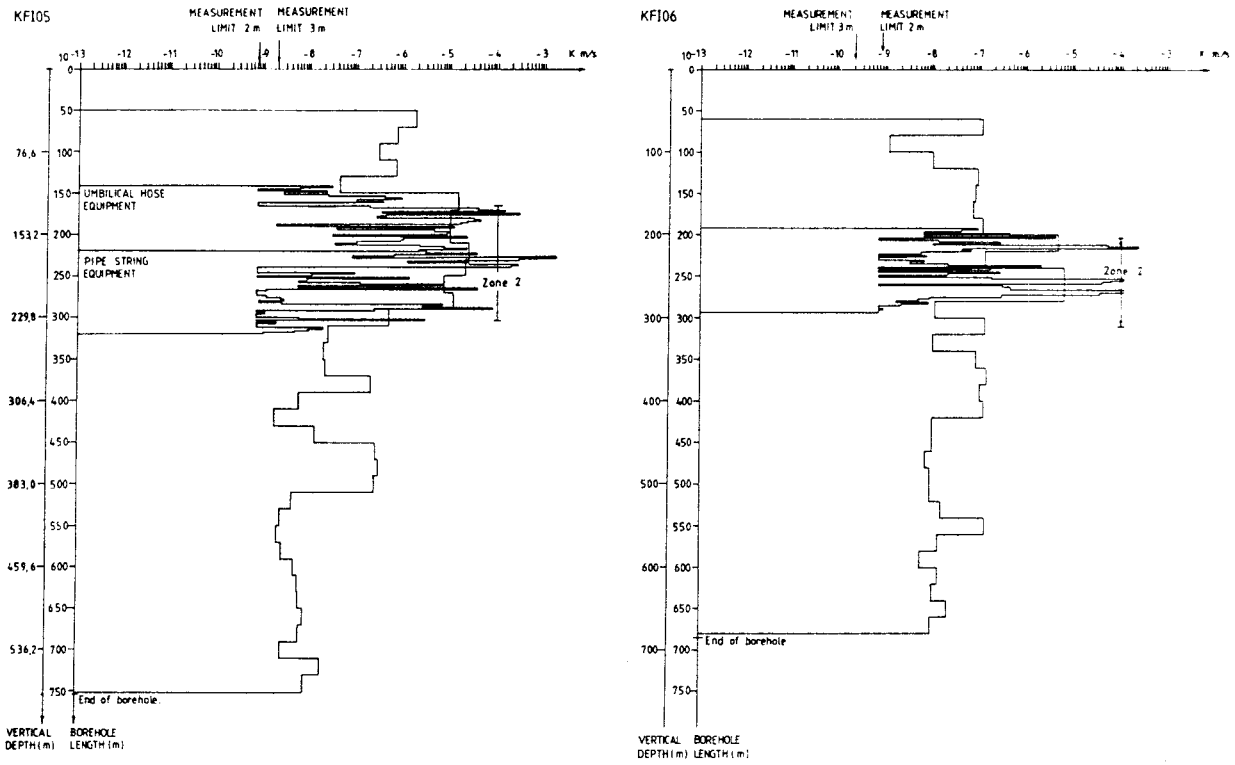

Figure 3.1 The hydraulic conductivity in two boreholes within the Brändan area, illustrating the general trend of decreasing conductivity versus depth (from Andersson et al. 1988).

aquifer. The latter was confirmed by the pressure registrations during drilling of the booster drilled borehole BFI01, where very rapid pressure responses within Zone 2 between the pumping borehole BFI01 and the observation boreholes were observed (Ahlbom et al. 1987).

The single hole tests (Andersson et al. 1988) have corroborated the "sandwich" structure of Zone 2 revealed by geological and geophysical investigations. Comparably thin sections of tectonized, low-resistive and high-conductive rock are interrupted by relatively long intervals of more competent, medium- or low-conductive rock. The high-conductive sections, which often reach hydraulic conductivity values around 1E-4 m/s,

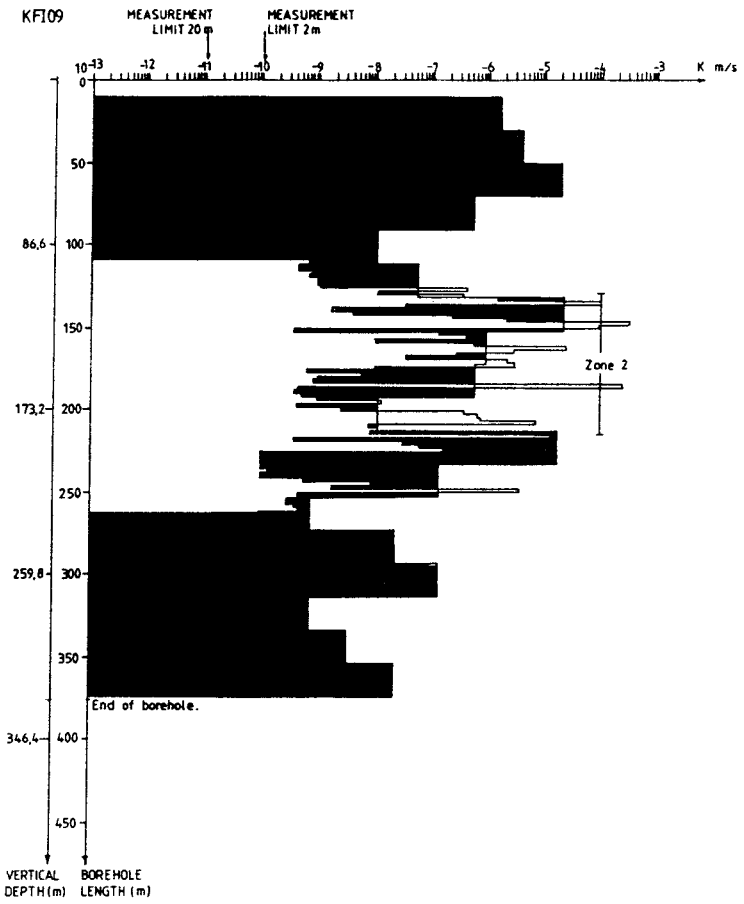

Figure 3.2 The hydraulic conductivity in borehole KFI09, illustrating high-conductivity peaks interrupting the general trend of decreasing conductivity versus depth (from Andersson et al. 1988).

have in some reports been denominated "subzones". Water injection tests in 2 m long sections have shown that the width of the subzones is limited to maximum 6 m (most often much less) and that the intermediate low-conductive parts vary from a few metres up to several tenths of metres (Figures 3.1-3.3).

A special study of the conductivity distribution within different subzones, performed as water injection tests in 0.11 m-sections in the pumping borehole, BFI02, (Ekman et al. 1988) proved, that the widths of the high-conductive parts were restricted to a few decimetres (Figure 3.4). It seems likely, that the widths of the high-conductive parts of the subzones are overestimated also in other boreholes when judged only from 2 m- (or longer) tests.

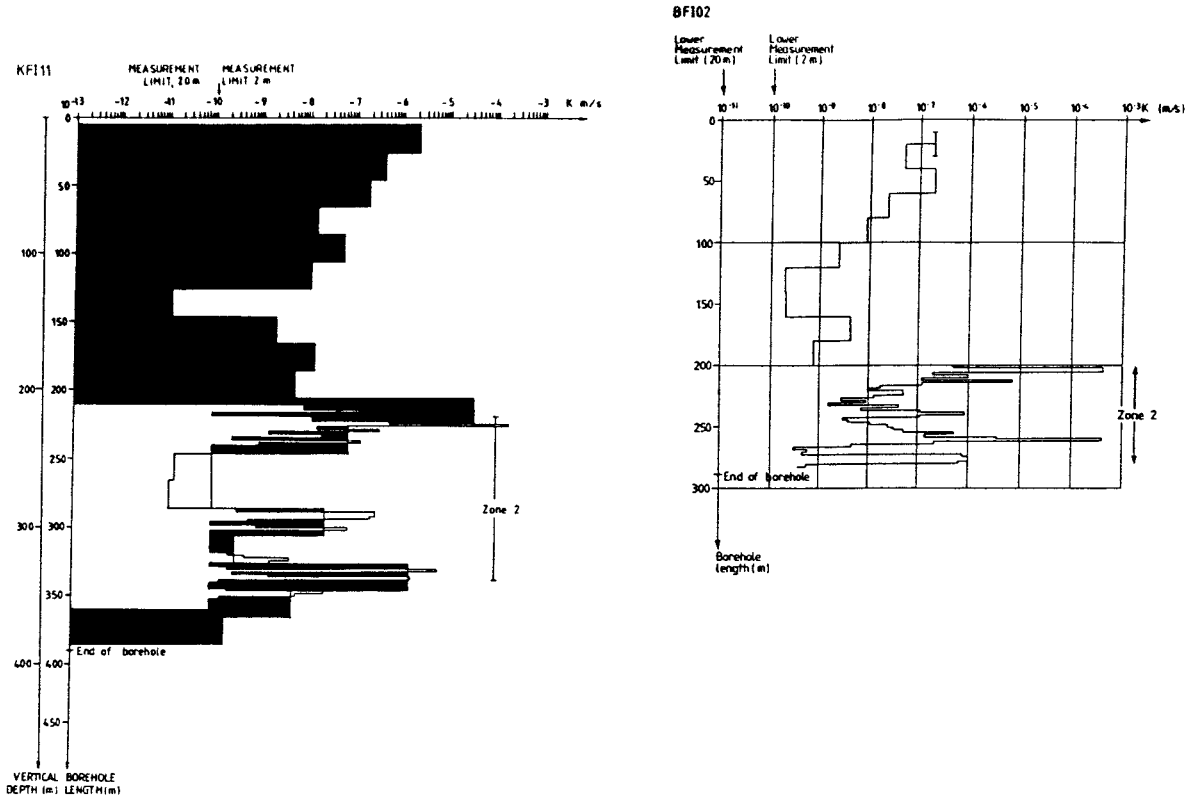

Figure 3.3 The hydraulic conductivity in boreholes KFI11 and BFI02, illustrating the large conductivity contrast between Zone 2 and the abovelying rock (from Andersson et al. 1988 and Ekman et al. 1988).

Table 3.1 illustrates transmissivity values of three different subzones in the pumping borehole. The T-values are calculated from 2 m-tests as well as from 0.11 m-tests.

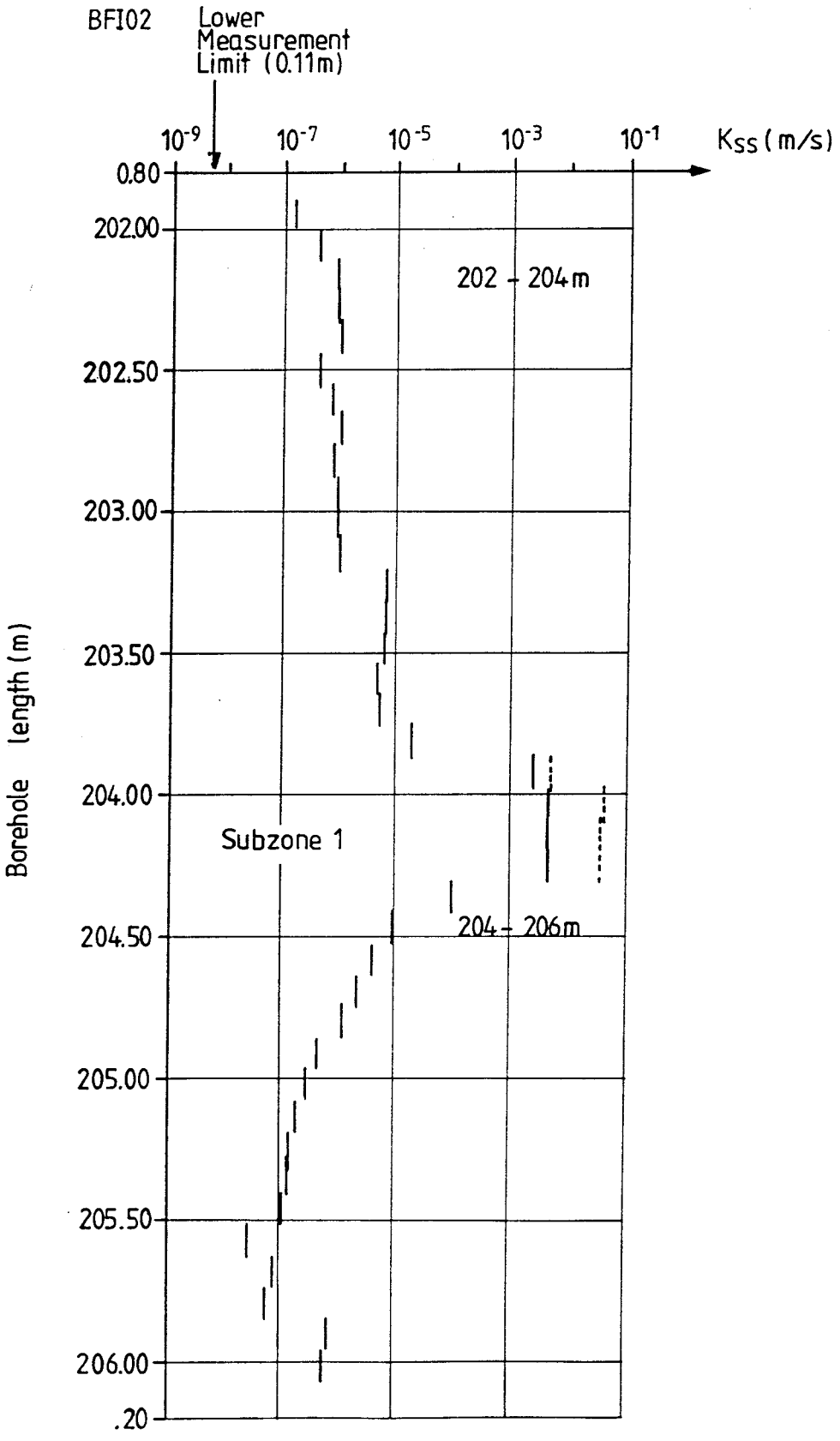

Figure 3.4 The hydraulic conductivity in 0.11 m-sections in the uppermost subzone of Zone 2 in borehole BFI02 (from Ekman et al. 1988).

Table 3.1 Values of hydraulic transmissivity calculated from 2 m-tests and 0.11 m-tests (from Ekman et al. 1988).

2 m-sections (m)	T_{2m} (m^2/s)	0.11 m-sections (m)	$T_{0.11\ m}$ (m^2/s)	Rock unit
202-204	8.6E-4	202.00-203.98	2.9E-4	
204-206	8.6E-4	203.98-206.07	1.6E-3	Subzone 1
202-206*	1.7E-3	202.00-206.07	1.9E-3	
212-214	1.4E-5	212.00-214.09	4.3E-5	Subzone 2
258-260	7.0E-6	258.00-259.98	3.2E-5	
260-262	8.4E-4	259.98-262.18	1.6E-3	Subzone 3
258-262**	8.4E-4	258.00-262.18	1.6E-3	

* Transmissivity values for the total of Subzone 1

** Transmissivity values for the total of Subzone 3.

3.3 Groundwater head conditions

The groundwater head measurements indicated a groundwater flow directed from W to E in the Brändan area but with a turning towards SE in the eastern part, i.e. in the vicinity of the Brändan zone (Ahlbom et al. 1987). This is relevant for the superficial part of the rock as well as for the upper part of Zone 2 and for the rock below Zone 2. In other words, the Brändan zone is recharging much of the groundwater of the Brändan area down to considerable depths in the bedrock and discharges the groundwater towards NE. The situation is illustrated in the head maps in Figure 3.5. The gradient is for the groundwater table varying between 1 m/450 m (2.2 %) in the western part of the area to 1 m/150 m (6.7 %) in the eastern

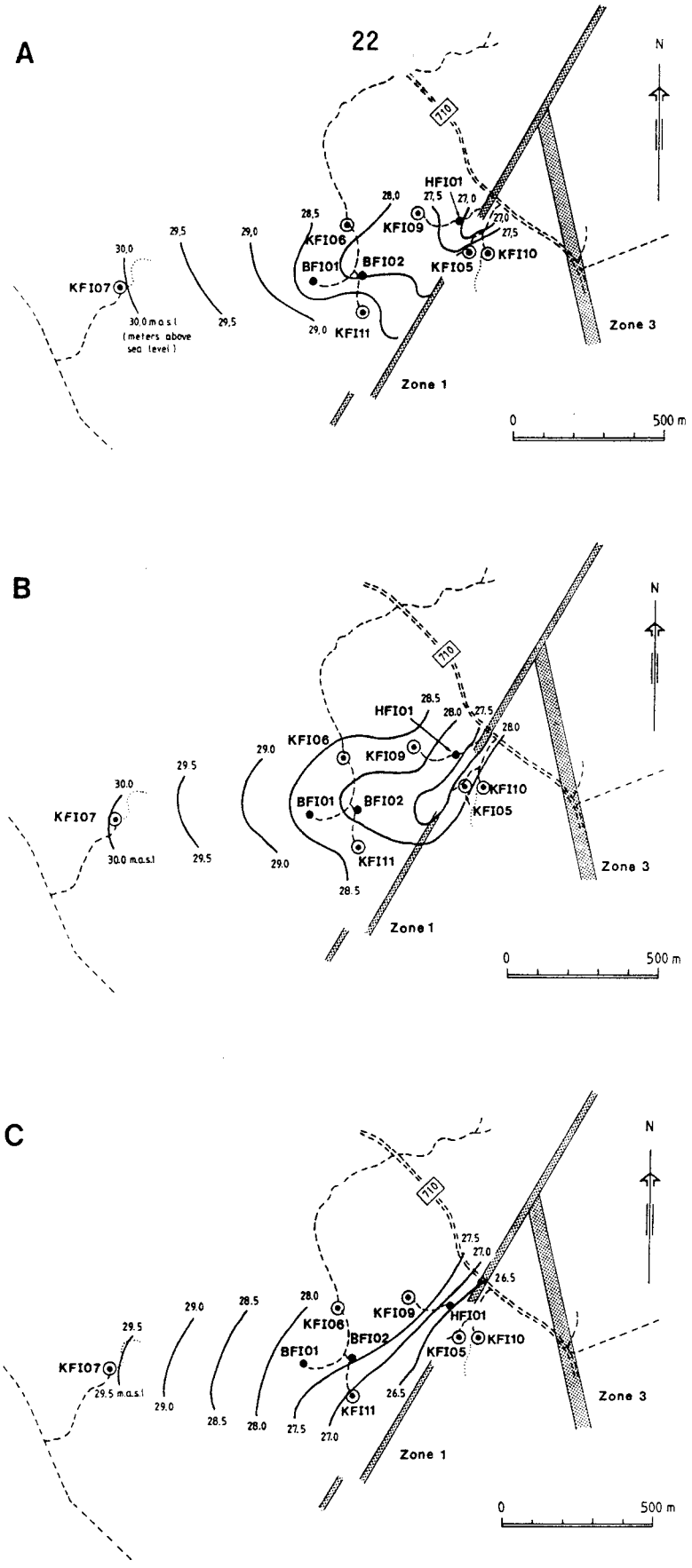

Figure 3.5 The groundwater head distribution in the Brändan area: A) superficially in the bedrock, B) in the upper part of Zone 2 and C) below Zone 2 (from Ahlbom et al. 1987).

part. For the upper part of Zone 2 as well as below the zone the corresponding values were determined to 1 m/450 m respectively 1 m/300 m (3.3 %). The latter value may, however, be overestimated (see Section 3.4).

The vertical head distribution in the western parts of the area is different from that in the eastern parts. To the west, Zone 2 is recharging groundwater from higher parts of the bedrock and possibly also from the bedrock below the zone. To the east, on the other hand, the pressure gradient is directed upwards from Zone 2. The boreholes KFI11 and HFI01 illustrate the two different situations (Figure 3.6).

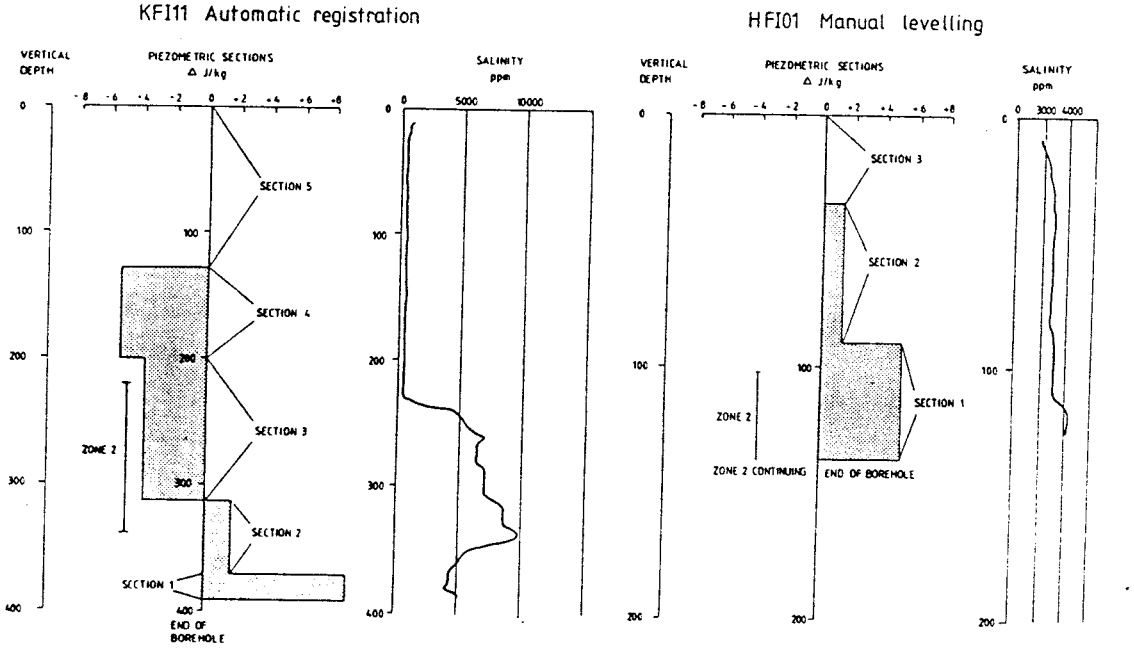

Figure 3.6 The vertical head distribution in KFI11 (situated to the west) and in HFI01 (situated to the east in the Brändan area) (from Ahlbom et al. 1987).

3.4 Groundwater flow rate

By hydraulic tests (single hole tests and interference tests) the hydraulic conductivity, i.e. the potential of the rock/ fractures to conduct water at a certain hydraulic gradient, is determined. If a value of the natural gradient is assumed, the groundwater flow rate and groundwater Darcy velocity can be calculated.

With the point dilution technique a semi-quantitative method for in situ measurements of groundwater flow rate under natural hydraulic gradient and in the natural flow direction is provided. Measurements with this method were during the summer 1987 performed in two boreholes, HFI01 and BFI01, within the Brändan area. Methods, equipment and results are described in Gustafsson and Eriksson (1988).

The measurements were performed in packed off sections at different levels within the boreholes. Most sections were short, 2 m, but also sections of considerable length, up to 180 m, were used, see Table 3.2.

As can be seen from the table, the upper and lower parts of Zone 2 as well as the abovelying country rock were included in the investigation in BFI01, whereas in HFI01, which is penetrating only the upper part of Zone 2, only this and the abovelying shallow country rock could be investigated.

The results of the point dilution measurements are summarized in Figures 3.7 and 3.8. From Figure 3.7 one interesting conclusion about the flow conditions of Zone 2 can be drawn. In the upper high-conductive part of the zone (242-246 m) the flow rate is considerable, whereas in the lower high-conductive part no measurable flow was observed. This confirms that the driving force, i.e. the hydraulic gradient in this part of Zone 2, is very low, which is consistent with the results from the

Table 3.2 Selected borehole sections for groundwater flow measurements (from Gustafsson and Eriksson 1988).

Borehole	Section	K (m/s)	Remarks
HFI01	38- 40	7.2E-5	Fracture zone in the shallow rock
"	108-110	3.8E-5	Upper part of Zone 2
"	112-114	1.9E-4	"
"	104-124	2.3E-5	"
"	84-129	1.3E-5	Upper part of Zone 2 and affected country rock above
BFI01	242-244	3.0E-4	Upper part of Zone 2
"	244-246	3.4E-4	"
"	264-266	1.1E-6	Within Zone 2
"	352-354	1.7E-5	Lower part of Zone 2
"	354-356	3.5E-5	"
"	9- 50	8E-6	Highly conductive shallow rock
"	50-230	5.6E-8	Low-conductive part between shallow rock and Zone 2

hydrochemical investigations (Section 3.5), which indicate stagnant groundwater below the upper part of Zone 2. Figure 3.7 also indicates, that the groundwater flow through the shallow, fractured and high-conductive parts of the bedrock is high. Below this rock there is almost 200 m of medium- to low-conductive rock, where the groundwater circulation is small. In the table in Figure 3.7 groundwater Darcy velocities, v_f, calculated from the groundwater flow rate values determined with the point dilution method are presented together with those calculated from the K- and I-values determined from hydraulic tests and piezometric measurements, v_{fc}. The v_f and v_{fc} values are in fairly good agreement in the upper part of Zone 2 as well as in the abovelying country rock. However, the Darcy velocities calculated in the lower part of Zone 2 from K- and I-values, v_{fc}, were overestimated with four orders of

DILUTION MEASUREMENTS IN BOREHOLE BFI01, FINNSJÖN STUDY SITE

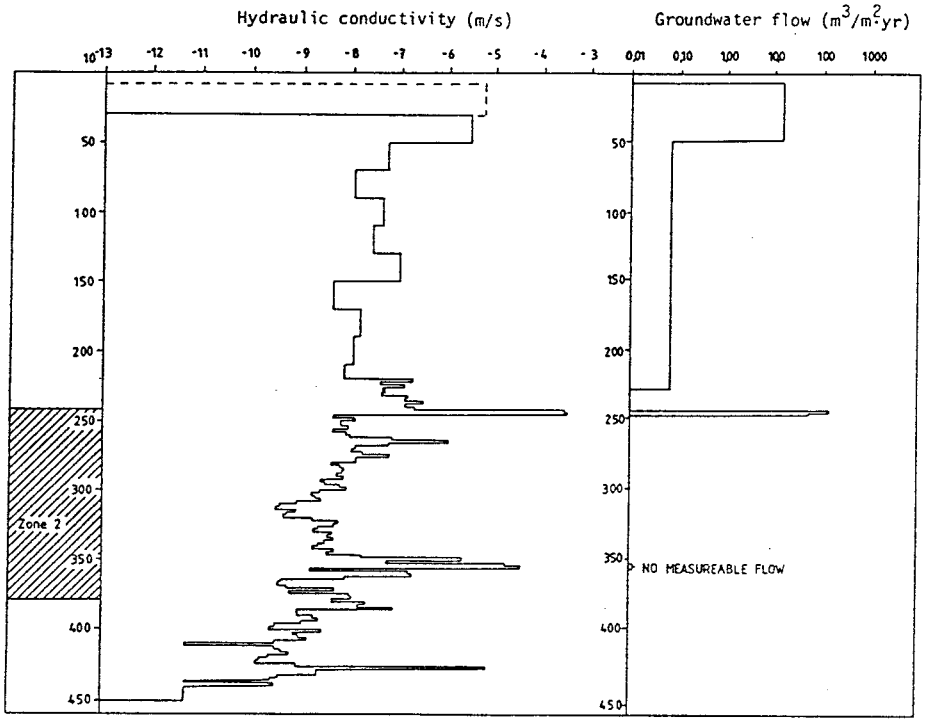

Section (m)	K (m/s)	Q_w (ml/min)	Q_f ($m^3/m^2 \cdot yr$)	v_f (m/s)	v_f (m/d)	v_{fc}* (m/s)
9- 50	8 E-6	381.2	14.2	4.5 E-7	0.039	0.4 E-7
50-230	3.1 E-8	7.9	0.07	2.2 E-9	0.0002	8.9 E-11
242-244	3.0 E-4	169.4	131.7	4.2 E-6	0.361	0.8 E-6
244-246	3.4 E-4	61.9	48.3	1.5 E-6	0.132	0.9 E-6
352-354	1.7 E-5	no measurable flow		3 E-11		0.5 E-7
354-356	3.5 E-5	"		3 E-11		0.9 E-7

* calculated with I=1/200 in the uppermost section and 1/350 in the other sections

Figure 3.7 Results of point dilution measurements in borehole BFI01. The results are compared to the hydraulic conductivity (from Gustafsson and Eriksson 1988).

magnitude compared to those determined from the dilution measurements. This result indicates that determinations of the hydraulic gradient in specific groundwater flow paths from piezometric measurements in relatively few observation points can be ticklish, especially when groundwater layers of different densities are involved, which is the case in the Brändan area.

In borehole HFI01, Figure 3.8, probably a minor discrepancy in the length determination between the hydraulic test equipment and the point dilution equipment caused apparently low flow rates in the two high-conductive 2 m-sections within the upper part of Zone 2. The point dilution measurements in the 20 m-section 104-124 m clearly proves, that the upper part of Zone 2 also in HFI01 exhibits a high flow rate. A relatively high flow rate corresponds to the high conductivity in the shallow 2 m-section 38-40 m. This indicates, like in BFI01, a large shallow groundwater circulation in HFI01.

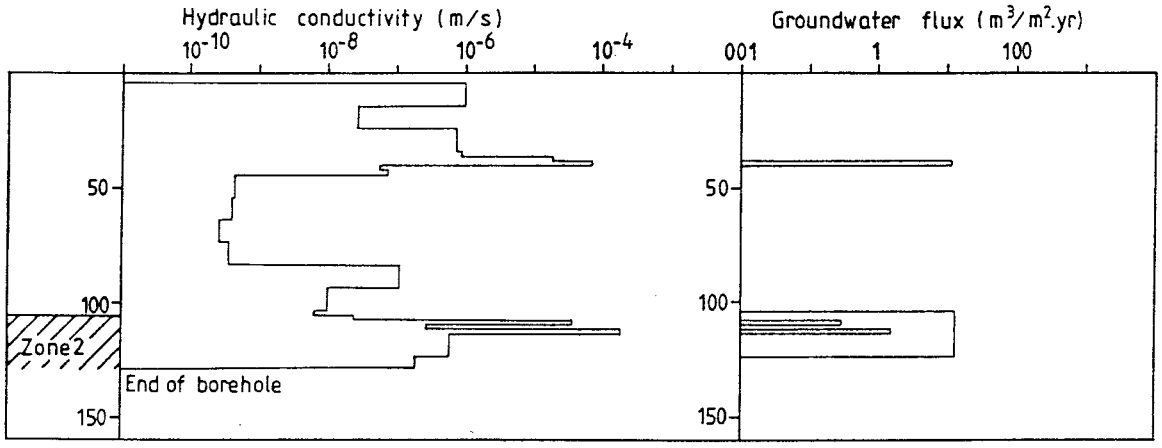

Figure 3.8 Results of point dilution measurements in borehole HFI01. The results are compared to the hydraulic conductivity (from Gustafsson and Eriksson 1988).

3.5 Groundwater chemistry

Studies on the groundwater chemistry in the Brändan area (e.g. Ahlbom et al. 1986, Smellie et al. 1987, Puigdomenech and Nordstrom 1987) constitute a relatively small part of the overall programme. However, these studies have been of great importance. Basic facts about the groundwater quality are necessary for the planning of the future large scale migration experiments, and the water chemistry investigations have also greatly helped to unravel the bedrock hydraulics in the area.

A more detailed account of the results of the groundwater chemical studies is beyond the scope of this chapter. The most important result is the fact that the salinity of the groundwater is low above Zone 2 but starts to increase drastically at the upper boundary of Zone 2, irrespective of the altitude of the zone, reaching a maximum value close to the lower boundary. The salinity content of the groundwater below Zone 2 remains more or less constant at this maximum value (Ahlbom et al. 1986). The situation is illustrated in Figure 3.9 where the electrical conductivity of the groundwater as well as pH are plotted versus depth. In Figure 3.10 some selected anions respectively cations are plotted versus depth. From these figures it is obvious, that the presence or absence of saline water throughout the Brändan area and its occurrence at different levels within the bedrock is determined by the structural geometry, which is dominated by Zone 2. This zone seems to function as a subhorizontal hydraulic boundary between superficial young, nonsaline groundwater and deep old, saline water. The age of the deep saline groundwater is from C^{14}-datings estimated at c. 12 000 years. This water is regarded to comprise waters resulting from several different processes: the Yoldia/Litorina marine transgressions, mecanical rupture of fluid inclusions and rock/water interactions over long residence times. Part of the deep saline groundwater may also consist of residual igneous/methamorphic fluids.

Figure 3.11 is a tentative model of the groundwater flow within the Brändan area, seen in a vertical section illustrating flow, piezometric and salinity conditions as well as the boundary effect of Zone 2.

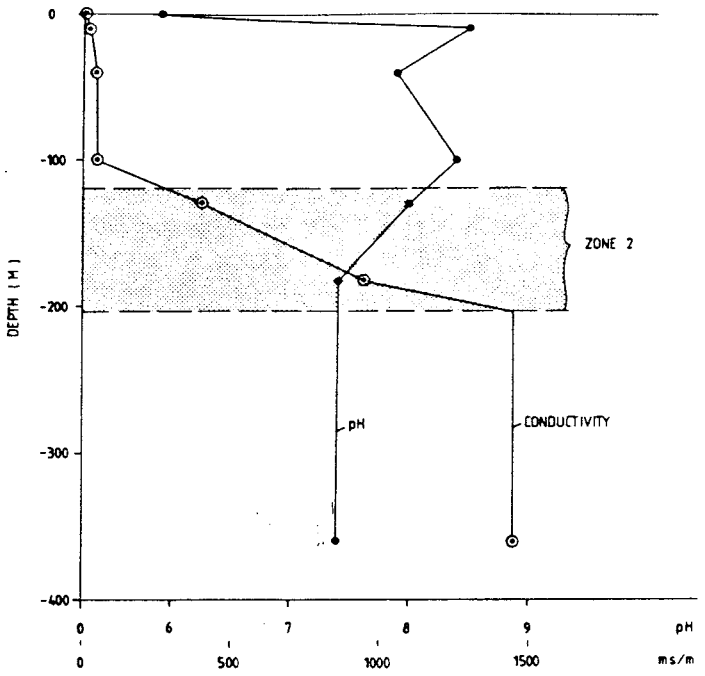

Figure 3.9 Variation of electrical conductivity and pH with depth in the Brändan area (boreholes HFI01 and KFI09) (from Ahlbom et al. 1986).

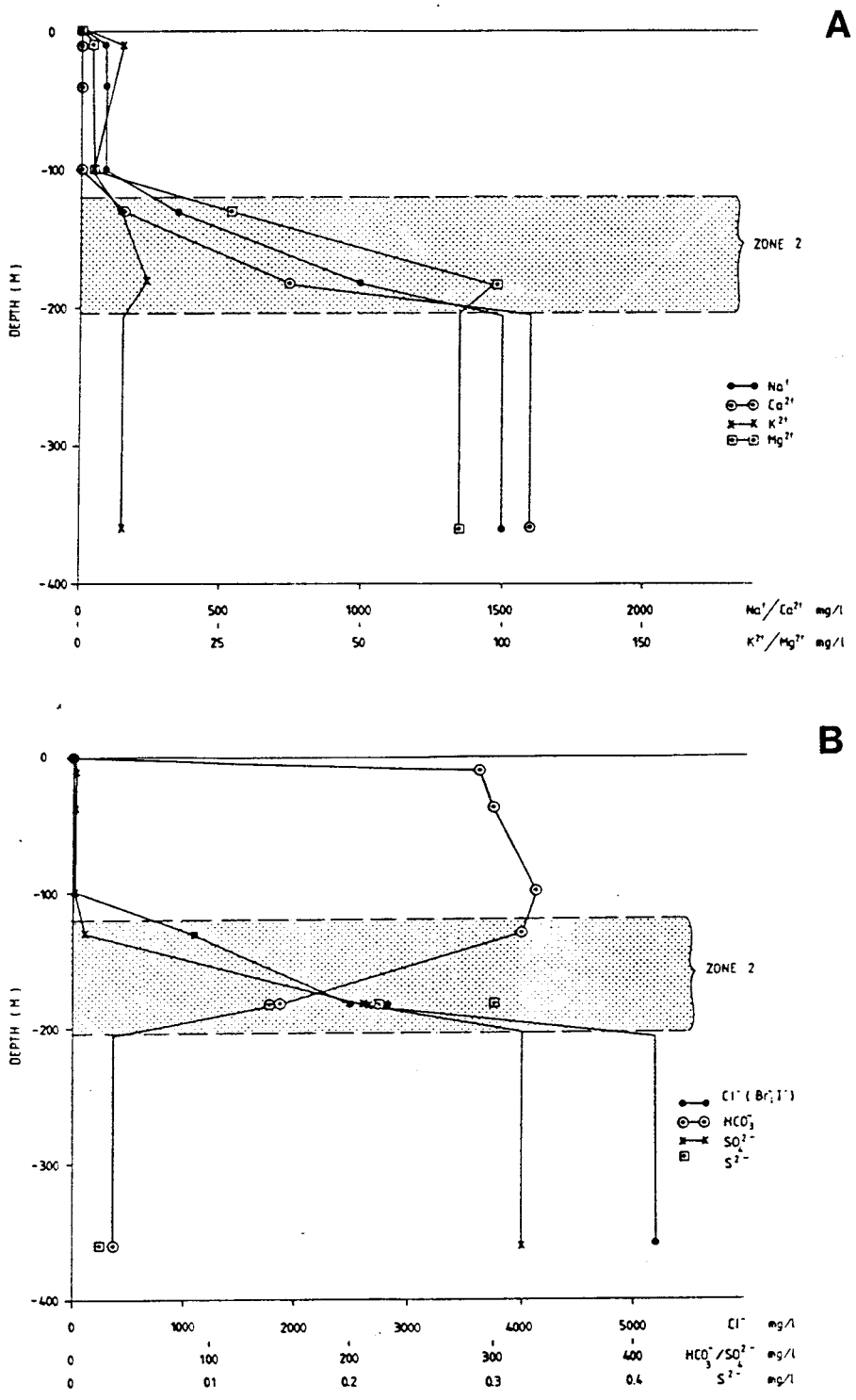

Figure 3.10 Variation of: A) selected cations and B) selected anions with depth in the Brändan area (boreholes HFI01 and KFI09) (from Ahlbom et al. 1986).

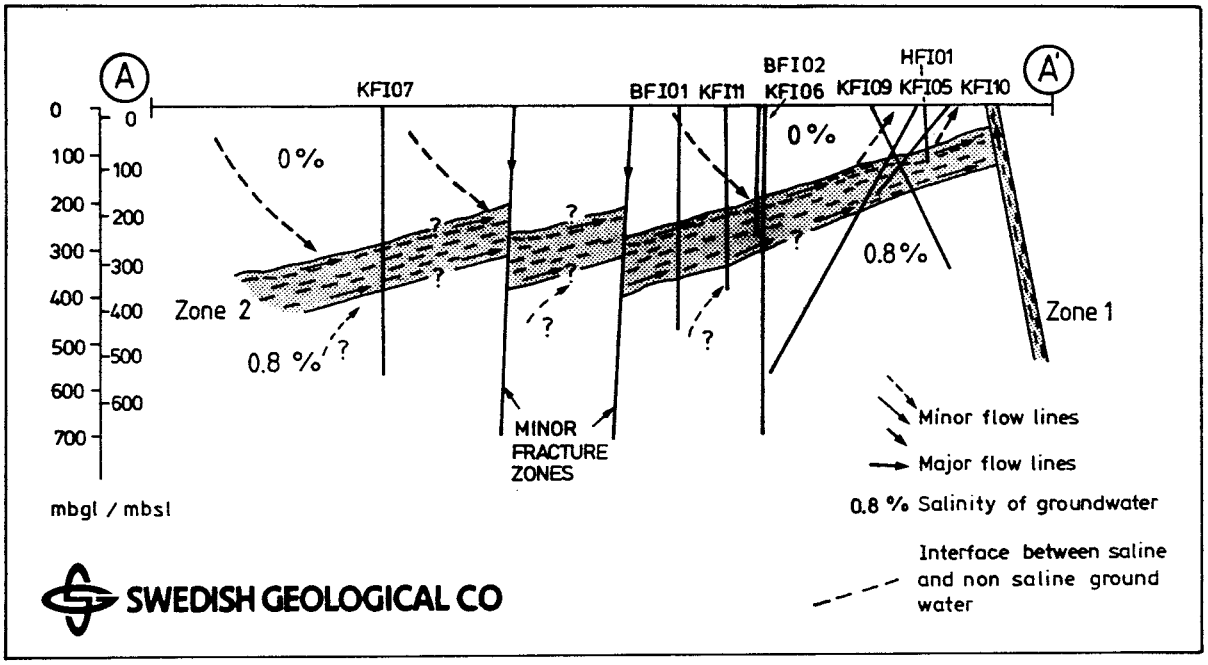

Figure 3.11 Tentative model of groundwater flow during undisturbed conditions in a vertical section through the Brändan area. The location of section A - A´ is given in Figure 1.2 (from Ahlbom et al. 1986).

4. DESIGN AND PERFORMANCE OF THE INTERFERENCE TESTS

4.1 Background

A part of the Finnsjön test site is illustrated by the map in Figure 1.2. The subarea denominated "the Brändan area" including the boreholes KFI05, KFI06, KFI07, KFI09, KFI10, KFI11, HFI01, BFI01 and BFI02 is located NW of Zone 1, whereas the part towards SE including the core boreholes KFI01, KFI02, KFI03, KFI04 and KFI08 as well as the percussion boreholes HG01-17 is considered to be located outside the Brändan area. The inclined boreholes KFI05 and KFI10 are, although starting east of Zone 1, regarded to belong to the Brändan area.

The profile A-A´ in Figure 1.2 is illustrated in Figure 1.3. The most important information in this figure is the position of the dominating tectonic structures in the area and the projected interceptions of the boreholes with Zone 2.

Figure 4.1 is a 3-dim picture of the eastern part of the Brändan area, seen from SW. The upper and lower boundaries of Zone 2 are marked in the figure. These boundaries are in the figure idealized planes calculated with the least square fitting method from the vertical depth values of the borehole interceptions with the respective boundaries. The equations of the resulting regression planes are for the upper boundary:

$$Z = -562.88 + 0.1516\ Y + 0.2379\ X \qquad (4.1)$$

and for the lower boundary:

$$Z = -805.88 + 0.2117\ Y + 0.3187\ X \qquad (4.2)$$

Equation 4.1 is much resembling the corresponding equation (6.1) in Ekman et al. (1988).

The general picture of the test site given by these three figures should be kept in mind for the discussion below.

The interference tests described in this report were preceded by a series of preliminary interference tests described by Ahlbom et al. (1987). The latter series was performed as pressure registrations in observation boreholes during drilling of the percussion borehole BFI01, using the air-flush system of the drilling rig as a high-capacity pump. BFI01 was pumped as an open borehole. In all, five interference tests were performed at different drilling depths of borehole BFI01. Zone 2 was not completely penetrated until the last two inter-

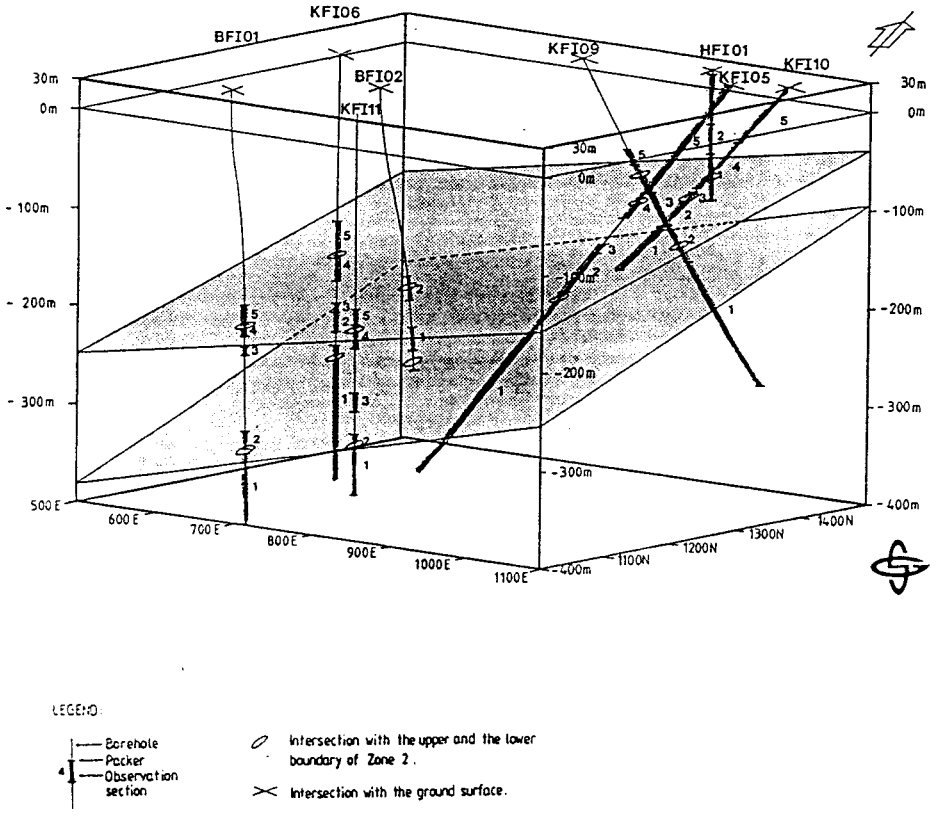

Figure 4.1 3-dimensional picture (seen from SW) of the eastern part of the Brändan area with boreholes, packer positions and pressure observation sections used during the interference tests.

ference tests. The pressure registration was undertaken in packed off sections in all boreholes within the Brändan area. However, at that occasion borehole BFI02 did not yet exist. The principle for the packer configuration in the observation boreholes was to isolate the entire Zone 2 in all boreholes completely penetrating the zone, and to make pressure observations within Zone 2 as well as above and below the zone in (maximum) five sections in each borehole. Since the interference tests were of second interest (the primary interest was the drilling of BFI01), all circumstances for a satisfactory interpretation of the tests could not be accomplished. For example the duration of the tests was only between one and 13 hours, which made it impossible to draw definite conclusions about hydraulic boundaries and the longterm drawdown behaviour. Another problem was the sometimes rather large flow rate variations in the pumphole. A third problem was, that the extremely rapid pressure propagation within Zone 2, which today is well-known, at that time was not expected. Therefore the pressure registration systems used were not ideal for recording the rapid initial responses. Finally, the pumping borehole was not instrumented for pressure registration.

Nevertheless, much valuable information could be derived from this series of tests. Preliminary T-, S- and hydraulic diffusivity parameters for Zone 2 as a whole could be evaluated, although not from very early parts of the pressure response curves. Also the extremely rapid pressure responses were recognized and conclusions about the flow pattern within Zone 2 and adjacent parts of the bedrock could be deduced. Tendencies of anisotropy were found. All this information was of value for the design of the interference tests described below.

Another valuable source of information for the design of the present interference tests was the detailed single hole water injection tests performed with 2 m packer spacing within and immediately outside Zone 2 in all boreholes of the Brändan

area and the special study with 0.11 m-sections in BFI02 (cf. Section 3.2).

Finally, all available information of hydraulic conditions were used for accomplishing a model for groundwater flow simulation in Zone 2 (Nordqvist and Andersson 1988). The flow model was used partly as a tool for aiding of the interference test design. However, the main objective of the modelling process was to set up a prediction for the interferece test results. After completion of the tests, the model was calibrated according to the actual results, in order to obtain a stepwise improvement of the model parameters.

The high-conductive intervals are in Ekman et al. (1988) denominated "subzones". In (almost) all boreholes, the upper boundary of Zone 2 is associated with a high-conductive zone, Subzone 1. The number of subzones below Subzone 1 is varying from borehole to borehole. If a subzone is defined as having a conductivity exceeding 1E-6 m/s, the total number of subzones varies between two (borehole KFI11) and seven or eight (borehole KFI05). In the present report, the concept "subzone" is used, especially for the pumping hole, BFI02. Since it is a delicate thing to interconnect specific subzones between different boreholes, also the less precise words "upper, lower and middle part of Zone 2" are often used for description of the conditions in the observation boreholes during the tests.

4.2 Objectives

The information obtained from the previously performed series of interference tests should, according to the packer configuration used, be representative for the entire Zone 2. In other words, the information was gained from the integrated response of all subzones in the different observation boreholes when pumping in (primarily) the total of Zone 2 (Ahlbom et al. 1987).

One of the most important objectives of the present interference tests was to investigate the properties of isolated subzones, primarily Subzone 1 and a subzone close to the lower boundary of Zone 2, but also, if possible, subzones in between. The primary goals of the interference tests were:

1) To determine the hydraulic properties within the entire Zone 2 and in specific subzones.
2) To investigate the persistence of subzones between different boreholes.
3) To investigate if different subzones are hydraulically isolated from each other, or if there exist interconnections between subzones, which would result in a leakage between two subzones if a drawdown is created in one of them.
4) To investigate the hydraulic boundaries of Zone 2.

In order to achieve a comprehensive set of data, also from the early, as well as the late stages of the pumping, it was important for the design of the tests to improve the quality of the data acquisition system and the other technical arrangements, compared to those of the previous preliminary series of interference tests.

Another point in the strategy of the planning of the present interference tests was to use water quality data (chemical composition, mainly salinity, measured as electrical conductivity, and groundwater temperature) and simple tracer tests as a support for the evaluation of the interference tests.

In the next sections the design and performance are described. The design includes packer configuration, technical arrangements in the pumping hole and at the well site and, finally, the data acquisition system. The performance describes the time schedule and the most important events during the tests.

4.3 Design

4.3.1 Hydraulic conductivity distribution in the pumping borehole

The single hole water injection tests performed in the pumping borehole BFI02 revealed a number of subzones of Zone 2 (Section 3.2). If a subzone is defined to have a hydraulic conductivity exceeding 1E-6 m/s, the number of subzones in BFI02 is four. Of these four subzones, Subzone 1 and Subzone 3 (Figure 4.2) are dominating concerning the magnitude of the hydraulic conductivity. In both cases K > 1E-4 m/s. The transmissivity values T, calculated for Subzone 1 and 3 respectively, as well as for the entire Zone 2, are as follows (Table 4.1):

Table 4.1 Comparison of hydraulic parameters for different hydraulic units in borehole BFi 2.

Hydraulic unit	Width (m)	K m/s	T m^2/s
Subzone 1	4	4.3E-4	1.7E-3
Subzone 3	4	3.5E-6 - 4.1E-4	8.4E-4
Zone 2	84	3.0E-10 - 4.3E-4	2.6E-3

The table shows, that the transmissivity of Subzones 1 and 3 is about 98.6 % of the transmissivity of the entire Zone 2, which implies that the same proportion of the total flow within Zone 2 occurs in these two subzones, if the gradient is uniform all over the zone.

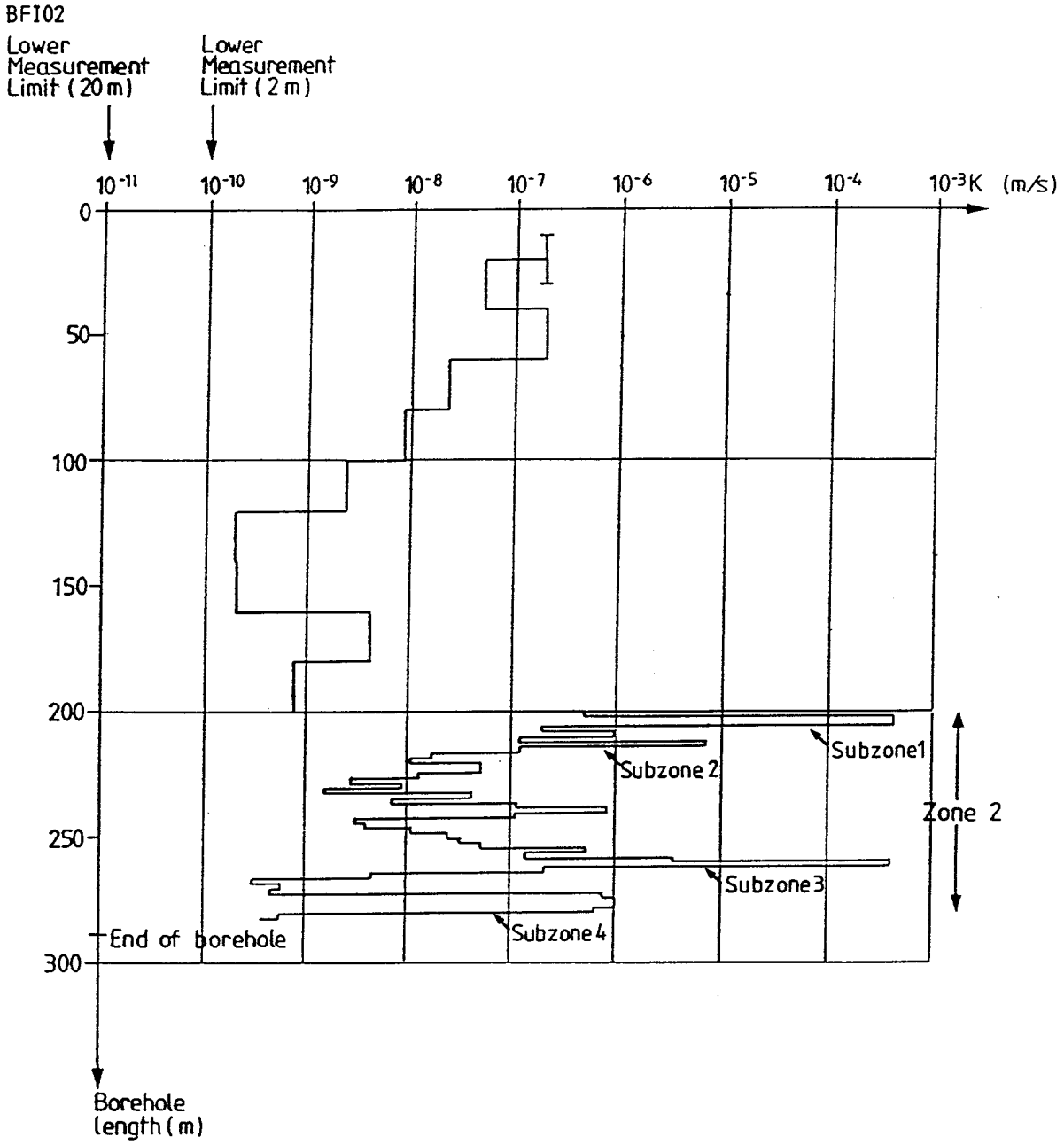

Figure 4.2 Hydraulic conductivity in 20 m- and 2 m-sections in borehole BFI02. Zone 2 with subzones is illustrated (from Ekman et al. 1988).

4.3.2 Packer configuration

Pumping borehole

The basis for the planning of the interference tests was the above mentioned fact, that Subzones 1 and 3 are totally dominating in Zone 2 concerning K- and T-values. It was therefore decided, that a series of three interference tests were to be performed: 1) one pumping in Subzone 3, 2) one pumping in Subzone 1, and 3) one last pumping in the entire Zone 2 (due to technical problems, two such pumpings were made, see below). Figure 4.3 schematically illustrates the packer configurations in the pumping borehole during the different interference test.

In tests 1 and 2, a double packer assembley with a packer spacing of 24 m was isolating the respective subzones from the above-/belowlying rock, whereas in tests 3A and 3B (explained below), a single packer isolated the interval between 193 m and the borehole bottom (288.69 m).

Due to a technical problem after start of the third pumping, it was necessary to stop the pump after c. 23 hours for repairing of the flow regulation system. After a recovery period of c. 20 hours, the pump was restarted and a new test initiated. Of these two tests, the first (short) pumping/recovery was called interference test 3A, the second (longer) interference test 3B.

Observation boreholes

Like in the pumping borehole, BFI02, the single hole injection tests have indicated that there in many other boreholes in the Brändan area exist at least one subzone below Subzone 1 with a

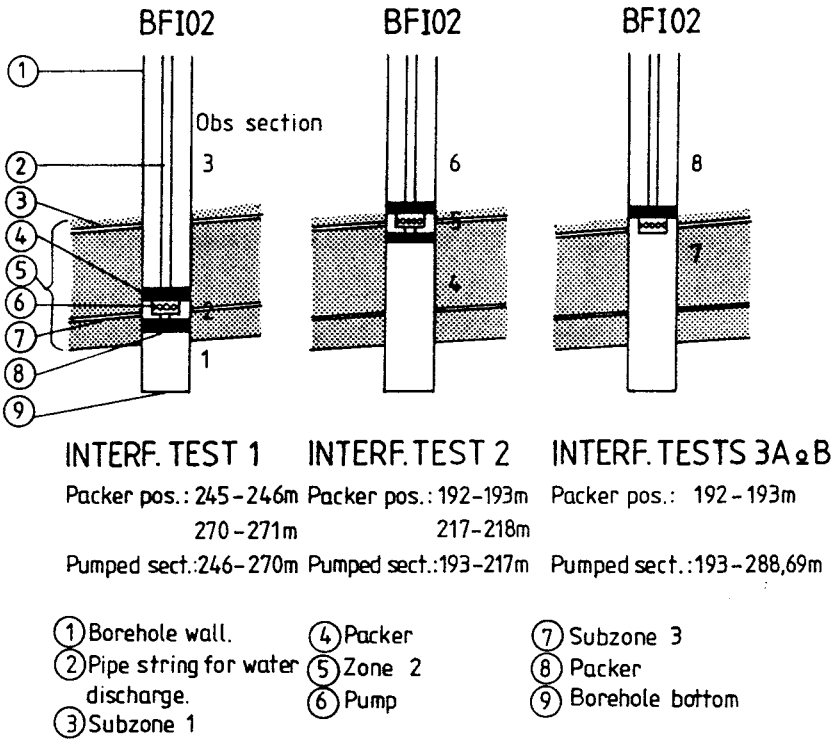

Figure 4.3 Schematic illustration of the packer configurations in the pumping hole during the different interference tests. The numbering of the observation sections is also marked in the figure.

hydraulic conductivity either higher (KFI05 and KFI10), equal to (KFI09) or slightly lower (KFI06) than that of Subzone 1. In all these cases the hydraulic conductivity is close to or exceeding 1E-4 m/s according to the 2 m-tests. In a couple of boreholes (KFI11 and BFI01) all subzones below Subzone 1, however, have hydraulic conductivities significantly lower than that of Subzone 1. In these two cases the subzone with the second highest conductivity seems to be associated with the lower boundary of Zone 2. It is possible that the high-conductivity intervals below Subzone 1 are interconnected, more or less directly, in the same way as Subzone 1 in the different boreholes is believed to be one persistent unit

within the area. However, looking at the model of fracturing of Zone 2 (Figure 2.4) it seems probable that the conditions are more complicated, especially when subzones between the upper and lower boundaries of Zone 2 are studied.

The main principle governing the packer configuration in the observation boreholes during the interference tests was to isolate the high-conductive parts (subzones) from each other. The boreholes closest to the pumping borehole are of special interest for the future investigations, and for these it was decided to, if there is space enough, use more than one packer between each observation section in order to minimize the risk of pressure by-pass within the borehole. For selection of suitable packer positions, the hydraulic conductivity diagrams from Andersson et al. (1988) were studied in detail. In Figure 4.4 the principle for selection of packer positions is illustrated with the hydraulic conductivity diagram for borehole KFI11.

In KFI11, Subzone 1 is outstanding concerning transmissivity: 3.6E-4 m/s at 223.94-225.94 m. If the above definition of a subzone is used, there exist only two subzones in KFI11, where Subzone 2 is associated with the lower boundary of Zone 2 and has a transmissivity of 1.5E-5 m/s. However, between Subzones 1 and 2 there is another marked hydraulic conductivity increase at the interval c. 288-294 m (and at c. 300-302 m), where the K-values in 2 m-sections vary between 8E-8 m/s and 3E-7 m/s.

The strategy for packing off KFI11 was to isolate and make pressure observations in all high-conductive intervals within Zone 2 but also to observe the pressure in one section above and in one section below Zone 2. The possible number of observation sections with the automatic system is for technical reasons restricted to five in the core drilled boreholes (Almén et al. 1986). The uppermost section (groundwater table) in a

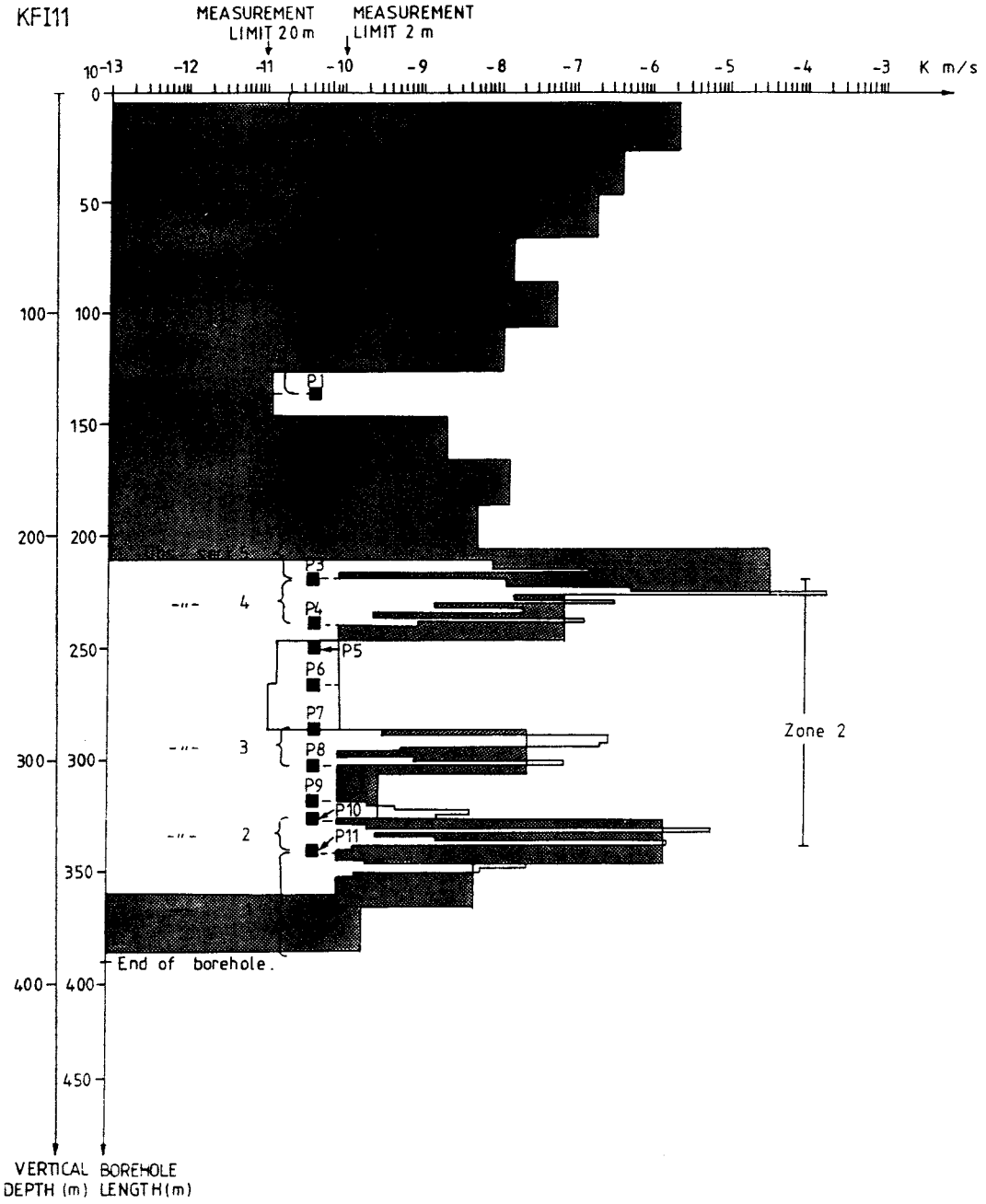

Figure 4.4 The conductivity diagram for borehole KFI11 and the packer configuration during the interference tests.

borehole can be either manually or automatically recorded (or both) depending on how many sections are occupied below the uppermost section. In KFI11 this section was only manually monitored. It was also desirable for the performance of the preliminary tracer test (Chapter 7) not to have too long observation sections. If possible, two packers (or more) between each observation section should be used in order to minimize pressure by-pass. The most important criterium for choosing a good position for the respective packers was to find an interval as low-conductive as possible, which diminishes the risk for water by-pass via water-conductive fractures.

The packer configuration and the configuration of observation sections for each observation borehole is found in Appendix 1. The figures are based on the hydraulic conductivity diagrams from Andersson et al. (1988). For each borehole a similar discussion as for KFI11 preceded the packer locations. The packer locations and observation sections are also illustrated in Figure 4.1. Finally, the borehole intervals for the observation sections of every actual borehole is found in Table 4.2 together with the values of hydraulic transmissivity for the observation sections situated within Zone 2.

4.3.3 Observation boreholes outside the Brändan area

Due to the rapid pressure responses also in distant boreholes within the Brändan area during pumping in Zone 2, a fact that was discovered already during the previous interference tests with BFI01 as a pumping borehole and confirmed at the beginning of the presently described tests, it was realized that also boreholes outside the Brändan area might react when pumping in BFI02. Therefore a number of boreholes, four core boreholes and one percussion borehole, south of the Brändan area were selected for groundwater level observations during the interference tests. These boreholes were all open, i.e. without packers,

Table 4.2 The borehole intervals for the observation sections in all active boreholes within the Brändan area (except KFI07) during the interference tests together with values of hydraulic transmissivity for the observation sections within Zone 2. The T-values were calculated from single hole tests in 2 m-sections.

Borehole	Section (no)	Interval (m)	T (m^2/s)	Part of Zone 2	Remarks (t=test)
KFI05	5(M)*	0-162	-	above	
	4	163-189	1.2E-3	upper	
	3	227-240	4.2E-3	middle	
	2	241-296	2.6E-4	lower	
	1	297-751	-	below	
KFI06	M**	0-165	-	above	
	5	166-201	-	above	
	4	202-227	5.6E-4	upper	
	3	250-259	4.0E-4	middle	
	2	260-279	2.7E-4***	lower	
	1	293-691	-	below	
KFI09	M**	0-100	-	above	
	5	101-118	-	above	
	4	119-151	1.0E-3	upper	
	3	152-188	5.8E-4	middle	
	2	189-230	1.2E-4	lower	
	1	231-376	-	below	
KFI10	5(M)*	0- 75	-	above	
	4	76-134	2.7E-4	Zone 1	
	3	139-158	1.2E-4	upper	
	2	159-193	7.6E-5	middle	
	1	194-255	2.2E-4	lower	
KFI11	M**	0-135	-	above	
	5	200-216	-	above	
	4	217-240	3.7E-4	upper	
	3	285-304	1.8E-6	middle	
	2	327-340	1.5E-5	lower	
	1	341-390	-	below	
HFI01	3(M)*	0- 50	-	above	
	2	51- 81	-	above	
	1	82-129	4.6E-4	upper	

Table 4.2 continued.

Borehole	Section (no)	Interval (m)	T (m^2/s)	Part of Zone 2	Remarks (t=test)
BFI01	M**	0-218	-	above	
	5	219-238	-	above	
	4	239-250	1.3E-3	upper	
	3	261-270	2.5E-6	upper	
	2	345-364	1.1E-4	lower	
	1	364-459	-	below	
BFI02	3(M)*	0-245	-	-	
	2	246-270	8.3E-4	lower	pumped in test 1
	1	271-288.7	-	-	
	6(M)*	0-192	-	above	
	5	193-217	1.7E-3	upper	pumped in test 2
	4	218-288.7	-	-	
	8(M)*	0-192	-	above	
	7	193-288.7	2.6E-3	whole	pumped in test 3A, 3B

* M = manually and automatically monitored section
** (M) = manually monitored section
*** = section 270.35-272.40 not injection tested.

and were either manually levelled with a sounding probe or automatically recorded with a pressure transducer or a water level gauge. Also KFI07, which is situated within the Brändan area but at a large distance from BFI02, was recorded in the same way. The actual borehole names, their depths, inclinations and distances to the pumping borehole (along the ground surface) as well as the method of groundwater level registration are presented in Table 4.3.

Table 4.3 Borehole data for KFI07 and the observation boreholes outside the Brändan area.

Borehole	Depth (m)	Inclination ^{o}	Distance to BFI02 (m)	Method of registration
KFI01	500.85	90	1 540	Manually
KFI02	698.70	50	1 380	Manually
KFI04	602.90	80	940	Transducer
KFI07	552.71	85	800	Manually
KFI08	464.35	60	1 310	Manually
HGB02	94	90	1 270	GW-gauge

4.3.4 Technical arrangements in the pumping borehole

The downhole equipment during test 1 was identical with that during test 2, naturally with exception of the packer positions during the respective tests. The equipment arrangements during tests 1 and 2 are illustrated in Figure 4.5. Some measures and technical data are specified for a) the submersible pump (Table 4.4), b) the pumping hole packers (Table 4.5) and c) the pressure transducers (Table 4.6).

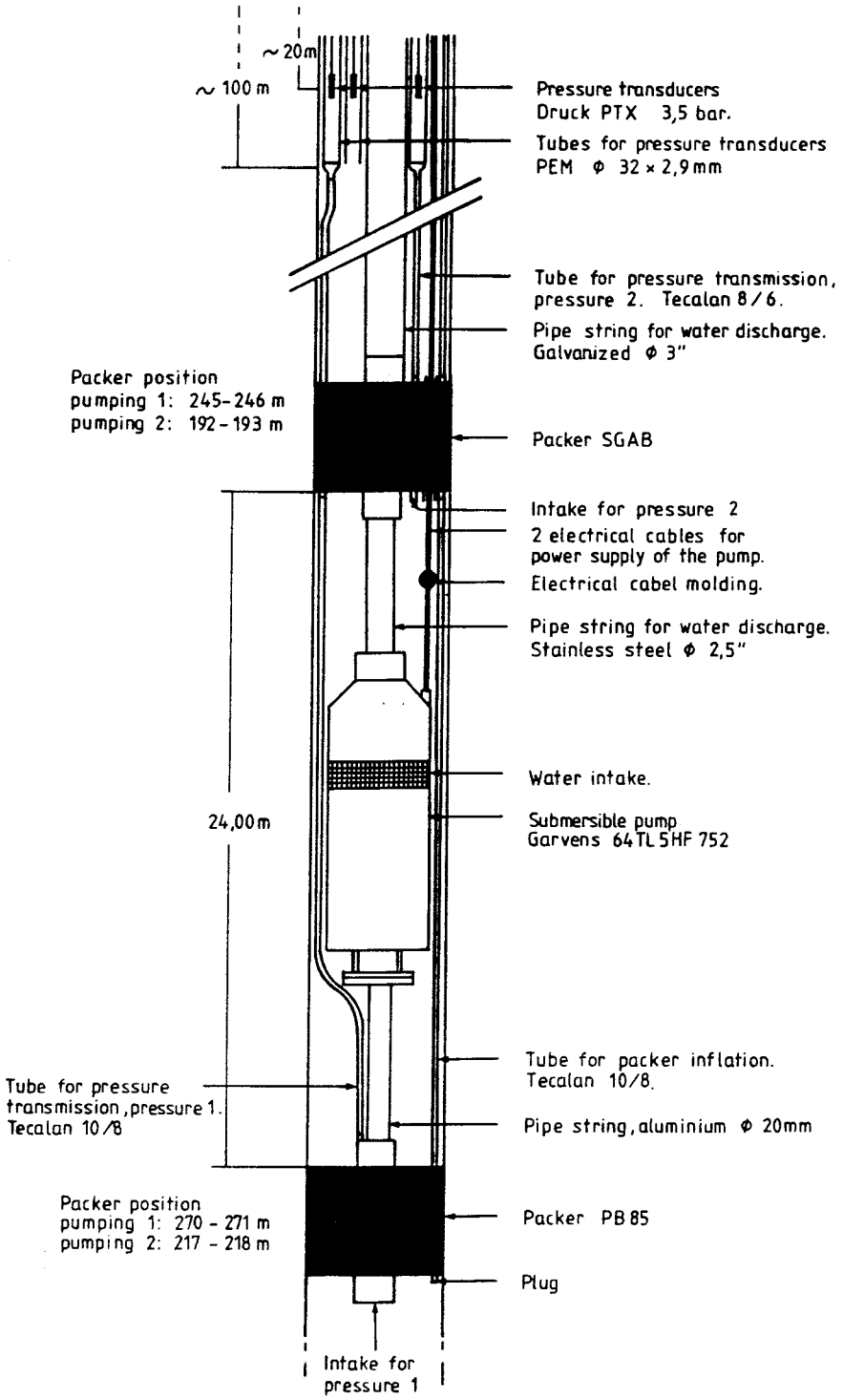

Figure 4.5 The down-hole equipment arrangements in the pumping hole BFI02 during tests 1 and 2.

Table 4.4 Specifications and technical data for Submersible pump type Garvens 64 TL 5HF752.

Measure (mm)	A	1866
	B	890
	C	147
	T	1390
Weight (kg)		85
Nominal effect (kW)		9.2
Max detachable effect (kW)		7.5
Max detachable current at 380V (A)		16.3
Degree of efficiency 3/4		79.5
Direct start JA/JN*		5.1
Y/D-start JA/JN*		1.65
Flow capacity at a total head of 30 m (l/min)		1000

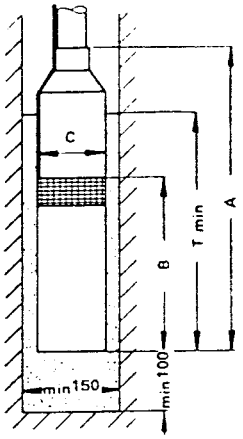

* JA = current at start
JN = operating current

Table 4.5 Specifications and technical data for the packers used in the pumping borehole.

	PACKER TYPE	
	PB 1-85	SGAB
Total length (mm)	1670	1600
Rubber length (mm)	1000	1000
Rubber diameter, uninflated (mm)	85	148
Inflated to 150 mm at (bars)	c. 3	c. 2

Table 4.6 Specifications and technical data for the pressure transmitters used in the pumping borehole.

Type	PTX 160/D
Operating pressure range	3.5 bar
Standard accuracy	0.1 %
Linearity and hysteresis	+ 0.1 %
Thermal stability	∓ 0.3 % total error band at -2° to 30°C
Accepted overpressure without calibr. change	2x
Pressure media	Fluids compatible with quartz and titanium
Transduction principle	Integrated silicon strain gauge bridge
Transmitter supply voltage	0-30 V d. c.
Output current	4-20 mA
Operating temp range	-20° to +60°C
Dimensions	17.5 mm diam x 220 mm length
Weight	113 gms nominal

The downhole instrumentation configuration in the pumping borehole during tests 3A and 3B was somewhat different from that during tests 1 and 2. The reason was, that the instrumentation was planned to have a double purpose: 1) instrumentation for pumping and pressure registration in two observation sections during interference tests 3A and 3B and 2) instrumentation for pumping, pressure registration and injection of tracers during the tracer tests, which are planned to follow immediately after the interference tests.

Figure 4.6 demonstrates the instrumentation in BFI02 during tests 3A and 3B. The pressure at the level 260.8 m was not registered during the interference tests. This part of the equipment is restricted to the later tracer tests.

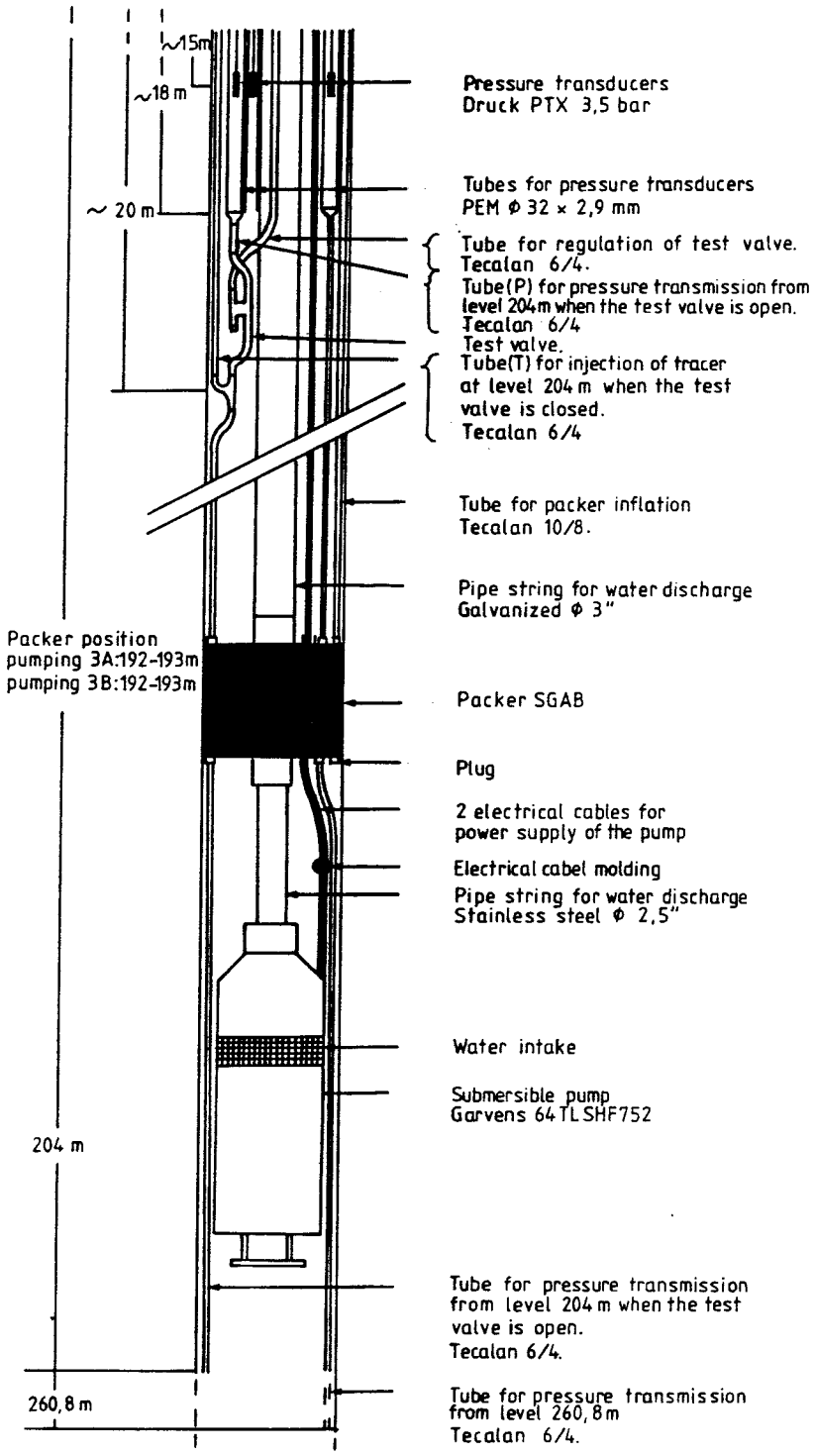

Figure 4.6 The down-hole equipment arrangements in the pumping hole BFI02 during tests 3A and 3B.

The pressure tube from level 204 m (obs. section 1) is connected to a so called test valve, a sliding valve, which can be either in an open or closed position. When open, the pressure in obs. section 1 (level 204 m) can be registered by the transducer. With the test value in closed position, tracer can be injected via the parallell Tecalantube, T, into obs. section 1 without being forced back to the ground surface via the pressure tube, P. One disadvantage for the tests with this arrangement was, that for practical reasons a tube with an innerdiameter of 4 mm (Tecalan 6/4) was used for the pressure transmission from level 204 m. With this narrow tube, a much larger delay in pressure transmission time occurred compared to during tests 1 and 2, when Tecalan 10/8 (8 mm inner diameter) was used. This fact had a negativ influence on the interpretation of hydraulic parameters in the pumping borehole during tests 3A and 3B (Section 6.2.1).

4.3.5 Well site equipment

The technical arrangements at the well site of the pumping hole BFI02 are summarized in Figure 4.7. The instruments can be grouped together in five different systems:

1) the pipe-line for water discharge on which the flow meter and flow regulation systems are connected,
2) the sensors for the electrical conductivity and temperature of the discharged water (connected to the pipe-line),
3) the water chemistry sampling unit (also connected to the pipe-line),
4) the packer regulation system, and
5) the data acquisition system.

Some technical data for the flow meter "Copa-X" are found in Table 4.7.

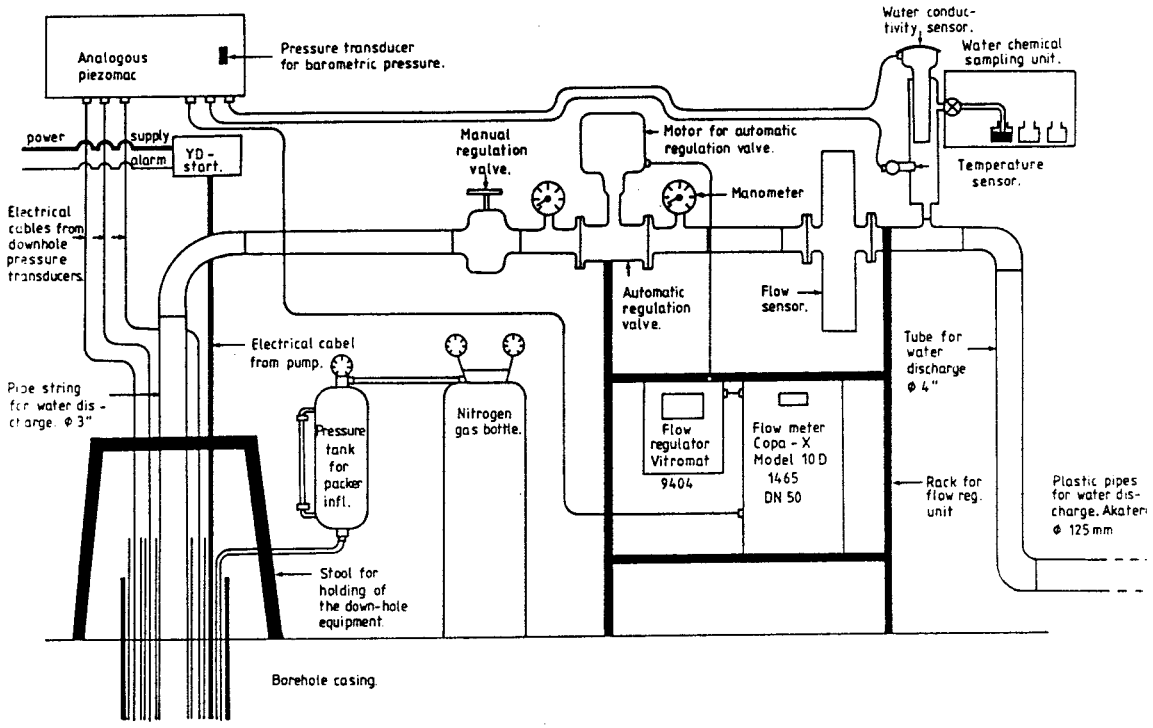

Figure 4.7 The technical arrangments at the well site of the pumping borehole BFI02.

Table 4.7 Specifications and technical data for the flow meter "Copa-X".

Range of flow rate (m^3/h)	min 0 - 3
	max 0 - 60
Max allowable operating pressure at 20°C	40 bars
Output signal, analogous output	0.4 - 20 mA
Power consumption	< 20 watts
Weight	4 kg

4.3.6 Data acquisition

The data acquisition system is illustrated schematically in Figure 4.8. The relevant parts of this system used during the interference tests are described in the following.

Pressure was monitored continuousely in all observation boreholes using multi-pressure probes, and in the pumping hole with single-pressure transmitters (Almén et al. 1986). Monitoring frequencies during all the tests were generally 30 minutes for the observation holes and 15 minutes for the pumping hole. Exceptions from this were close to pump start or pump stop, when the measuring interval was set to approximately 2 minutes and thereafter increased logarithmically to a constant interval.

Other variables measured were flow rate of the discharged water during pumping, electric conductivity and temperature of the discharged water and, finally, atmosperhic pressure.

The pressure was registrered with the Piezomac system (Almén et al. 1986). Data was dumped directly from the Piezomac units to a portable IBM-compatible PC. This unit is provided with means for immediate plotting in the field, but this option was only used to a very limited extent during the interference tests.

The raw data transferred from the Piezomac units to the portable IBM was then transferred to a DEC computer, where all the files for each separate dumping were stored.

In order to provide output for the aquifer analyses in form of diagrams of various formats, the raw data was organized into files covering each test and converted to a suitable format for the plotting facilities (Nyberg 1988). Plots were produced as logarithmic and semi-logarithmic pressure versus time diagrams

for each pump and recovery phase, in addition to linear plots covering each test.

In addition to automatically collected data, manual levelling was performed daily in all boreholes, both for calibration purposes and for monitoring of boreholes not registered automatically. This data was entered manually directly to the DEC computer.

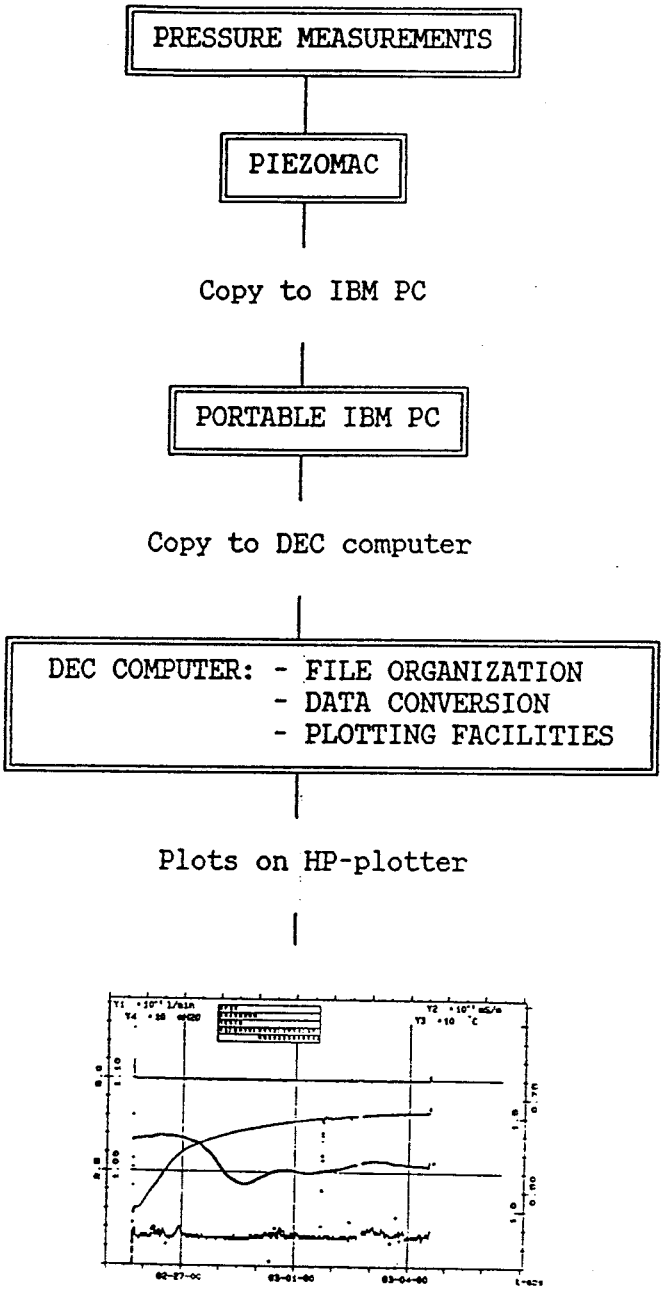

Figure 4.8 The data acquisition system applied during the interference tests.

4.4 Performance of the interference tests

4.4.1 Time schedule and flow rates applied

Subzone 1 is regarded as of special interest for the investigation, because it has been associated in (almost) every borehole with the upper boundary of Zone 2. Subzone 1 has in every borehole a high hydraulic conductivity, seldom exceeded by the conductivity of other subzones further down in Zone 2. It seems to constitute the boundary between nonsaline and saline water, and the water transport during natural gradient conditions has been found to be considerable (Ahlbom et al. 1987) and (Gustafsson and Eriksson 1988). In order to gain as much information from Subzone 1 as possible, it was decided to let the test in Subzone 1 to continue twice the time of the tests in Subzone 3 respectively in the entire Zone 2. A preliminary tracer test with injection of three different tracers was also performed during the pumping in Subzone 1 (see Chapter 7). In order not to spread these tracers to lower parts of Zone 2 (which is of importance for the major tracer tests planned later in phase 3 of the Fracture Zone Project), it was important that the pumping in Subzone 3 was made before the pumping in Subzone 1. Otherwise possibly lingering tracers could be forced downwards by a gradient created during pumping in Subzone 3. A schematic illustration of the time schedule for the three pumpings with intervening recovery periods is found in Figure 4.9. The figure also illustrates different events during the tests, e.g. injection of tracers and pumpstops.

In order to determine suitable flow rates for the three different interference tests, a short pumping test with three flow rate steps was performed four days before interference test 1. Drawdown was observed in the pumping hole and in the

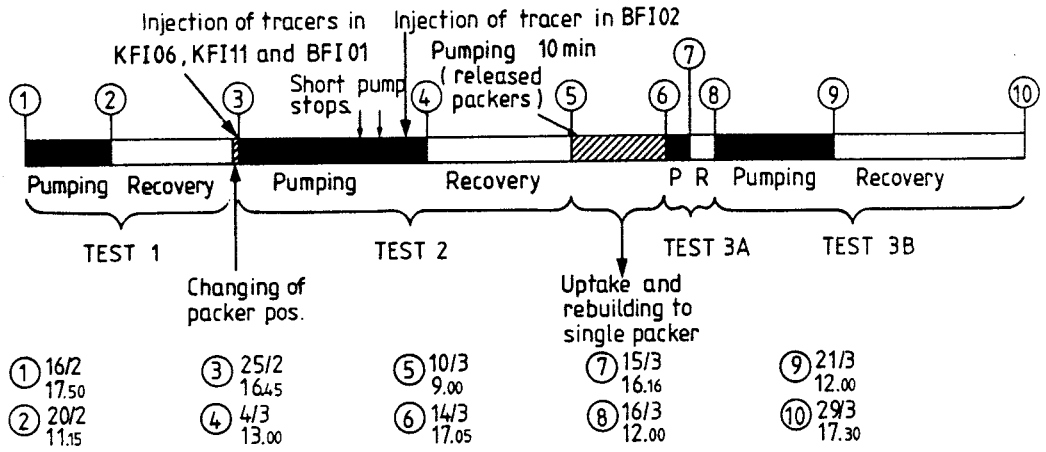

Figure 4.9 A schematic illustration of the time schedule for the three different pumping periods with intervening pressure recovery periods during the interference tests.

observation boreholes. From the results of this step pumping test and with aid from the previous knowledge about the hydraulic properties of the subzones as well as about the total of Zone 2, a flow rate of 500 l/min was decided for all tests. The flow rate during tests 1 and 2 was very stable and turned out to be very close to 500 l/min, 500 $\pm$ 2 l/min (the accuracy of the flow meter is 1 %). However, during test 3A the automatic flow regulation system failed, and therefore the flow rate increased from 500 l/min to c. 700 l/min after 13 h of pumping. Continued problems of keeping the flow at 500 l/min made it necessary to chose the flow rate 700 l/min also for test 3B. The flow regulation was during this test made manually and was therefore less accurate than with the automatic equipment. This did, however, not decrease the quality of the data collected from test 3B in any determining way.

4.4.2 Summary of the interference tests

Test 1

During the first interference test, section 246-270 m in borehole BFI02, i.e. the dominating subzone in the lower part of Zone 2, was pumped with a capacity of 500 l/min. Automatic pressure registrations were undertaken in three sections in the pumping hole, five sections in boreholes KFI05, KFI06, KFI09, KFI10, KFI11 and BFI01 and finally in three sections in HFI01. I.a. for calibration purposes, the groundwater table was also manually levelled in all boreholes. Due to the large pressure responses in all observed boreholes after a short time of pumping, it was regarded of great interest to make pressure registrations also in the boreholes KFI07, 800 m W of BFI02 in the Brändan area and in KFI01 and KFI04 outside the area, 1 540 respectively 940 m from the pumping hole. Therefore, after c. 2 days of pumping a pressure transmitter was installed in KFI04, whereas in KFI01 and KFI07 manual levelling was performed twice a day. These three boreholes were registered as open holes. It was also decided, that a percussion borehole, HG02, situated about 1 270 m from BFI02 and recorded with a groundwater level gauge (for another project), should be included in the registrations.

About two respectively three days after pumpstop, during recovery, two other distant boreholes, KFI08, 1 310 m from BFI02, and KFI02, inclined towards Zone 1 and at the ground surface located 1 380 m from BFI02, was included in the group of manually levelled boreholes.

Unfortunately the pressure registration probe in KFI05 failed after c. 2 days of recovery and was out of function during the rest of test 1.

Test 2

Test 2 was the test of longest duration (see Figure 4.9) due to the great interest attached to the tested section: 193-217 m, Subzone 1, i.e. the uppermost part of Zone 2. The pumping capacity was again 500 l/min. The same observation boreholes as during the end of the recovery phase of test 1 were used, i.e. altogether 13 boreholes. The pressure registration probe in KFI05 was out of function until a new probe was installed after seven days of the recovery phase.

After c. 5 days of pumping a power failure caused a pump stop during approximately one hour. About 16 hours later a similar incident occurred. This time the pump stop lasted less than half an hour.

During test 2, two tracer tests were performed. The first test was a radially converging test, where three different tracers were injected in respectively KFI06, KFI11 and BFI01 a few hours before pumpstart. After pumpstart water samples were frequently taken in the pumphole, until the pulses of tracers had arrived, which occurred after a rather short time (Chapter 7).

The second tracer test was made as a control of the isolating effect of the lower packer in the pumping borehole. A certain amount of the tracer Uranine was injected into the section below the lower packer (218-288.7 m) about 17 hours before pumpstop. Due to the gradient directed from this section towards the pumped section, the tracer was expected to be transported to the latter. If the isolation by the lower packer should be insufficient, the tracer ought to be found in the pumped section after only a short time. However, frequent water sampling during the next 20 hours of pumping showed no sign of Uranine whatsoever. This demonstrated that the packer isolation between the two sections was efficient (Chapter 7). The path-

ways for the water leaking from the lower section to the pumped section, which is proved to occur (Section 5.1.1), therefore have to be the natural fractures at varying distances from the pumping borehole between the two sections.

After 6 days of recovery, the packers in the pumping hole were realesed, and water was pumped from the borehole during a period of 10 min with a capacity of 500 l/min. 65% of the injected amount of Uranine was thereby recovered. The remaining part of the tracer was recovered during the pumping phase of test 3A.

The recovery period during test 2 was for BFI02 about six days, before the packers were released. The duration of uptake of the downhole equipment, rebuilding to a single-packer configuration for test 3 and lowering into the borehole was 4 days and 8 hours. The recovery period for the observation boreholes, in which the registrations continued, while the work in BFI02 was ongoing, was in other words more than ten days.

Test 3A

Test 3, performed in the entire Zone 2 (section 193-288.7 m), was intended to last four days and the pumping capacity was determined to 500 l/min. However, after c. 13.5 hours the automatic flow regulation system failed to function, and the capacity increased to about 700 l/min. It was decided to end the test and to restart after a period of recovery. Pumpstop occurred after 23.2 hours and the recovery lasted for 19.7 hours. This short test was called test 3A. All observation sections were functioning during the test.

Test 3B

The automatic flow regulation system was not possible to repair immediately, and therefore the next test (3B), again in

section 193-288.7 m, was performed with manual flow regulation and flow rate measurements. The accuracy of flow regulation and flow rate measurements was thereby decreased (see flow rate diagrams in Appendices 2-5) but acceptable. For practical reasons the capacity was increased to 700 l/min.

The pressure registrations was, due to technical reasons, interrupted in KFI05 during the pump phase from one to 13 hours after pumpstart. During the recovery phase the pressure registration failed in the pumping borehole between 10 and 33 hours after pumpstop.

In table 4.7 the basic facts about the performance of the interference tests are summarized.

Table 4.7 The performance of interference tests in the Brändan area, Finnsjön study site. Summing up of basic facts.

Test number	Pumped sect	Duration	Disch. rate	Special events
Test 1, P	246-270 m	3 days 17.4 h	500 l/min	After 2 days: manual levelling in KFI01 and KFI07 and automatic registration in KFI04 started.
Test 1, R	-	5 days 5.5 h	-	1)After 2 days: probe in KFI05 fails 2)After 2 days: manual levelling in KFI08 started 3)After 3 days: manual levelling in KFI02 started
Test 2, P	193-217 m	7 days 20.25 h	500 l/min	1)Injection of tracer in KFI06, KFI11 and BFI01 immediately before pump start 2)Probe in KFI05 still out of function 3)After 5 days: short pumpstop (c. 1 h) 4)After 6 days: another short pumpstop (c. 0.5 h) 5)After 7 days: injection of tracer in sect. 1 in BFI02
Test 2, R	-	5 days 20 h in BFI02 10 days 4,1 h in the other boreholes	-	1)Probe in KFI05 still out of function 2) After 6 days: packers realesed in BFI02 and pumping during 10 min with a capacity of 500 l/min (for collection of injected tracer) 3)After 7 days: new probe installed in KFI05.
Test 3A, P	193-288.7	23.2 h	500-700 l/min	After 13.5 h: The automatic flow regulation system fails
Test 3A, R	-	19.7 h	-	-

Table 4.7 continued.

Test number	Pumped sect	Duration	Dish. rate	Special events
Test 3B, P	193-288.7	5 days	700 l/min	1)The automatic flow regulation system out of function. Manual pressure regulation. 2)Pressure registrations in KFI05 interrupted 1-13 h after pump start.
Test 3B, R	-	8 days 5.5 h	-	3)Pressure registrations in BFI02 interrupted 10-33 h after pump stop.

P = pumping

R = recovery

5. QUALITATIVE INTERPRETATION OF THE TESTS

5.1 Boreholes within Zone 2

5.1.1 Interference test 1

As described in Section 4.3.2 the first interference test was performed by pumping of the lowermost subzone of Zone 2 in borehole BFI02. Registrations of the drawdown were undertaken in isolated sections within Zone 2 in the adjacent boreholes and also above and below the zone, see Fig 4.1. After stop of pumping, the recovery of the groundwater head was measured in the same sections and boreholes.

The drawdown and recovery measured for the pumped interval and the observation sections are shown in logarithmic graphs in Appendix 2 together with the recorded flow rate, salinity of the discharged water, downhole temperature of the water in BFI02 and the barometric pressure head. The latter four parameters are presented both on a linear time scale (Appendix 2:1) and on a logarithmic time scale (Appendix 2:2). The symbols used for the measured parameters and different observation sections are shown in the legend at the beginning of the Appendix section.

The flow rate was very stable at c. 500 l/min (8.33 l/s) after about 1 minute of pumping. The barometric pressure head was constant at c. 10.20 m of water in the beginning of the test, decreased slightly to c. 10.14 m at 700 minutes and increased to c. 10.40 m by the end of the test. The water temperature was constant at c. 9.7°C after about 15 minutes of pumping throughout the test.

The electric conductivity of the discharged water decreased from c. 1250 mS/m at the beginning of the test to c. 1150 mS/m by the end of the test. This demonstrates that a significant

leakage from the upper parts of Zone 2 (the electric conductivity of the water is here about 450 mS/m) to the lower part of the zone took place during pumping, see below.

The graphs in Appendix 2 show that the induced pressure wave propagated very rapidly from BFI02 to the observation boreholes. A considerable drawdown was measured at very short times after start of pumping in all sections within Zone 2, e.g. borehole KFI11, also at long distances from BFI02, e.g. HFI01. This indicates a high hydraulic diffusivity, i.e. transmissivity divided by the storage coefficient, in the lateral direction of Zone 2. From the single-hole tests it is known that individual subzones within Zone 2 have a high transmissivity, see Chapter 3.

The borehole section(s) in each borehole showing the fastest response to the pumping and the largest drawdown is likely to represent the primary pathway of the pressure wave between the pumped section in BFI02 and the actual observation section. The other borehole sections should then represent more diffuse pathways resulting in succesively more delayed and attenuated responses. The distances (in space) from the midpoint of the pumped section in BFI02 to the midpoints of each observation section during interference test 1 are shown in Table 5.1.

The drawdown graph from borehole BFI02 in Appendix 2:3 indicates that the largest drawdown occurred in the pumped section but a significant drawdown also took place below and above this section. The difference in drawdown between the borehole sections was persistent during the entire test. Also in the observation boreholes a certain drawdown difference between sections in the same borehole generally occurred, see Appendix 2:4-10. This fact indicates that the different borehole sections are hydraulically interconnected (in the vertical direction) over long distances but also that certain

Table 5.1 Distances to observation sections from BFI02 during interference test 1.

Borehole	Section no	Distance (m)	Borehole	Section no	Distance (m)
KFI05	5	332	KFI11	5	159
	4	261		4	154
	3	225		3	156
	2	209		2	170
	1	264		1	187
KFI06	5	205	BFI01	5	169
	4	197		4	167
	3	193		3	167
	2	193		2	194
	1	307		1	230
KFI09	5	307	HFI01	3	391
	4	305		2	369
	3	305		1	353
	2	308			
	1	331			
KFI10	5	411			
	4	350			
	3	310			
	2	285			
	1	243			

flow restrictions must occur to maintain the observed drawdown differences between sections in the same borehole during the test. At larger distances from BFI02 the drawdown differences between sections tend to decrease, e.g. boreholes KFI09 and HFI01. The hydraulic interaction within Zone 2 is also manifested by the change in electric conductivity of the discharged water during the test, see Appendix 2:1-2.

The differences in drawdown between sections in the same borehole in general seem to be persistent both in time and with distance from BFI02. However, in the more distant boreholes KFI09 and HFI01 no differences in drawdown in the observation

sections within Zone 2 were observed during the test. In borehole KFI09 only the section located above the zone (section 5) responded differently. This may either be interpreted as an unusually good hydraulic communication between the pumped section in BFI02 and all observation sections in borehole KFI09 within Zone 2, both in the horizontal and vertical direction, or alternatively, that the drawdown differences between sections naturally will diminish with radial distance from BFI02, c.f. Section 6.4. The geological interpretation suggests the presence of interconnecting fractures between the different subzones of Zone 2, see Figure 2.4. In borehole HFI01 the drawdown curves in the lower two sections coincide, whereas the uppermost section responds differently. In this borehole only the lowermost section is located (in the upper part) of Zone 2. The uppermost section represents the groundwater table.

By studying the initial response pattern (the order of reponse of sections) in the different boreholes and the measured drawdown in the sections after a short time of pumping, a schematic picture of the propagation of the induced pressure wave within Zone 2 can be deduced. The response pattern of the observation sections, the primary response (PR) sections and their location within Zone 2 together with the maximal drawdown of the primary responses are shown in Table 5.2. In the table, sections with (nearly) coinciding responses are lumped together within brackets. The section numbers refer to the location of the observation sections in the boreholes as listed in Table 4.2.

A schematic picture of the propagation of the primary pathways within Zone 2, extending from BFI02 to the midpoints of the primary observation sections during interference test 1 is shown in Figure 5.1. The section numbers in Figure 5.1 refer to the location of the observation sections in the boreholes as listed in Table 4.2. This figure constitutes a vertical profile through the CAD-picture of Zone 2 shown in Figure 4.1.

Table 5.2 Response pattern of borehole sections, primary response (PR) sections together with their location within Zone 2 and maximal drawdown during interference test 1.

Borehole	Resp. pattern section number	PR-section(s) number	Part of Zone 2	Maximal drawdown (m)
KFI05	2-1-3-4-5	2	lower	(6.78)
KFI06	3-2-4-5-1	3	lower	(6.52)
KFI09	3-4-2-1-5	3,4	whole	6.51
KFI10	1-3-2-4-5	1,3	whole	6.64
KFI11	3-2-1-4-5	3	lower	7.39
BFI01	4-3-1-2-5	4	upper	5.38
HFI01	1-2-3	1,2	(upper)	6.52
BFI02	2-1-3	2	lower	10.20

NB. Values within brackets are uncertain.

The boreholes are projected onto the profile which is oriented in S65W-N65E in the RAK-system. The profile is viewed parallel to the upper and lower (extrapolated) surfaces of Zone 2. The actual borehole intersections with the upper and lower boundaries of Zone 2 are marked in the figure together with the observation sections within the zone.

Table 5.2 and Figure 5.1 show that the primary responses in the observation boreholes generally occurred in the lower part of Zone 2 in the boreholes nearest to BFI02 whereas at larger distances all borehole sections within Zone 2 responded almost simultaneously, e.g. KFI09 and KFI10. However, in BFI01 the primary response occurred in the upper part of Zone 2. The response in BFI01 was also somewhat slower compared to KFI06 and KFI11, which boreholes are located at about the same distance from BFI02. This may indicate deviating geological

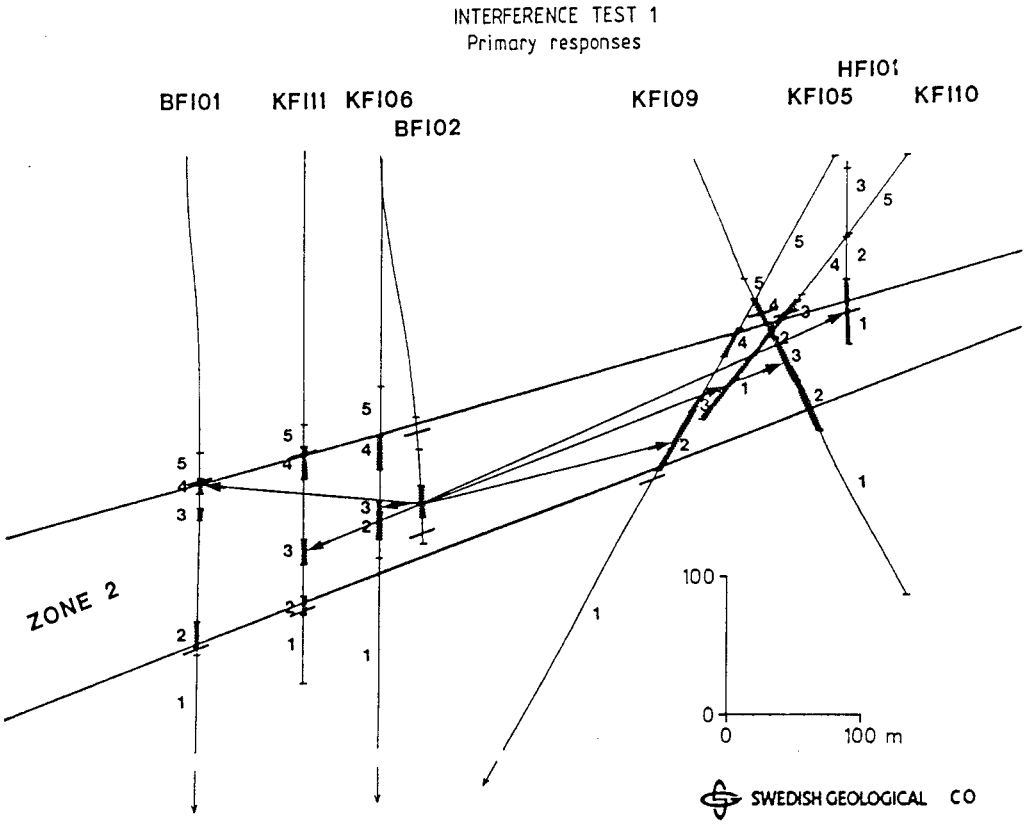

Figure 5.1 Schematic picture of the propagation of the primary responses during interference test 1.

conditions between BFI01 and BFI02, cf. Section 6.3. It should be observed that only the upper part of Zone 2 is penetrated by the borehole HFI01.

Table 5.2 also shows that the slowest responses generally occurred above Zone 2 (section 5) except in KFI06 where the section below the zone (section 1) shows the slowest response. The temporary decrease in drawdown at about 60 minutes in KFI06, see Appendix 2:5, is not clear. It may be due to technical problems (e.g. leakage) with the multipacker system in this borehole. Also during the recovery phase in KFI06 a similar head change occurred by the end of the test. This

remarkable drawdown behaviour does not appear in any of the other boreholes or in other tests.

In Figures 5.2a and b the primary drawdown responses, i.e. the fastest responding section with the largest drawdown in each borehole, according to Table 5.2, during the first interference test are plotted versus time in semilogarithmic graphs. It should be observed that the response in the pumping borehole BFI02 is delayed up to about ten minutes due to technical problems, see Section 4.3.4. The vertical scale shows the drawdown in the borehole sections. As indicated in the figures the values on this scale should be multiplied by a factor of 10. The distances of the borehole sections from BFI02 are listed in Table 5.1.

The figures clearly show that the primary drawdown responses are very similar in all boreholes during the entire test irrespectively of the distance to BFI02. While the actual drawdown differs somewhat between the near-region boreholes, it is almost identical in the distant-region boreholes. The rate of drawdown is virtually the same, independently of distance to BFI02. Thus, within the investigated area, the rate of drawdown with time is (nearly) constant at all points, i.e the hydraulic gradient is constant. This situation, which is known as the pseudosteady-state flow period, can only occur in a bounded system, i.e. an aquifer surrounded by hydraulic boundaries (Earlougher 1977). The steep shape of the drawdown curves in the logarithmic graphs at intermediate times indicates that Zone 2 is bounded by negative (barrier) hydraulic boundaries. This is consistent with the geological interpretation of the outer boundaries of Zone 2, see Chapter 2. Here, Zone 2 is described as a triangular-shaped area surrounded by fracture zones.

Figures 5.2a and b also show that the primary drawdown responses in some of the nearest observation boreholes deviate

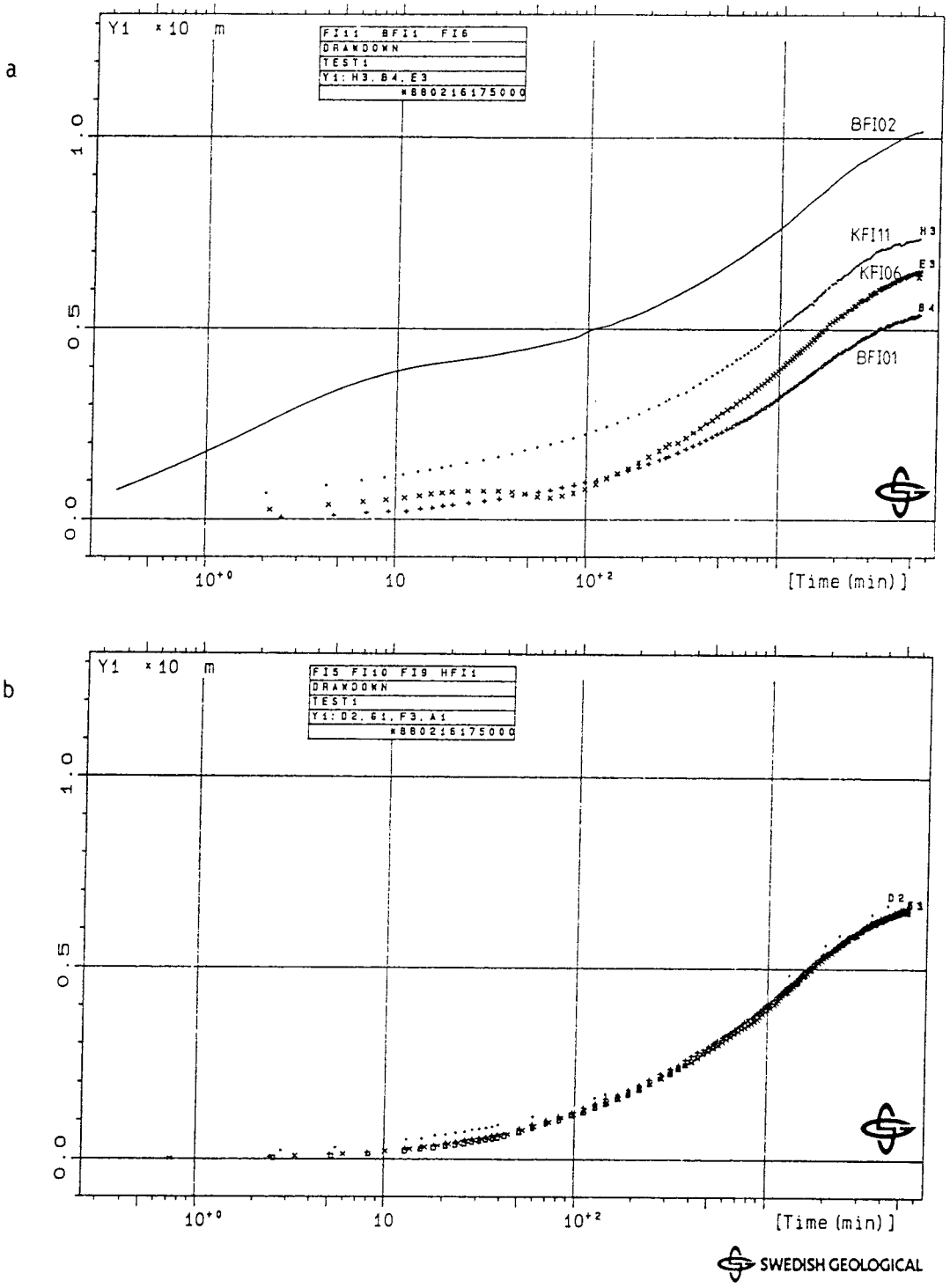

Figure 5.2 The primary drawdown responses in the boreholes within Zone 2 during interference test 1.
a) boreholes BFI02, KFI06, KFI11 and BFI01.
b) boreholes KFI05, KFI09, KFI10 and HFI01.

significantly from the drawdown in the other boreholes, e.g. KFI11 and BFI01. As stated above, the drawdown in KFI06 is probably not representative for intermediate times. Borehole KFI11 responded very rapidly indicating almost immediate hydraulic communication with BFI02 whereas borehole BFI01 responded somewhat slower than the other boreholes (but still very fast) indicating a more delayed (possibly indirect) hydraulic communication with BFI02, see Section 6.3.

After long pumping times (about 5000 minutes) all drawdown curves shown in Appendix 2 tend to flatten out, indicating a major inflow of water to Zone 2 from external sources, c.f. test 2. This inflow may possibly be transmitted along Zone 1 (the Brändan zone), which extends towards southwest to Lake Finnsjön, see Chapter 2. Zone 1 may be in hydraulic connection with Lake Finnsjön. Other fracture zones may also be potential sources of inflow to Zone 2.

Graphs of the recovery of the groundwater head after stop of pumping are also shown in Appendix 2. The recovery is in this case plotted versus equivalent time (Agarwal 1980), since a certain drawdown trend still existed by the end of the pumping period. If a (near) steady-state is reached during the drawdown period, the recovery should be plotted versus real time since stop of pumping, cf. test 2. The recovery curves are in general almost identical to the drawdown curves, which is consistent with theory. Thus, all observations and conclusions drawn from the drawdown phase are confirmed by the recovery phase. This fact also strengthens the confidence of the interference test results.

A rough estimation of the magnitude of leakage from the upper part of Zone 2 to the lower part during pumping can be obtained from the measured electric conductivity of the water. Knowing the initial water conductivities in the upper and lower parts of Zone 2 and assuming that the discharged water is a

mixture of these two sources only the following balance equation can be set up:

$$EC_1 \times Q_1 + EC_2 \times Q_2 = EC_t \times Q \qquad (5.1)$$

and $Q_1 + Q_2 = Q$

where EC_1, EC_2 and EC_t = initial electric conductivity of water in the upper part of Zone 2, in the lower part of Zone 2 and of the discharged water by the end of the test, respectively.

Q_1, Q_2 and Q = leakage flow rate from upper part of Zone 2, flow rate from lower part of Zone 2 and total flow rate, respectively.

Assuming that EC_1 = 450 mS/m, EC_2 = 1250 mS/m, EC_t = 1150 mS/m (see Appendix 2:1-2) and Q = 500 l/min gives Q_1 = 62.5 l/min and Q_2 = 437.5 l/min, i.e. the leakage rate to the lower, pumped part of Zone 2 is about 60 l/min from above by the end of the test. This rough estimation may be misleading if leakage also occurred from the rock below Zone 2 (with higher electric conductivity) during pumping. If such leakage was significant, the actual leakage from above would be higher than 60 l/min, to obtain a decreasing electric conductivity of the discharged water, see Section 6.4.

5.1.2 Interference test 2

The second interference test was carried out by pumping in the uppermost part of Zone 2 in the same borehole (BFI02), see Section 4.3.2. The observation boreholes and sections were basically identical with those during the first interference test (except KFI05). After stop of pumping the recovery of the groundwater head was measured in the same sections.

The variations of the flow rate, barometric pressure head, downhole temperature and electric conductivity of the discharged water during the drawdown phase are shown in Appendix 3:1-2. The flow rate was again held constant at c. 500 l/min (after about 10 minutes) throughout the test. The barometric pressure head was stable at c. 10.35 m water column to about 2000 minutes when it dropped to c. 9.85 m to again increase to c. 10.10 m by the end of the drawdown period.

The temperature of the water initially rose from c. 7.5°C to c. 8.5°C and stayed at this value with a tendency of slightly increasing temperature by the end of the drawdown period. The change of electric conductivity was more pronounced at interference test 2 compared to test 1. The electric conductivity increased from initially c. 450 mS/m to c. 720 mS/m by the end of the drawdown period. This indicates that a significant leakage from the lower part of Zone 2 to the upper part takes place during pumping, see below.

The drawdown and recovery curves from the second interference test are shown in logarithmic graphs in Appendix 3. The recovery is plotted versus real time (instead of equivalent time) since a steady-state was reached by the end of the drawdown period of interference test 2. The drawdown graph from BFI02 again shows that the largest drawdown occurred in the pumped section. A significantly lower drawdown took place below this section whereas the section above was unaffected by the pumping until about 1000 minutes when the drawdown started to increase. This section represents the groundwater level in BFI02.

The above facts indicate that the pumped section in BFI02 is more effectively (hydraulically) isolated from the overlying rock during interference test 2 compared to the first test. The isolation above the pumped section seems to be very efficient and indicates a large hydraulic conductivity contrast between

Zone 2 and the overlying rock. This fact is also known from the single-hole tests, see Chapter 3. The drawdown in the section above the pumped section in BFI02 in the first interference test and in the section below the pumped section in the second test is however very similar. The drawdown in these sections is dominated by the upper and lower subzones of Zone 2, respectively. This indicates that the hydraulic properties of these subzones are similar.

As will be described in Chapter 7, a tracered volume of water was injected just below the lower packer in BFI02 during the second interference test to check the possible bypass of water around the lower packer during pumping. This experiment showed that no bypass of water could be detected and thereby confirmed that the pumping in BFI02 was effectively concentrated to the uppermost part of Zone 2 during interference test 2.

Similar total drawdowns and rates of drawdown were measured in the observation sections during interference test 2 as in test 1. The main differences between the tests are that the propagation of the primary pressure wave from BFI02 was more concentrated to the upper part of Zone 2 in most of the observation boreholes during interference test 2. This indicates that the induced pressure wave from BFI02 propagated more directly along the upper part of the zone, particularly towards the nearest boreholes, and caused an even more rapid and appreciable drawdown at short times in these boreholes, e.g. KFI11.

The distances from the midpoint of the pumped section in BFI02 to the midpoints of the observation sections during the second interference test are shown in Table 5.3. The response pattern of the observation sections, the primary response (PR) sections and their location within Zone 2 and maximal drawdowns are shown in Table 5.4. A schematic picture of the propagation of the primary response during interference test 2 is shown in

Figure 5.3. The designations of the borehole sections are the same as in Table 5.2 and Figure 5.1, respectively. In Table 5.4, sections with almost identical responses are lumped together within brackets.

Table 5.3 Distances to observation sections from BFI02 during interference test 2.

Borehole	Section no	Distance (m)	Borehole	Section no	Distance (m)
KFI05	5	309	KFI11	5	153
	4	245		4	155
	3	217		3	177
	2	206		2	200
	1	293		1	222
KFI06	5	189	BFI01	5	165
	4	189		4	168
	3	195		3	174
	2	200		2	221
	1	345		1	265
KFI09	5	286	HFI01	3	367
	4	288		2	349
	3	294		1	338
	2	302			
	1	339			
KFI10	5	391			
	4	331			
	3	294			
	2	272			
	1	234			

By comparing Tables 5.2 and 5.4 it can be seen that the general response patterns for test 1 and test 2 are similar with the exception that the primary responses in the nearest boreholes (KFI06 and KFI11) now occur in the upper part of Zone 2. Compared to test 1, the primary responses in KFI06, KFI11 and BFI01 are more direct during interference test 2 which results in larger drawdowns in these sections at short times, cf. section 4 in KFI11 where the drawdown is about 1.5 m after c. 2 minutes of pumping. This indicates a very high

hydraulic diffusivity (high transmissivity and low storativity) along the upper part of Zone 2, particularly between BFI02 and KFI11. In BFI01 the primary response again occurs in section 4 as in test 1.

Table 5.4 Response pattern in the boreholes, primary response (PR) sections together with their location within Zone 2 and maximal drawdowns during interference test 2.

Borehole	Resp. pattern section number	PR-section(s) number	Part of Zone 2	Maximal drawdown (m)
KFI05	not used during interference test 2			
KFI06	4-5-2-3-1	4	upper	6.98
KFI09	4-3-2-1-5	4,3	whole	6.39
KFI10	1-3-2-4-5	1,3	whole	6.46
KFI11	4-5-3-2-1	4	upper	7.87
BFI01	4-3-1-2-5	4	upper	5.91
HFI01	1-2-3	1,2	(upper)	6.38
BFI02	5-4-6	5	upper	11.15

The other sections in KFI06, KFI11 and BFI01 and in the more distant boreholes from BFI02 (KFI09, KFI10 and HFI01) respond in a similar manner as in test 1. In the latter boreholes very small drawdown differences between sections were observed as in test 1. The maximal primary drawdowns in the most distant boreholes (KFI09, KFI10 and HFI01) were less in test 2 than in test 1 despite the longer pumping time for test 2, see Table 4.7. For the nearest boreholes the opposite is true, cf. Tables 5.2 and 5.4. This may possibly be explained by somewhat different outer boundary conditions and recharge (and leakage) conditions for the upper and lower parts of Zone 2.

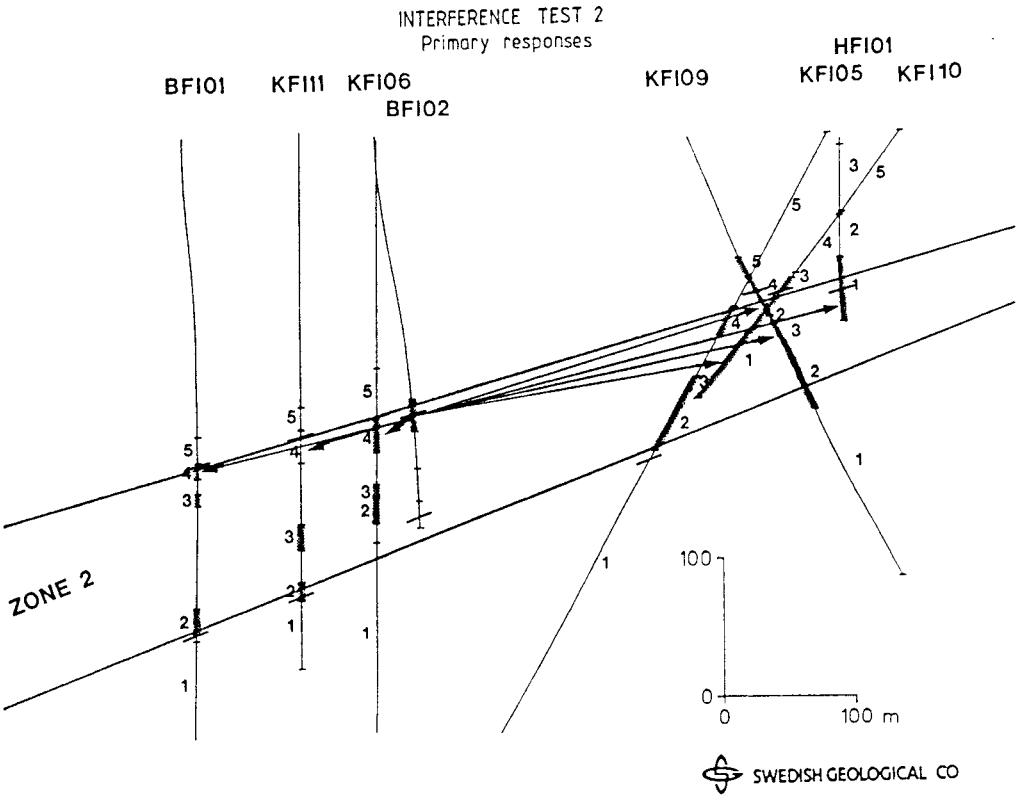

Figure 5.3 Schematic picture of the propagation of the primary responses during interference test 2.

The slowest responses still occurred above Zone 2 except in KFI06 and KFI11 where the sections below the zone responded slowest. This again confirms the good hydraulic isolation between the pumped section in BFI02 and the overlying rock. In the boreholes KFI05, KFI10 and HFI01 the slow responses above the zone may also be due to open borehole conditions in these sections (no packers).

Figures 5.4a and b show the primary drawdown response in each borehole versus time in semilogarithmic graphs during interference test 2, cf. Figure 5.2. As in test 1, the drawdown in the pumped section in BFI02 was delayed up to about 10

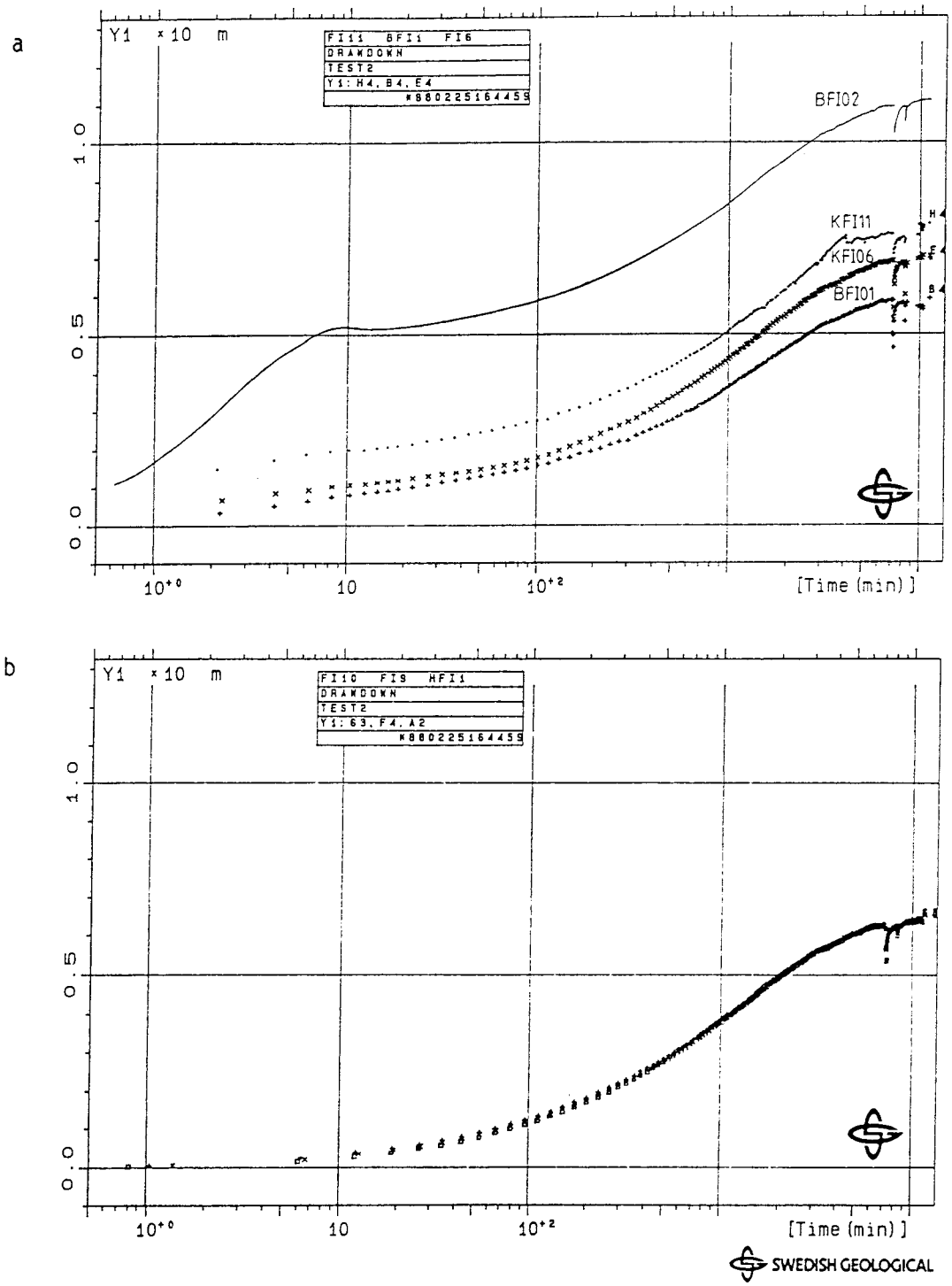

Figure 5.4 The primary drawdown responses in the boreholes within Zone 2 during interference test 2.
a) boreholes BFI02, KFI06, KFI11 and BFI01.
b) boreholes KFI09, KFI10 and HFI01.

minutes. The curves exhibit the same general pattern as in test 1, i.e. the rate of drawdown was very similar in all boreholes, independently of the distance to BFI02. This confirms the bounded nature of Zone 2 in a hydrogeologic sense. As in test 1, the (primary) drawdowns in the nearest observation boreholes (KFI06, KFI11 and BFI01) deviate significantly from the primary drawdowns in the other boreholes. The drawdown (and recovery) curves from interference test 2 ultimately flattened out and a steady-state was reached by the end of the test, indicating major (external) sources of water recharging Zone 2, cf. test 1.

The recovery curves after stop of pumping together with the drawdown curves are shown in Appendix 3. As for test 1, the recovery curves are almost identical to the drawdown curves. This means that the results and conclusions obtained from the drawdown period are confirmed by the recovery phase.

The electric conductivity of the discharged water increased from about 450 mS/m to about 720 mS/m during test 2. Using the same assumptions as for test 1, the leakage from the lower part of Zone 2 to the uppermost part during pumping may be estimated. Using the same initial electric conductivities as for test 1, Q_1 = 331 l/min and Q_2 = 169 l/min, i.e. the estimated leakage rate from the lower parts of Zone 2 is about 170 l/min (2.8 l/s) by the end of the drawdown period. This is about one third of the total discharge rate from BFI02 during test 2. Thus, the estimated leakage from below during test 2 is significantly higher than from above during test 1, see Section 6.4.

5.1.3 Interference test 3

Test 3A

The third interference test was performed by pumping of the entire Zone 2 below a single packer in borehole BFI02, see Section 4.3.2. The observation sections and boreholes were basically identical to the ones used in the previous two interference tests. Due to technical problems with the flow regulation system (see Section 4.4.2) this drawdown test was terminated after about 24 hours. After stop of pumping the recovery was measured. This test (drawdown and recovery) is denoted test 3A on the graphs.

The flow rate, downhole temperature and electric conductivity of the discharged water during the drawdown period together with the barometric pressure head are shown in Appendix 4:1-2. The flow rate was constant at c. 500 l/min until about 13.5 hours after start of pumping. After this time the flow rate recorded was unreliable. Subsequent calibrations with tank and stop watch showed that the real flow rate had increased to about 700 l/min by the end of the test.

The barometric pressure head was stable at about 10.1 m during the drawdown period and decreased to 10.0 m during the recovery period. The temperature of the water was relatively stable at 9.5°C but the temperature recording also become unstable by the end of the test. The electric conductivity initially increased from c. 950 mS/m to 990 mS/m and then decreased to a stable value of c. 970 mS/m by the end of the test. This indicates that the discharged water during this test is more evenly distributed from both the upper and lower parts of Zone 2 with a slightly increasing portion coming from the upper parts, cf. tests 1 and 2.

The drawdown and recovery curves from test 3A are shown in logarithmic graphs in Appendix 4. The drawdown recorded in

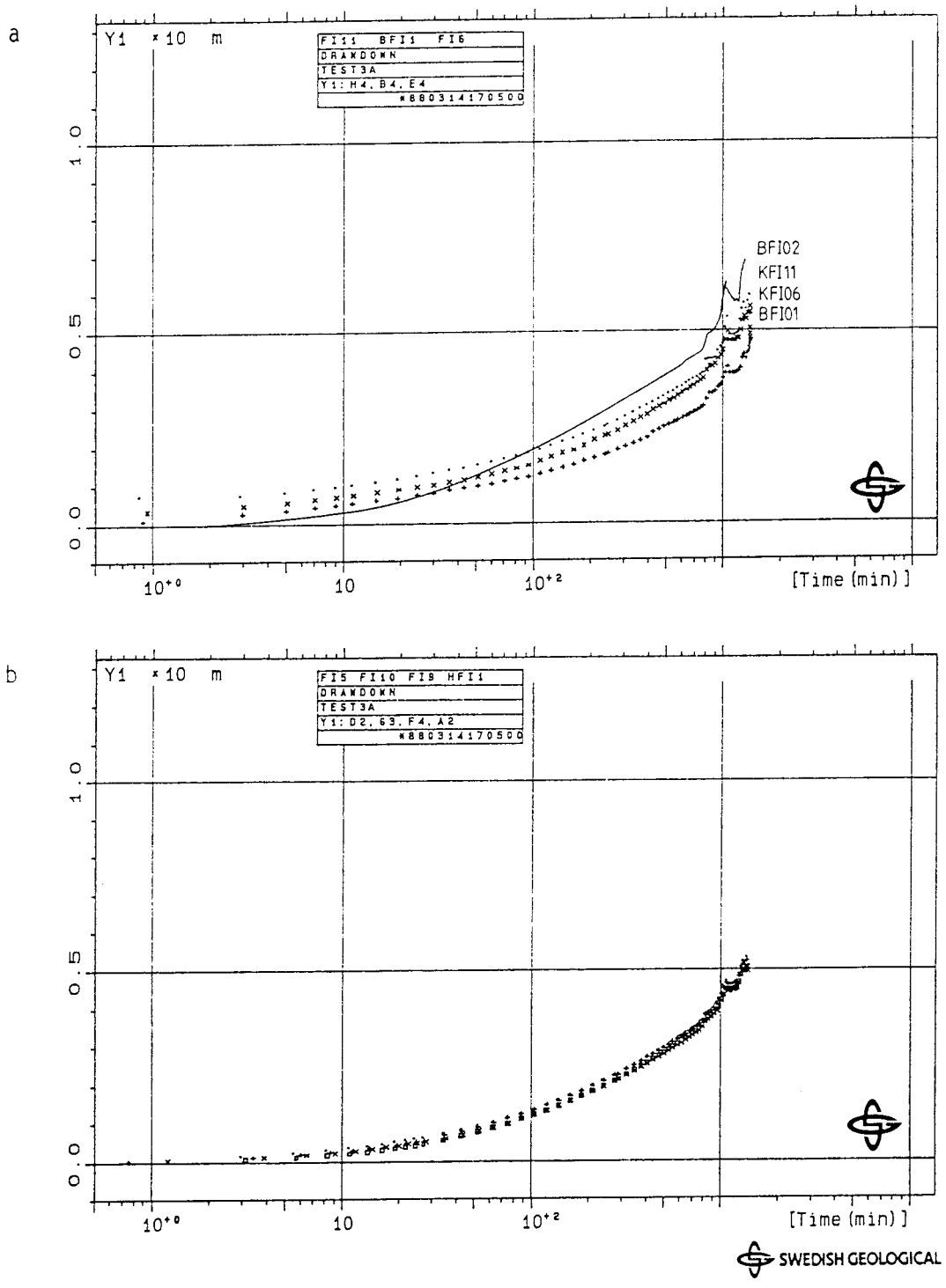

Figure 5.5 The primary drawdown responses in the boreholes within Zone 2 during interference test 3 A.
a) boreholes BFI02, KFI06, KFI11 and BFI01.
b) boreholes KFI05, KFI09, KFI10 and HFI01.

BFI02 (pumped borehole) at the beginning of the test was significantly delayed due to the technical arrangement in BFI02 during this test, see Section 4.3.4. As for test 2, the section above the packer was effectively isolated from the pumped section.

The drawdown (and recovery) behaviour of test 3A was very similar to the first 24 hours of test 2. The first part of test 3A is directly comparable with test 2 since the flow rates were identical. Both the magnitude and rate of drawdown and the response patterns are similar, see Table 5.6. The main difference between the tests is that the primary drawdown in the nearest boreholes (KFI06, KFI11 and BFI01) was somewhat less in test 3A. Since the responses are similar to test 2, the distances to BFI02 shown in Table 5.3 should also be (approximately) representative for test 3A (and 3B). The drawdown of the primary response sections during interference test 3A is shown in Figures 5.5a and b. The figures show that the drawdowns in the nearest boreholes do not deviate much from the other boreholes as in test 2.

As for the previous interference tests the recovery curves are very similar in shape to the drawdown curves, thus confirming the results from the latter test. The recovery measured in the boreholes is though somewhat higher than the corresponding drawdown for test 3A due to the increase in flow rate that happened by the end of the drawdown test. The maximal primary drawdown in each observation borehole during test 3A (and 3B) is presented in Table 5.5.

Test 3B

After recovery of test 3A, a new drawdown test was carried out. This test is denoted 3B on the graphs. Also during this test problems with the flow regulation system occured, see Section 4.4.2. The flow rate, barometric pressure head, electric

Table 5.5 Maximal primary drawdowns at certain times of tests 3A and 3B.

Borehole	Maximal drawdown (m)	
	Test 3A t=1367 min	Test 3B t=7200 min
KFI05	5.33	7.71
KFI06	5.50	7.80
KFI09	5.06	7.41
KFI10	5.22	7.56
KFI11	5.83	8.08
BFI01	4.48	6.45
HFI01	5.06	7.42
BFI02	6.90	9.95

conductivity and temperature of the water during this test are shown in Appendix 5:1-2. The flow rate decreased slightly from c. 715 l/min and stabilized at c. 700 l/min. After about 3.5 days the flow rate increased to c. 800 l/min but returned to c. 700 l/min by the end of the test. The temperature of the water was relatively constant at c. 9.5°C during the test. The barometric pressure head increased from c. 10.10 m of water column to c. 10.25 m after about 2.5 days and stayed relatively constant at this level. The electric conductivity decreased almost linearily from c. 970 mS/m to c. 880 mS/m by the end of the test.

The drawdown and recovery curves from test 3B are shown in Appendix 5. The graph from BFI02 shows that the section above the packer was slowly responding after about 700 minutes. This again demonstrates a good hydraulic isolation between the pumped section and the overlying rock. The drawdown (and recovery) behaviour in the observation boreholes was very similar to those during test 3A. The only difference between

the tests is that the drawdown (recovery) was higher during test 3B due to the higher flow rate used. The drawdown is roughly proportional to the flow rate at all times during pumping. The maximal primary drawdown in each borehole at specified times for tests 3A and 3B is shown in Table 5.5.

The response pattern of the sections in the boreholes, the primary response (PR) section(s) in each borehole and the corresponding part of Zone 2 during tests 3A and 3B are shown in Table 5.6.

Table 5.6 Response pattern of sections in the boreholes, the primary response (PR) sections and their location within Zone 2 during interference tests 3A and 3B.

Borehole	Resp. pattern sections number	PR-section(s) number	Part of Zone 2
KFI05	2-1-3-4-5	2	lower
KFI06	4-5-2-3-1	4	upper
KFI09	4-3-2-1-5	4,3	whole
KFI10	1-3-2-4-5	1,3	whole
KFI11	4-3-2-5-1	4	upper
BFI01	4-3-1-2-5	4	upper
HFI01	1-2-3	1,2	(upper)
BFI02	7-8	7	whole

By comparing Tables 5.4 and 5.6 it can be seen that both the response patterns and the primary response sections were very similar for test 2 and tests 3A, 3B, respectively. The main difference between the tests is that the drawdown curves in the nearest boreholes were more closely spaced together in tests 3A and 3B compared to test 2 (and test 1). This is probably due to

the fact that the discharge was more evenly distributed within Zone 2 during tests 3A and 3B.

In borehole KFI05 (which was not used in test 2) the primary response occurred in the lower part of Zone 2 (as in test 1), see Table 5.2. The response pattern above and below Zone 2, particularly in borehole KFI11, was somewhat different between test 2 and tests 3A, 3B. In the latter two tests the uppermost section (5) responded somewhat slower than during test 2.

Another difference in KFI11 is that the drawdown in the lowermost section (1) increased more rapidly during tests 3A and 3B compared to test 2. This may also be explained by the more uniformily distributed discharge from Zone 2 during tests 3A and 3B. As before, the recovery curves were almost identical to the drawdown curves.

Figures 5.6a and b show the primary drawdown response in each borehole versus time in semi-logarithmic graphs during interference test 3B. The curves are similar to those for test 2 but the (primary) drawdowns in the nearest boreholes were less in test 3B, particularly at early times. Thus, the (primary) drawdowns appear more averaged in test 3B (and 3A) and also more correlated to the distance from BFI02, see Section 6.2.

A rough estimation of the proportions of the total discharge derived from the upper and lower parts of Zone 2, respectively, during test 3B may be obtained from the measured electric conductivity of the discharged water. Assuming that the discharged water is a mixture of water from the upper and lower parts of Zone 2 only, the actual flow rates by the end of test 3B may be estimated from Eqn 5.1. Using EC_1 = 450 mS/m, EC_2 = 1250 mS/m as before and EC_t = 880 mS/m and Q = 700 l/min gives Q_1 = 324 l/min and Q_2 = 376 l/min from the upper and lower parts of Zone 2, respectively. This indicates that

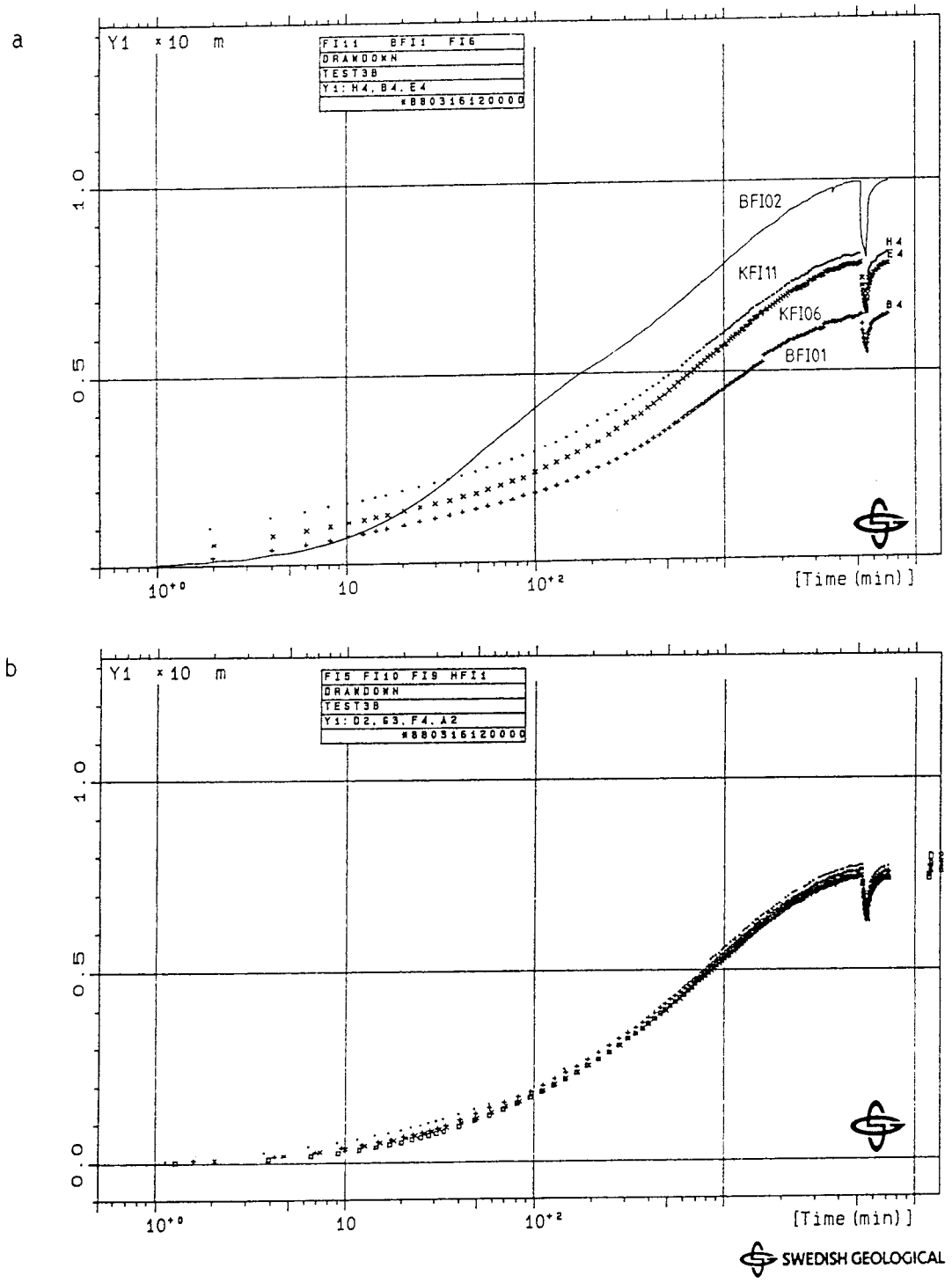

Figure 5.6 The primary drawdown responses in the boreholes within Zone 2 during interference test 3B.
a) boreholes BFI02, KFI06, KFI11 and BFI01.
b) boreholes KFI05, KFI09, KFI10 and HFI01.

approximately the same proportions were discharged from the upper and lower parts of Zone 2 by the end of test 3B.

5.1.4 Summary of test responses

Since all interference tests (except 3 B) were performed with the same flow rate, the drawdown (and recovery) responses may be directly compared between the tests. As described above, different responses can be distinguished between the near-region and the more distant region from the pumping borehole. In the near region, primary responses dominated whereas responses were more averaged at longer distances. The drawdowns at longer times were very similar in all tests (except test 3 B). A schematic picture of the observed drawdown (and recovery) responses within Zone 2 during each test are shown in logarithmic graphs in Figure 5.7. In the near-region the upper and lower curve correspond to the primary and secondary responses in the Zone, respectively. In the distant-region the single curve corresponds to the secondary (averaged) responses.

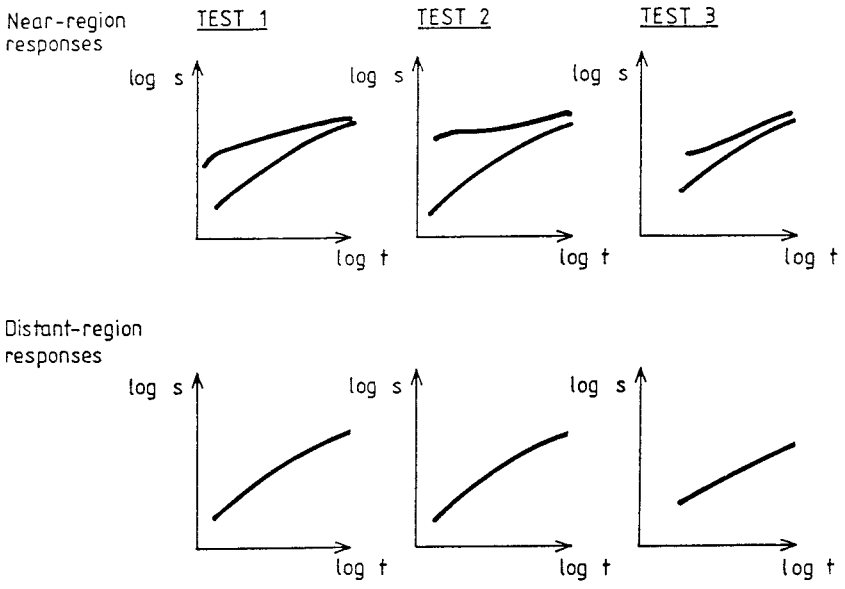

Figure 5.7 Schematic picture of observed drawdown (and recovery) responses during the different interference tests.

During test 1 and test 2 the primary responses in the near-region normally occurred in the sections representing the pumped parts of Zone 2, respectively. The primary response were more accentuated during test 2, compared to test 1. During test 3A and 3B the separation between the primary and secondary response curves was less, compared to test 1 and 2. The response pattern during tests 3A and 3B was similar to that of test 2, i.e. the upper part of the zone responded fastest. In the distant-region boreholes all response curves within Zone 2 almost coincide. The secondary responses in the near-region are very similar to the responses in the distant-region during all tests.

During each test, the primary responses were similar in all boreholes except BFI01 and KFI11, which boreholes show somewhat deviating (primary) responses, particulary during test 1 and test 2. Both the actual head change and rate of head change of the primary responses were similar, (almost) independently of the distance to the pumping borehole. This facts indicate that the aquifer system is surrounded by hydraulic boundaries. Since all response curves have a steep shape in the logarithmic graphs negative (barrier) boundaries are suggested. During the final stage of test 2 (which had the longest duration) a steady-state was reached. This indicates that Zone 2 is reacharged from external sources, possibly other fracture zones. The changes in electric conductivity of the discharged water from the pumping borehole and the estimated discharge from the upper and lower parts of Zone 2 by the end of each test are shown in Table 5.7.

Table 5.7 Changes in electric conductivity (E.C.) of the discharged water from BFI02 and estimated discharge from the upper (U) and lower (L) part of Zone 2 by the end of the interference tests.

Test no	Part of Zone 2	Discharge (l/min)	Initial E.C. (mS/m)	Final E.C. (mS/m)	Est. discharge (l/min)
1	lower	500	1250	1150	U = 62 L = 438
2	upper	500	450	720	U = 331 L = 169
3B	whole	700	970	880	U = 324 L = 376

5.1.5 Variation of the groundwater table in the boreholes

Manual registrations of the groundwater table in the boreholes within Zone 2 were also undertaken twice a day during the interference tests. The groundwater table in these boreholes corresponds to the upper, open borehole intervals above the uppermost packer. It should be noted that in the boreholes BFI02, KFI05, KFI10 and HFI01 the groundwater table corresponds to the uppermost observation section (Section 5) used in the interference tests. In these boreholes the groundwater table was thus also monitored by the Piezomac system, see Section 4.3.2.

The manual registrations of the groundwater head (taking the inclination of the boreholes into account) in the boreholes within Zone 2 during the interference tests are presented in

Appendix 6. The graphs show that the groundwater head in the observation boreholes responds significantly during the different drawdown and recovery periods. However, the drawdown of the groundwater head is normally much less than the observed drawdown in the observation sections within Zone 2.

Small drawdowns of the groundwater head were observed in the boreholes BFI01 and BFI02 indicating good hydraulic isolation towards the overlying rock in these boreholes. Large drawdown of the groundwater head was observed in borehole KFI09. This is consistent with the hydraulic conductivity profile in this borehole which indicates high conductivities above Zone 2.

5.2 Boreholes outside Zone 2

The groundwater levels in peripheral boreholes outside Zone 2 were also measured during the interference tests. These boreholes were open (without packers) and the groundwater levels were generally recorded manually twice a day. The peripheral boreholes manually registered were KFI01, KFI02, KFI04, KFI07 and KFI08. The geological interpretation in Chapter 2 indicates that it is uncertain whether borehole KFI07 is located within or outside Zone 2. From interference test 2 and onwards a pressure transducer was installed in borehole KFI04 for continuous registration of the groundwater level. Finally, recordings of the groundwater level by a chart recorder in the percussion borehole HGB02 (in Zone 3) near KFI08 were also available. The approximate distances from BFI02 to the top and bottom of these boreholes are listed in Table 5.8.

Graphs showing the variation of the groundwater head in the peripheral boreholes during the entire interference test period are shown in Appendix 7. The drawdown and recovery periods of the different interference tests are marked on the graphs. The

graphs show that all peripheral boreholes clearly responded to the different drawdown and recovery periods, even the most distant boreholes KFI01, KFI08 and HG 2. The exact drawdown and recovery in these boreholes is however difficult to quantify due to the natural variations of the groundwater level in the boreholes during the actual periods and the sparse recording density.

The first part of the interference test period generally coincides with a freezing period with a general slight natural decrease of the groundwater levels. The natural decrease was estimated to amount only to a few centimetres during the different test periods. A larger natural decrease of the groundwater levels would have totally obscured the recovery periods in the most distant boreholes. During tests 3A and 3B the natural groundwater levels are assumed to be relatively stable.

Table 5.8 Approximate distances from BFI02 to the top and bottom of the peripheral boreholes.

Borehole	Distance from BFI02 (m)	
	top	bottom
KFI01	1540	1540
KFI02	1380	940
KFI04	940	920
KFI07	800	810
KFI08	1310	1420
HG02	1260	1260

Significant responses to the drawdown and recovery periods occured in the boreholes KFI04 and KFI07. For example, by the

end of interference test 3B the drawdown in these boreholes amounted to c. 0.7 m and c. 1.6 m, respectively.

No quantitative interpretation of the responses in the peripheral boreholes has been performed. Since these boreholes are open, the measured groundwater head represents an integrated head value over the entire borehole lengths. Thus, the measured head changes in these boreholes are not directly comparable with those obtained in isolated sections in the boreholes within Zone 2. Also, the small drawdowns registered relative to the natural variations of the groundwater level) in the mostperipheral boreholes make it difficult to prepare representative drawdown and recovery curves for quantitative analysis.

Nevertheless, the significant responses of the peripheral boreholes during the interference tests, particularly boreholes KFI04 and KFI07, indicate a certain hydraulic communication between Zone 2 and areas outside the zone, possibly via other fracture zones, see Chapter 2.

6. QUANTITATIVE INTERPRETATION OF THE TESTS

6.1 Theoretical considerations

The quantitative analysis of the aquifer system of Zone 2 is rather complicated due to its complexity and bounded character. The qualitative interpretation of the first two tests indicates that the lower and upper part of Zone 2, respectively, can be regarded as pumped aquifers in the analysis of these tests. However, significant drawdowns also occurred within the entire Zone 2, indicating good hydraulic communication in the vertical direction of the zone. Since a certain difference in drawdown generally occurred between sections in the same borehole, flow restrictions must though exist between the upper and lower parts of the zone.

The analysis should thus be based on a theory which takes vertical anisotropy of hydraulic conductivity into account. One possible approach is to treat Zone 2 as composed of two aquifers, i.e. the upper and lower parts, separated by a (equivalent) semi-permeable layer between the aquifers (leaky aquifer system). In this case, the lower part of Zone 2 is regarded as the pumped aquifer and the upper part as the unpumped aquifer during interference test 1. In test 2 the reversed situation then prevails. Alternatively, Zone 2 may also be regarded as one aquifer system with vertical anisotropy (layered aquifer). In this case both test 1 and test 2 may be analysed according to theory for a partially penetrating borehole in an anisotropic aquifer. The first approach is used in this study. In the following sections both time-drawdown and distance-drawdown analysis methods will be described. Data from the recovery phases may also be used in the same manner.

6.1.1 Time-drawdown analysis

Theories for flow in leaky aquifer systems are presented in the literature by e.g. Neuman and Witherspoon (1969a,b) and Hantush (1967). The first theory takes into account the storage capacity of the assumed semi-permeable layer while this storage is neglected in the latter theory. Since the flow transfer between the subzones of Zone 2 is assumed to be controlled by discrete fractures with low storage capacity rather than flow through a porous medium, see Chapter 2, the theory by Hantush (1967) should to be justified in this case. A diagrammatic representation of such a leaky aquifer system is shown in Figure 6.1.

A special case of this theory presumes (approximately) equal hydraulic diffusivities (T/S) in both the pumped and unpumped aquifer. The theory is further simplified by assuming that the transmissivities (and consequently also the storage coefficients) in the two aquifers are (approximately) equal. By considering the uppermost and lowermost parts of Zone 2 as the two main subaquifers, the latter assumptions also seem to be justified as discussed in Chapter 3. The hydraulic single-hole tests in boreholes BFI01 and BFI02 indicated similar hydraulic properties of these two parts of Zone 2.

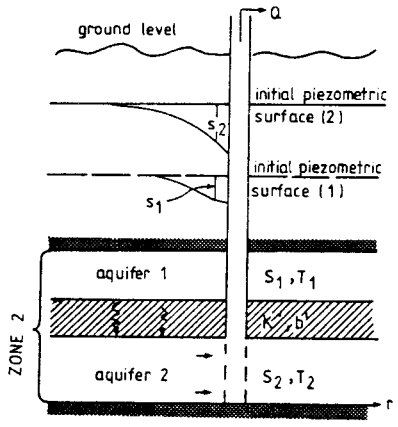

Figure 6.1 Diagrammatic representation of a leaky aquifer system (after Hantush, 1967).

From the special case of the theory by Hantush (1967) the transmissivity and storage coefficient of the pumped (and unpumped) aquifer may be calculated. The theory also permits estimation of the vertical hydraulic conductivity of the assumed semi-permeable layer between the aquifers.

The leakage coefficient is defined as the equivalent hydraulic conductivity (in the vertical direction) of the semi-permeable layer divided by the thickness of this layer. In this case, when the semi-permeable layer is assumed to be intersected by discrete fractures, the leakage coefficient expresses the leakage (flow rate) per unit area and unit hydraulic gradient in an eqivalent porous medium (according to Darcy´s law). Depending on the number, location and aperture of the fractures the actual (vertical) hydraulic conductivity of the semi-permeable layer may locally significantly exceed the calculated (average) hydraulic conductivity of this layer to achieve the same leakage rate through the layer.

Using the special theory by Hantush (1967) the theoretical drawdown in the pumped and unpumped aquifers can be calculated. Thus, type curves in logarithmic diagrams for the theoretical drawdowns in the pumped and unpumped (infinite) aquifer can be constructed for a particular value of the leakage factor of the semi-permeable layer, see Figure 6.2. Using the nomenclature in Figure 6.1 the drawdown in the pumped and unpumped aquifers (assuming identical hydraulic properties of the two aquifers) can be expressed as:

$$s_1 = \frac{Q}{8 \pi T_2} \left[W(u) - W(u, \beta) \right] \qquad (6.1)$$

$$s_2 = \frac{Q}{8 \pi T_2} \left[W(u) + W(u, \beta) \right] \qquad (6.2)$$

s_1 = drawdown in the unpumped aquifer (m)
s_2 = drawdown in the pumped aquifer (m)
Q = flow rate (m^3/s)
$T_2 = T_1$ = transmissivity of pumped (and unpumped) aquifer (m^2/s)
$W(u)$ = well function for nonleaky aquifer (-)
$W(u, \beta)$ = well function for leaky aquifer (-)

$$u = r^2 S_2 / 4 T_2 t \qquad (6.3)$$

$$\beta = (r/B) \sqrt{2} = \text{leakage factor} \qquad (6.4)$$

r = radial distance (m)
$S_2 = S_1$ = storage coefficient of pumped (and unpumped) aquifer (-)
$T_2/S_2 = T_1/S_1$ = hydraulic diffusivity of pumped (and unpumped) aquifer (m^2/s)
t = time (s)

$$B = \sqrt{T_2 / (K'/b')} \quad (m/s) \qquad (6.5)$$

K'/b' = leakage coefficient (s^{-1})
K' = vertical hydraulic conductivity of semi-permeable layer (m/s)
b' = thickness of semi-permeable layer (m)

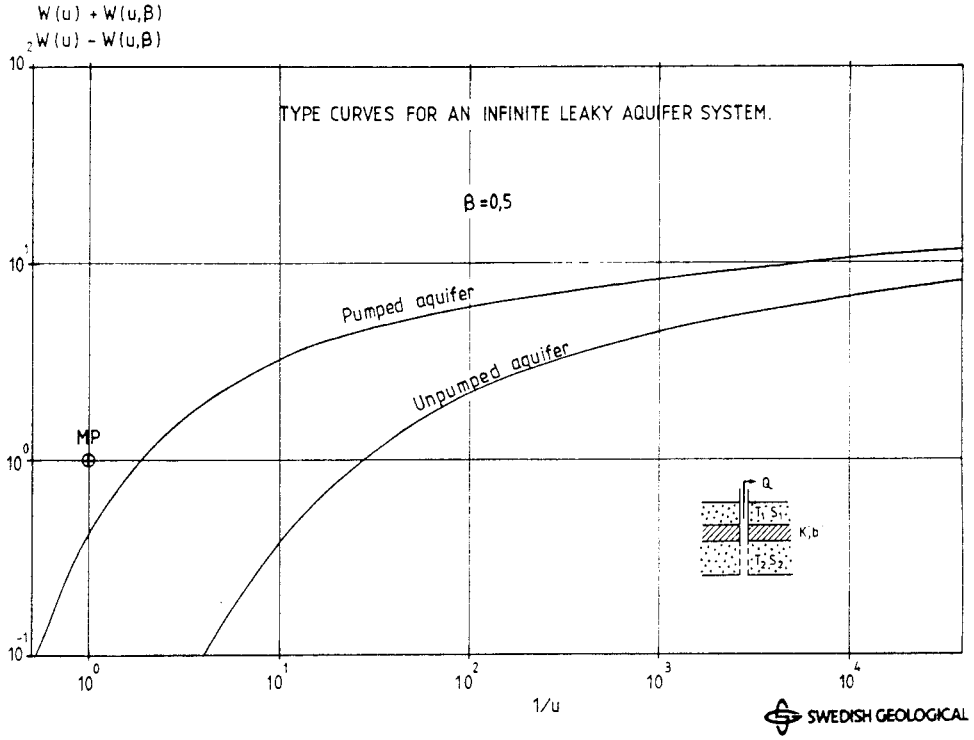

Figure 6.2 Example of type curves for infinite, leaky aquifer system.

As an example, Figure 6.2 shows the theoretical drawdown in a pumped and unpumped infinite aquifer, respectively, according to Eqns (6.1) and (6.2) for $\beta = 0.5$. Similar type curves can be constructed for other values of the β-parameter, which characterizes the leakage between the pumped and unpumped aquifer. By matching the data curves with such type curves the transmissivity of the pumped (and unpumped) aquifer may be calculated from Eqn (6.1) as follows if the matchpoint on the type curve diagram is chosen at (1,1):

$$T_2 = T_1 = \frac{Q}{8 \pi s_m} \qquad (6.6)$$

where s_m is the drawdown at the matchpoint on the data curve diagram. The storage coefficient of the pumped (and unpumped) aquifer may be calculated from Eqn (6.3) accordingly:

$$S_2 = S_1 = \frac{240\ T_2\ t_m}{r^2} \qquad (6.7)$$

where t_m is the time on the data curve at the match-point. Alternatively, the hydraulic diffusivity of the aquifers may be calculated as

$$T_2 / S_2 = T_1 / S_1 = r^2 / 240\ t_m \qquad (6.8)$$

The leakage coefficient may be determined by combining Eqns (6.4) and (6.5):

$$K' / b' = \frac{T_2 \beta_m^2}{2r^2} \qquad (6.9)$$

where β^2_m corresponds to the β-value used for the type curve matching.

The main problem with the time-drawdown analysis is the system of hydrogeologic boundaries surrounding Zone 2 in combination with high hydraulic diffusivity of the zone. As discussed in Chapter 2, Zone 2 may (hydrogeologically) be represented by a triangular-shaped area delimited by other fracture zones. The exact positions of the boundaries are however difficult to delineate. Also the precise nature of the boundaries in a hydrogeologic sense is difficult to deduce. Since a significant drawdown also occurred in boreholes outside Zone 2 at long distances, see Section 5.2, it may be concluded that at least some of the boundaries of Zone 2 are semi-permeable but with significantly lower hydraulic conductivity compared to Zone 2. Possibly, these boundaries (e.g. fracture zones) may also act as water conduits from external sources recharging Zone 2, ultimately leading to an approximate steady-state drawdown, cf. test 2, after relatively long time.

Due to the above facts, a time-drawdown analysis with analytical methods (imaginary well theory) is complicated. In addition, to quantitatively analyze the response in a completely bounded aquifer system, an infinite array of imaginary wells would be required. The main problem is to obtain a unique evaluation of the hydraulic parameters since the effects of the boundaries become significant after short times. However, a distance-drawdown analysis may provide a first means to obtain estimates in the correct order on the hydraulic parameters.

6.1.2 Distance-drawdown analysis

As discussed in Section 5.1 a pseudosteady-state drawdown behaviour was reached very quickly in the boreholes within Zone 2. This implies that the shape of the cone of depression will not change with time within the pseudosteady-state area. This means that the straight lines in a semilogarithmic distance-drawdown graph at different times of pumping will (ideally) be parallel to each other within the pseudosteady-state area. Thus, the transmissivity of the aquifer should be rather well defined by a distance-drawdown analysis (provided the aquifer is homogeneous and isotropic). In a semi-logarithmic graph the transmissivity and storage coefficient of the aquifer may be estimated (Carlsson and Gustafsson 1984) as:

$$T = \frac{0.366\ Q}{\Delta s} \qquad (6.10)$$

where Δs = slope of the straight line (m)

$$S = \frac{135\ T\ t}{r_e^{\,2}} \qquad (6.11)$$

r_e = extrapolated radius (m)

The storage coefficient should be calculated before any outer boundary effects have become appreciable, i.e. at short times.

6.2 Interpretation

The interpretation of the interference tests is based on both distance-drawdown and time-drawdown analyses. The former method was mainly used for the analysis of the primary drawdown response in the boreholes, i.e. analysis of responses in the lateral direction. The latter method was used to analyse the multi-section responses in each borehole, i.e analysis of responses in the vertical direction. In the following sections each interference test is described separately.

6.2.1 Interference test 1

Distance-drawdown analysis

A semi-logarithmic distance-drawdown graph for the primary response (PR) sections in the observation boreholes at three different times during interference test 1 is shown in Figure 6.3. The actual drawdowns and times in the observation boreholes and the pumping borehole are listed in Table 6.1. The drawdowns of the primary responses by the end of the tests are listed in tables in Chapter 5. Time-drawdown graphs of the primary responses in the observation boreholes are also shown in figures in Chapter 5. In Tables 6.1-4 the most representative primary response (PR) section in each borehole is listed (in boreholes where primary responses occur in more than one section).

Table 6.1 Drawdown of the primary responses at different pumping times during interference test 1.

Bore-hole	PR-section no	Distance (m)	Drawdown (m) t=10min	t=300min	t=1000min
KFI05	2	209	0.43	(2.52)	(4.30)
KFI06	3	193	0.55	(2.02)	3.93
KFI09	3	305	0.20	2.16	3.91
KFI10	3	310	0.23	2.26	4.05
KFI11	3	156	1.15	3.29	5.03
BFI01	4	167	0.20	1.76	3.20
HFI01	1	353	0.16	2.16	4.00
BFI02	2	-	(3.90)	6.00	7.70

N.B Values within brackets are uncertain.

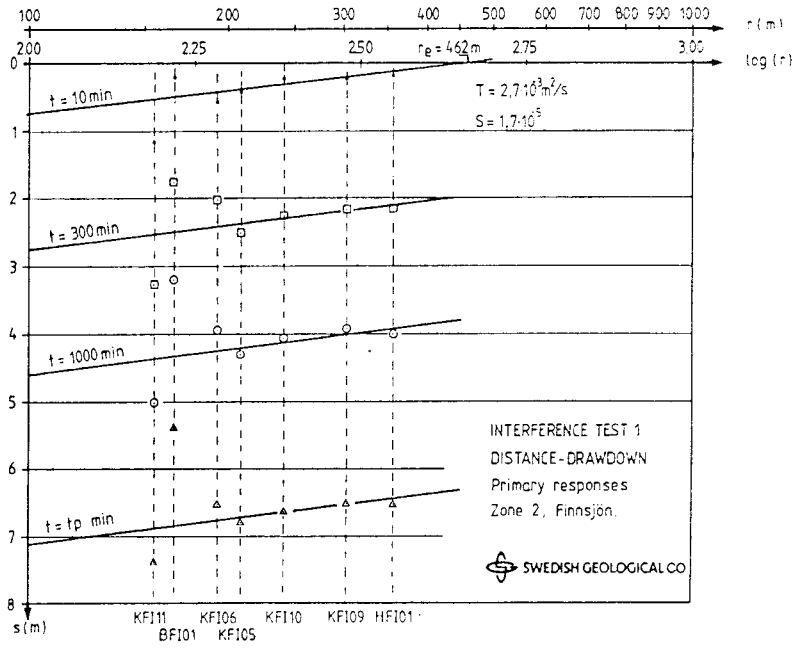

Figure 6.3 Drawdown of the primary responses versus distance to BFI02 during interference test 1.

As can be seen from Figure 6.3 and Table 6.1 the straight lines in the distance-drawdown graph are approximately parallel to each other at different pumping times. The drawdowns measured in the more distant observation sections fairly well conform to the straight line, whereas the drawdowns measured in the closest sections to BFI02 show large deviations from the straight line. This is a common feature for all interference tests performed, particularly test 1 and 2, which is assumed to depend on local heterogenities between these boreholes and BFI02, see below. The distance-drawdown analysis shown in Figure 6.3 is based on the most distant observation sections. The transmissivity is calculated according to Eqn (6.10). An estimation of the storage coefficient by Eqn (6.11) is made from the first straight line before the boundary effects have become significant.

The distance-drawdown analysis is considered as approximative only, due to the uncertainties in the determination of (representative) distances to BFI02 to be used in the analysis and the relatively few data points utilized. Besides the analytical interpretation, numerical simulations were performed to check the ability to reproduce the measured responses within Zone 2 for different T-and S-values, see Chapter 8. The numerical simulations confirmed that the hydraulic parameters determined from the distance-drawdown analysis were in the correct order.

Time-drawdown analysis

An approximative time-drawdown analysis, as described in Section 6.1.1, was also performed by matching the first few points of the data curves shown in Appendix 2 with type curves such as the ones shown in Figure 6.2. The analysis was made before the effects of the outer boundaries of Zone 2 have become appreciable. The transmissivity and storage coefficient are calculated from Eqns (6.6-7). By the time-drawdown analysis

of test 1 the lower part of Zone 2 is considered as the pumped aquifer and the upper part as the unpumped aquifer. An example of time-drawdown analysis by type curve matching is presented in Figure 6.4. This figure shows that the outer boundary effects become significant after about 10 minutes of pumping.

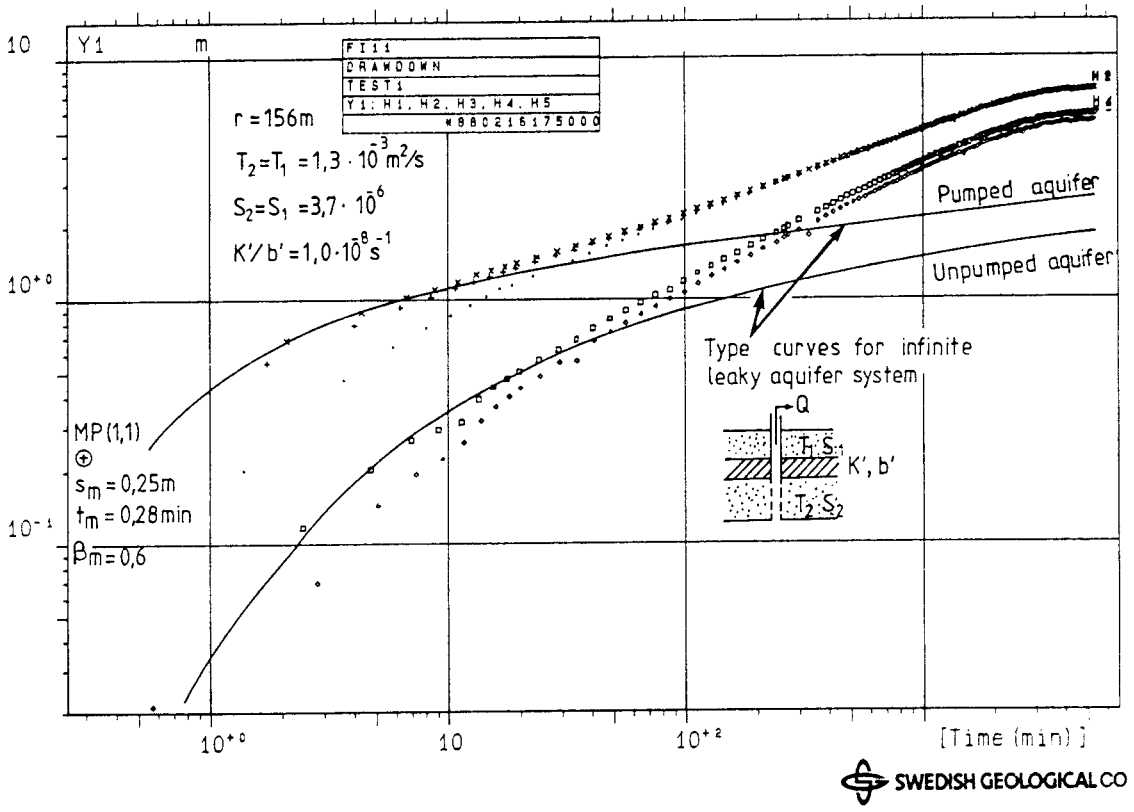

Figure 6.4 Example of time-drawdown analysis from borehole KFI11 by type curve matching.

The leakage coefficient, which represents the leakage from the upper part of Zone 2 to the lower part during pumping, is calculated from Eqn (6.9). The β-value is obtained by type curve matching from the separation of the measured drawdown curves for the pumped and unpumped aquifer. From the boreholes KFI09 and HFI01 no value on the leakage coefficient can be obtained since the response curves for the pumped and unpumped aquifer (within Zone 2) coincide in these boreholes. Although not strictly consistent with the theory used (equal transmissivities of the pumped and unpumped aquifers are assumed), a rough estimation of the leakage to Zone 2 from the overlying rock in the distant boreholes KFI09, KFI10 and HFI01 was also made using the present theory. The (in general) delayed and attenuated responses occurring above and below Zone 2 indicate that the zone is in most boreholes rather effectively isolated from the over- and underlying rock during pumping.

Since the recovery curves almost coincide with the drawdown curves, as discussed in Chapter 5, the former curves are mainly used in a complementary manner in the time-drawdown analyses.

The results of the time-drawdown analysis of interference test 1 are presented in Table 6.2. The observation sections in different parts of Zone 2 representing the pumped and unpumped aquifer, respectively, are also included in the table. The estimated values on the leakage coefficient are listed besides the unpumped aquifer. These values are mainly based on the separation between the drawdown curves for the pumped and unpumped aquifer by the end of the test. No values on the leakage coefficient can be calculated from the responses in the primary sections only.

The calculated values on the hydraulic parameters are considered as approximative since very few data points were used in the quantitative analyses due to the boundary effects.

Nevertheless, model simulations show that the calculated values on the hydraulic parameters accurately can reproduce the measured data curves, see Chapter 8. A discussion of the representativity of the calculated values on the hydraulic parameters in the different tests is given in Section 6.4.

No rigorous quantitative interpretation from the sections in the pumping borehole BFI02 was made due to the delay in pressure responses in this borehole in the beginning of the tests, see Section 4.3.4. However, from a semi-quantitative analysis of the early drawdown data from BFI02 during test 1 the skin factor was estimated at c. -2.5 which corresponds to an effective borehole radius of BFI02 of c. 1.0 m. This radius is consistent with the estimated (primary) drawdown in BFI02 according to the distance-drawdown graph.

Table 6.2 Estimated hydraulic parameters of Zone 2 and parts thereof from the time-drawdown analysis of interference test 1.

Borehole	T (m^2/s)	S	K´/b´ (s^{-1})	Observation sections no	Part of Zone 2
KFI05	1.6E-3	1.0E-5	-	2	lower
			4.1E-8	4	upper
KFI06	1.6E-3	7.1E-6	-	3	lower
			4.8E-8	4	upper
KFI09	2.4E-3	2.0E-5	-	3,4,2,1	whole
			1.3E-8	5	above
KFI10	2.0E-3	2.2E-5	-	1,3	whole
			7.1E-8	4	above (Zone 1)
KFI11	1.3E-3	3.7E-6	-	3	lower
			1.7E-8	4	upper
BFI01	2.4E-3	5.7E-5	-	4	upper
			4.2E-8	1,2	lower
HFI01	3.9E-3	2.3E-5	-	1,2	(upper)
			1.4E-9	3	above

6.2.2 Interference test 2

A semi-logarithmic distance-drawdown graph for the primary responses at three different pumping times during interference test 2 is shown in Figure 6.5. The actual drawdown of the primary response (PR) sections at the corresponding times are listed in Table 6.3.

Table 6.3 Drawdown of the primary responses at different pumping times during interference test 2.

Bore-hole	PR-section no	Distance (m)	Drawdown t=10min	t=300min	t=1000min
KFI0	not used during interference test 2				
KFI06	4	189	1.05	2.71	4.37
KFI09	4	288	0.29	2.13	3.81
KFI10	1	234	0.33	2.22	3.87
KFI11	4	155	1.98	3.60	5.10
BFI01	4	168	0.79	2.23	3.63
HFI01	1	338	0.23	2.10	3.77
BFI02	5	-	(5.25)	6.80	8.50

NB. Values within brackets are uncertain.

For interference test 2, the upper part of Zone 2 is regarded as the pumped aquifer and the lower part as the unpumped aquifer in analogy with test 1. Leakage occurred from the lower part to the upper part of the zone. The distance-drawdown analysis of the primary responses is based on the most distant observation sections from BFI02. Again, the drawdowns of the primary responses in the nearest boreholes BFI01 and KFI11 deviate from the interpreted straight lines indicating local heterogeneities. As for test 1 the straight lines are almost parallel at the different pumping times. The results of the distance-drawdown analysis from interference test 2 are shown in Fig 6.5.

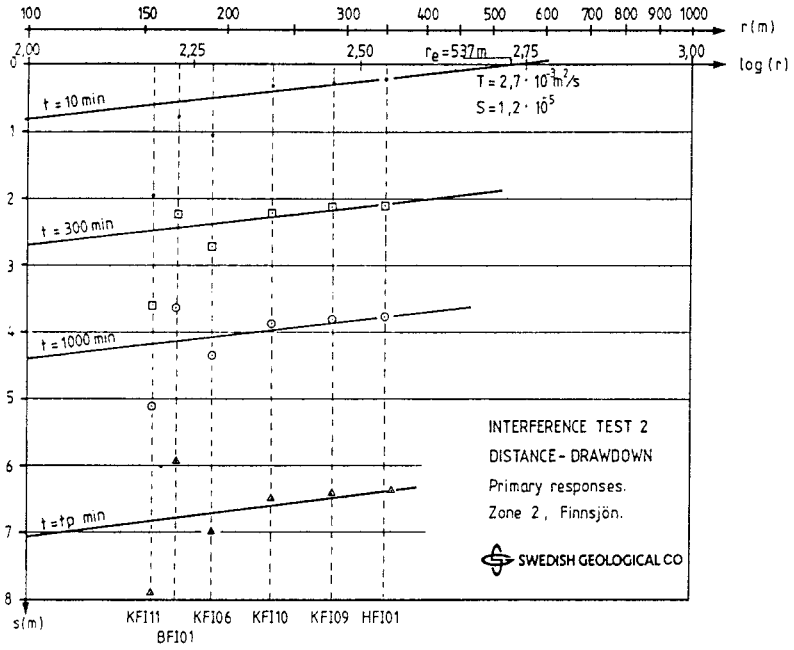

Figure 6.5 Drawdown of the primary responses versus distance to BFI02 for interference test 2.

An approximative time-drawdown analysis of the first part of the data curves shown in Appendix 3 was also performed in analogy with test 1. The time-recovery curves were used as complementary information. The results of the time-drawdown analysis of interference test 2 are presented in Table 6.4. As for test 1 the values on the calculated hydraulic parameters are considered as approximative. A comparison of Tables 6.2 and 6.4 shows that the calculated values on the hydraulic parameters for the lower and upper parts of Zone 2, respectively, are very similar. This is consistent with the assumptions in the theory used. A discussion of the results of test 2 is given in Section 6.4.

Table 6.4 Estimated hydraulic parameters of Zone 2 and parts thereof from the time-drawdown analysis of interference test 2.

Borehole	T (m^2/s)	S	K´/b´ (s^{-1})	Observation section(s) no	Part of Zone 2
KFI05	(not used during interference test 2)				
KFI06	1.4E-3	2.4E-6	-	4	upper
			4.5E-8	2,3	lower
KFI09	2.5E-3	9.9E-6	-	4,3,2	whole
			1.5E-8	5	above
KFI10	2.5E-3	1.0E-5	-	1,3	whole
			9.3E-8	4	above (Zone 1)
KFI11	1.4E-3	5.7E-7	-	4	upper
			2.9E-8	3,2	lower
BFI01	1.4E-3	9.4E-6	-	4	upper
			1.6E-8	1,2	lower
HFI01	2.4E-3	1.5E-5	-	1,2	(upper)
			1.3E-9	3	above

6.2.3 Interference test 3

Distance-drawdown graphs of the primary responses at different pumping times during interference tests 3A and 3B are shown in Figures 6.6 and 6.7, respectively. The drawdown of the primary response (PR) sections are listed in Tables 6.5 and 6.6.

Table 6.5 Drawdown of the primary responses at different pumping times during interference test 3 A.

Bore-hole	PR-section no	Distance (m)	Drawdown (m) t=10min	t=300min	t=1000min
KFI05	2	206	0.37	2.35	4.37
KFI06	4	189	0.72	2.51	4.51
KFI09	4	288	0.25	2.19	4.13
KFI10	3	234	0.28	2.32	4.31
KFI11	4	155	1.01	2.77	4.72
BFI01	4	168	0.51	1.97	3.77
HFI01	1	338	0.20	2.19	4.16
BFI02	7	-	(0.30)	3.30	(5.60)

Table 6.6 Drawdown of the primary responses at different pumping times during interference test 3 B.

Bore-hole	PR-section no	Distance (m)	Drawdown (m) t=10min	t=300min	t=1000min
KFI05	2	206	0.57	(3.47)	5.57
KFI06	4	189	1.10	3.66	5.69
KFI09	4	288	0.36	3.14	5.28
KFI10	3	234	0.40	3.32	5.43
KFI11	4	155	1.65	4.16	6.05
BFI01	4	168	0.74	2.83	4.54
HFI01	1	338	0.28	3.16	5.30
BFI02	7	-	(0.70)	5.75	7.85

NB. Values within brackets are uncertain.

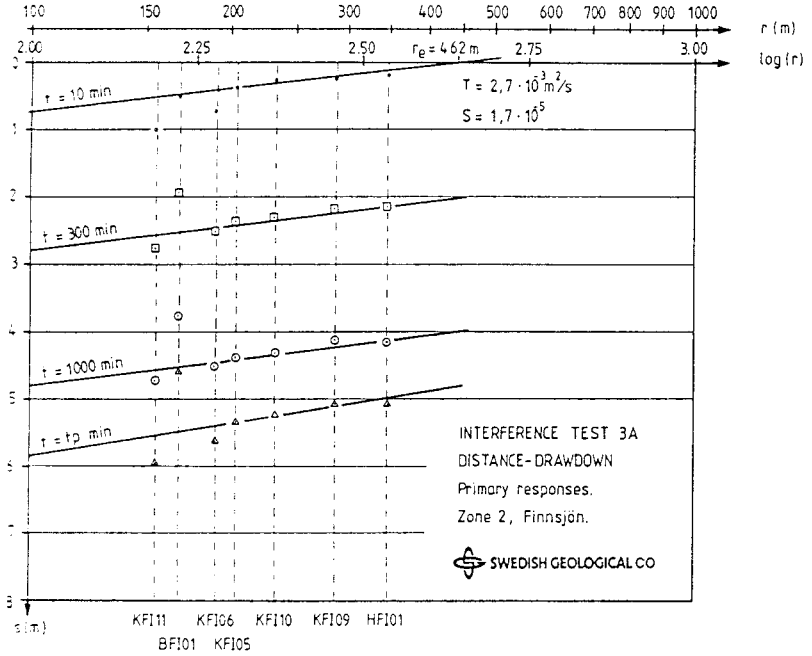

Figure 6.6 Drawdown of the primary responses versus distance from BFI02 for interference test 3A.

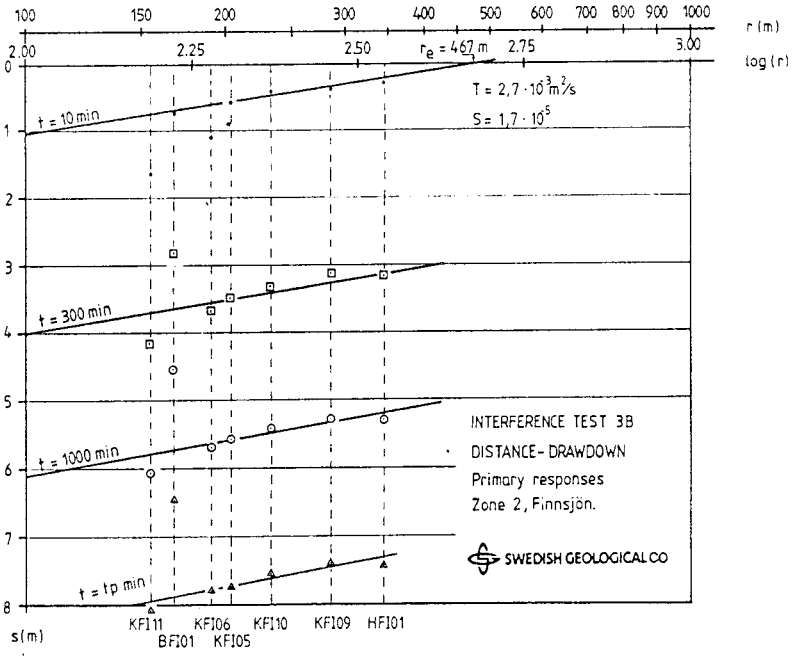

Figure 6.7 Drawdown of the primary responses versus distance from BFI02 for interference test 3B.

It should be recalled that the flow rate for test 3 A was constant at about 500 l/min during the first c. 800 minutes but increased to c. 700 l/min after that time. This means that only the drawdowns at t = 10 min and t = 300 min during test 3 A could be directly compared with corresponding drawdowns during tests 1 and 2. Comparing Table 6.5 with Tables 6.1 and 6.3 at t = 10 min and t = 300 min reveals that the drawdowns in the boreholes situated closest to the pumping borehole generally was less for test 3 A compared to tests 1 and 2. This is probably a reflection of the different discharge conditions in BFI02 during these tests.

The results of the distance-drawdown analyses of tests 3A and 3B are shown in Figures 6.6 and 6.7, respectively. As before, the drawdown of the primary responses in the closest borehole sections deviate from the interpreted straight lines but not as pronounced as during tests 1 and 2.

An approximative time-drawdown analysis was also carried out for tests 3A and 3B. Since the drawdown behaviour during tests 3A and 3B was similar to that of test 2 the same analysis technique was used. However, this is not quite consistent with the theory used since the entire Zone 2 was pumped in tests 3A and 3B, implying different flow conditions during the tests, see Section 6.4. Accordingly, the calculated values should be regarded as approximative only. Moreover, the values calculated on the leakage coefficient are regarded as apparant due to the deviations of the actual flow pattern from that assumed by the theory. The results of the time-drawdown analysis of interference tests 3A and 3B are presented in Tables 6.7 and 6.8, respectively.

Table 6.7 Estimated hydraulic parameters of Zone 2 and parts thereof from the approximative time-drawdown analysis of interference test 3A.

Borehole	T (m^2/s)	S	K´/b´ (s^{-1})	Observation section, no	Part of Zone 2
KFI05	2.2E-3	9.7E-6	-	2	lower
			1.0E-7	3,4	upper
KFI06	2.2E-3	2.3E-6	-	4	upper
			7.0E-8	2	lower
KFI09	3.3E-3	1.0E-5	-	4,3,2	whole
			7.2E-9	5	above
KFI10	2.2E-3	1.5E-5	-	1,3	whole
			8.0E-8	4	above (Zone 1)
KFI11	2.2E-3	5.6E-7	-	4	upper
			4.6E-8	2	lower
BFI01	2.2E-3	1.5E-5	-	4	upper
			1.9E-8	1,2	lower
HFI01	2.8E-3	1.7E-5	-	1,2	(upper)
			1.4E-9	3	above

Table 6.8 Estimated hydraulic parameters of Zone 2 and parts thereof from the approximative time-drawdown analysis of interference test 3B.

Borehole	T (m^2/s)	S	K'/b' (s^{-1})	Observation section, no	Part of Zone 2
KFI05	1.7E-3	1.3E-5	-	2	lower
			6.9E-8	3,4	upper
KFI06	1.4E-3	3.8E-6	-	4	upper
			4.1E-8	2	lower
KFI09	3.5E-3	1.7E-5	-	4,3,2	whole
			1.0E-8	5	above
KFI10	2.4E-3	1.8E-5	-	1,3	whole
			8.7E-8	4	above (Zone 1)
KFI11	1.3E-3	2.6E-6	-	4	upper
			1.1E-7	2	lower
BFI01	2.0E-3	2.0E-5	-	4	upper
			1.3E-8	1,2	lower
HFI01	3.5E-3	1.9E-5	-	1,2	(upper)
			1.4E-9	3	above

6.3 Evidence of anisotropic conditions within Zone 2

To investigate possible anisotropic conditions in the lateral and vertical directions of Zone 2, the response times, t_e, for the primary observation borehole sections were calculated. The response time is here defined as the time after start of pumping when a drawdown of 0.02 m was measured in the actual observation section. Since most of the primary drawdown responses occurred very rapidly, the frequency of drawdown measurements was insufficient at very short times in some of the boreholes. In these cases the measured drawdown curves have

been extrapolated backward at short times by using appropriate type curves, see Section 6.1.1.

Knowing the response time and the distance, r, to the pumping borehole section, the ratio t_e/r^2 may be calculated for the primary observation sections in the boreholes. This ratio is an indicator of the homogeneity of an aquifer assuming radial flow conditions. In a homogeneous and isotropic aquifer the ratio should be equal for all observation sections. The ratio is also inversely proportional to the hydraulic diffusivity, T/S, of the aquifer. For comparison, an apparent mean velocity (r/t_e) of the induced primary pressure wave towards the different observation sections, assuming one-dimensional flow, are calculated. The drawdown response times for the primary observation sections, the distances to BFI02, the ratio t_e/r^2, the hydraulic diffusivity and the estimated mean velocity, v, of the primary pressure wave are shown in Table 6.9 for the different interference tests. The values on the hydraulic diffusivity are calculated from the tables of results presented in the previous section.

The table show that the estimated mean velocities are highest (t_e/r^2 lowest) towards the boreholes KFI06 and, in particular, KFI11 during all tests. The calculated hydraulic diffusivity is very high towards these borehole, particularly for test 2. However, towards borehole BFI01 the mean velocity of the pressure wave is much slower (particularly for test 1) despite that this borehole is located rather close to BFI02. During tests 2 and 3 the estimated mean velocity towards BFI02 is only slightly higher than that towards the more distant boreholes, e.g. KFI09 and HFI01. The ratio t_e/r^2 is accordingly higher (lower T/S) towards BFI01. These differences in responses between the near-region observation boreholes are also observed during the tracer tests, see below.

Table 6.9 Drawdown response times for the primary observation sections, distances to BFI02, ratio t_e/r^2, hydraulic diffusivity and the mean velocity (v) of the pressure wave for different interference tests.

Borehole	t_e (s)	r (m)	$t_e/r^2 \times 10^4$ (s/m^2)	T/S (m^2/s)	v (m/s)
	Interference test 1				
KFI05	25	209	5.7	160	8.4
KFI06	16	193	4.3	225	12
KFI09	93	305	10	120	3.3
KFI10	87	243	15	91	2.8
KFI11	4	156	1.6	351	39
BFI01	93	167	33	42	1.8
HFI01	126	353	10	170	2.8
	Interference test 2				
KFI06	3.6	189	1.0	583	52
KFI09	40	288	4.8	253	7.2
KFI10	30	234	5.5	250	7.8
KFI11	0.4	155	0.2	2460	352
BFI01	18	168	6.4	149	9.3
HFI01	47	338	4.1	160	7.2
	Interference test 3A				
KFI05	24	206	5.7	227	8.6
KFI06	2.3	189	0.6	957	82
KFI09	44	288	5.3	330	6.5
KFI10	36	234	6.6	147	6.5
KFI11	1.4	155	0.6	3930	111
BFI01	16	168	5.7	147	10.5
HFI01	72	338	6.3	165	4.7

Table 6.9 also shows that the estimated mean velocity of the pressure propagation and the hydraulic diffusivity are significantly higher during test 2, i.e. in the uppermost part of Zone 2. Borehole KFI11 responded almost instantaneously during test 2. The estimated mean velocities and ratios of t_e/r^2 were similar during test 2 and 3. The individual ratios of t_e/r^2 were also rather equal between the tests although somewhat higher during test 1 (with the exception of the closest boreholes to BFI02). This indicates similar (averaged) hydraulic properties at longer distances from BFI02. However, in the region close to BFI02 anisotropic conditions occur along Zone 2.

The multiple-section borehole responses are discussed in section 5.1, see Figs. 5.1 and 5.3 for test 1 and 2, respectively. These responses may provide a picture of the propagation of the pressure wave in the vertical direction of Zone 2. In Table 6.10 both the primary drawdown responses (as in Table 6.9) and the non-primary responses in the opposite (lower/upper) part of Zone 2 towards the near-region boreholes are characterised. The table shows that the estimated mean velocity of the pressure wave is significantly lower in the non-primary response (NPR) sections, particularly during test 2 compared to the primary response (PR) sections. The estimated mean velocities towards the NPR-sections are rather similar for test 1 and 2 for all boreholes whereas the velocities towards the PR-sections differ significantly between boreholes and tests. Also the calculated ratios t_e/r^2 are similar for the NPR-sections for test 1 and 2 but much higher (lower T/S) compared to the PR-sections. As discussed above, the separation between the PR- and NPR-curves decreased during tests 3A and 3B due to changed flow conditions when the entire zone was pumped.

Table 6.10 Drawdown response times for the primary (PR) and non-primary (NPR) borehole sections, distance to BFI02, ratio t_e/r^2 and estimated mean velocity of the pressure wave towards the near-region boreholes for different interference tests.

Bore-hole	Section no	Part of Zone 2	t_e (s)	r (m)	$t_e/r^2 \times 10^4$ (s/m^2)	v (m/s)	Remarks
	Interference test 1						
KFI06	3	lower	16	193	4.3	12	PR
	4	upper	43	197	11.1	4.6	NPR
KFI11	3	lower	4	156	1.6	39	PR
	4	upper	42	154	17.7	3.7	NPR
BFI01	4	upper	93	167	33	1.8	PR
	2	lower	318	194	84.5	0.6	NPR
	Interference test 2						
KFI06	4	upper	3.6	189	1.0	52	PR
	2	lower	52	200	13.0	3.8	NPR
KFI11	4	upper	0.4	155	0.2	352	PR
	2	lower	53	200	13.2	3.8	NPR
BFI01	4	upper	18	168	6.4	9.3	PR
	2	lower	192	221	39.3	1.2	NPR
	Interference test 3A						
KFI06	4	upper	2.3	189	0.6	82	PR
	2	lower	11	200	2.7	18	NPR
KFI11	4	upper	1.4	155	0.6	111	PR
	2	lower	4.8	200	1.2	42	NPR
BFI01	4	upper	16	168	5.7	10.5	PR
	2	lower	177	221	36.2	1.2	NPR

As discussed in Section 5.1 the primary drawdown responses generally propagated along the lower and upper parts of Zone 2 during test 1 and 2, respectively, except for borehole BFI01. In this borehole the primary drawdown response occurred in the upper part of Zone 2 both during test 1 and 2. This may possibly indicate the presence of a fault between boreholes BFI01 and BFI02.

6.4 Summary and discussion of results

Based on the overall interpretation of the interference tests, a schematic picture of possible flow patterns during the different tests is shown in Figure 6.8. This figure indicates that different flow patterns should prevail for observation boreholes located relatively close to BFI02 and at larger distances from BFI02. From this tentative interpretation it follows that the primary responses in the closest boreholes should be more representative for the hydraulic properties of the lower and upper parts of Zone 2 during test 1 and 2, respectively. For tests 3A and 3B the primary responses in these boreholes were slightly more averaged since the entire Zone 2 was pumped.

In observation boreholes located at longer distances from BFI02, the drawdown responses were similar during all tests. Also the magnitude of drawdowns in these boreholes were similar for all tests (except test 3B in which a higher flow rate was used). This indicates that all tests are governed by approximately the same (long-term) values on the hydraulic parameters.

The above interpretation regarding flow patterns suggests that the leaky-aquifer (time-drawdown) analysis described in Section 6.1.1 should be more applicable to the responses in the closest

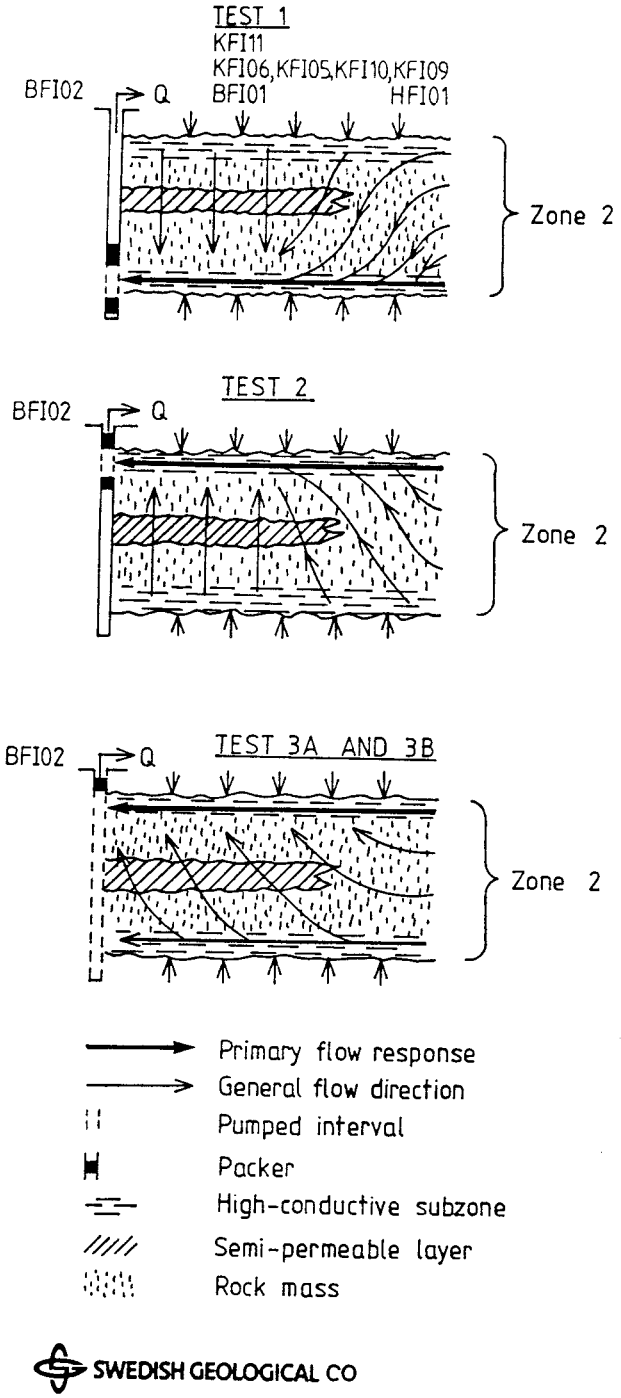

Figure 6.8 Schematic picture of possible flow patterns during the different interference tests.

observation boreholes during test 1 and 2. The calculated hydraulic parameters in these boreholes should thus represent the properties of the lower and upper parts of Zone 2, respectively. On the other hand, the calculated hydraulic parameters from the most distant observation boreholes should, accordingly, be more representative of the average properties of the entire Zone 2.

During tests 3A and 3B the anisotropic properties of Zone 2 in the vertical direction were less accentuated due to the different discharge conditions. The changes of electric conductivity of the discharged water during the tests indicate that approximately the same proportions were discharged from the upper and lower parts of the zone by the end of the tests. Thus, both the upper and lower part of the zone were pumped during tests 3A and 3B. The graphs in Appendix 4 and 5 show that the separation between the curves within Zone 2 for broeholes in the near-region was less during these tests, compared to tests 1 and 2. It is also assumed that cross-flow between the upper and lower part of the zone took place during the tests.

6.4.1 Time-drawdown analysis

The values on the hydraulic parameters calculated from the time-drawdown analyses are rather similar for all tests. From test 1 and 2 the hydraulic properties of the lower and upper part of Zone 2, respectively, may be estimated from the short time (primary) responses in the closest observation boreholes (KFI06, KFI11 and BFI01). The transmissivities, which are similar for these parts of Zone 2, are estimated at about 1.5E-3 m^2/s.

The corresponding values on the storage coefficient from the closest boreholes are, however, somewhat different between the

tests. From test 1 the estimated storage coefficient of the lower part of Zone 2 normally ranges betewen 4-7E-6. From BFI01 an apparently high value on the storage coefficient was calculated. This is likely to be an effect of the assumed inhomogeneities between BFI01 and BFI02, see below. From test 2, lower values on the storage coefficient was calculated for the upper part of Zone 2, ranging between 6E-7 - 2E-6 in the closest boreholes. Again, a significantly higher storage value was obtained from BFI01.

The time-drawdown analyses of the most distant observation boreholes (which are assumed to give more representative values on the hydraulic parameters of the entire Zone 2) yield similar transmissivity values from all tests, ranging between 2.5 - 3.5E-3 m^2/s. Also the estimated values on the storage coefficient from the distant observation boreholes are similar for all tests, ranging between 1-2E-5.

Values on the leakage coefficient between the upper and lower parts of Zone 2 were calculated from the separation of the drawdown curves, both at short and long pumping times. The values presented in the tables are mainly determined from the separation of the curves by the end of the tests. It was found that the calculated leakage coefficients increased with the pumping time, particularly during test 2 but also for test 1 and tests 3A and B. This is consistent with the assumed flow patterns shown in Figure 6.8 and the changes of the electric conductivity of the discharged water during the tests. The latter measurements indicate an increasing leakage rate, particularly during test 2, see Appendix 3:1-2.

The calculated values on the leakage coefficients within Zone 2 are rather similar for test 1 and test 2. They range between 2-5E-8 s^{-1}. The corresponding values for test 3A and 3B are generally somewhat higher (particularly for KFI11). These values are considered as apparent only due to the different

flow conditions in Zone 2 during these tests. The values on the leakage coefficient estimated between Zone 2 and the overlying rock from the distant observation boreholes generally range between 1E-9 s^{-1} in HFI01 to 1E-8 s^{-1} in KFI09. However, in KFI10 the hydraulic communication with the overlying rock (including Zone 1) is improved and the values estimated on the leakage coefficient range between 7-9E-8 s^{-1}.

Although the estimated values on the leakage coefficient are similar between test 1 and 2 the changes of the electric conductivity (salinity) of the discharged water during these tests indicate that the leakage rate would be higher during test 2 compared to test 1, see Section 5.1. This may be explained by the fact that the hydraulic communication between Zone 2 and the underlying rock is better than that of the overlying rock. This would possibly explain the relatively slow decrease of salinity during test 1 (performed in the lower part of Zone 2) and the relatively strong increase of salinity during test 2 (performed in the upper part of Zone 2). This explanation is also supported by the drawdown response patterns during test 1 and test 2. The drawdown responses are generally slower in the overlying rock than in the underlying rock, see Tables 5.2 and 5.4.

The representativity of the calculated leakage coefficients can be checked by a simple estimation of the leakage rate by the end of test 2. The leakage rate may be calculated from the following equation (Carlsson and Gustafsson 1984):

$$Q_L = K' / b' \cdot \Delta h_m \cdot A_L \qquad (6.12)$$

where Q_L = leakage rate (m^3/s)
K'/b' = leakage coefficient (s^{-1})
Δh_m = average head difference between aquifers (m)
A_L = leakage area (m^2)

The leakage area may for this purpose, according to the drawdown responses, be approximated by a circular area with a radius of about 300 m concentric to BFI02. At larger distances no significant head difference between the upper and lower part of Zone 2 exists. If the leakage coefficient is assumed to 2 E-8 s^{-1} the estimated leakage rate would be about 2.8 l/s (168 l/min) by the end of test 2 (see Section 5.1.2). This corresponds to an average head difference of about 0.5 m between the upper and lower partsof the zone. This value seems reasonable according to the measured differences in drawdown (and recovery) between the upper and lower part of Zone 2 by the end of test 2, see Appendix 3.

Assuming a thickness of the semi-permeable layer of about 50 m the value on the leakage coefficient used in the above calculations corresponds to an average (bulk) vertical hydraulic conductivity of 1E-6 m/s of the (equivalent) porous semi-permeable layer. As discussed above this value may locally be significantly exceeded due to the actual fracture pattern within Zone 2, see Chapter 2. Using a transmissivity of 3E-3 m^2/s of Zone 2 and a total thickness of 100 m, the average hydraulic conductivity of Zone 2 in the lateral direction is about 3E-5 m/s. This corresponds to an (average) anisotropy ratio of about 30 between the lateral and vertical hydraulic conductivity of Zone 2. However, as described above, this ratio may locally be much higher.

Finally, treating Zone 2 as one stratified anisotropic aquifer system in the analyses of the interference tests, as discussed in Section 6.1.1, would most likely yield very similar values on the hydraulic properties in the lateral direction. The latter analysis method might possibly provide more representative values on the hydraulic conductivity in the vertical direction of Zone 2.

6.4.2 Distance-drawdown analysis

The distance-drawdown graphs of the primary responses confirm the above interpretation of possible flow patterns during the interference tests shown in Figure 6.8. The drawdowns of the primary responses in the closest boreholes generally deviate from the drawdowns in the more distant boreholes, particularly for tests 1 and 2. While the (primary) drawdowns in the former boreholes vary significantly between tests, the drawdowns in the latter boreholes are rather similar for all tests (except test 3B with higher flow rate). This again indicates that the drawdowns in the nearest boreholes represent the hydraulic properties of the most rapid (primary) pathways between BFI02 and these boreholes and that the drawdowns at longer distances from BFI02 should be more averaged and representative of the entire Zone 2. The similar drawdowns observed at long distances and pumping times during all tests (except test 3B) indicate that similar (long-term) values on the hydraulic parameters should prevail in all tests. According to the assumed flow patterns these representative values correspond to the hydraulic properties of the entire Zone 2.

The distance-drawdown analyses for different pumping times were performed with emphasis on the more distant observation boreholes. Thus, the hydraulic parameters calculated from these analyses should represent the properties of the entire Zone 2. It should be pointed out that the distance-drawdown analyses are considered as rather approximate due to the few data points utilized and the uncertainties in the determination of the (representative) distances to the borehole sections. However, in tests 3A and 3B the interpreted straight lines are more well-defined. The drawdowns observed at short pumping times are regarded to yield the most representative values on the storage coefficient of Zone 2. At later times boundary effects may influence the drawdown curves. Thus, the storage coefficient of

Zone 2 was calculated from the shortest time (t = 10 min) in the distance-drawdown graphs.

From the distance-drawdown analyses of the (primary) responses in test 1 the transmissivity of Zone 2 was estimated at T = 2.7E-3 m^2/s and the storage coefficient at S = 1.7E-5. For test 2 the same transmissivity of Zone 2 was calculated but a slightly lower storage coefficient, S = 1.2 E-5. The distance-drawdown analyses of tests 3A and 3B are considered as the most representative for the determination of the hydraulic properties of the entire Zone 2. The values calculated from the distance-drawdown analyses are in good agreement with those from the time-drawdown analyses.

From the calculated transmissivity values the hydraulic conductivity of the uppermost and lowermost subzones of Zone 2 may be estimated. Assuming a thickness of 0.5 m for these subzones, as was indicated from the detailed single hole tests in BFI02 (Ekman et al 1988), the (average) hydraulic conductivity of the subzones is about 3E-3 m/s. This value may locally be significantly higher since the (effective) thickness of the subzones locally may be less than 0.5 m.

The distance-drawdown graphs show that the drawdown pattern in the boreholes generally is persistent at different pumping times, i.e. the rate of drawdown of the primary responses is nearly the same in all borehole sections at all times. As discussed above, the (primary) drawdown in the nearest boreholes (KFI11, BFI01 and KFI06) generally deviates from the straight lines, particularly in KFI11 and BFI01, both at short and long pumping times. This is probably a reflection of local heterogeneities which in general will be more accentuated close to the pumped borehole (See section 6.3). At longer distances such effects will normally tend to average out.

The nature of such local heterogeneities may vary, e.g. transmissivity anisotropy, lithology variations due to faults or flow in restricted paths in the rock (channeling). The latter two causes may be reflected in the calculated storage coefficients and response times, cf. BFI01 and KFI11. In BFI01 a high (apparent) storage coefficient and a relatively slow response time was calculated. According to the geological interpretation (Chapter 2) a local fracture zone exists between BFI01 and BFI02. The zone, which also may be faulted, could possibly decrease the hydraulic communication across the zone (indirect response). On the other hand, the zone may also (partially) act as a recharge source, thus decreasing the measured drawdown in BFI01. Both causes would result in a high apparent storage coefficient calculated.

In KFI11 (and KFI06) a larger (primary) drawdown and a faster response time were observed than in the other boreholes. This is only partially explained by the shorter distance to BFI02. The higher drawdown would normally indicate a lower transmissivity between BFI02 and KFI11. The calculated storage coefficients in KFI11 (and KFI06) are significantly lower than in the other boreholes, particularly in tests 1 and 2. The drawdown response in Fi 11 may be interpreted as flow in a restricted (low-porosity) channel in the rock rather than a general decrease in transmissivity between BFI02 and KFI11. A brief discussion of transmissivity anisotropy associated with the boreholes BFI01 and KFI11 is given in Chapter 8. A comparison of responses from the interference tests and tracer tests in these boreholes is presented in Chapter 7.

6.5 Comparison of results from previous investigations

As described in Chapter 3, single-hole tests in boreholes within Zone 2 and preliminary interference tests during drilling of BFI01 have previously been performed in the Brändan

area. The latter tests were also simulated by numerical modeling (Nordqvist and Andersson 1987). The transmissivities corresponding to the observation borehole intervals used in the interference tests, calculated from the single-hole tests, are presented in Table 6.11.

The agreement between the results of the present interference tests and the single-hole tests regarding calculated transmissivities is in general rather good. However, the transmissivities calculated from the single-hole tests are in general somewhat lower than those from the interference tests. It should be pointed out that the single-hole test results in the most high-conductive parts of the observation borehole intervals are above the (practical) upper measurement limit of the test equipments used as discussed by Andersson et al. (1987).

The preliminary interference tests during drilling of BFI01 were of rather short duration and the tests were merely aimed at the design of the present interference tests. Thus, no firm conclusions about the actual outer boundary conditions of Zone 2 could be deduced from these tests. Accordingly, the tests were evaluated by theory for aquifers of infinite areal extent. This generally resulted in an underestimation of the transmissivity and an overestimation of the storage coefficient of Zone 2 by factors of 2-5 compared to the results of the present interference tests. However, in some boreholes good agreement between the results of the preliminary and the present interference tests was obtained. Also the basic conclusions drawn from the preliminary tests regarding the flow conditions within and adjacent to Zone 2 are in good agreement with the present results.

The numerical simulations of the preliminary interference tests during drilling also suffered from a relevant representation of the outer boundary conditions of Zone 2. However, these

simulations helped in deducing the relevant outer boundary conditions and in the determination of the hydraulic parameters of Zone 2 from the present interference tests, see Chapter 8.

Table 6.11 Total transmissivities of the observation borehole sections within Zone 2 used in the interference tests, calculated from single-hole tests in 2 m sections.

Borehole	Observation section, no	Interval (m)	T (m^2/s)	Part of Zone 2	Remarks
KFI05	4	163-189	1.2 E-3	upper	
	3	227-240	4.2 E-3	middle	
	2	241-296	2.6 E-4	lower	
KFI06	4	202-227	5.6 E-4	upper	
	3	250-259	4.0 E-4	lower	
	2	260-279	2.7 E-4*	lower	
KFI09	4	119-151	1.0 E-3	upper	
	3	152-188	5.8 E-4	middle	
	2	189-230	1.2 E-4	lower	
KFI10	4	76-134	2.7 E-4	Zone 1	
	3	139-158	1.2 E-4	upper	
	2	159-193	7.6 E-5	middle	
	1	194-225	2.2 E-4	lower	
KFI11	4	217-240	3.7 E-4	upper	
	3	285-304	1.8 E-6	lower	
	2	327-340	1.5 E-5	lower	
BFI01	4	239-250	1.3 E-3	upper	
	3	261-270	2.5 E-6	upper	
	2	345-364	1.1 E-4	lower	
HFI01	1	82-129	4.6 E-4	(upper)	
BFI02	pumped	193-217	1.7 E-3	upper	Test 2
	"	246-270	8.3 E-4	lower	Test 1
	"	193-288	2.6 E-3	whole	Tests 3A, 3B

* Section 270.35 - 272.40 not measured.

7. TRACER TESTS

7.1 General

In order to optimize the design and performance of the radially converging tracer experiment, which is the first of three proposed tracer experiments in phase 3 of the Fracture Zone Project at Finnsjön, a series of preliminary tests were suggested. In this chapter a preparatory tracer run, performed in the upper highly conductive part of Zone 2 during interference test 2, is presented. Tracers were injected in the boreholes BFI01, KFI06 and KFI11 located west, north and south of the pumping hole BFI02, at a radial distance of approx. 160 metres (Figure 7.1). The water discharging from borehole BFI02 was then sampled and analysed for tracer contents.

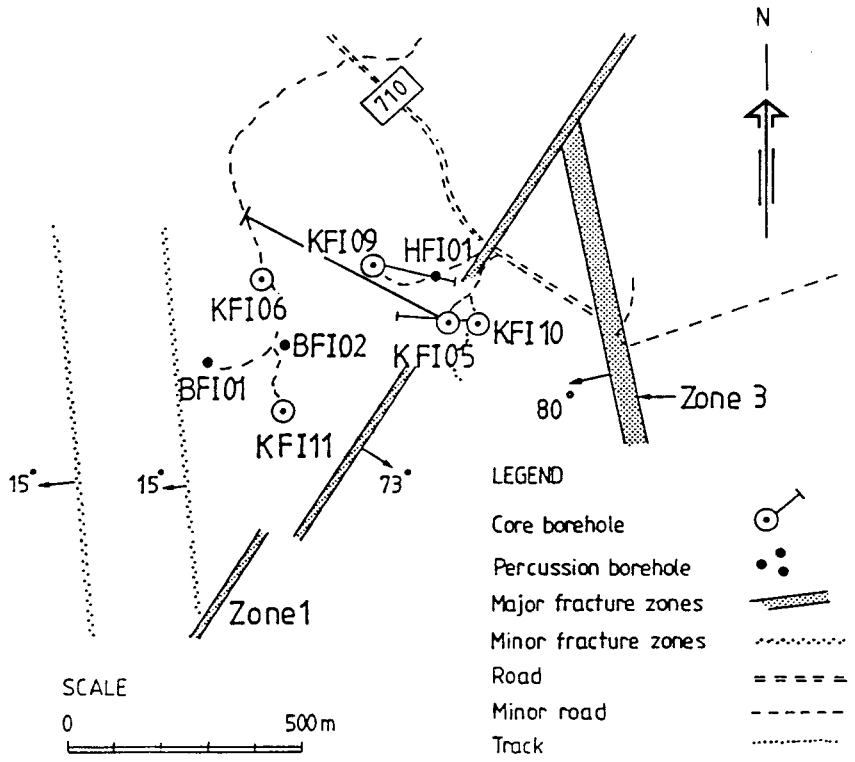

Figure 7.1 Map of the Brändan area showing borehole locations and fracture zones.

7.1.1 Objectives

The specific objective of this test was primarily to establish hydraulic connections between the pumped section in borehole BFI02 and the injection sections in the surrounding boreholes. Ideally estimates of the following parameters would be possible from tracer arrivals in three directions:

- residence time
- first arrival
- hydraulic fracture conductivity
- flow porosity
- fracture aperture
- dispersivity

Directional variations of the parameters governed by the solute transport will give a measure on the degree of heterogeneity, since they should be the same in all directions in a homogeneous and isotropic medium.

As non-sorbing tracers were used in a highly conductive fracture zone with a large induced hydraulic gradient the possible effects of sorption and matrix diffusion was assumed to be negligible and thus not included in the evaluation of the tracer runs.

Secondly, in the pumping hole BFI02 bypass of water from below, if any, around the lower packer and into the pumped section was checked by an injection of tracer labelled water just below the lower packer. Bypass around the packer would then be indicated by the precence of tracer in the discharging water.

7.2 Pulse injection of tracers

7.2.1 Design and performance

During interference test 2 tracers were injected in section no 4 in the observation boreholes BFI01, KFI06 and KFI11. These sections represent the upper, highly conductive part of Zone 2 in the boreholes (Appendix 1:2, 1:5 and 1:6). In Figure 7.2 the relative position of the boreholes used is shown and the pumping/sampling and injection sections intersecting the upper highly conductive part of Zone 2 are marked. Basic data about the tracer test are presented in Tables 7.1 - 7.4. The tracers Uranine, Iodide and Amino G Acid were injected as pulses through the pressure connection tubes in the multi-pressure probes of the Piezomac system. The tracers were injected according to the following scheme:

- Registration of natural piezometric head in the borehole sections.
- Injection of tracer slugs (50 - 125 litres) in the boreholes BFI01, KFI06, and KFI11.
- Flushing with groundwater and distilled water (50 - 125 litres) in order to force the tracer some distance into the fractures and to rinse the tubing from tracer.
- Registration of piezometric head.
- Start of pumping in borehole BFI02 for the interference test when natural piezometric head was reached in all sections.

As was expected for these highly conductive sections, the piezometric head immediately reached natural levels after the injection and flushing was completed. The pump was then started in borehole BFI02 for a continuous water discharge during approximately 8 days at a capacity of 500 l/min (Table 4.7). Sampling of the discharged water for tracer analysis was

performed with an automatic sampling equipment (Figure 7.3). The time between the sampling events was determined by the predicted time of first arrival. The first day samples were taken at every hour, followed by sampling at every second hour.

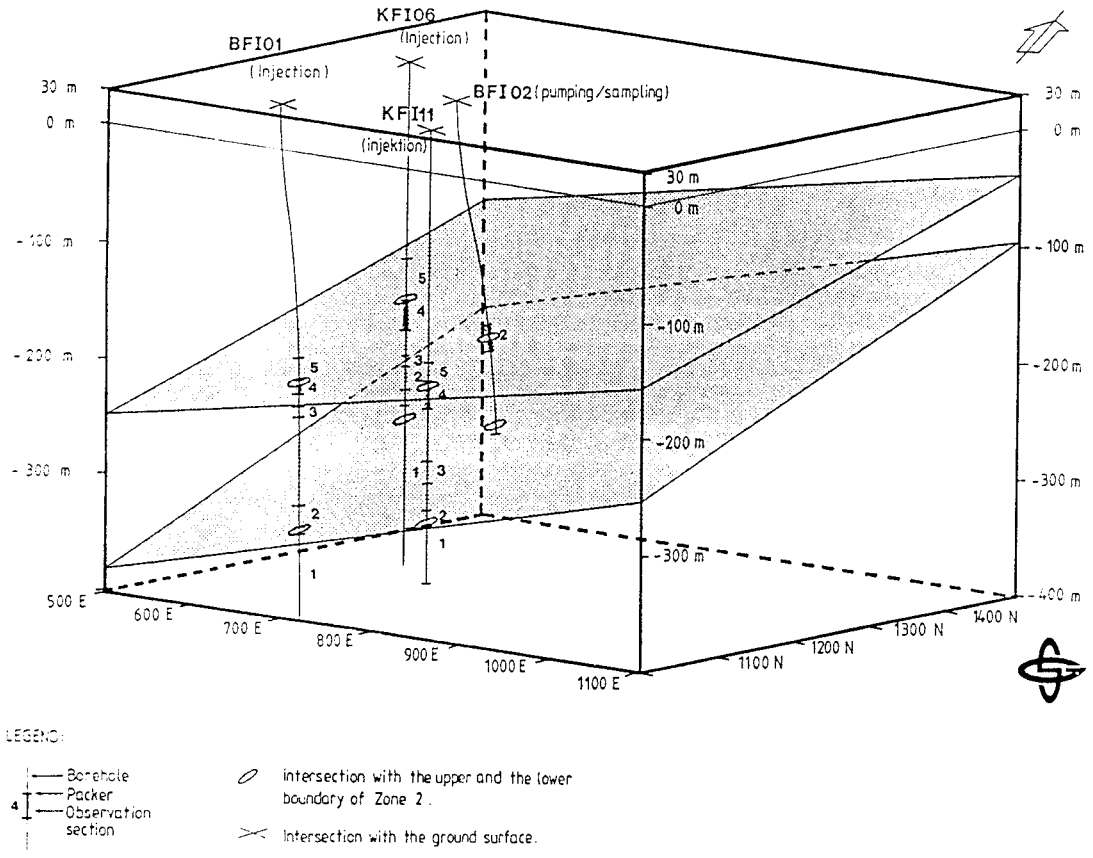

Figure 7.2 Relative positions of the boreholes and pumping/ sampling resp. injection sections used in the tracer tests.

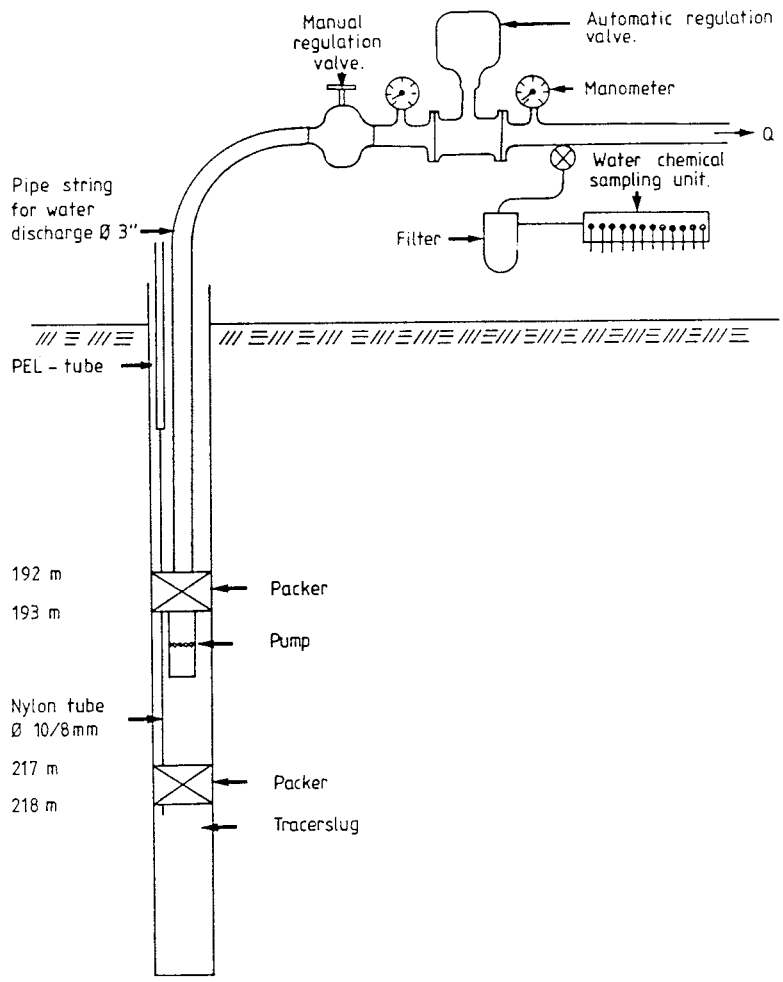

Figure 7.3 Packer configuration and equipment set up in borehole BFI02.

Table 7.1 Pumping/sampling and injection sections.

Borehole	Section (m)	Distance* (m)	T** (m^2/s)	Remarks
BFI02	193 - 217	---	1.7E-3	pumping/sampling
BFI01	239 - 250	168	1.3E-3	injection
KFI06	202 - 227	189	5.6E-4	injection
KFI11	217 - 240	155	3.7E-4	injection

* Distance to the injection sections from the pumped section in BFI02.

** Calculated from single-hole water injection tests in 2 m sections (from Table 6.11).

Table 7.2 Estimated hydraulic parameters of the upper part of Zone 2 from the time-drawdown analysis of interference test 2 (from Table 6.4).

Route	T (m^2/s)	S
BFI01 - BFI02	1.4E-3	9.4E-6
KFI06 - BFI02	1.4E-3	2.4E-6
KFI11 - BFI02	1.4E-3	5.7E-7

Table 7.3 Volumes of borehole sections and pressure connection tubing.

Borehole	L (m)	Diam. (mm)	Volumes (litres) section	tubing	total
BFI02	24	158	450	880	1330
BFI01	11	168	234.5	11.3	245.8
KFI06	25	56	48.6	2.6	51.2
KFI11	23	56	43.4	2.8	46.2

Table 7.4 Tracers, concentrations and volumes injected.

Borehole	Tracer	Concentration (ppm)		Volumes (litres) tracer sol.	flushing
BFI01	Uranine	10.000		125	125
KFI06	Iodide	126.900	(1 M)	50	50
KFI11	Amino G Acid	20.000		50	50

7.2.2 Methods of interpretation

The interpretation of the breakthrough curves is made under the assumption of a homogeneous and isotropic radially converging steady-state flow field. A conceptual model of the tracer test is shown in Figure 7.4.

Assuming that Darcy's law is valid and that the flow in the aquifer is concentrated to one single fracture, the hydraulic fracture conductivity for the equivalent single fracture can be determined with the geometry and the withdrawal rate, Q, as the basic variables.

$$K^{q}_{esf} = \left[\frac{Q \cdot \ln(r/r_w) \cdot (g)^{1/2}}{2 \cdot \pi \cdot \Delta h \cdot (12\nu)^{1/2}} \right]^{2/3} \qquad (7.1)$$

where r = distance from pumping hole (m)
r_w = radius of pumping hole (m)
Δh = head difference between pumping and injection borehole (m)

If a tracer is injected at an arbitrary distance or direction from a pumping borehole, the hydraulic conductivity for the equivalent single fracture can be determined with the residence time, t_o, as the basic variable.

$$K^{t}_{esf} = \frac{(r^2 - r_w^2) \cdot \ln(r/r_w)}{2 \cdot t_o \cdot \Delta h} \qquad (7.2)$$

where t_o = residence time

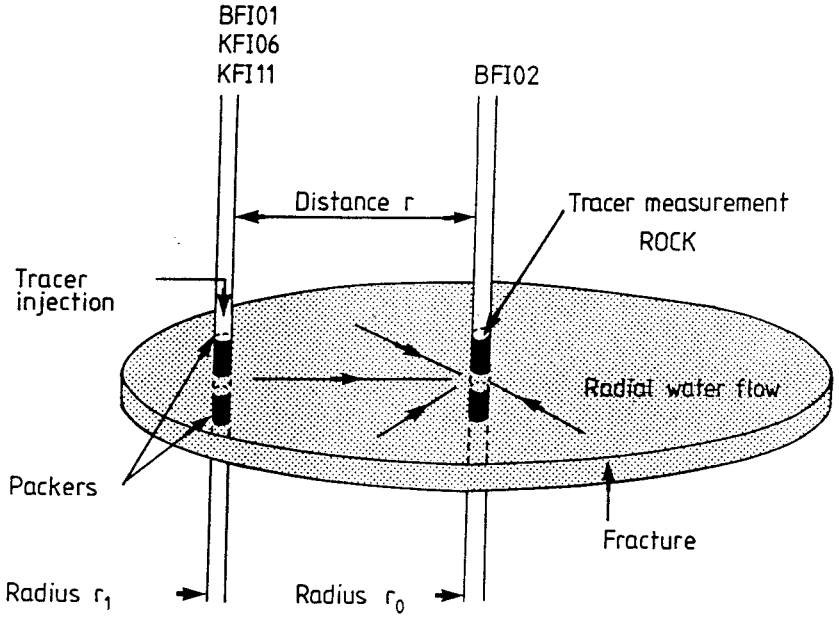

Figure 7.4 Conceptual model of the tracer test

Calculations of the hydraulic fracture conductivity utilizing Equations (7.1) and (7.2) require a constant head difference Δh, i.e. a steady-state. Examination of the breakthrough curves and comparison with the drawdown in the pumping and injection sections (Figures 7.6 - 7.8 and Table 7.5) shows that the first arrival and residence time has been reached and most of the tracers have been recovered in the pumping hole long before steady-state is reached. However, even though the drawdown is not constant, the head difference, especially between the boreholes KFI06 - BFI02 and KFI11 - BFI02, is fairly constant with time during the process of tracer transport from the injection boreholes to the centrally located pumping hole BFI02 (Table 7.6), cf. section 5.1.1. The error introduced by assuming constant Δh values is relatively small. For calculations of the hydraulic fracture conductivities, K^q_{esf} and K^t_{esf} respectively, the values of Δh underlined in Table 7.6 have been used. The Δh values in Table 7.6 are calculated by addition of 0.5 m to the drawdown differences (from Table 7.5) between the pumed borehole interval and the injection intervals, respectively. The 0.5 m addition is due

to the reference level beeing 0.5 metre lower in borehole BFI02 than in the other boreholes.

Table 7.5 Drawdown (metres) in the pumping and injection sections during interference test 2.

Borehole	Drawdown (m) versus time (h)							
	0.1	1.0	5.0	10.0	15.0	33.3	66.6	100
BFI02	4.9	5.6	6.8	7.7	8.4	9.7	10.6	11.0
BFI01	0.6	1.4	2.2	3.0	3.6	4.7	5.5	5.8
KFI06	1.0	1.6	2.8	3.7	4.3	5.6	6.4	6.9
KFI11	1.8	2.6	3.6	4.4	5.0	6.2	7.5	7.5

Table 7.6 Head differences (metres) between the pumped section and the injection sections at different times during interference test 2.

Route	Δh (m) versus time (h)								steady state
	0.1	1.0	5.0	10.0	15.0	33.3	66.6	100	
BFI01 - BFI02	4.8	4.7	5.1	5.2	5.3	5.5	5.6	5.7	5.7
KFI06 - BFI02	4.4	4.5	4.5	4.5	4.6	4.6	4.7	4.6	4.6
KFI11 - BFI02	3.6	3.5	3.7	3.8	3.9	4.0	3.6	4.0	3.7

The fracture aperture, defined as the aperture of one equivalent single fracture, e_{esf}, can be determined by using Equation (7.3) for laminar flow between two smooth parallel plates (Snow, 1968) and inserting the value of K_{esf} determined from Equation (7.1) or (7.2). The different fracture apertures will be denoted by e^q_{esf} and e^t_{esf} respectively.

$$e^x_{esf} = (K^x_{esf} \cdot 12 \cdot \upsilon / g)^{1/2} \qquad (7.3)$$

where x = q or t

υ = kinematic viscosity of the water (m^2/s)

g = acceleration due to gravity (m/s^2)

The aperture can also be calculated from the mass balance, by dividing the volume of the fracture by the area of the fracture plane according to Eqn.(7.4).

$$e^m = Q \cdot t_o / (\pi(r^2 - r_w^2)) \qquad (7.4)$$

The transmissivity of a fractured aquifer can be calculated by multiplying the equivalent single fracture conductivity (K^q_{esf} or K^t_{esf}) by the aperture (e^q_{esf}, e^t_{esf} or e^m) denoted T^q, T^t and T^m, respectively. In the hypothetical case of a single parallel-plate fracture aquifer these calculated transmissivities will coincide.

The flow porosity, $\emptyset_k$, defined as the volume of rock available for transport of water (Norton and Knapp, 1977) can be determined as the ratio between the hydraulic conductivity of the rock mass, K, and the conductivity of one equivalent single fracture, K^t_{esf} or K^q_{esf}, assuming equal gradient over the rock mass and over the fracture and that Darcy´s law applies.

$$\emptyset_k{}^x = K / K^x_{esf} \qquad (7.5)$$

where $x = q$ or t

The flow porosity can also be determined as the ratio between the volume of flowing water in the rock mass and the total volume of the rock mass. In radially convergent flow the ratio is

$$\emptyset_k{}^m = Q \cdot t_o / (\pi \cdot r^2 \cdot L) \qquad (7.6)$$

where L = thickness of the aquifer (m)

Note that by definition e^m and $\emptyset_k{}^m$ will be equal if determined for a one metre thick aquifer.

Contrary to the porous medium case, porosity values determined in a heterogeneous rock aquifer from equation (7.5) or (7.6) are dependent on the length of the interval where K was determined, or on L being the assumed thickness of the aquifer contributing to the flow. For example in the case of one single fracture (or a few narrow-spaced fractures) in an otherwise low conductive rock mass.

If the flow porosity is calculated according to Equation (7.5) the hydraulic conductivity of the rock mass, K, can be determined as a mean value from single-hole hydraulic testing according to Equation (7.7), or alternatively by utilizing transmissivity values from hydraulic interference tests.

$$K = (T_p / L_p + T_i / L_i) / 2 \qquad (7.7)$$

where T_p = transmissivity of pumping section (m^2/s)
T_i = transmissivity of injection section (m^2/s)

Hydrodynamic dispersivity, A, is defined as the spreading in time and space of a water-soluble substance transported with the groundwater due to the velocity distribution in the aquifer and molecular diffusion in the flow paths. In the table of results (Table 7.8) the dispersivities are estimated from the breakthrough curves according to Equation (7.8), which is the solution for convergent radial flow in a single fracture (Gelhar, 1987).

$$A = 3 \cdot r(dt/t_0)^2/64 \qquad (7.8)$$

where dt and t_0 are defined as depicted schematically in Figure 7.5.

Eqn.(7.8) takes into account the varying velocity and dispersion coefficient associated with the radial flow system and is strictly valid for Peclet numbers Pe > 10, i.e. A/r < 0.1.

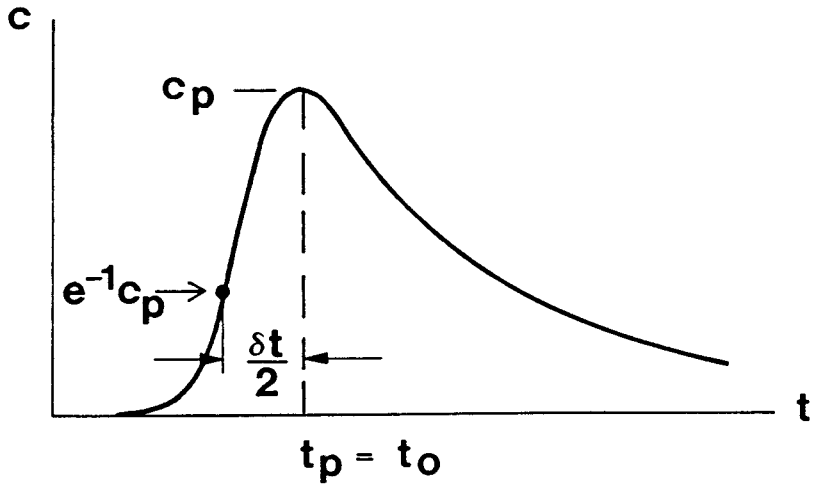

Figure 7.5 Schematic tracer breakthrough curve for convergent radial flow tracer test with pulse injection (Gelhar, 1987).

To distinguish more than one possible main flow path from the observed breakthrough curves the one-dimensional solution given by Lenda and Zuber (1970) and Kreft et al.(1974) can be used.

$$C = \frac{m}{V}\left[\frac{1}{\left[4 \cdot \pi \cdot n \cdot (t/t_o)^3\right]^{1/2}}\right] \cdot \exp\left[\frac{-(1 - t/t_o)^2}{4 \cdot n\,(t/t_o)}\right] \quad (7.9)$$

where C = concentration
n = A/x
x = distance in the direction of flow
m = total mass of tracer injected
V = total volume available for water flow

This one-dimensional solution will overestimate the magnitude of the dispersivity, A, by a factor of 1.33 as it does not account for the varying velocity and dispersion coefficient developed in the radial flow field (Gelhar, 1987). However, the fact that it is not possible to determine whether there are more than one flow path contributing to the solute transport with the solution given by Gelhar (Eqn. 7.8), the factor 1.33 is not large compared to the difference in dispersivity and residence time, t_o, that can be expected between existing main flow paths/fractures.

The residence time, t_o, also called the mean transport time of a solute, is determined as the time to peak concentration according to the theories of Gelhar (1987). However, in nuclear safety analysis the time of first arrival and the early part of the breakthrough curve of the solute are also important, "whereas later flow fractions represent lower levels of radiotoxicity due to radioactive decay. This marks a distinct difference from common approaches in chemical engineering and heat extraction" (Brotzen, 1986).

The residence time or the time of first arrival provides a possibility to estimate any anisotropic conditions of an aquifer, because in a homogeneous and isotropic aquifer where a tracer is injected at an arbitrary direction and distance r from a withdrawal borehole, the ratio between the residence time and the distance squared, t_o/r^2, should be constant.

To evaluate the above discussed transport parameters, calculated according to Equations (7.1) - (7.6), two brief statements regarding fracture flow can be utilized.

The first one is that in a single fracture the flow rate is proportional to the aperture cubed, but the velocity to the

aperture squared. The fracture conductivity calculated with the flow rate as the basic variable will thus coincide with that calculated from the residence time of a solute only in the case of parallel planar plates representing the fracture surfaces. Hence, in a natural fracture plane with patches of elevated aperture constituting the flow paths the quotient K^q_{esf}/K^t_{esf} will increase from unity the more pronounced the fracture flow paths differ from parallel planar plates.

The second one is that if the transmissivity of the aquifer remains constant, the magnitude of the transport parameters determined with the flow rate as the basic variable are insensitive to the number of fractures contributing to the flow. If, on the other hand, the transport parameters are determined with the residence time as the basic variable, then the magnitude is very sensitive to the number of fractures involved in the solute transport.

The impact on the magnitude of the transport parameters by the number of fractures contributing to the flow can be easily demonstrated by an example, summarized in Table 7.7. One aquifer constitutes of a single parallel-plate fracture with the aperture 1.00 mm and the other of five parallel-plate fractures with the aperture 0.58 mm, making up a transmissivity of 6.24E-4 m^2/s in both aquifers.

From Table 7.7 it is obvious that the magnitude of the hydraulic fracture conductivity and the aperture determined with the flow rate as the basic variable, K^q_{esf} and e^q_{esf} respectively, are insensitive to the number of fractures involved. This flow rate determined aperture and conductivity will hence be insufficient for calculations of solute transport. For example in the aquifer with five fractures, the wetted surface area, calculated as the total fracture surface area divided by the total volume of water per unit width of

aquifer, will be calculated to 2.0E3 m^{-1}, but the actual value is 3.4E3 m^{-1}.

Table 7.7 Example of differences in the magnitude of the determined transport parameters arising when two different basic variables are used in the calculations.

Parameter	Aquifer with parallel-plate fractures	
	one fracture (1.00 mm)	five fractures (0.58 mm)
T (m^2/s)	6.24E-4	6.24E-4
Q (m^3/s) *	1.0E-2	1.0E-2
Δh (m) **	19.25	19.25
K^q_{esf} (m/s)	0.624	0.624
K^t_{esf} (m/s)	0.624	0.213
e^q_{esf} (m)	1.00E-3	1.00E-3
e^t_{esf} (m)	1.00E-3	0.58E-3
e^m (m)	1.00E-3	2.92E-3
t_o (hours)	1.96	5.74

* r_w = 0.08 m , ** r = 150 m

In the five fracture aquifer also the actual velocity of solute transport is about three times slower than what would be calculated from the value of K^q_{esf}. Hence, the possibilities for sorption is better than flow rate determined parameters show. The hydraulic fracture conductivity and aperture determined with the residence time as the basic variable, K^t_{esf}, e^t_{esf} and e^m respectively, will in contrary give a correct measure on the transport properties of the parallel-plate fracture system. Note that e^m gives a measure on the sum of the apertures in the fracture system and the quotient e^m/e^t_{esf} the number of fractures.

7.2.3 Results

Tracers from all three boreholes reached the pumping/sampling borehole BFI02. The resulting breakthrough curves of the tracers are presented as normalized tracer concentrations versus time in Figures 7.6 - 7.8. A summary of the parameters determined from the pulse injection of tracers is presented in Table 7.8.

Utilizing the statements and the example given in the previous section regarding fracture flow, the results presented in Table 7.8 indicate that not more than 3 - 4 fractures/main flow paths are involved in the solute transport from the boreholes KFI06 and KFI11, if parallel-plate fractures are assumed. As the natural fractures most probably have a wave shaped variation of the aperture, the number of fractures or flow paths contributing to the solute transport must be even smaller in the direction towards KFI06 and KFI11. However, the results indicate a larger number, 10 - 15, of fractures/main flow paths contributing to the solute transport in the direction towards borehole BFI01.

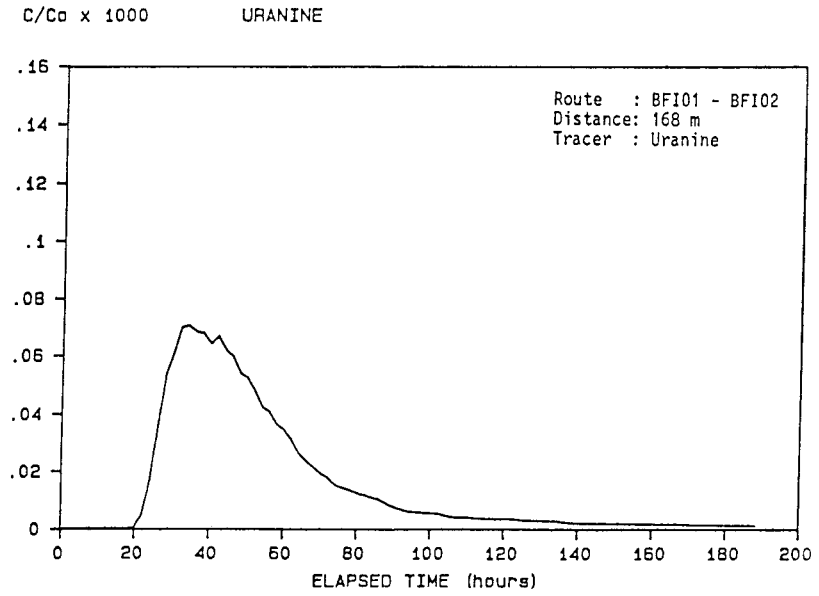

Figure 7.6 Breakthrough curve for Uranine in borehole BFI02 resulting from pulse injection in borehole BFI01.

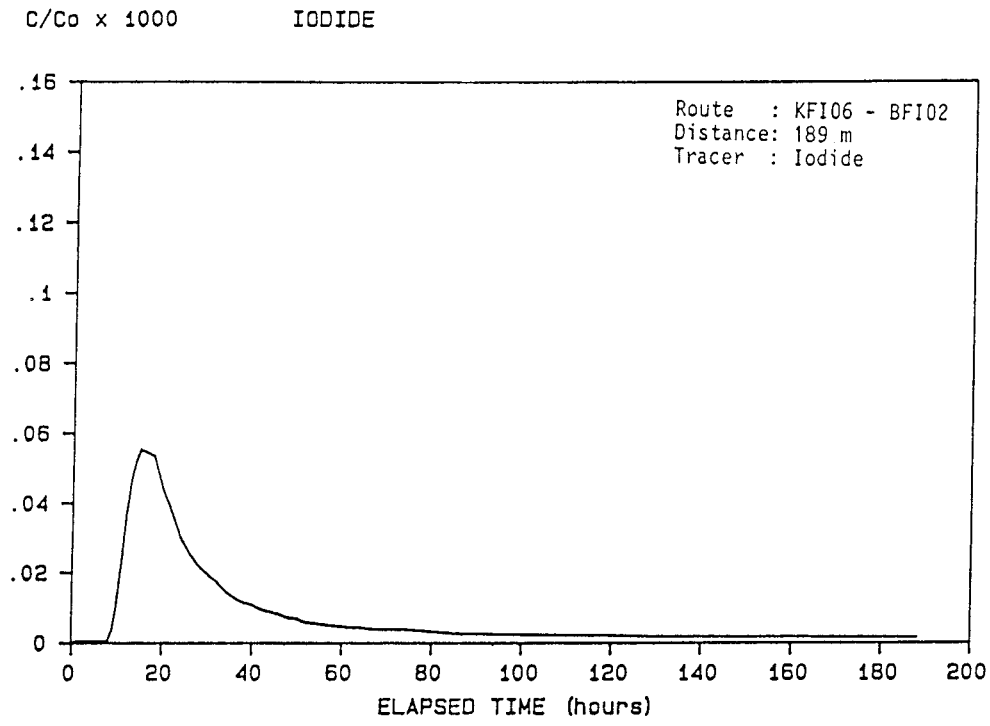

Figure 7.7 Breakthrough curve for Iodide in borehole BFI02 resulting from pulse injection in borehole KFI06.

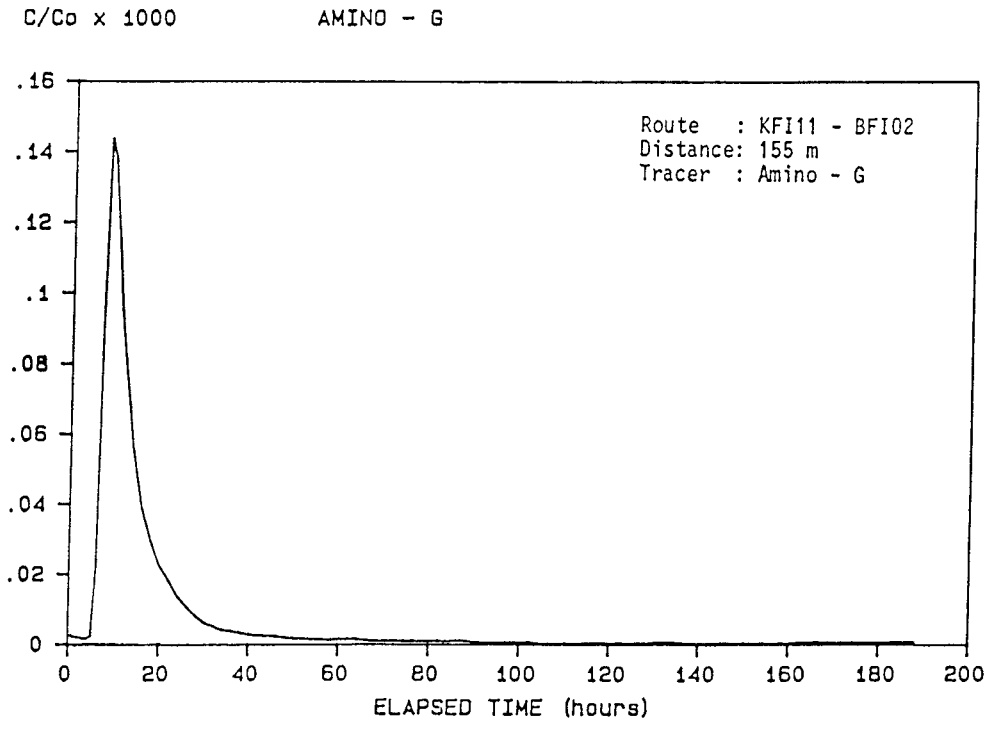

Figure 7.8 Breakthrough curve for Amino G Acid in borehole BFI02, resulting from injection in borehole KFI11.

Table 7.8 Summary of parameters determined from pulse injections of tracers during interference test 2.

Route	BFI01 - BFI02	KFI06 - BFI02	KFI11 - BFI02
Tracer	Uranine	Iodide	Amino G Acid
Distance (m)	168	189	155
Δh (m)	5.3	4.5	3.7
K^q_{esf} (m/s)	1.3	1.5	1.7
K^t_{esf} (m/s)	1.6E-1	6.1E-1	9.7E-1
e^q_{esf} (m)	1.4E-3	1.5E-3	1.6E-3
e^t_{esf} (m)	5.1E-4	9.9E-4	1.2E-3
e^m (m)	1.2E-2	4.3E-3	3.2E-3
T^q (m^2/s)	1.8E-3	2.3E-3	2.7E-3
T^t (m^2/s)	8.2E-5	6.0E-4	1.2E-3
T^m (m^2/s)	1.9E-3	2.6E-3	3.1E-3
$\emptyset_k{}^q$ (1 m section)+	1.1E-3	9.4E-4	8.2E-4
$\emptyset_k{}^t$ (1 m section)+	8.8E-3	2.3E-3	1.4E-3
$\emptyset_k{}^m$ (1 m section)	1.2E-2	4.3E-3	3.2E-3
t (hours)	20	8	5
t_o (hours)*	35	16	8
t/r^2 (s/m^2)	7.1E-4	2.2E-4	2.1E-4
t_o/r^2 (s/m^2)	1.2E-3	4.5E-4	3.3E-4
A (m)**	2.4	3.9	1.3
Pe	70	49	118
Recovery (%)	68	81	70

+ K in Eqn. (7.5) determined from interference test data, (Table 7.2)

* t_o = time at peak concentration.

** assuming flow in one single fracture, according to Eqn.(7.8)

The number of possible fractures/flow paths was also evaluated by regression estimates from the breakthrough curves. The results of these estimates are presented in Table 7.9 and Figures 7.9 - 7.12. In Figure 7.9 the experimental breakthrough curve for Iodide (injected in KFI06) is presented together with a theoretical curve fitted only to the ascending part of the breakthrough, according to the single fracture theory by Gelhar, (1987). The dispersivity, A, and the residence time, t_0, of the theorethical curve are given in Table 7.8.

Figure 7.9 indicates that the experimental breakthrough curve obtained in borehole BFI02 must be the result of solute transport in more than one fracture/main flow path from the injection point in borehole KFI06. This is also evident from the regression estimate on the entire breakthrough curve with only one flow path, presented in Figure 7.10, which does not describe the experimental data completely.

Two main flow paths, as presented in Figure 7.11 give on the other hand a better description of the experimental data. Note that the residence time of the primary flow path, 17.5 hours, is very close to that obtained by the fit with one flow path to the ascending part of the breakthrough curve, i.e. 16 hours (Fig 7.9). A comparison of the dispersivities of these two flow paths (Tables 7.8 and 7.9) shows that they differ by a factor of 1.8, which is slightly more than what is expected if the residence times are nearly the same (factor 1.3).

A regression estimate with three flow paths to the experimental data of the Uranine breakthrough in borehole BFI02, obtained from injection in borehole BFI01 is presented in Figure 7.12. In this case the second partial curve has the largest mass transfer. If there exist several fractures with almost identical residence times and dispersivities this will also reflect the result of the regression estimate.

Table 7.9 Regression estimate of dispersivity and residence time, with Eqn (7.8) on the experimental data.

Route and Tracer	Flow paths		t_0 (hours)	A (m)	Pe
BFI01 - BFI02 Uranine	One,	1A	47.0	10.9	15
	Three,	3A	31.9	2.4	70
		3B	48.6	6.8	25
		3C	99.3	14.8	11
KFI06 - BFI02 Iodide	One,	1A	21.1	13.7	14
	Two,	2A	17.5	7.2	26
		2B	40.7	31.3	6
KFI11 - BFI02 Amino G Acid	One,	1A	11.0	8.5	18
	Two,	2A	8.8	2.7	57
		2B	14.8	11.4	14

The hydraulic fracture conductivity in the upper highly conductive part of Zone 2 was calculated with both the withdrawal rate, Q, and the residence time of a tracer, t_0, as the basic variable, denoted K^q_{esf} and K^t_{esf} respectively (Table 7.8). The fracture conductivities calculated are notably high (K^q_{esf} = 1.3 - 1.7 and K^t_{esf} = 1.6E-1 - 9.7E-1 m/s), but are only a factor 5-50 higher than the average hydraulic conductivity, K_{ss}, determined by hydraulic single-hole tests in 0.11 m sections of borehole BFI02 (Ekman et al., 1988). The calculated K^t_{esf} values can also be compared with the results from a previously performed flushing water tracer test in Zone 2 (Gustafsson and Andersson, 1989) where tracer labelled flushing water from borehole KFI11 entered the drilling water supply well (borehole HFI01) at a distance of about 400 m (Fig. 7.1). The hydraulic fracture conductivity calculated, K^t_{esf}, ranged between 1.7E-2 - 1.5E-1 m/s, depending on the assumed flow regime and hydraulic gradient.

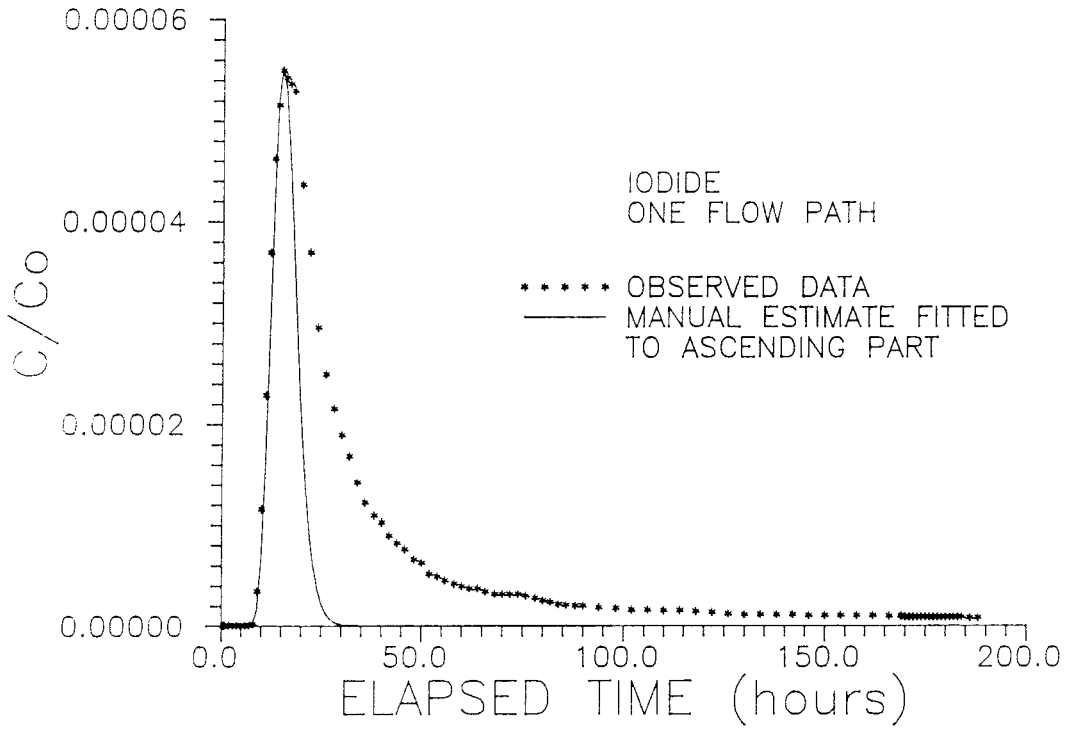

Figure 7.9 Experimental breakthrough curve for Iodide and fit with one fracture/flow path, weighted to the ascending part of the breakthrough.

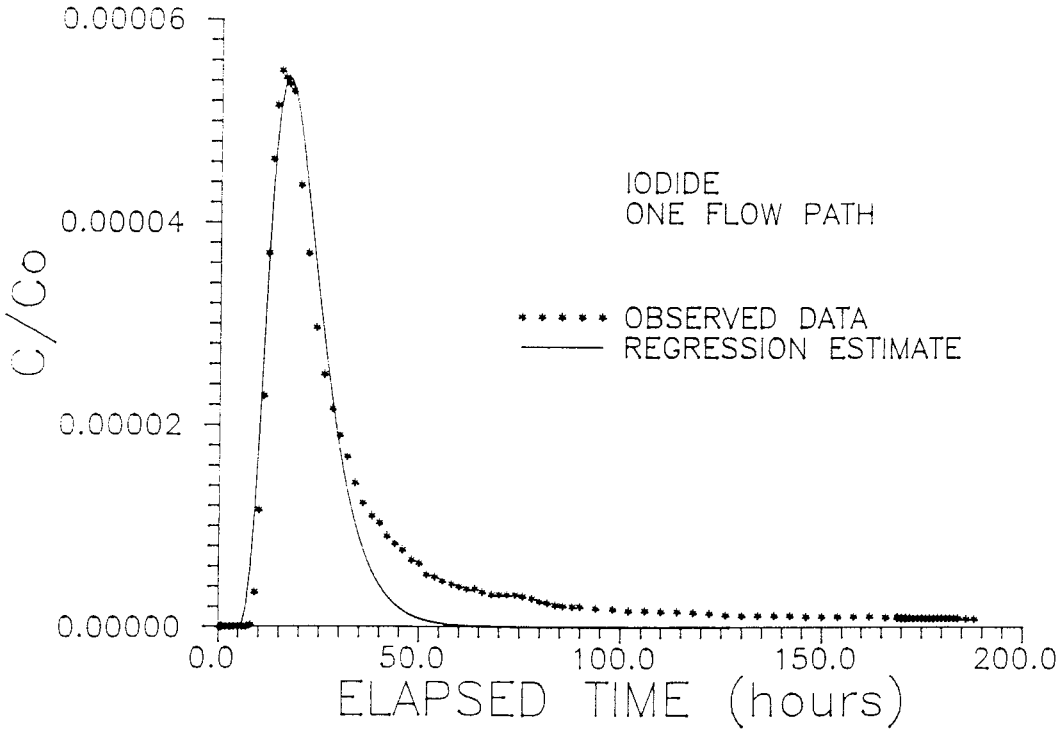

Figure 7.10 Regression estimate with one flow path to the experimental Iodide data.

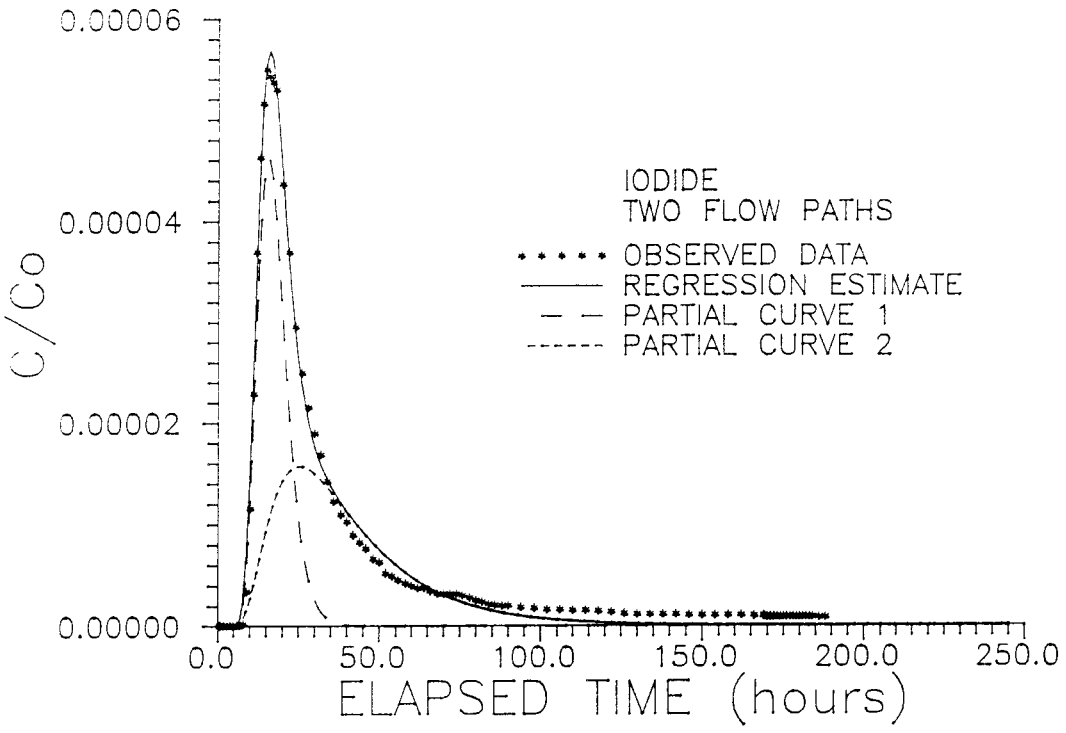

Figure 7.11 Regression estimate with two flow paths to the experimental Iodide data.

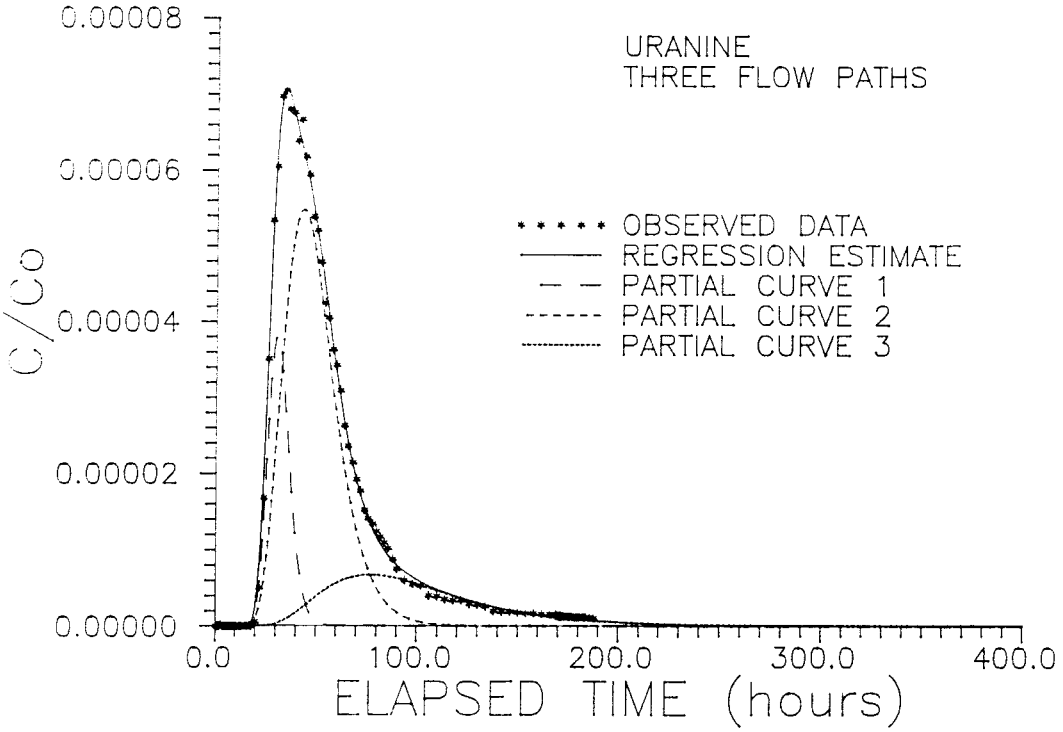

Figure 7.12 Regression estimate with three flow paths to the experimental Uranine data.

Tracer tests have also been conducted in a minor fracture zone at Gåvastbo, in the vicinity of the area of the present tracer test (Gustafsson and Klockars, 1981). The fracture conductivities calculated (K^q_{esf} = 1.4E-2 and K^t_{esf} = 2.7E-3) were approx. two orders of magnitude lower than in Zone 2, cf. Table 7.8. Interestingly the same ratio also applies to the transmissivity values, 4.4E-6 compared to 1.4E-3 m^2/s.

The transmissivities in the different directions of Zone 2, calculated from the tracer test, T^q, T^t and T^m respectively, are to be compared with those calculated from the interference test, T. The T^q, T^m and T values are all in good agreement, ranging between 1.4E-3 - 3.1E-3 m^2/s. The T^t value reflects on the other hand the transmissivity of a single fracture/flow path and is consequently smaller, 8.2E-5 - 1.2E-3 m^2/s.

The flow porosity values were determined from tracer runs in the upper highly conductive part of Zone 2. From the geological and hydrogeological interpretations it can be concluded that, in the upper part of Zone 2, the main part of groundwater flow actually occurs in a less than one metre thick subzone. Hence, the flow porosity is determined for a one metre thick zone, even though it was straddled in ca. 25 m long borehole intervals during the present tracer test. The values of the flow porosity, $\emptyset_k{}^m$ and $\emptyset_k{}^t$, determined from tracer arrivals in three directions over distances ranging between 155 - 189 metres are within 3.2E-3 - 1.2E-2 and 1.4E-3 - 8.8E-3, respectively. In the minor fracture zone investigated by Gustafsson and Klockars (1981) the flow porosity, $\emptyset_k{}^t$, was 1.6E-3 if calculated for a one metre thick zone. The value is close to that obtained in Zone 2.

In the above mentioned flushing water tracer test, the flow porosity, $\emptyset_k{}^t$, in Zone 2 was calculated to 6.7E-3 - 5.9E-2, depending on the assumed flow regime and hydraulic gradient. Considering the uncertainties in the latter calculation, the

flow porosity of the upper highly conductive part of Zone 2 seems to be consistent within about one order of magnitude. However, in the present tracer test, the flow porosity values determined with the residence time as the basic variable, $\emptyset_k{}^t$ and $\emptyset_k{}^m$, clearly show that the porosity is larger in the direction towards borehole BFI01 than in the direction to the other two boreholes (Table 7.8). This directional variation of the porosity is also evident from the storage coefficients calculated from the time-drawdown analysis of interference test 2 (Table 7.2).

The calculated dispersivities and Peclet numbers are presented in Tables 7.8 and 7.9. In all three directions the dispersivity is low in the primary flow paths, 1.3 - 7.2 m, and in most of the secondary flow paths, which implies that the solute transport in the groundwater flow paths studied, and at the distances involved, is dominated by advection whereas dispersion is of minor importance.

The recovered mass of injected tracers was calculated after 188 hours of pumping (Table 7.8). The recovery was about 70% for Uranine and Amino G and 81% for Iodide. The Iodide and Uranine had not reached background values at the time of stop of pumping at 188 hours.

Heterogeneity of Zone 2 is evident from directional comparisons between the parameters governing the solute transport (Table 7.8). Within the radius of the present tracer test the upper highly conductive part of Zone 2 is fairly homogeneous regarding transmissivity, but the other parameters essential to solute transport show directional variations indicating anisotropic conditions. In the direction of the dip, i.e. towards borehole BFI01, the aperture and the hydraulic conductivity of the fractures or flow paths contributing to the solute transport are lower than in the direction of the strike, i.e. towards the boreholes KFI06 and KFI11. The number of fractures or flow paths involved is on the other hand larger in the direction towards

BFI01, giving a higher porosity but longer residence time in this direction compared to the direction towards KFI06 and KFI11. The anisotropic conditions of Zone 2, which may be due to an intersecting minor fracture zone or fault, is also reflected in the t_o/r^2 values presented in Table 7.8.

In summary, the performed tracer test reveal the following regarding solute transport in the the upper highly conductive part of Zone 2:

- The hydraulic fracture conductivity, determined in three different directions from the residence time of the tracers, K^t_{esf}, assuming one single fracture, is in the range of 1.6E-1 - 9.7E-1 m/s.

- The number of fractures/main flow paths contributing to the solute transport is about 1 - 4 in the direction to the boreholes KFI06 and KFI11, whereas towards BFI01 the evaluation indicates a larger number, 10 - 15.

- The fracture apertures, e^t_{esf}, calculated as equivalent single fractures are in the range of 5.1E-4 - 1.2E-3 m.

- The flow porosity, $\emptyset_k^m$, determined from the mass balance in the one metre thick upper subzone of Zone 2, is 3.2E-3 and 4.3E-3 in the direction to the boreholes KFI06 and KFI11, respectively. The porosity calculated is enhanced in the direction to BFI01, 1.2E-2.

- The results obtained indicate the wetted surface area per volume of water being larger in the direction towards BFI01 than towards KFI06 and KFI11. If parallel-plate fractures are assumed, the ratios are about 1.8E3 and 3.9E3 m^{-1} respectively.

- Heterogeneity of Zone 2 is evident from directional comparisons between the parameters governing the solute transport. Within the radius of the present tracer test the upper highly conductive part of Zone 2 is fairly homogeneous regarding transmissivity, but the other parameters essential to solute transport show directional variations indicating anisotropic conditions. In the direction of the dip, i.e. towards borehole BFI01, the calculated hydraulic conductivity and aperture of the flow paths are lower than in the direction of the strike of Zone 2, i.e. towards the boreholes KFI06 and KFI11. The apparent number of fractures or flow paths contributing to the solute transport is on the other hand larger in the direction towards BFI01, giving a higher porosity but longer residence time in this direction compared to the direction towards KFI06 and KFI11. The anisotropic conditions of Zone 2, also reflected in the t_o/r^2-values presented, may be due to an intersecting fracture zone, which according to the geological interpretations exists between the boreholes BFI01 and BFI02.

- The dispersivities calculated are small in all three directions, 1.3 - 7.2 m in the primary flow paths, or expressed as Peclet numbers, 118 - 26. This implies that the solute transport in the groundwater flow paths studied, at the distances and residence times involved, is dominated by advection whereas dispersion is of minor importance.

- No perceptible effect of sorption or matrix diffusion was observed of the non-sorbing tracers used in the highly conductive fracture zone studied.

7.3 Water Bypass Test

7.3.1 Design and performance

Subsequent to the tracer pulse test a bypass test was conducted in the pumping borehole BFI02 during interference test 2, in purpose to check if there was any bypass of water from below around the lower packer into the pumped section at 193 - 217 m. The tracer, Uranine, was injected below the lower packer as a pulse through the pressure connection tube, see Figure 7.3. The tracer was dissolved in groundwater and groundwater was also used to flush the tracer through the tubing.

Uranine was also used as a tracer in the preceding pulse injections, described in Section 3.2, and was injected in borehole BFI01. However, in the bypass test the Uranine tracer slug was injected 171 hours after the injection in BFI01. The peak concentration of Uranine in the pumped section in BFI02, originating from BFI01, had then already passed more than 100 hours ago and the breakthrough was on its latter, declining part, c.f Figure 7.6.

Basic data about concentration and volumes are given in Table 7.10. Sampling of the discharged water was done at every 20 minutes during the first three hours, followed by sampling at every hour.

Table 7.10 Tracer, concentration and volumes in the bypass test.

Tracer	Conc. (ppm)	Volumes (litres)		
		tracer sol.	flushing	inj. tubing
Uranine	200	25	50	35

7.3.2 Results

No tracer was detected in the discharged water during the 17 hours that the pumping continued after time of tracer injection. Any water bypass of importance, as indicated by the increasing salinity of the discharged water during the interference test 2, would have been measureable well above the detection limit.

When interference test 2 was finished and the packers were deflated for rearrangement to interference test 3A, the pump was restarted for 10 minutes. A volume of 5180 litres was discharged containing a total of 3.24 g Uranine, which make up about 65 % of the injected mass of tracer. When interference test 3A started, the discharged water was sampled and the remaining part of the tracer (1.76 g) was recovered within 5 hours.

The test performed demonstrated that there existed no measureable bypass of water around the lower packer into the pumped section during interference test 2. This fact in turn indicates that the hydraulic isolation of the pumping interval during interference test 2 was efficient.

8. NUMERICAL SIMULATION OF THE INTERFERENCE TESTS

8.1 Modeling approach

8.1.1 Objectives

There were two main objectives with the numerical simulations described in this chapter. One objective was to support the analytical interpretation of the interference test data, with regard to evaluation of hydraulic parameters and boundary configuration. The approach in this case was :
1. To compare previous model predictions to measured responses from the present interference tests.
2. To obtain an updated groundwater flow model calibrated to fit the observed data from the present interference tests. In this process much consideration was given to geological interpretations (Chapter 2) to define hydrogelogical boundaries.

The other objective was that the calibrated flow model for the Brändan area could be used for future numerical predictions of planned tracer tests (Gustafsson et al 1987, Nordqvist 1988). Ideally, the calibrated model can be extrapolated to predict flow conditions in two dimensions for different pumping strategies.

8.1.2 Groundwater flow model

The groundwater flow model employed here assumes a porous medium, where variables and parameters describing flow can be described on a continuum basis. The model can be stated mathematically as (Freeze and Cherry, 1979):

$$T \frac{\partial^2 h}{\partial x^2} + T \frac{\partial^2 h}{\partial y^2} - Q = S \frac{\partial h}{\partial t} \qquad (8.1)$$

where T = transmissivity (L^2/T)
S = storage coefficient
h = hydraulic head (L)
Q = fluid sources or sinks (L/T)

Eqn. (8.1) is based on Darcy's law and a continuity equation, and assumes constant density of fluid and confined saturated flow. Further, Eqn. (8.1) assumes that the flow medium is isotropic. Accounting for anisotropic flow conditions, Eqn. (8.1) can be expressed as (Freeze and Cherry 1979) :

$$\frac{\partial}{\partial x}\left(T_x \frac{\partial h}{\partial x}\right) + \frac{\partial}{\partial y}\left(T_y \frac{\partial h}{\partial y}\right) - Q = S \frac{\partial h}{\partial t} \qquad (8.2)$$

During the simulations it was generally assumed that the flow medium is isotropic. Thus, Eqn. (8.1) was used to obtain a calibrated flow model. However, some calculations were also carried out using Eqn (8.2) in order to study effects of anisotropic conditions.

Eqns. (8.1) and (8.2), subjected to boundary and initial conditions, is solved and hydraulic head over the entire region is calculated. The solution in this case was obtained by using the two-dimensional finite element code SUTRA, version 1284-2D (Voss 1984). Although there are a number of techniques available for solving equations for a porous medium in two dimensions, a finite element technique is considered to be appropriate in this case where transient conditions as well as large contrasts in hydraulic parameters are modelled. In addition, irregular shapes can easily be accomodated with finite elements.

Data required to solve Eqns. (8.1) and (8.2) consists of the following:

- geometry for the flow domain

- hydraulic parameters for the flow domain

- boundary and initial conditions

- location and strength of fluid sinks or sources.

8.2 Previous transient flow modeling

Previous efforts to model transient flow in the Brändan area were carried out in order to aid the design and planning of the present hydraulic interference tests (Nordqvist and Andersson 1987). These calculations were based on somewhat limited data and a relatively simple model geometry, and were used mainly to study effects on groundwater flow of stratification in the vertical direction. Nevertheless, the predicted results were directly comparable to the actual interference test data. In this case, any of the different tests can be compared, since this modeling was carried out in a vertical profile, assuming radial symmetry. Four different scenarios were modelled; pumping in subzone 1, pumping in subzone 2, pumping in subzone 3, and pumping in the entire Zone 2. The different subzones refer to the upper, middle and lower parts of Zone 2, respectively. The model geometry and parameter distribution used for the predictive simulations is shown in Figure 8.1. In Figure 8.1, the layer with the K - value (hydraulic conductivity) of 1.0E-05 represents subzone 3 (pumping section for test 1), and the the with a K - value of 2.0E-04 Subzone 1 (pumping section for test 2).

Comparisons between predicted responses for tests 1, 2 and 3B will be discussed in the following sections. The comparisons are presented in Appendices 9.1-12, with the interference test results plotted together with the predicted primary responses and predicted groundwater level responses (or the uppermost

section). The predicted primary responses should be compared to the uppermost observed curve, while the predicted groundwater level responses should be compared to the lowermost observed drawdown curve. The remainder of the predicted sections are here omitted for clarity, and only the predicted extremes are plotted.

8.2.1 Predictions of test 1

Test 1 was performed with the lowermost section of Zone 2 (called subzone 3) as the pumping section, with a discharge rate of 500 l/min. Comparisons of predicted versus measured responses to pumping for test 1 are presented in Appendix 9.1-4.
Assessment of the accuracy of the predictions clearly shows that drawdowns are not predicted well for all the boreholes. For the observation sections located far from the pumped hole (KFI09, KFI10, HFI01), predicted responses are reasonably accurate. However, the general shape of the drawdown curves does not match and steady state appears to be reached too soon in the predictive calculations. As for the sections closest to the pumped section (KFI06, KFI11, BFI01), predicted drawdowns are generally significantly greater than the observed. At some instants, the discrepancies are of the order of one magnitude.

In order to analyze the reasons for the failure of this simple model to predict the responses during test 1, it is necessary to recall the assumed parameter distribution (Figure 8.1). From Figure 8.1 it is seen that the assumed transmissivity (hydraulic conductivity multiplied with the thickness) of subzone 3 is relatively low with low permeability layers surrounding in the vertical direction. Such a configuration will result in the steep gradients as is represented in the different predicted drawdown curves. What this really means, in terms of aquifer evaluation, is that the apparent hydraulic properties of Subzone 3 are different than was assumed in

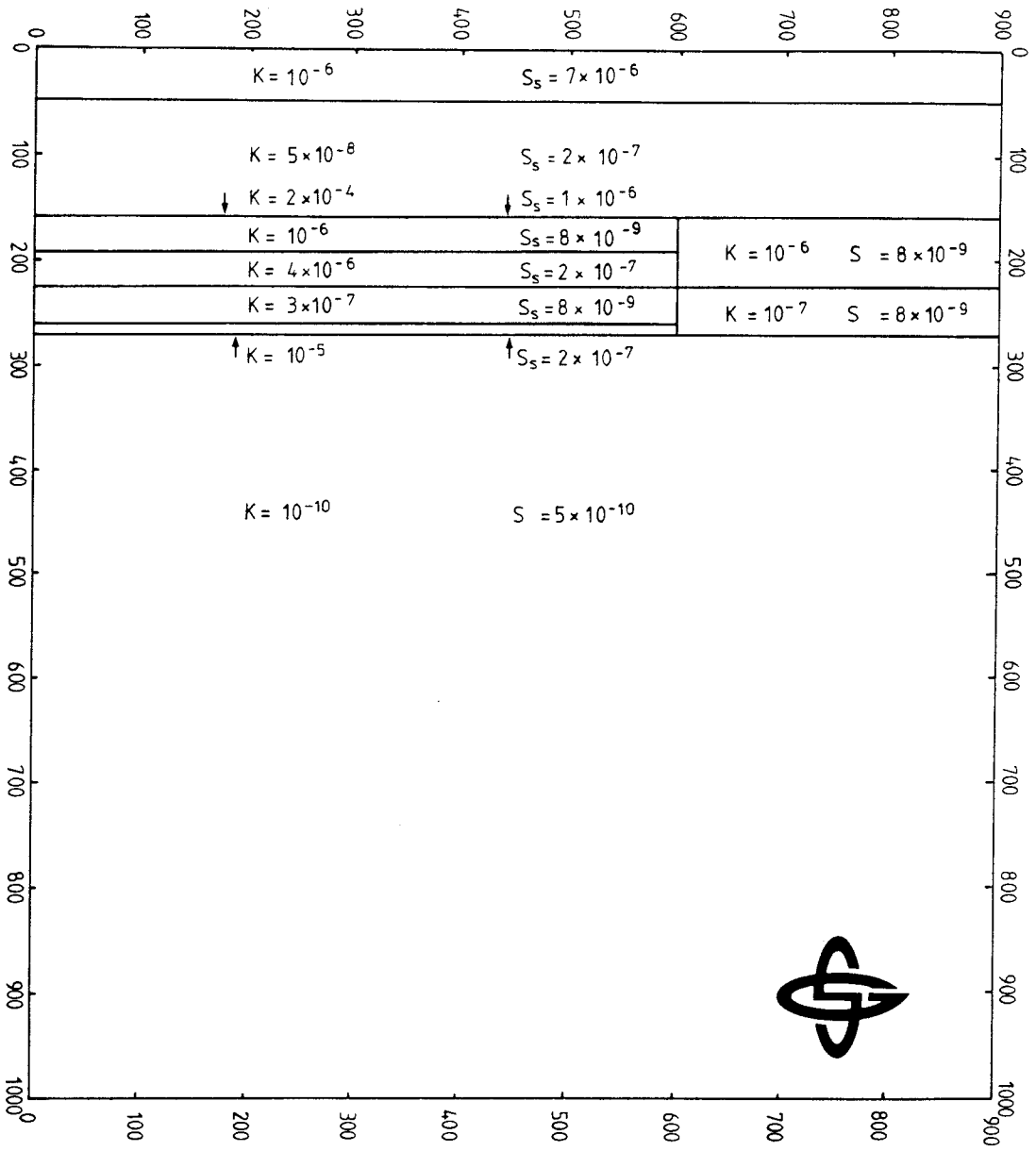

Figure 8.1 Model geometry and parameter distribution used for predictive simulations.

the model. Since the assumed transmissivity of Subzone 3 is reasonably close to what what is indicated from single hole tests (Ekman et al., 1988), one may interpret the result as an indication that Subzone 3 is not as hydraulically isolated (in the vertical direction) from the rest of Zone 2 as the model assumes. It could also be argued that this interpretation is supported by the fact that the separation between the different curves for the observation sections within Zone 2 is very moderate in most cases, indicating that Zone 2 acts more like a homogeneous unit rather than isolated separate subzones.

The failure to reproduce the general shape of the drawdown curves is attributed to a lack of a correct definition of hydraulic boundaries.

8.2.2 Predictions of test 2

The pumping section for this test was the uppermost section of Zone 2 (called subzone 1) with a pumping capacity of 500 l/min. Comparisons of predicted versus observed responses to pumping are presented in Appendix 9.5-8. There were no observations in observation hole KFI05 due to pressure probe failure.

The results in this case resembles those for test 1 to a large extent. Again, predicted responses close to the pumped section are by far too large, while predicted drawdowns in sections located farther away are reasonably accurate. However, neither in this case the general shape of the drawdown curves is accurately reproduced.

The interpretation of the comparison between predicted and measured responses for test 2 will essentially be the same as for test 1, that Zone 2 behaves hydraulically like one single aquifer. There should be no doubt that separate layers (the different subzones), at least piecewise continuous, of relatively high hydraulic conductivity exist within Zone 2, but

that these likely are interconnected by smaller essentially vertical fracture systems, see also Chapter 2. Thus, test 1 and test 2 may be thought of more as pumping of an aquifer with a partially penetrating well.

8.2.3 Predictions of test 3B.

Test 3B was performed in the entire Zone 2 with a pumping capacity of approximately 700 l/min. Comparisons of predicted versus measured responses to pumping are presented in Appendix 9.9-12.

The comparison in this case reveals that, just as for test 1 and test 2, predicted drawdowns are too large for the sections closer to the pumping section (KFI06, KFI11, BFI01). Thus, the interpretation presented above that the separate subzones are in reality not hydraulically isolated units is not sufficient to explain the prediction errors. An obvious additional interpretation would be that the transmissivity of Zone 2 in reality is greater than what was assumed in the prediction model, probably in some combination with incorrectly described boundary conditions.

8.2.4 Summary of model predictions

The numerical predictions were carried out based on somewhat limited data, and using a relatively simplified geometry (radial symmetry in a vertical profile). Zone 2 was modeled as a zone consisting of three highly conductive subzones of finite extension in the horizontal plane, and separated by layers of relatively low hydraulic conductivity.

Comparisons of predicted versus observed results from the interference tests show that the predictions generally are not accurate. The data available for the predictive modelling consisted mainly of single hole packer tests, and some limited

pump test data from pumping during drilling of BFI01. The latter consisted of short time series of a few hours duration. It is apparent that accurate predictions of this kind of interference tests are difficult to make based on the actual information that was available. However, by analyzing the discrepancies between predicted and measured results, some valuable information can be gained about Zone 2.

Both the model predictions as well as analytical interpretations (Chapter 6) indicate that the previously assumed transmissivity of Zone 2 is somewhat low. Further, the different subzones are not isolated units, but are hydraulically interconnected. This is indicated by the fact that measured drawdowns from different observation sections within Zone 2 for a particular observation borehole in most case merge to similiar values of drawdown as steady state is approached. The validity of this interpretation is also supported very nicely by some parameter sensitivity tests performed during the predictive modelling (Nordqvist and Andersson, 1987). In one of those tests the layers separating the subzones were assigned a significantly lower hydraulic conductivity than those in Figure 8.1. An example is shown in Figure 8.2 for a radial distance of 150 m from the pumping section. The result was a significant vertical difference in drawdowns between different subzones within Zone 2, which was generally not observed during the interference tests. However, it should be pointed out that since certain (but small) drawdown differences between different sections actually were observed, this may indicate a somewhat lower hydraulic conductivity in the vertical direction, see also Chapters 5 and 6. An additional important interpretation is that hydraulic boundaries are not accounted for correctly, which is indicated by the shape of the drawdown curves obtained from the interference tests.

In order to obtain an improved model that will describe flow in the Brändan area, some additional data needs are recognized. The most important is a better description of the geometrical framework, with respect to the extent of Zone 2 and the nature of its boundaries. Further, values of transmissivity of Zone 2 would have to be refined. In the following section an attempt to update the groundwater flow model is described. This is important for supporting analytical interpretations of the interference tests and for prediction of results from future tracer tests.

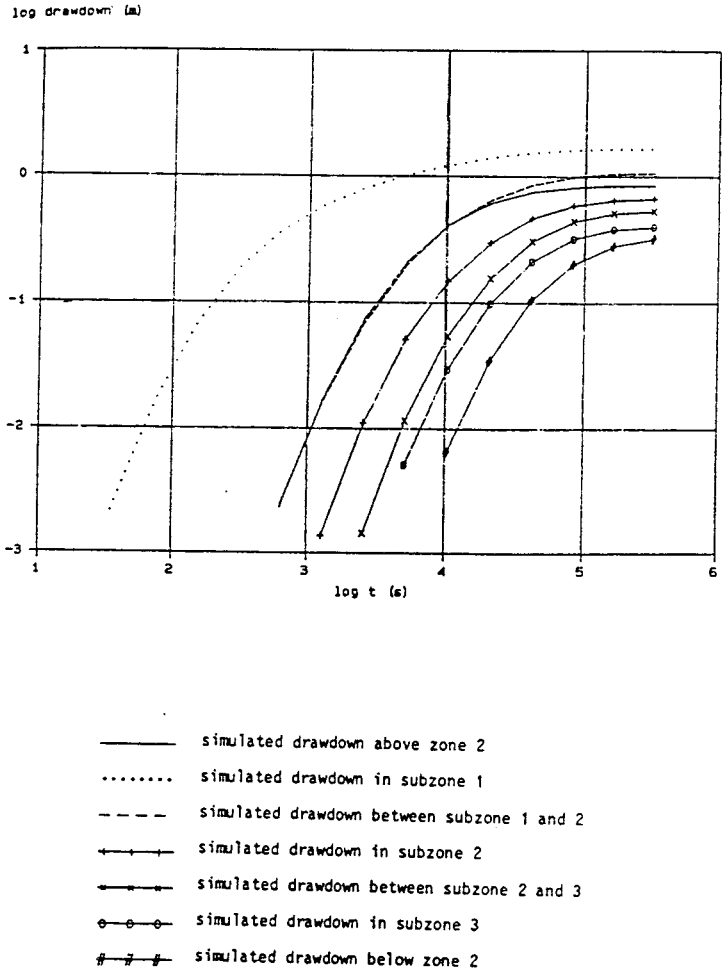

Figure 8.2. Example of low conductivity layers separating the highly conductive subzones.

8.3 Calibration of the updated groundwater flow model

8.3.1 Model Geometry

The flow domain chosen for the model calculations was based on updated interpretations of the geology of the Brändan area (see Chapter 2), and is considerably larger than in any of the previous modeling efforts in this area (Andersson and Andersson 1987, Nordqvist and Andersson 1987). The main justification for this was that data from the interference test were available from boreholes outside Zone 2, such as KFI01 and KFI04. Thus, modeling results outside Zone 2 could be verified, although in a somewhat qualitative manner. The flow domain used for the simulations is shown in Figure 8.3, with the boreholes of interest marked.

Figure 8.3 describes Zone 2 in a horizontal plane as a triangle lined by the vertically oriented Brändan zone along one edge. Along the left edge of the computational domain another vertical fracture zone is included, the Gåvastbo zone. Each rock unit is assumed to be homogeneous in the groundwater flow model.

The flow domain in Figure 8.3 was discretisized into a finite element mesh in order to provide input to the numerical model. The element mesh is shown in Figure 8.4, and consists of 1404 nodes and 1326 quadrilateral elements.

The modeling was performed only in a horizontal plane representing the entire thickness of Zone 2. Zone 2 was modeled as one hydraulic unit with boundary conditions as specified below. It was not considered relevant to attempt to model any of the subzones separately, since the interference test results indicated that a significant part of the flow originated from vertical flows within Zone 2, when pumping only in one of the

subzones. Thus, the test actually simulated is test 3B, pumping in the entire Zone 2 (see Chapter 4).

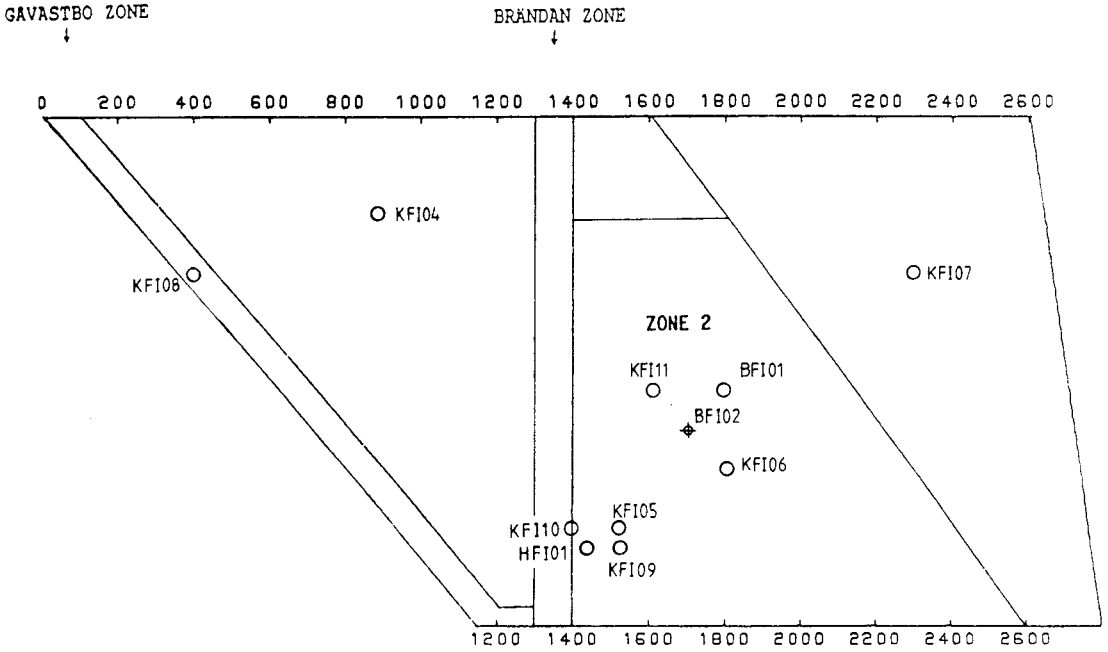

Figure 8.3 Flow domain used for the numerical simulations.

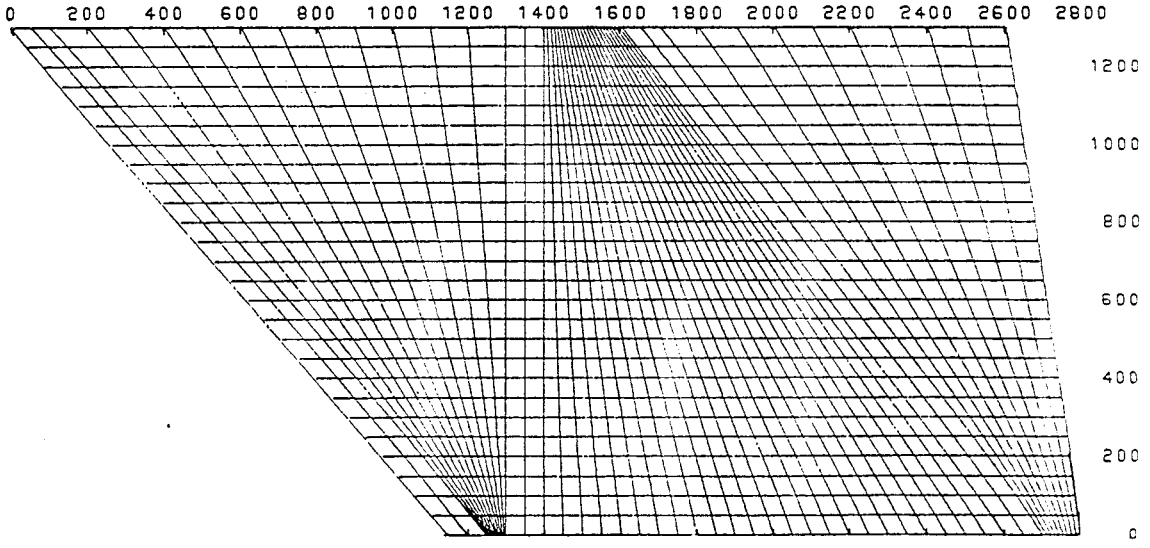

Figure 8.4 Finite element mesh for the modeled region.

8.3.2 Boundary Conditions

One of the main obstacles when attempting to model Zone 2 is to define the hydrogeological boundaries of the zone in the horizontal direction. In the simulations described here, boundaries were defined based on interpretations of the interference test data and geological information. The boundary conditions imposed on the modeled domain are shown in Figure 8.5. No natural gradient is considered, since it is inadequately defined for the model geometry and is judged not to influence the drawdown distribution significantly when pumping from Zone 2. A constant head is assigned to one end of the Brändan zone in order to account for inflow of groundwater possibly originating from lake Finnsjön, which location also approximately corresponds to the groundwater divide (see Figure 1.2). Flow is also allowed in the model to originate from the Gåvastbo Zone (due to the constant head along this boundary), thus entering Zone 2 close to the boreholes HFI01, KFI05, KFI09 and KFI10. The location and hydraulic description of all boundaries should be considered to be approximate.

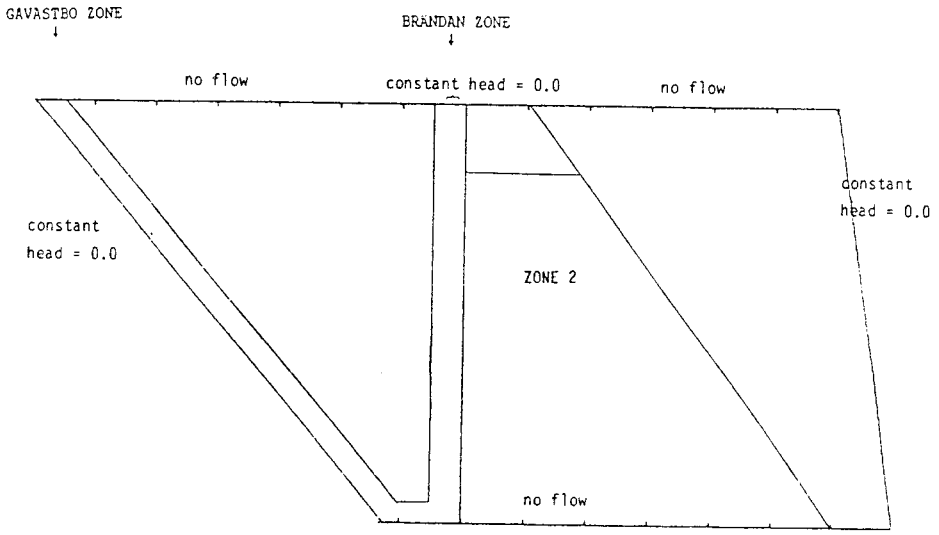

Figure 8.5. Boundary conditions for the modelled region.

As initial conditions for the transient conditions the hydraulic head is set to zero for the entire flow domain. Groundwater withdrawal rate is set to 700 l/min, which corresponds to the pumping rate for test 3B.

8.3.3 Calibration of the model

Calibration strategy and criteria

The approach chosen for calibration of the present flow model was to utilize as much geological and hydrogeological information as possible, in order to obtain an accurate description of the flow conditions in the Brändan area. This involved in addition to the detailed geological interpretations described in Chapter 2, the measured responses from the actual interference tests.

The general procedure was to simulate transient flow, using the assumed geometry of the flow domain, in such a way that an agreement between simulated and measured drawdowns of the primary responses would be achieved. This process is actually a trial and error procedure, which is often employed to solve this kind of inverse problem.

One very important point is that although data of high quality from the interference tests are available for calibration of the flow model, there is at present no way to verify that a calibrated model is a unique solution to this particular system. In order to verify a calibrated model data from a different hydraulic event, for example pumping of a different borehole, would be desirable.

The term calibration criteria refers here to the measure used in order to judge whether a calibration is satisfactory or not. The criterium employed here was simply to visually compare measured and simulated transient drawdown behaviour in

all the monitored boreholes. Differences in drawdown between boreholes were also used to some extent, but in a somewhat more qualitative manner.

The "tuning" parameters for the calibration were transmissivity and storage values, and to some extent the boundary conditions. Boundary effects are detected in the transient drawdown curves as deviations from corresponding type curves for infinite aquifers. A combination of transmissivities, storage coefficients and boundaries that would yield a good fit between measured and simulated primary responses, was considered as an indication that these parameters were correctly estimated. The storage coefficients were basically tuned using the initial stages of the compared curves, while transmissivity values entirely govern steady state drawdowns.

Results of calibrations

The calibrated flow model was arrived at by adjusting hydraulic parameters and boundary conditions until a satisfactory fit between observed and simulated drawdown behaviour was obtained. During this process, extensive interaction between modeling results and analytical aquifer analysis was maintained.

Using the assumed geometry, the parameter distribution yielding the best fit is shown in Figure 8.6. All the separate rock units in Figure 8.6 are here assumed to be homogeneous and isotropic. The separate section at the top of the triangular shape representing Zone 2, was introduced to eliminate undesired effects on flow in Zone 2 of the assigned constant head in the direction of Lake Finnsjön. The simulated and observed transient drawdown curves are shown in Appendix 10.1-4 for the boreholes within Zone 2, and the hydraulic head distribution near steady state is shown in Figure 8.7. Figure 8.7 shows a relatively low hydraulic head gradient within Zone 2 due to the high transmissivity, while steep gradients prevail

in the rock outside Zone 2. Budget calculations carried out by SUTRA indicate that approximately 60% of the discharged fluid in the model originates from the constant head boundary at the upper part of the Brändan Zone in Figure 8.5.

The transient curves show a relatively good agreement between simulated and observed primary responses. The main exception consists of borehole BFI01, where simulated drawdowns are significantly higher than the observed as steady state is approached. As been discussed in Section 6.3, measured responses in BFI01 (and to some extent in KFI11) are not consistent with those observed in other boreholes. The behaviour of KBF01 is not possible to model using the assumptions of the flow geometry and an isotropic medium.

As a qualitative check of the calibrated model, measured responses outside Zone 2 were also compared with the model results. Figure 8.8 shows an example of this, where data from KFI04 (see Figure 8.3 for location) are compared to model calculations. The slopes of the measured and modeled transient curves are similiar, while they differ somewhat timewise. The time discrepancy may be due to open-borehole effects in KFI04 (no packers) not accounted for in the numerical model.

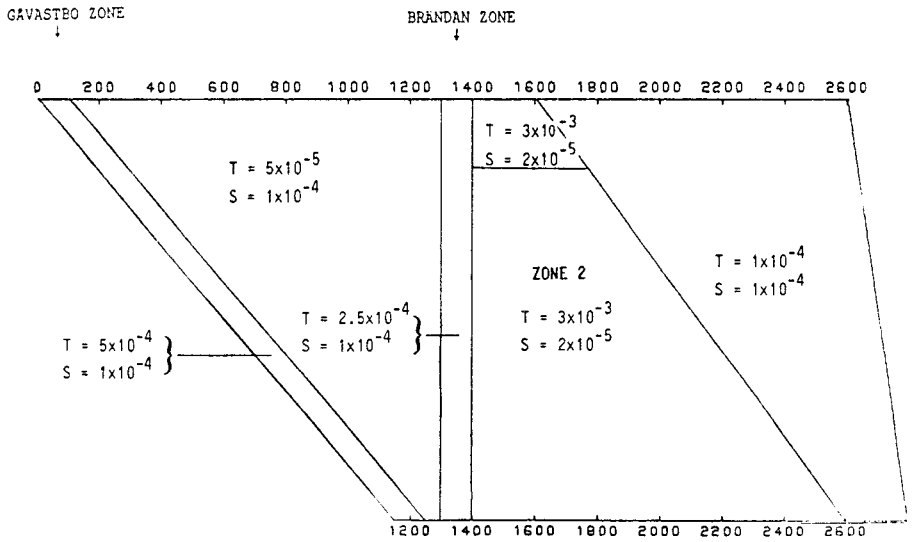

Figure 8.6 Parameter distribution for the calibrated model.

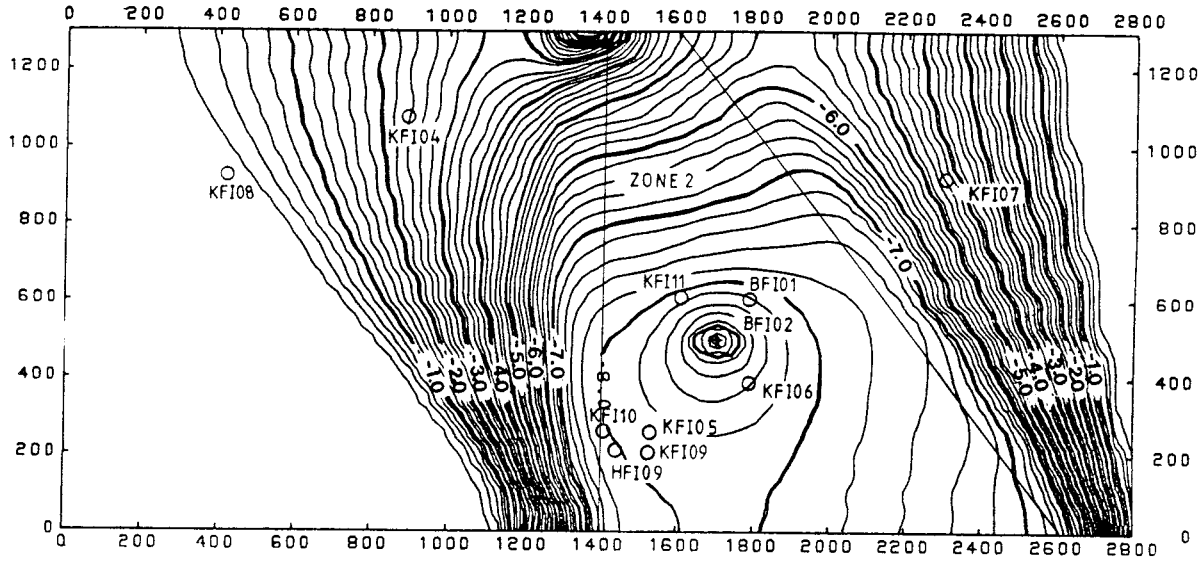

Figure 8.7 Hydraulic head distribution near steady state for the calibrated model.

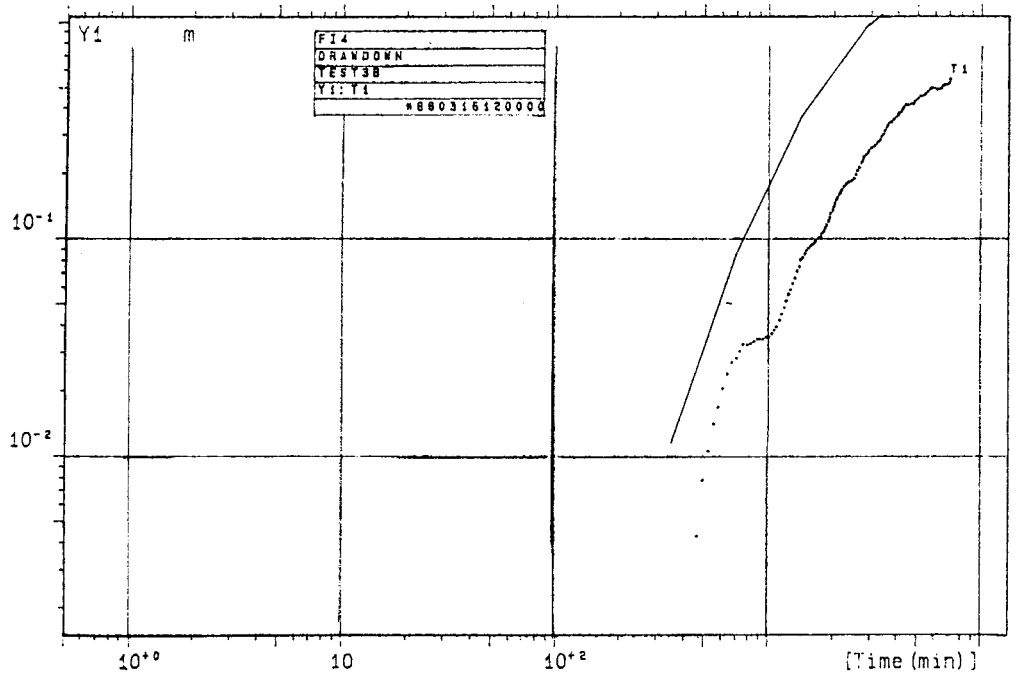

Figure 8.8 Simulated and observed transient responses in borehole Fi 4. Simulated results are represented with a solid line.

8.3.4 Parameter sensitivity

The term parameter sensitivity refers in this case to how flow conditions in the computational domain changes as hydraulic parameters are changed, and is not used as a measure of parameter uncertainty. The effects of parameter changes on the simulation results were not examined systematically, but during the calibration process two main features of the flow system became apparent:

- total drawdown within Zone 2 is generelly governed by the nature of surrounding boundaries. In Figure 8.9 the transmissivity within Zone 2 is increased by approximately one order of magnitude compared to Figure 8.7. Figure 8.9 demonstrates how changes in transmissivity within Zone 2 have very little effect on the magnitude of the drawdowns in the different boreholes.

- hydraulic gradients within Zone 2 are entirely governed by the transmissivity. This is also noted in Figure 8.9, where drawdowns approaching steady state are almost identical in all the boreholes within Zone 2 for the case of high transmissivity.

Figures 8.7 and 8.9 also demonstrates the "bathtub" effect that is a result of a bounded system such as this (see also Section 5.1.1). This means that the drawdown behaviour in general is very similiar between the boreholes within Zone 2. Thus, to explain the observed inconsistencies in observed responses in BFI01 one must include properties not accounted for in the present flow model. These may be local inhomogeneities close to the borehole causing somewhat lower hydraulic connection between BFI02 and BFI01. Another possibility is a general anisotropy within Zone 2. The latter will be examined in the next section.

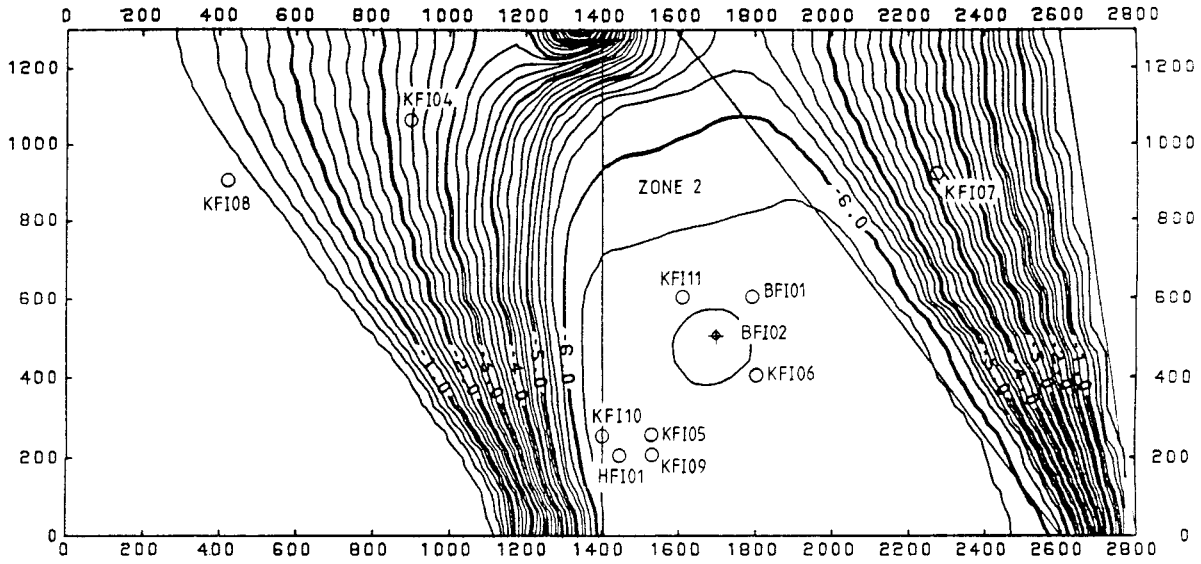

Figure 8.9 Hydraulic head distribution near steady state when using a transmissivity of one order of magnitude larger in Zone 2 than for the calibrated model. See Figure 8.7 for comparison.

8.3.5 Effects of anisotropy

The purpose of studying the effects of anisotropic transmissivity within Zone 2 was to see whether the inconsistent behaviour of the near-region boreholes (KFI06, KFI11, and BFI01) could be explained, while simultaneously simulating responses in the other boreholes. Evidence of anisotropic conditions within Zone 2 are discussed in section 6.3 and in Chapter 7.

The parameter distribution and anisotropy relations imposed on the flow domain in this case is shown in Figure 8.10. The principal directions of the anisotropy are rather arbitrary. It should be pointed out that there is no other observational basis for this anisotropy, than what is possibly indicated from the interference tests.

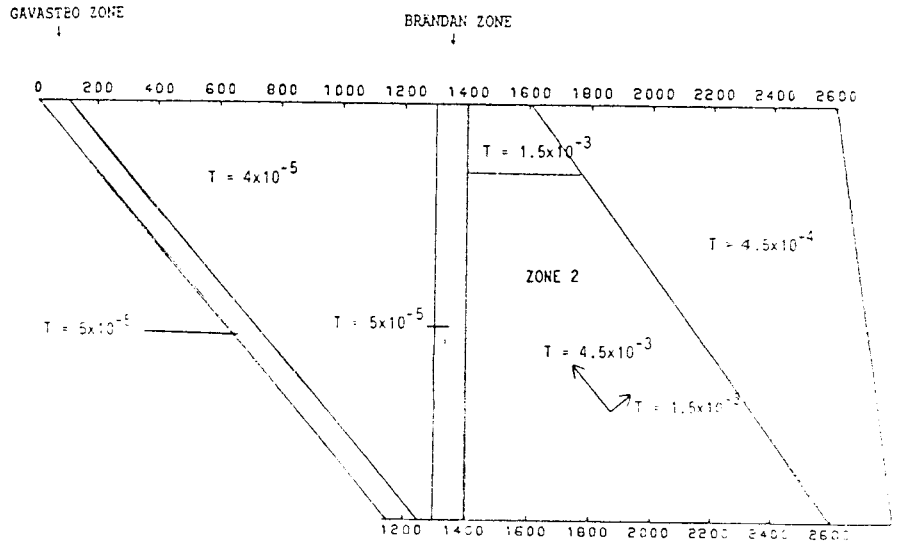

Figure 8.10 Parameter distribution used for the anisotropy studies. Storage values are the same as in Figure 8.6.

The results are shown in Appendix 10:5-8. These indicate that by accounting for anisotropy it may be possible to improve the calibrated model for the boreholes close to the pumped hole, BFI01, KFI06 and KFI11. However, the fits obtained for observation holes KFI05, KFI09, KFI10 and HFI01 are not entirely satisfactory. This could indicate that for this particular geometry responses in these boreholes can not be modeled using the assumed anisotropy relations. It is considered unlikely that further adjustment of hydraulic parameters and boundary conditions could resolve these discrepancies. The hydraulic head distribution near steady state in this case is shown in Figure 8.11.

The implications of the anisotropy modelling are essentially that more questions are raised than answered. With the assumptions of this particular flow geometry, a general anisotropy in Zone 2 may partly explain the observed

inconsistencies for the boreholes close to the pumping hole, but will not improve the calibrated model over the whole flow domain in general. This would suggest that local inhomogenities rather than a general anisotropy in Zone 2 cause the inconsistent drawdown behaviour in BFI01 (and to some extent KFI11 and KFI06), see also Section 6.3 and Chapter 7.

It should be pointed out that there is no way to verify any effects of anisotropy in the flow domain from the results from the interference test. Only pumping of a different borehole within Zone 2 would provide means for such a verification. Possibly will future tracer test be useful for this purpose.

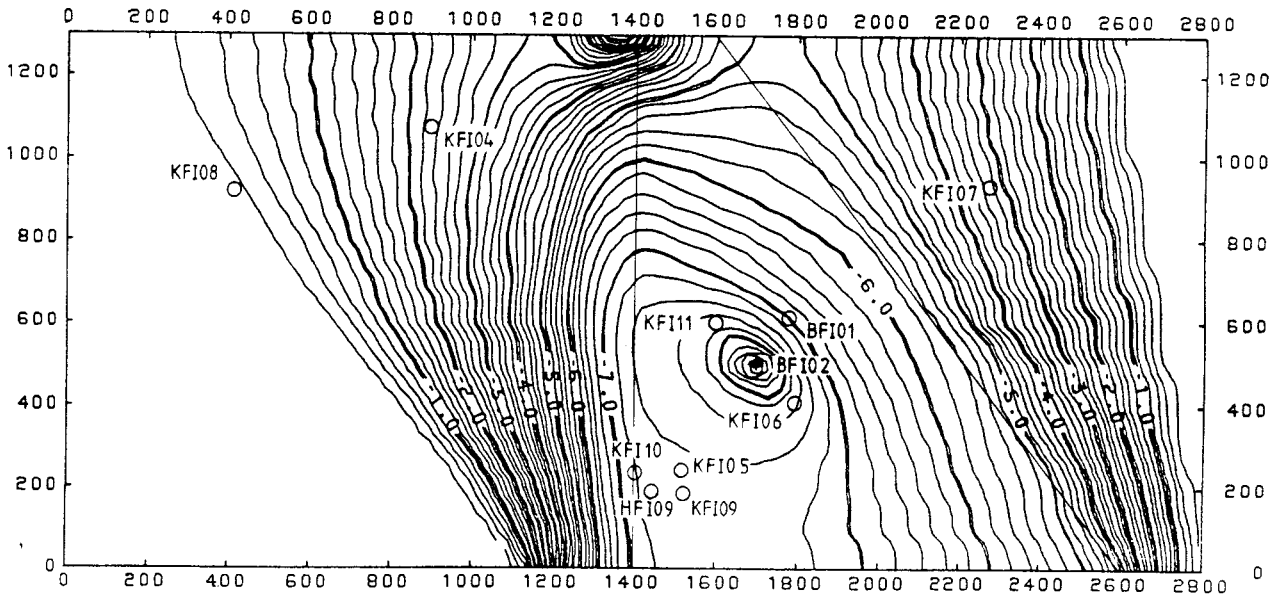

Figure 8.11 Hydraulic head distribution near steady state for the anisotropic case.

8.4 Summary of the numerical simulations

To summarize, the numerical simulations have proven to be very useful when analyzing the hydraulic properties of the Brändan area and Zone 2 in particular. It has been shown that using the assumed geometry of the flow domain, it is possible to simulate the observed responses of the interference test in the boreholes within Zone 2. However, in the boreholes closest to BFi 2 the agreement between measured and simulated responses is not entirely satisfactory.

A comparison of the results in these simulations with previous modeling efforts in Zone 2 indicates that a considerably better understanding of the flow conditions has been gained through the interference tests. The improvements are mainly due to the more detailed description of the flow geometry, which enables a better description of the boundaries of Zone 2.

Some comments should be made regarding the certainty of the parameter distribution obtained during the calibration. Using trial and error as a parameter estimation procedure based on data from a single event, one gets essentially no information about the uniqueness of the obtained parameters. More sophisticated parameter estimation schemes may or may not reveal that other parameter distributions also would explain the observed data. One implication of this is that confidence in predictive ability of the model has to be somewhat restricted. Only data from a different hydraulic event would enable this particular calibration to be verified.

The transmissitivity arrived at in Zone 2, and used in the model, is 3.0E-03 m^2/s, and the storage coefficient 2.0E-05. The limited sensitivity studies shows that the magnitude of the drawdown within Zone 2 is not very sensitive to changes in transmissivity in Zone 2, while hydraulic gradients within Zone

2 are entirely governed by the transmissivity (given the specified boundary conditions).

Applying anisotropic properties to Zone 2 may partly account for the inconsistencies observed in boreholes adjacent to BFI02. However, these calculations are of a somewhat hypothetical character and do not necessarily represent a physical reality.

9. CONCLUSIONS

The present series of interference tests have demonstrated the usefulness of conducting such tests by pumping and recording pressure changes in multiple borehole sections. This provides detailed studies of the propagation of the pressure waves created and the associated flow pattern within Zone 2 and adjacent rock.

The interference tests showed that different flow patterns were generated in regions close to the pumping borehole and at longer distances from this borehole. In the near-region the flow is dominated by the primary responses corresponding to the most rapid flow path between the pumping borehole and the actual observation borehole. These flow paths may be strongly influenced by local heterogeneities between the boreholes, e.g. restricted flow channels, faults etc. The secondary responses in the boreholes (in the near-region) were in general more delayed and attenuated, representing more averaged flow conditions.

In the distant region no dominating primary response generally occurs but instead all borehole responses within Zone 2 almost coincide. These responses are believed to represent the averaged hydraulic properties of the zone, whereas the primary responses in the near-region should represent the short-time behaviour of the system. This interpretation is supported by the fact that the long-term drawdown behaviour in all boreholes was very similar between the different tests, whereas the short-time behaviour in boreholes close to the pumping borehole varied considerably between tests. In these boreholes distinct primary responses were obtained at the beginning of interference tests 1 and 2 when the lower and upper subzones, respectively, were pumped individually. When the entire Zone 2 was pumped (test 3) more averaged responses were obtained both at short and long times.

The interference tests have proved that the upper and lower subzones of Zone 2 have a high hydraulic diffusivity (high transmissivity and low storativity). The transmissivity of each subzone was determined to about 1.5E-3 m^2/s from the time-drawdown analysis of the interference tests. Assuming an effective thickness of about 0.5 m each, the hydraulic conductivity of the subzones is about 3E-3 m/s. These values are in good agreement with the results from the single hole tests within Zone 2.

The storage coefficients calculated, corresponding to the primary responses in the subzones, are generally small, ranging from about 6E-7 to 7E-6 in the near-region boreholes (KFI11 and KFI06) during test 1 and test 2. The lowest storativity values were obtained from test 2, indicating particularly low-porosity flow paths in the uppermost subzone close to BFI02.

From the distance-drawdown analysis for the most distant observation boreholes the representative transmissivity of the entire Zone 2 was estimated to about 3E-3 m^2/s and the storage coefficient to about 2E-5. These values were applied for Zone 2 in the numerical simulations of the interference tests.

Except in the most distant boreholes, differences in drawdown (and recovery) were observed between sections (in Zone 2) in the same borehole. This indicates certain flow restrictions in the vertical direction of Zone 2. From the observed drawdown differences in the boreholes the leakage coefficient of the assumed semi-permeable layer between the subzones was estimated at about 1-5E-8 s^{-1}. Assuming a thickness of about 50 m of the semi-permeable layer, these values correspond to an equivalent porous medium hydraulic conductivity in the vertical direction of Zone 2 of about 1E-6 m/s. However, the actual flow transfer within Zone 2 is likely to be controlled by discrete fractures which locally may have much higher hydraulic conductivity.

Although the responses above and below Zone 2 in general are more slow and attenuated compared to those within Zone 2, they indicate a certain hydraulic interaction between the zone and the over- and underlying rock. However, tests 2 and 3 showed a slower response above the zone in the borehole BFI01 and in the pumping borehole BFI02, indicating good hydraulic isolation towards the overlying rock in these boreholes. During interference test 2 a considerable leakage was estimated from the lower (unpumped) parts of Zone 2, and possibly also from the rock below the zone, to the upper (pumped) part of the zone.

The interference test responses clearly show that Zone 2 hydrogeologically is bounded by outer delimitations. These boundaries are probably constituted by steeply dipping fracture zones as suggested by the geological interpretation. According to this interpretation the geometry of Zone 2 may be characterized by a triangular-shaped area.

Interference test 2 showed that a steady-state was reached by the end of the test, indicating major inflows to Zone 2 during pumping, possibly from adjacent fracture zones, e.g. the Brändan Zone (Zone 1), or other more distant zones.

Observations of the groundwater levels in open boreholes outside Zone 2 showed that significant drawdowns occured at long distances (up to 1.5 km) from BFI02 during the interference tests. This indicates a certain hydraulic interaction between Zone 2 and adjacent areas, possibly via fracture zones or via pressure propagation in the upper part of the bedrock.

The tracer test has confirmed the anisotropic conditions towards the near-region boreholes KFI06, KFI11 and BFI01. In the direction of the dip of Zone 2, i.e. towards borehole BFI01, the calculated hydraulic conductivity and aperture of the flow paths is lower than in the direction of the strike, i.e. towards the boreholes KFI06 and KFI11. The apparent number

of fractures or flow paths contributing to the solute transport is on the other hand likely to be larger in the direction towards BFI01, giving a higher porosity in this direction than in the direction towards KFI06 and KFI11. The residence time of a solute tracer will hence be longer in the direction towards BFI01 than towards the other boreholes. The anisotropic conditions governing the solute transport within the radius of the tracer test may be due to an intersecting fracture zone, which according to the geological interpretations exists between the boreholes BFI01 and BFI02.

The hydraulic fracture conductivities calculated from the tracer test in the upper highly conductive part of Zone 2 are notably high, ranging between 1.6E-1 and 9.7E-1 m/s, but are only a factor 5 - 50 higher than the average hydraulic conductivity determined by single-hole water injection tests in 0.11 m sections of borehole BFI02. The calculated conductivities are also in good agreement with the results from a previously performed flushing water tracer test in Zone 2, between the boreholes KFI11 and KFI11. Over a distance of about 400 m the calculated fracture conductivity ranged between 1.7E-2 - 1.5E-1 m/s, depending on the assumed flow regime and hydraulic gradient. The conclusion is that in the upper part of Zone 2 the fracture conductivities are consistently high over its entire extention.

As mentioned above, the flow porosity calculated for the approximately one metre thick upper zubzone of Zone 2 is larger in the direction towards borehole BFI01 than towards the boreholes KFI06 and KFI11, 1.2E-2 and 3.8E-3 respectively. These values should be compared with values from the flushing water tracer test, assuming flow in Zone 2 being concentrated to three one metre thick subzones. The value obtained from the latter test was 6.7E-3 - 5.9E-2 depending on the assumed flow regime and hydraulic gradient. In spite of the prevailing anisotropic conditions, the flow porosity in the the upper

highly conductive part of Zone 2 seems to be consistent within one order of magnitude.

The dispersivities calculated are low in the primary flow paths, 1.3 - 7.2 m, and in most of the subordinating flow paths, which implies that the solute transport in the groundwater flow paths studied, at the distances and residence times involved, is dominated by advection whereas dispersion is of minor importance. Also no perceptible effect of sorption or matrix diffusion was observed of the non-sorbing tracers used in the highly conductive fracture zone studied.

The responses of the present interference tests were compared to predicted responses from a previous numerical model based on the results from the preliminary interference tests during drilling of BFI01. Since the latter tests were of short duration, no information regarding the outer boundary conditions of Zone 2 could be deduced. This resulted in some discrepancies between predicted and observed responses of the present interference tests. The discrepancies are mainly explained by outer boundary effects and enhanced hydraulic interaction within Zone 2 in the subvertical direction, compared to that assumed in the predictive modeling.

The new model simulations, which take the outer boundary effects into account, have confirmed the chosen, representative values on the hydraulic parameters of Zone 2 calculated from the present interference tests. In general, a satisfactory agreement between simulated and observed drawdown was obtained in the most distant observation boreholes, both at short and long times. However, the agreement decreased for the nearest observation boreholes, particularly at short times. This is quite natural, considering the deviating hydraulic properties in these boreholes (particularly the storage coefficients), which are not incorporated in the model.

Attempts were also made to include a general transmissivity anisotropy within Zone 2 in the numerical model but the overall results were not significantly improved. It is more likely that local heterogeneities in the near-region boreholes dominate the responses in these boreholes than a general transmissivity anisotropy. This demonstrates the problem of scales in flow modeling in crystalline rock.

The overall technical performance of the interference tests, including the data acquisition system, was generally succesful, particularly during tests 1 and 2. The succesful technical performances of the tests are demonstrated by the almost identical data curves obtained from the corresponding drawdown and recovery periods (which is expected by theory). The monitoring of additional parameters in the pumping borehole, e.g. electric conductivity, proved to be very useful by the interpretation of the interference tests.

The interference tests also demonstrated the need of rapid data acquisition (e.g. pressure) during the initial stages of the tests. Need of rapid data sampling may always be expected when pumping and monitoring is performed in isolated borehole sections encompassing fracture zones with high hydraulic diffusivities, especially if, in addition, hydraulic boundary effects are involved.

The results of the present hydraulic interference tests and tracer tests may provide a basis for future development of models for flow and dispersion in fractured crystalline rock. Although Zone 2 within the Brändan area may appear unique in a geological and hydrogeological sense, fracture zones with similar properties are likely to be encountered at other sites. Combined use of hydraulic (interference) tests and tracer tests is recommended in future investigations.

10. REFERENCES

Agarwal R G 1980. A new method to account for producing time effects when drawdown type curves are used to analyze pressure buildup and other test data. Soc. Pet. Eng. Paper 9289, Dallas.

Ahlbom K, Andersson P, Ekman L, Gustafsson E, Smellie J, and Tullborg E-L 1986. Preliminary investigations of fracture zones in the Brändan area, Finnsjön study site. SKB Technical Report 86-05.

Ahlbom K, Andersson P, Ekman L and Tirén S 1987. Characterization of fracture zones within the Brändan area, Finnsjön study site. SKB Progress Report 88-09.

Almén K-E, Andersson O, Axelsen K, Fridh B, Gustafsson E, Hansson K, Johansson B-E, Nilsson G, Olsson O, Sehlstedt M and Wikberg P 1986. Site investigation. Equipment for geological, geophysical, hydrogeological and hydrochemical characterization. SKB Technical Report 86-16.

Andersson J-E and Hansson K 1986. Hydraulic testing in rock: Part 6: Interference tests (In Swedish). SKB Progress Report 86-22.

Andersson J-E, Andersson P and Ekman L 1987. Water injection tests in borehole Fi 10 at the Finnsjön test site. Comparison of tests performed with two different equipment systems. The effects of gas-lift pumping on hydraulic parameters. SKB Progress Report 87-33.

Andersson J-E, Ekman L and Winberg A 1988. Detailed investigations of fracture zones in the Brändan area, Finnsjön study site. Single hole water injection tests in detailed sections. Analysis of the conductive fracture frequency. SKB Progress Report 88-08.

Andersson J and Andersson P 1987. Flow Simulations in a Fracture Zone in the Brändan Area, Finnsjön. SKB Progress Report 87-26.

Brotzen O 1986. On groundwater travel times in granite and gneiss. Paper presented at the 2nd Intern. Conf. on Nuclear Waste Management of the Canadian Nuclear Society. Winnipeg.

Carlsson L, Gentzschein G, Gidlund G, Hansson K, Svenson T and Thoregren U 1980. Supplementary permeability measurements in the Finnsjön area (In Swedish). KBS Technical Report 80-10.

Carlsson L and Gustafson G 1984. Pumping tests as a geohydrological investigation method (In Swedish). R41:1984. ISBN 91-540-4106-6 Statens råd för byggnadsforskning, Stockholm.

Earlougher R C 1977. Advances in well test analysis. Monograph Series, Society of Petroleum Engineers of AIME, Dallas.

Ekman L, Andersson J-E, Andersson P, Carlsten S, Eriksson C-O, Gustafsson E, Hansson K, and Stenberg L 1988. Documentation of borehole BFi 2 within the Brändan area, Finnsjön study site. The Fracture Zone Project - Phase 3. SKB Progress Report in prep.

Freeze R A and Cherry J A 1979. Groundwater. Prentice-Hall.

Gelhar L W 1987. Applications of stochastic models to solute transport in fractured rocks. SKB Technical Report 87-05.

Gustafsson E and Andersson P 1989. Groundwater flow conditions in a low angle fracture zone at Finnsjön, Sweden. Paper for submission to Chemical Geology, In prep.

Gustafsson E, Andersson P and Larsson N-Å 1987. The Fracture Zone Project in Finnsjön, Phase 3. Proposal for tracer experiments. SKB Progress Report 87-34.

Gustafsson E and Eriksson C-O 1988. Characterization of Fracture Zones in the Brändan area, Finnsjön study site: Determination of groundwater flow by the point dilution method in packed off sections in the boreholes BFi 1 and HFi 1. SKB Progress Report in prep.

Gustafsson E and Klockars C-E 1981. Studies on groundwater transport in fractured crystalline rock under controlled conditions using non-radioactive tracers. SKB Technical Report 81-07.

Hantush M S 1967. Flow to wells in aquifers separated by a semipervious layer. J. Geophys Res. 72 (6) pp 1709-1720.

Kreft A, Lenda A, Turek B, Zuber A and Czauderna K 1974. Determination of effective porosities by the two-well pulse method. Isotope Techniques in Groundwater Hydrology. Proc. Symp. IAEA Vienna.

Larsson N-Å and Jacobsson J-Å 1982. Studies of the groundwater level above two fracture zones in the Finnsjön test site (In Swedish). SKB Progress Report 82-36.

Lenda A and Zuber A 1970. Tracer dispersion in groundwater experiments. Isotope Hydrology, Proceedings of a symposium, IAEA Vienna.

Munier R and Tirén S A. Geometry and kinetics of deformation zones in the Finnsjön area, central Sweden: A deformation system controlled by five sets of shear zones. SKB Progress Report (In prep.).

Neuman S P and Witherspoon P A 1969a. Theory of flow in a confined two aquifer system. Water Resour. Res. 5(4) pp 803-816.

Neuman S P and Witherspoon P A 1969b. Applicability of current theories of flow in leaky aquifers. Water Resour. Res. 5(4) pp 817-829.

Niva B 1987. Detailed investigations of fracture zones in the Brändan area, Finnsjön study site. Borehole radar measurements in the borehole BFi 1. SKB Progress Report 87-07.

Nordqvist R and Andersson J-E 1987. Transient flow simulations in a fracture zone in the Brändan area, Finnsjön. SKB Progress Report 88-11.

Nordqvist R 1988. Numerical predictions of a radially converging tracer test in a fracture zone in the Brändan area, Finnsjön. SKB Progress Report in prep.

Norton D and Knapp R 1977. Transport phenomena in hydrothermal systems: The nature of porosity. Amer. Journal of Science. Vol 277, pp 913-936.

Nyberg G 1988. Manual for data acquisition in hydrotesting at the Swedish Hard Rock Laboratory (In Swedish). SKB Technical PM 25-88-003.

Puigdomenech I and Nordstrom K 1987. Geochemical interpretation of groundwaters from Finnsjön Sweden. The Royal Institute of Technology, Stockholm / US Geological Survey, Menlo Park, California. SKB Technical Report 87-15.

Smellie J, Gustafsson E and Wikberg P 1987. Groundwater sampling during and subsequent to air-flush rotary drilling: Hydrochemical investigations at depth in fractured crystalline rock. SKB Progress Report 87-31.

Snow D T 1968. Rock fracture spacings, openings and porosities. J. Soil Mech. Found. Div. Proc. ASCE, Vol 14, No SM 1.

Stenberg L 1987. Detailed investigations of fracture zones in the Brändan area, Finnsjön study site. Investigations with the Tubewave method in boreholes Fi 6 and BFi 1. SKB Progress Report 87-08.

Voss C 1984. A finite-element simulation model for saturated-unsaturated fluid-density-dependent groundwater flow with energy transport or chemically reactive single species solute transport. U.S. Geological Survey, Water Resources Investigations Report 84-4369, 1984.

APPENDICES

Contents of Appendices

APPENDIX 1

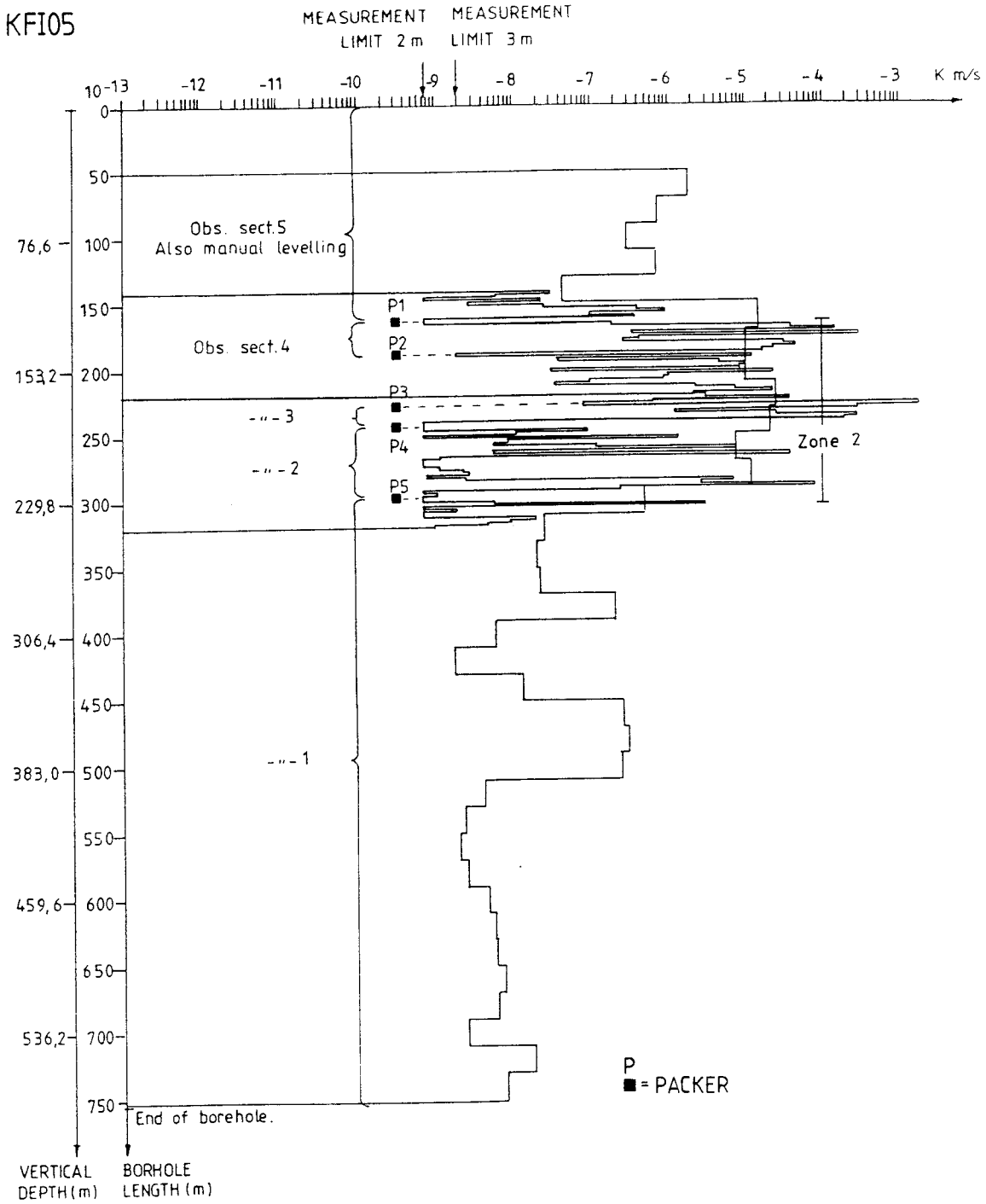

Appendix 1:1 Packer configuration in observation borehole KFI05.

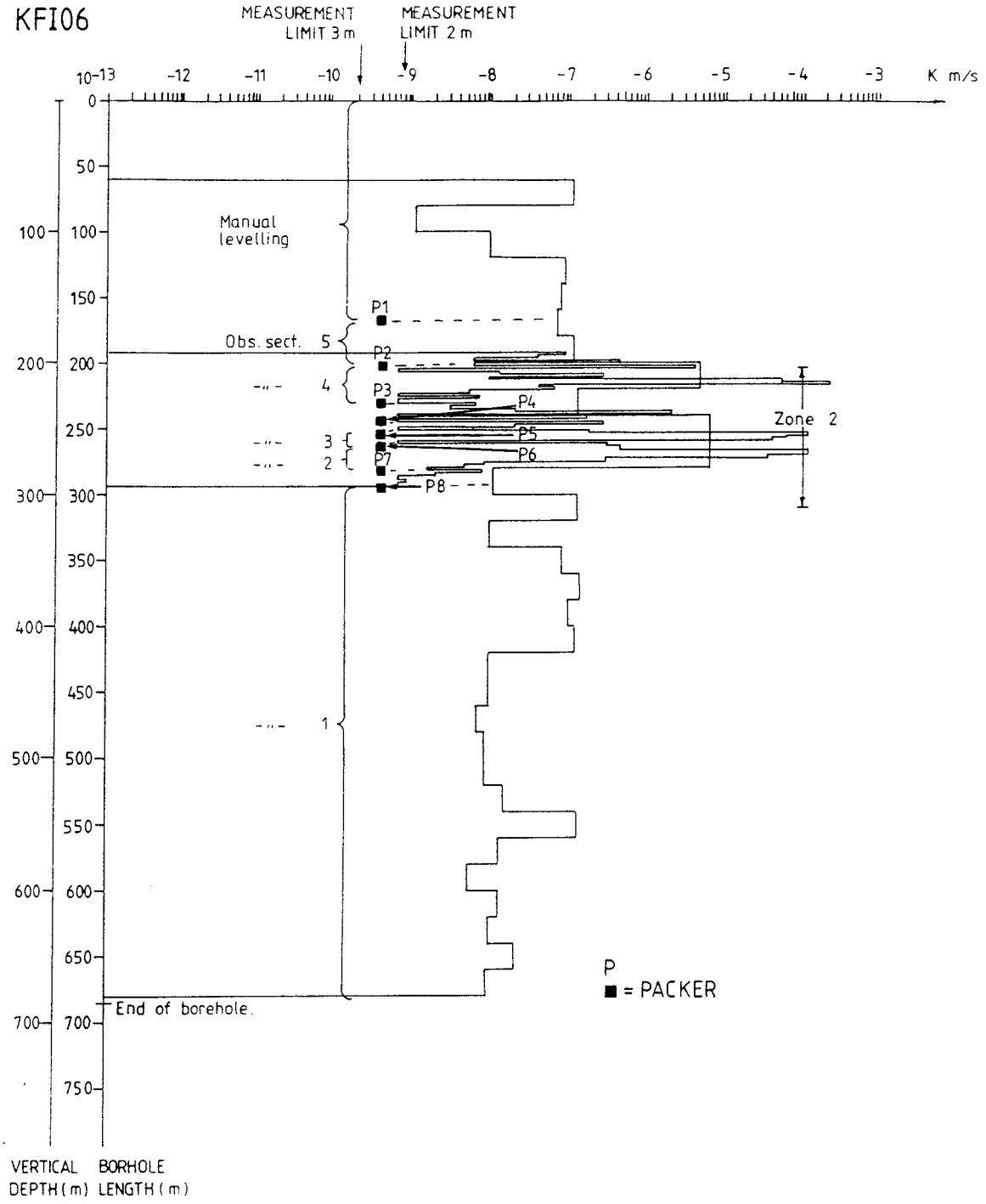

Appendix 1:2 Packer configuration in observation borehole KFI06.

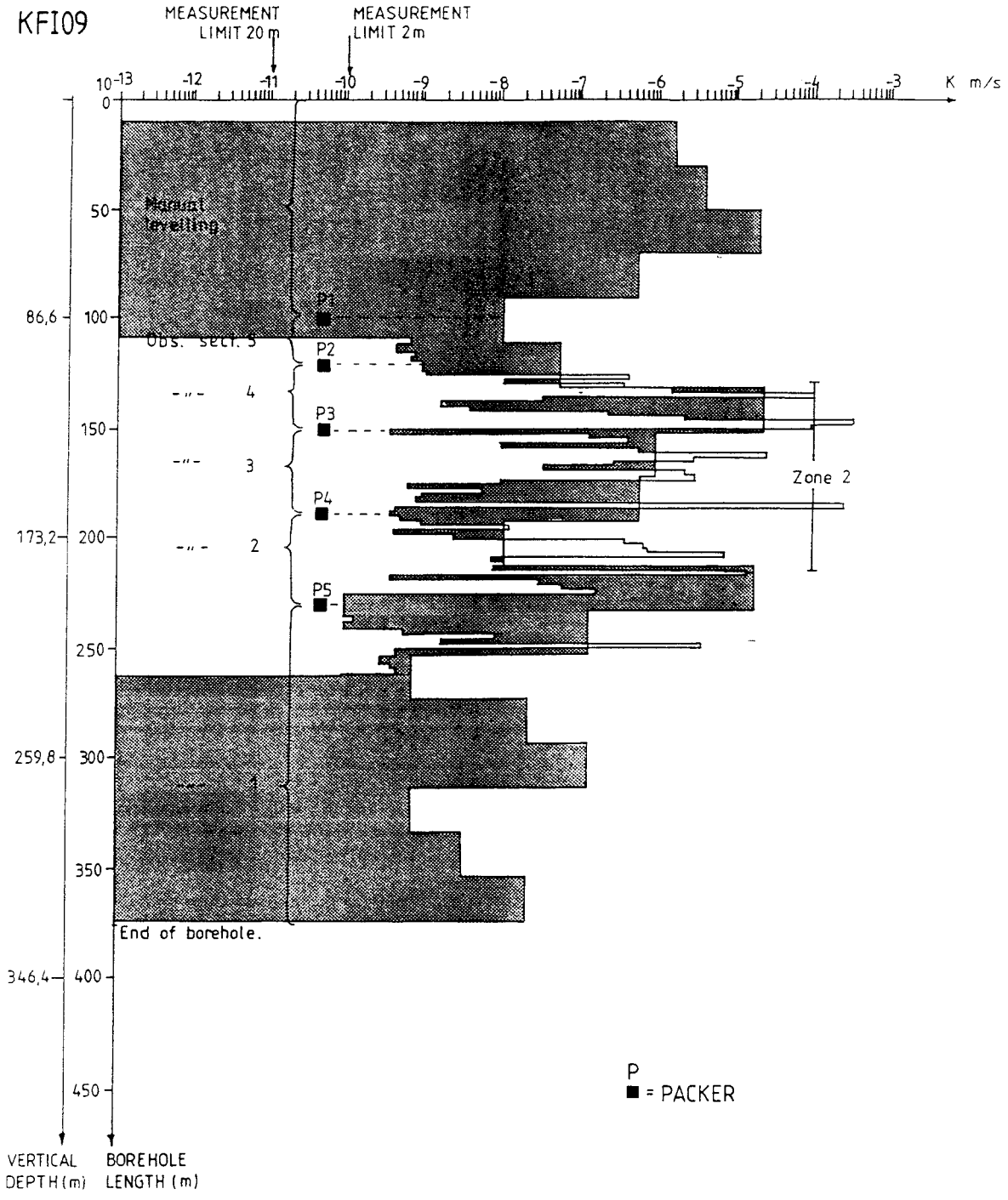

Appendix 1:3 Packer configuration in observation borehole KFI09.

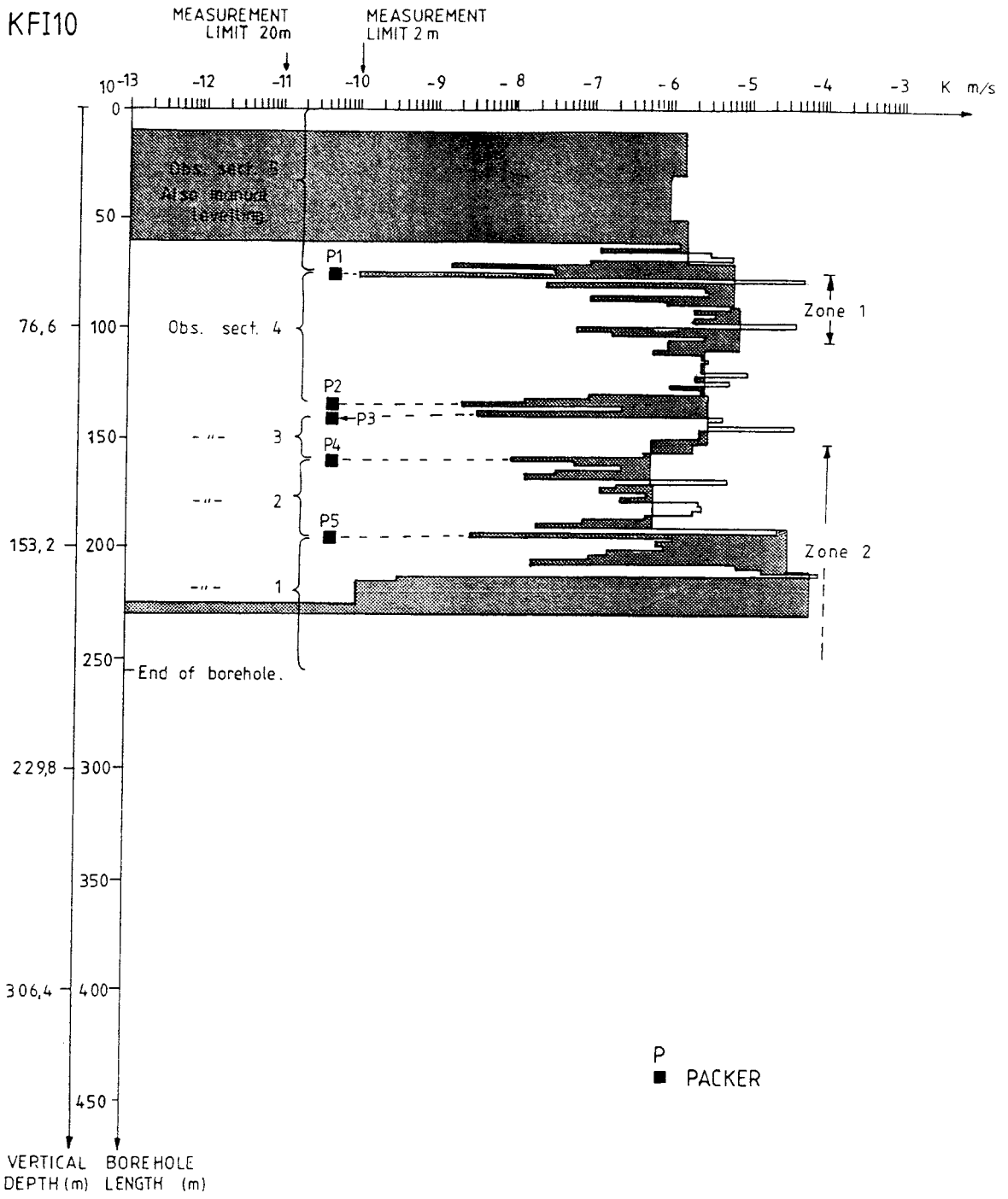

Appendix 1:4 Packer configuration in observation borehole KFI10.

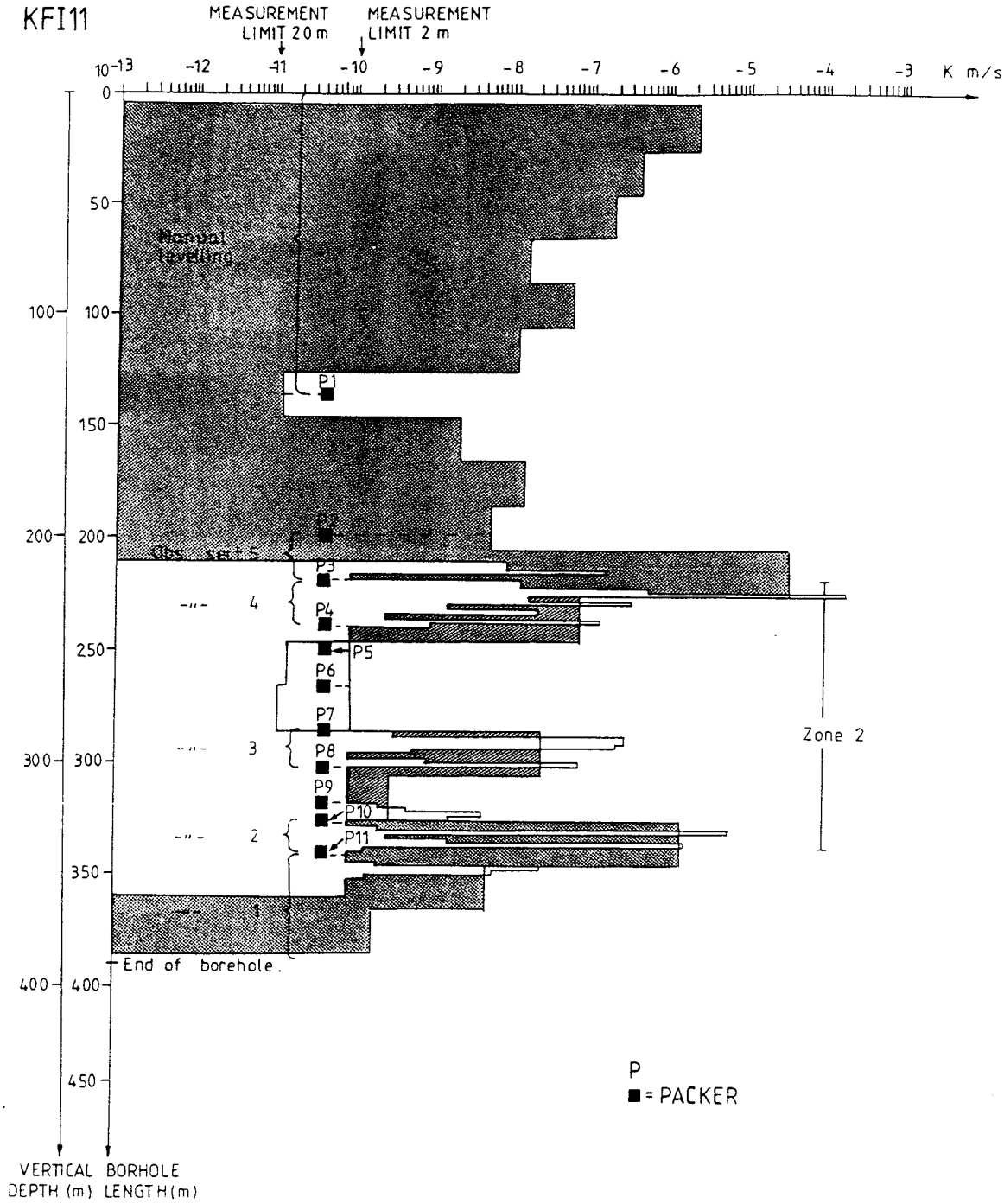

Appendix 1:5 Packer configuration in observation borehole KFI11.

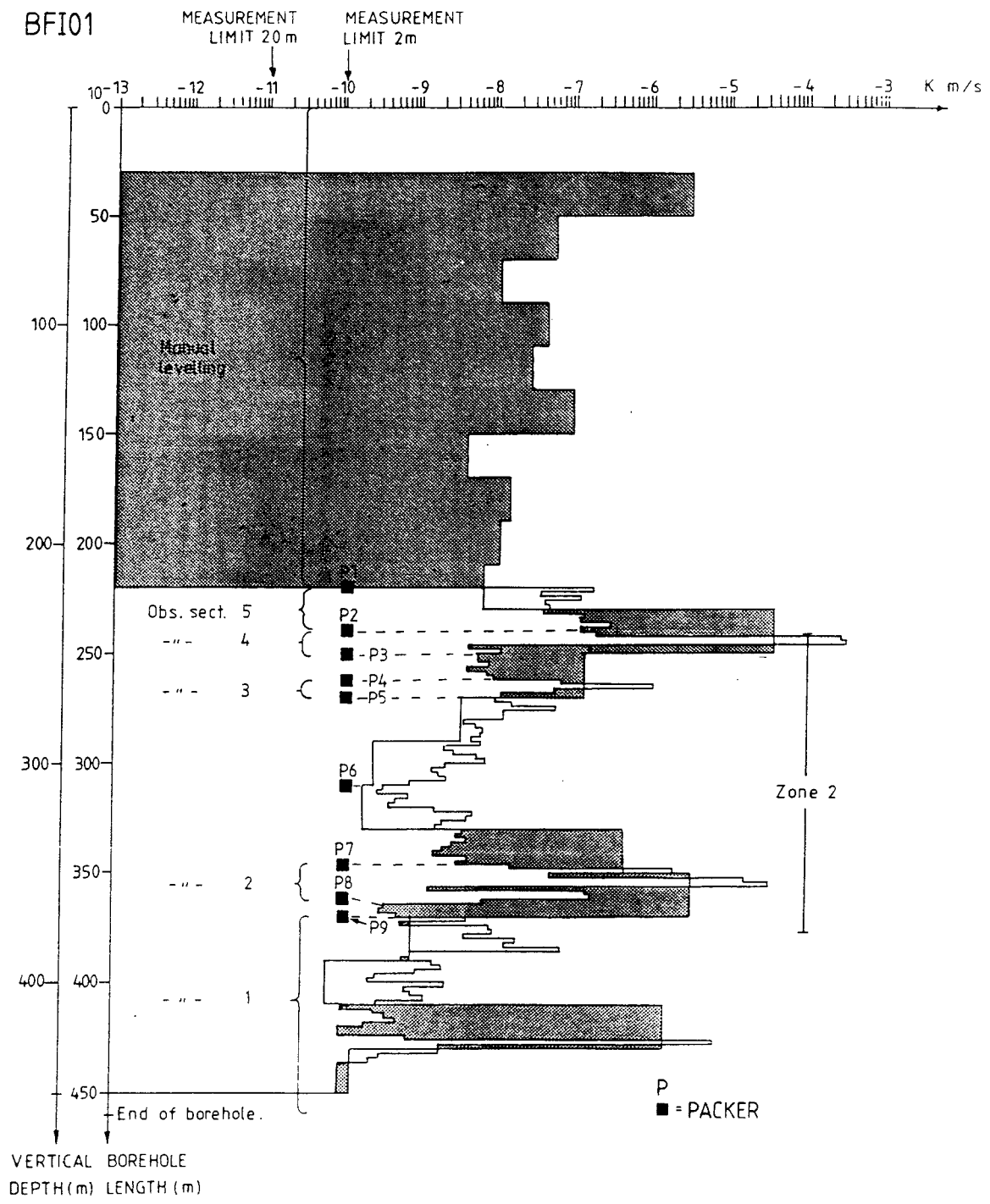

Appendix 1:6 Packer configuration in observation borehole BFI01.

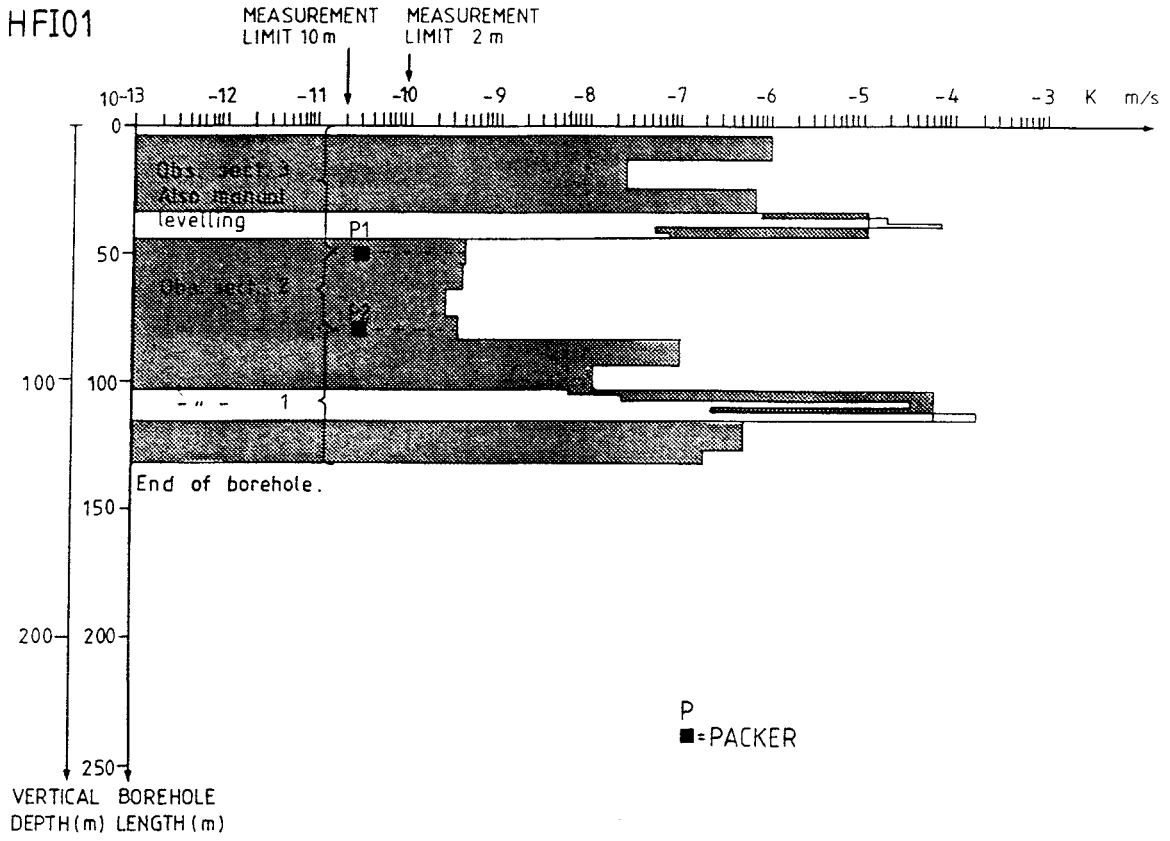

Appendix 1:7 Packer configuration in observation borehole HFI01.

LEGEND

Symbols used for parameters measured in the pumping borehole BFI02 and for sections in the observation boreholes.

Pumping borehole

⋯⋯	flow rate
+ + + + +	electric conductivity
▫ ▫ ▫ ▫ ▫	barometric pressure head
× × × × ×	temperature

Observation boreholes

◆ ◆ ◆ ◆ ◆	section 5 (upper)
▫ ▫ ▫ ▫ ▫	section 4
× × × × ×	section 3
+ + + + +	section 2
⋯⋯	section 1 (lower)

Note that the numbers on all linear scales should be multiplied by factors specified at the top of each scale.

APPENDIX 2

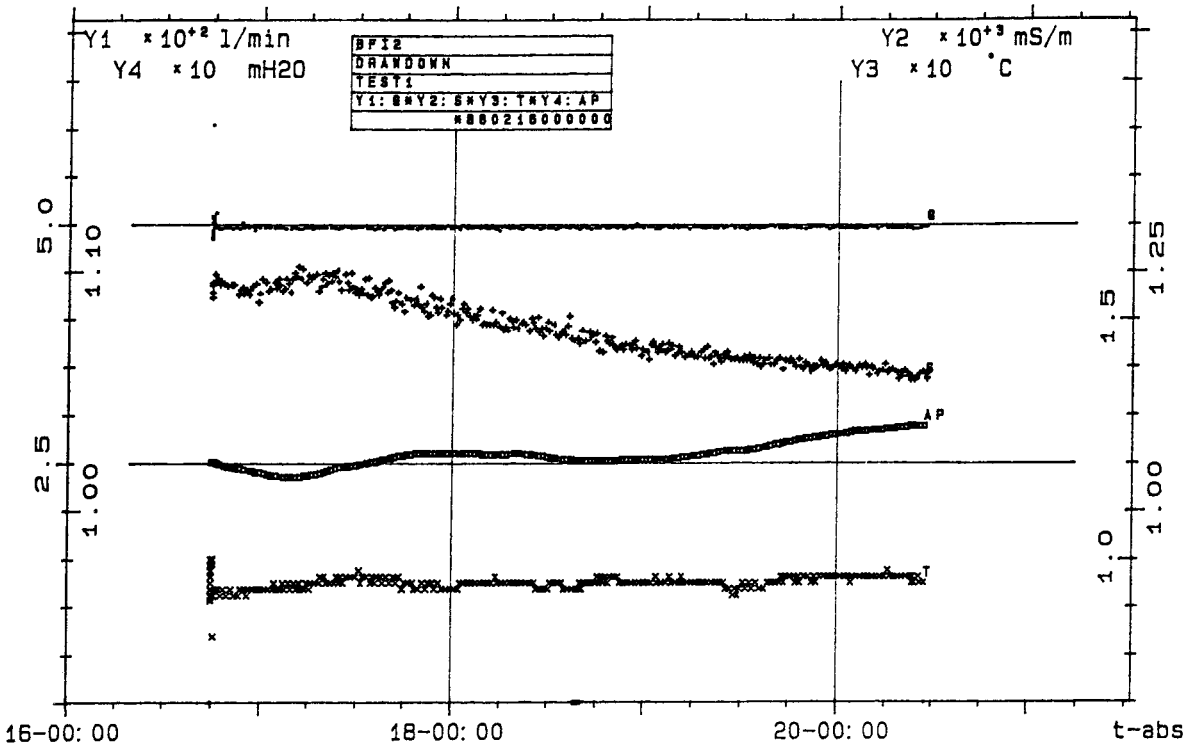

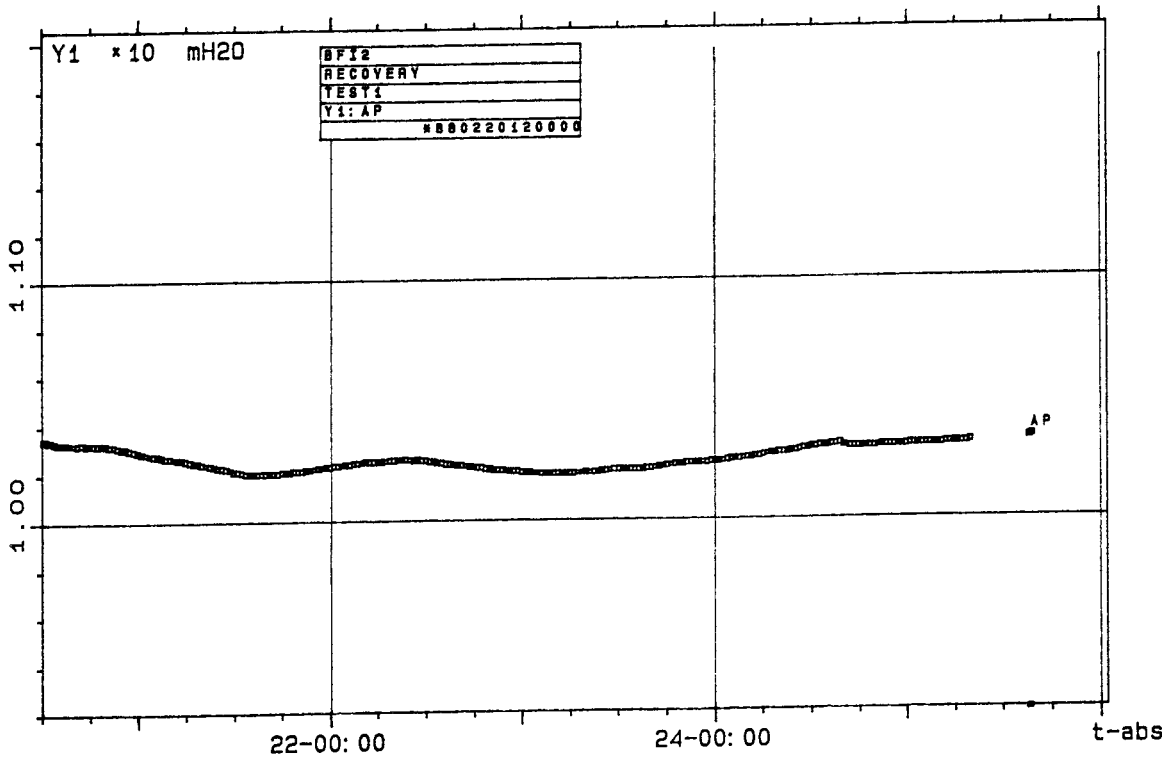

Appendix 2:1 Flow rate, electric conductivity, barometric pressure head and temperature during interference test 1 (linear time scale).

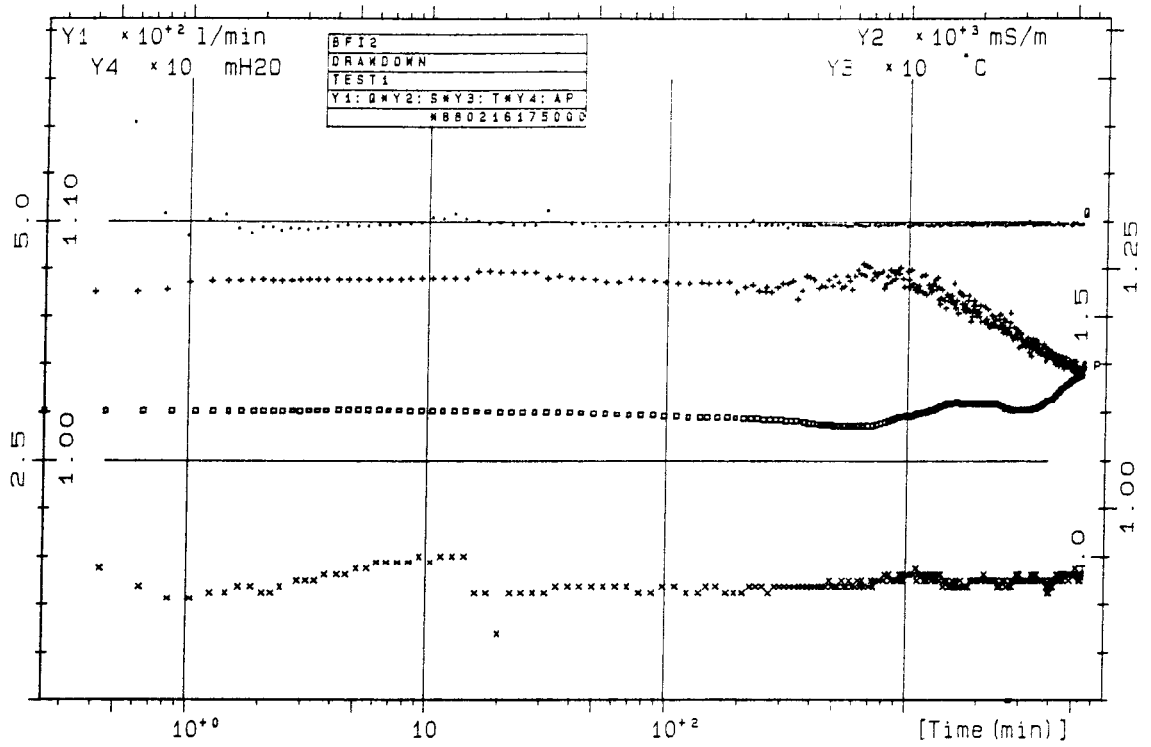

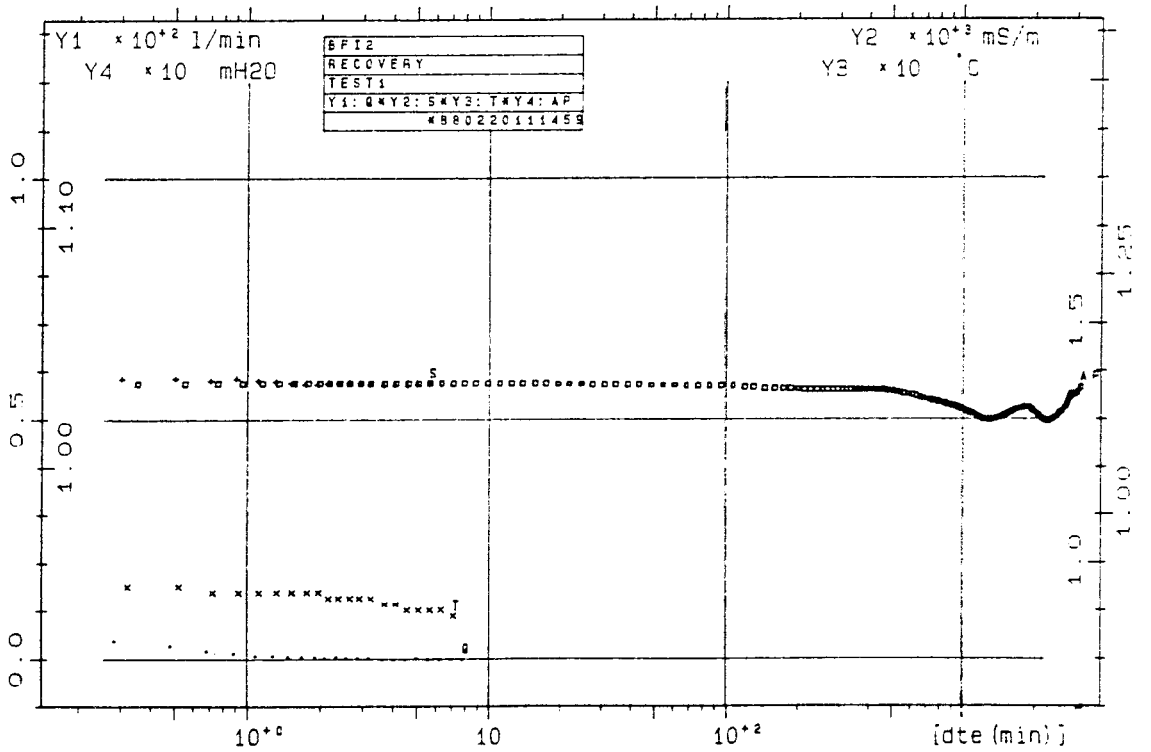

Appendix 2:2 Flow rate, electric conductivity, barometric pressure head and temprature during interference test 1 (logarithmic time scale).

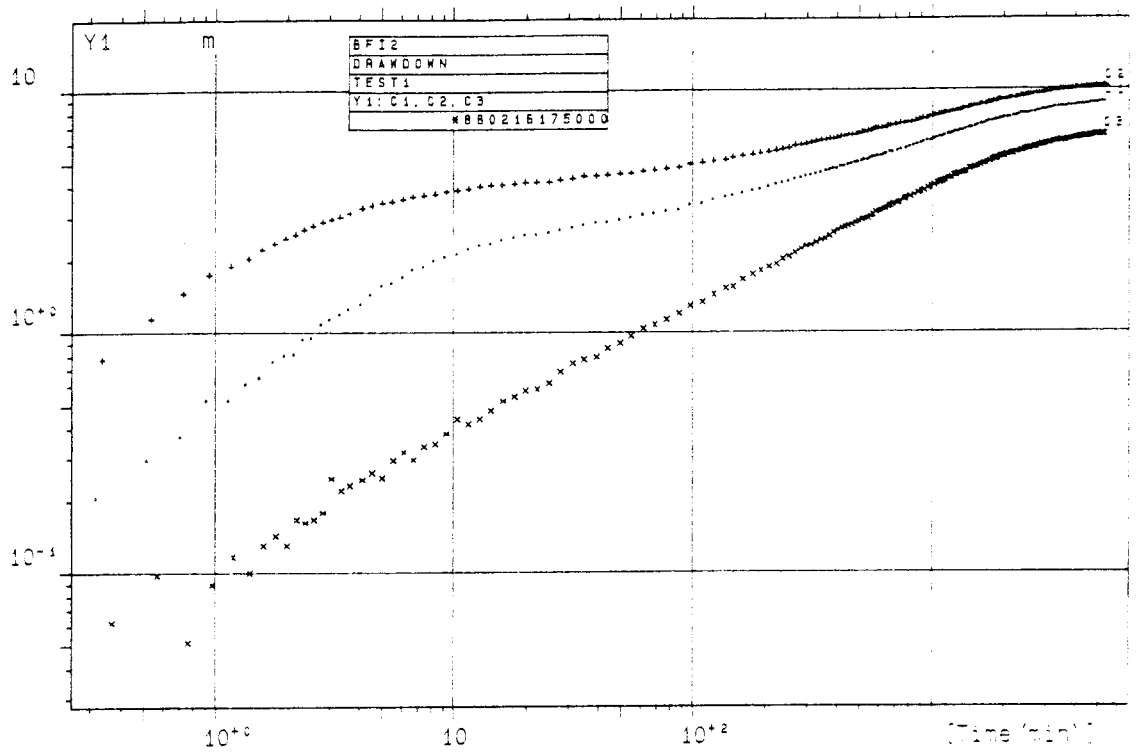

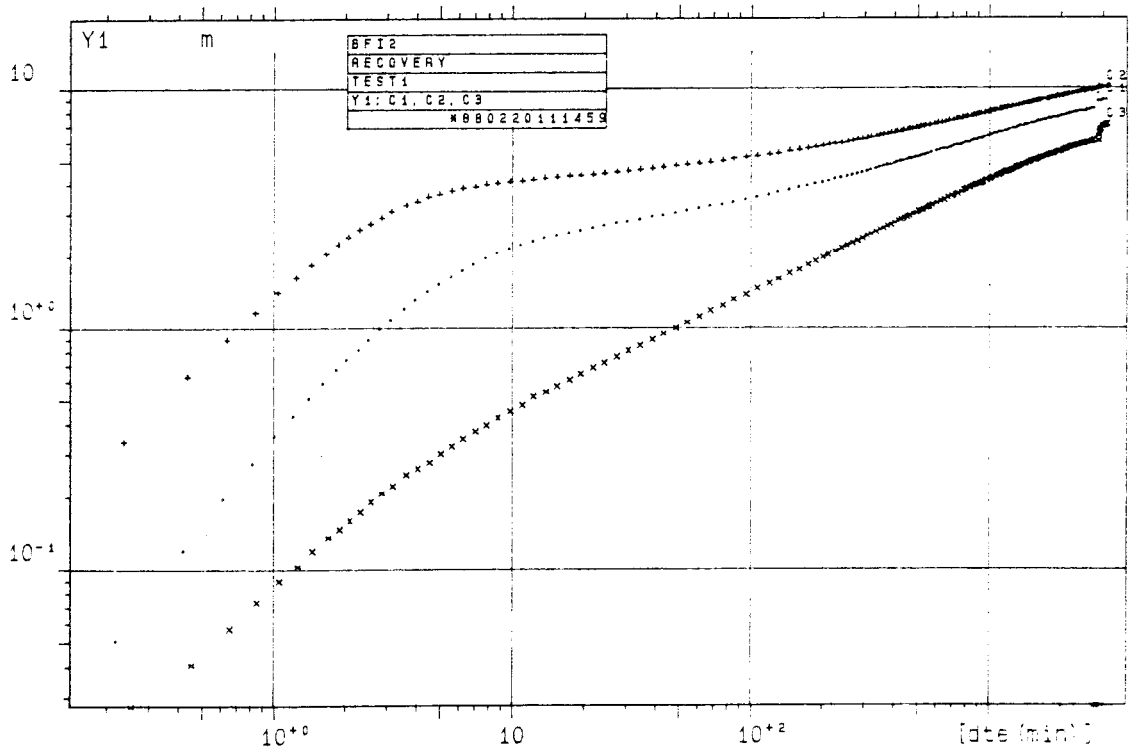

Appendix 2:3 Observed drawdown and recovery in borehole BFIC2 during interference test 1.

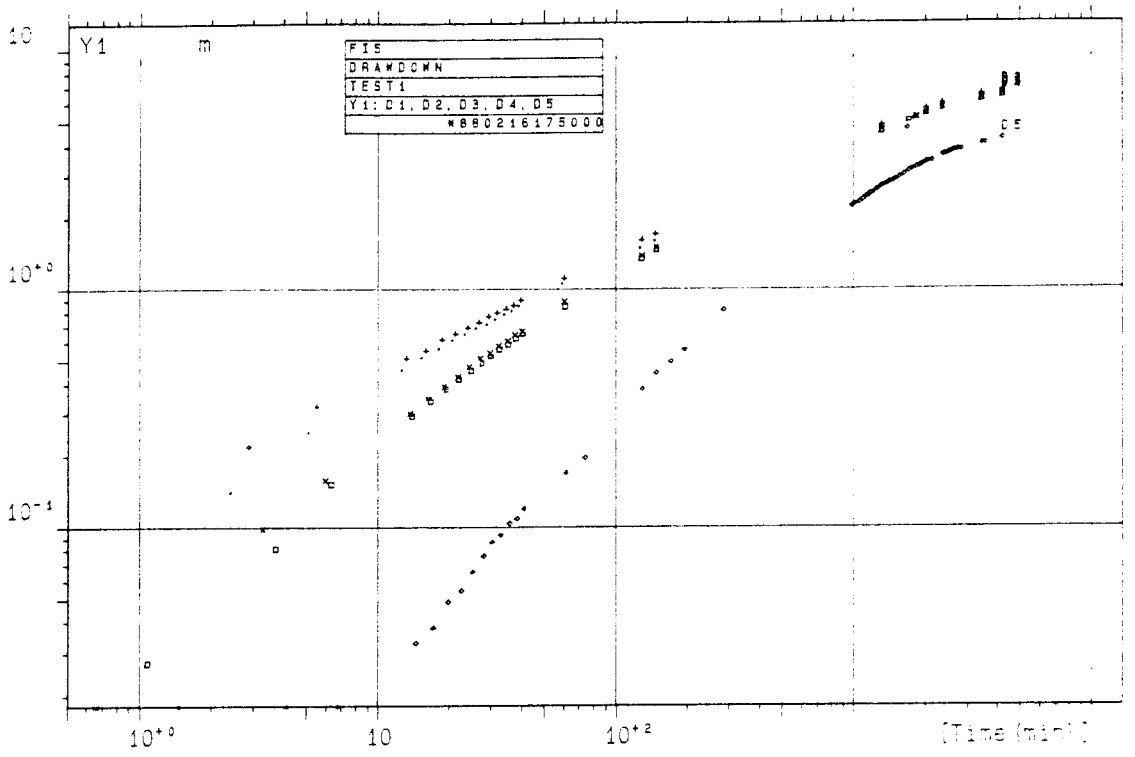

Appendix 2:4 Observed drawdown in borehole KFI05 during interference test 1 (recovery not measured).

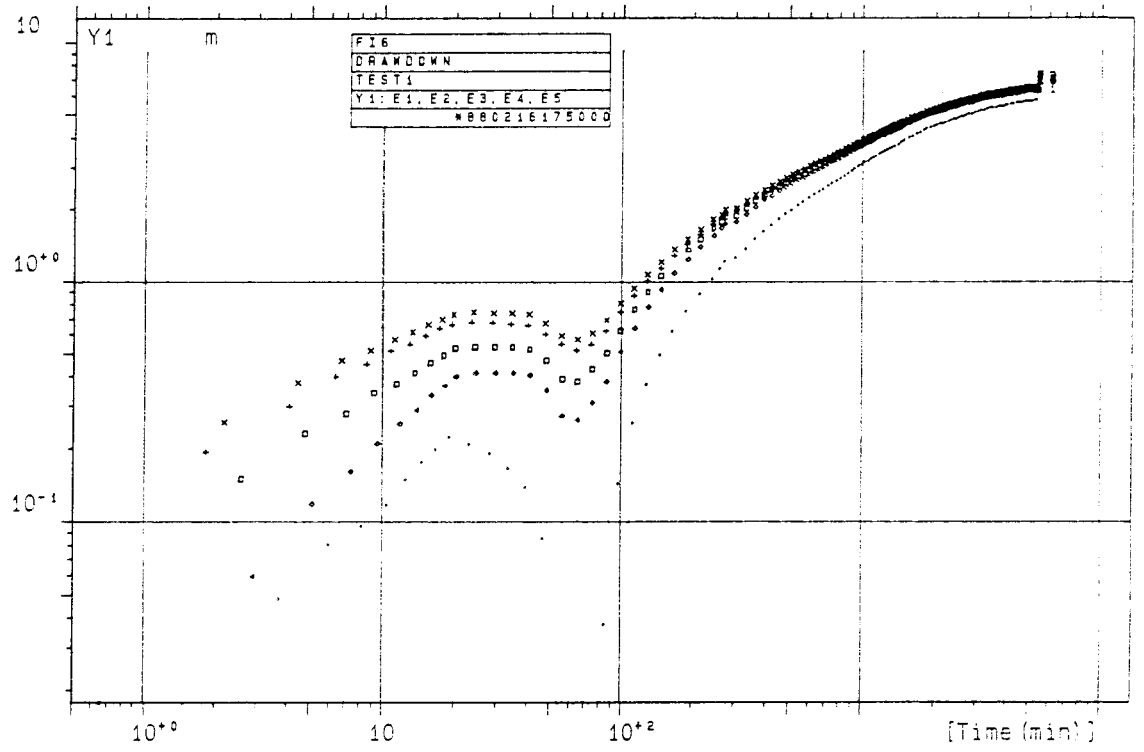

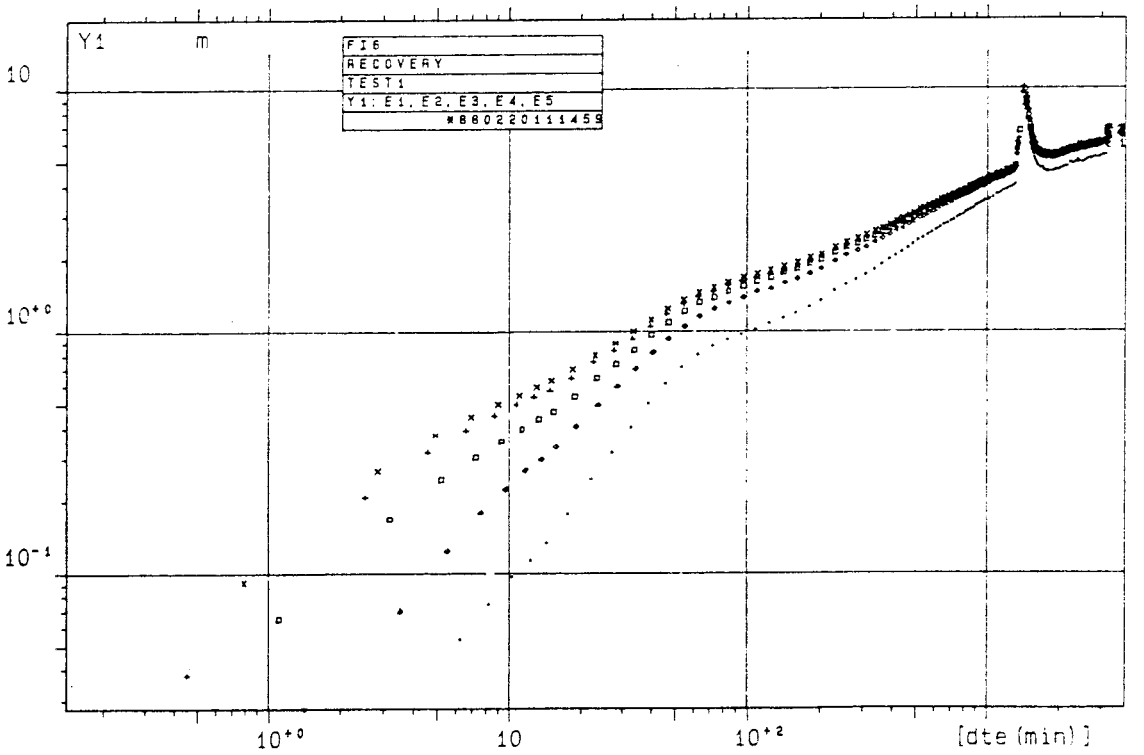

Appendix 2:5 Observed drawdown and recovery in borehole KFI06 during interference test 1.

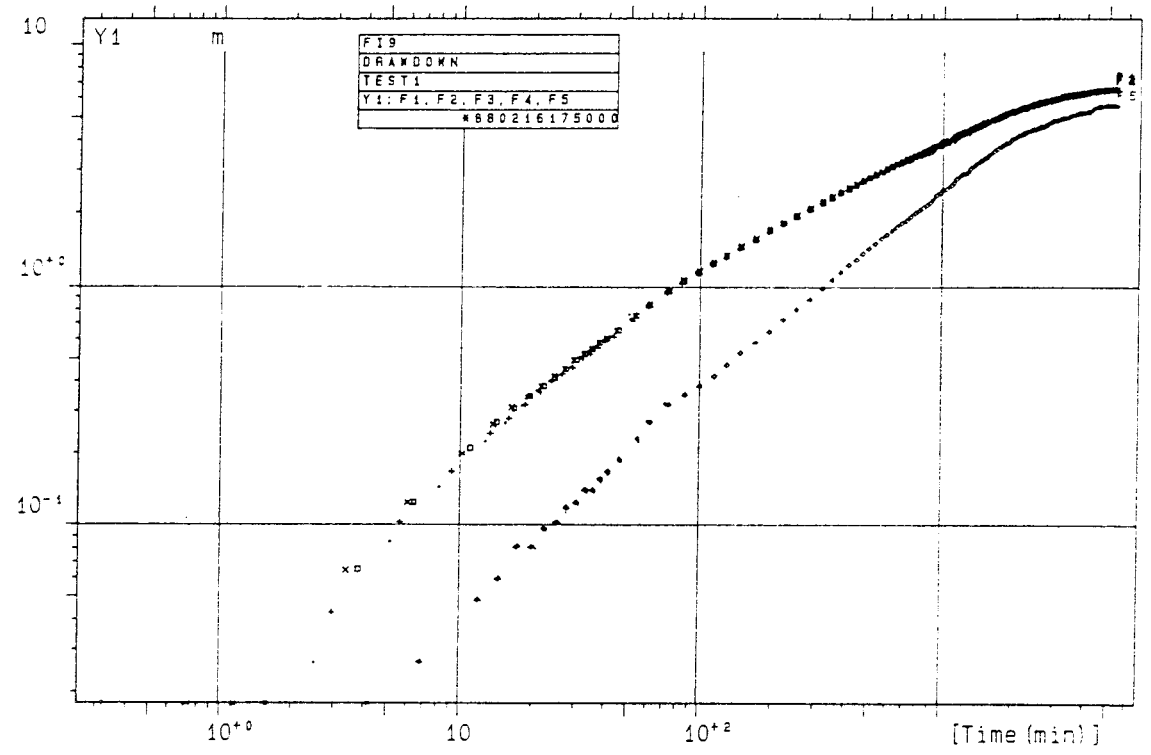

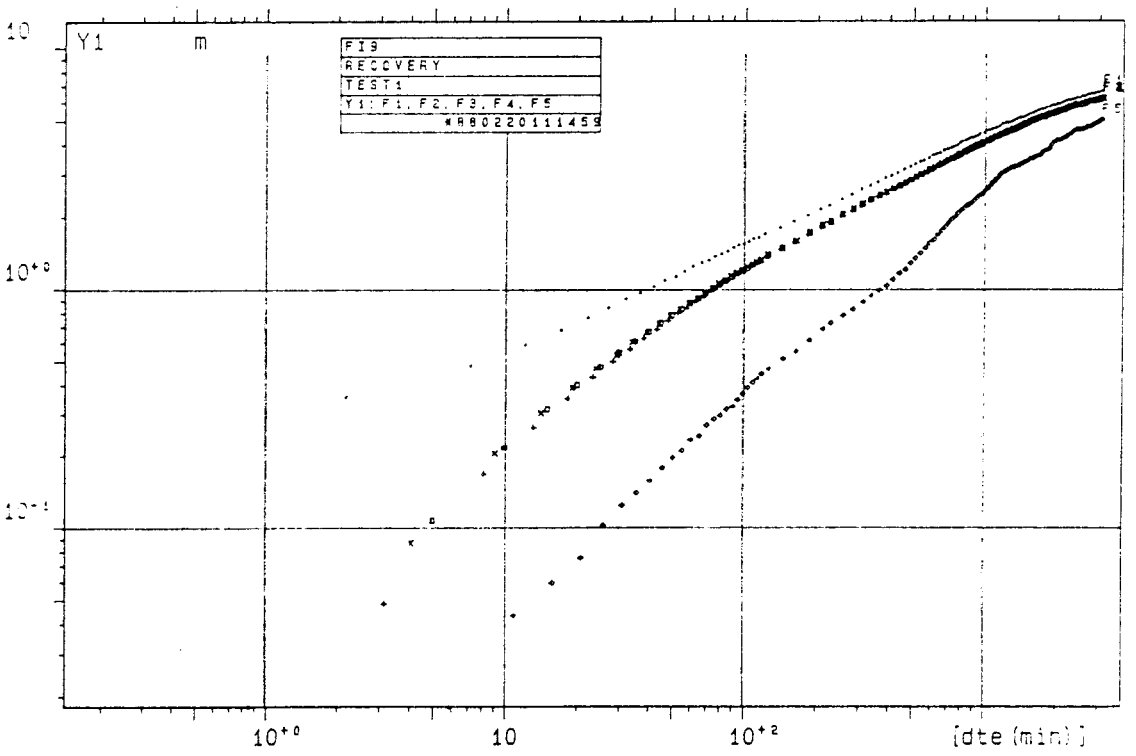

Appendix 2:6 Observed drawdown and recovery in borehole KFI09 during interference test 1.

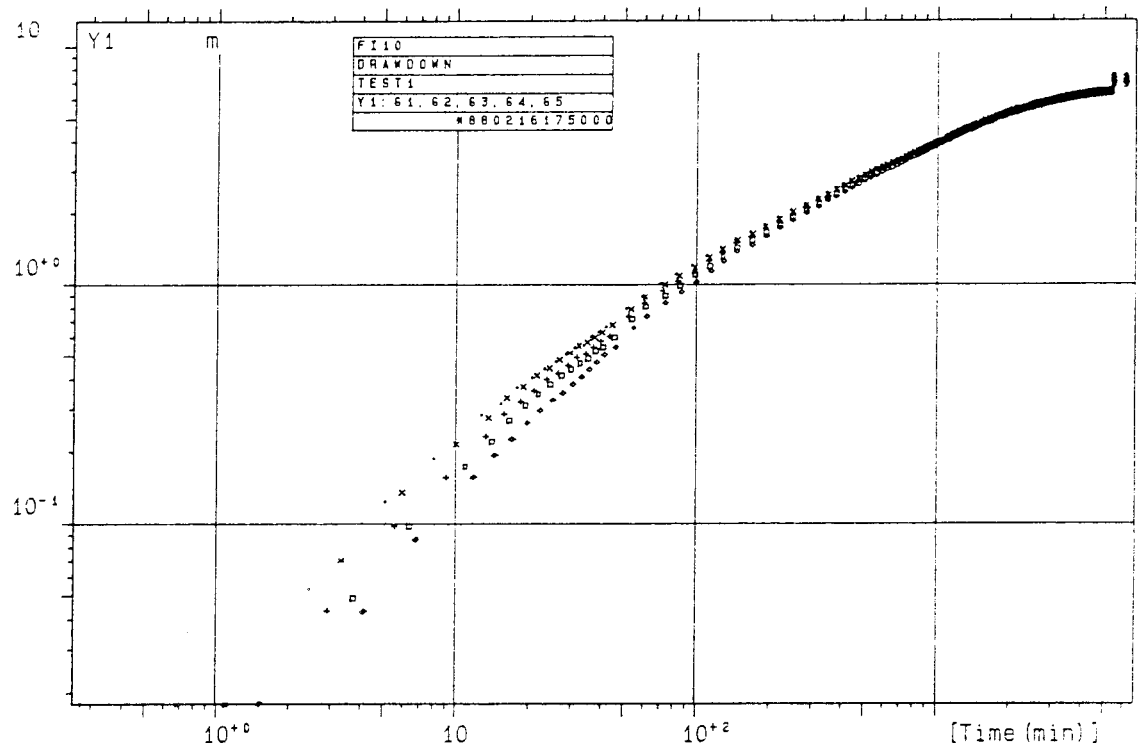

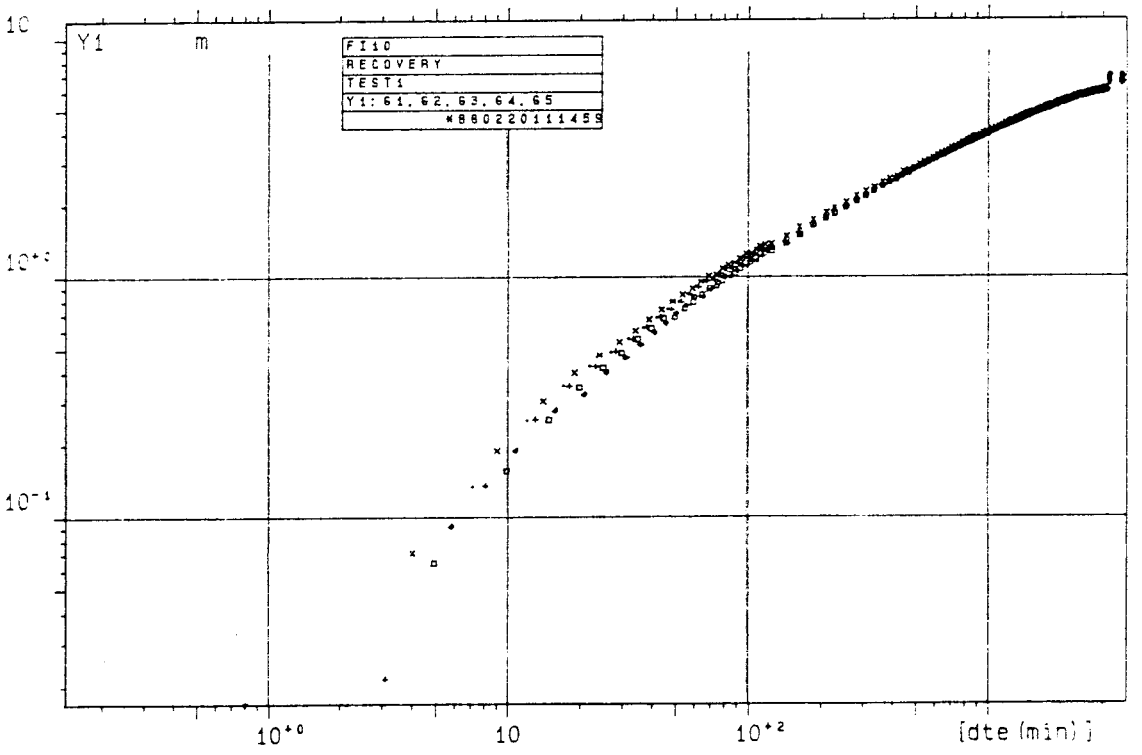

Appendix 2:7 Observed drawdown and recovery in borehole KFI10 during interference test 1.

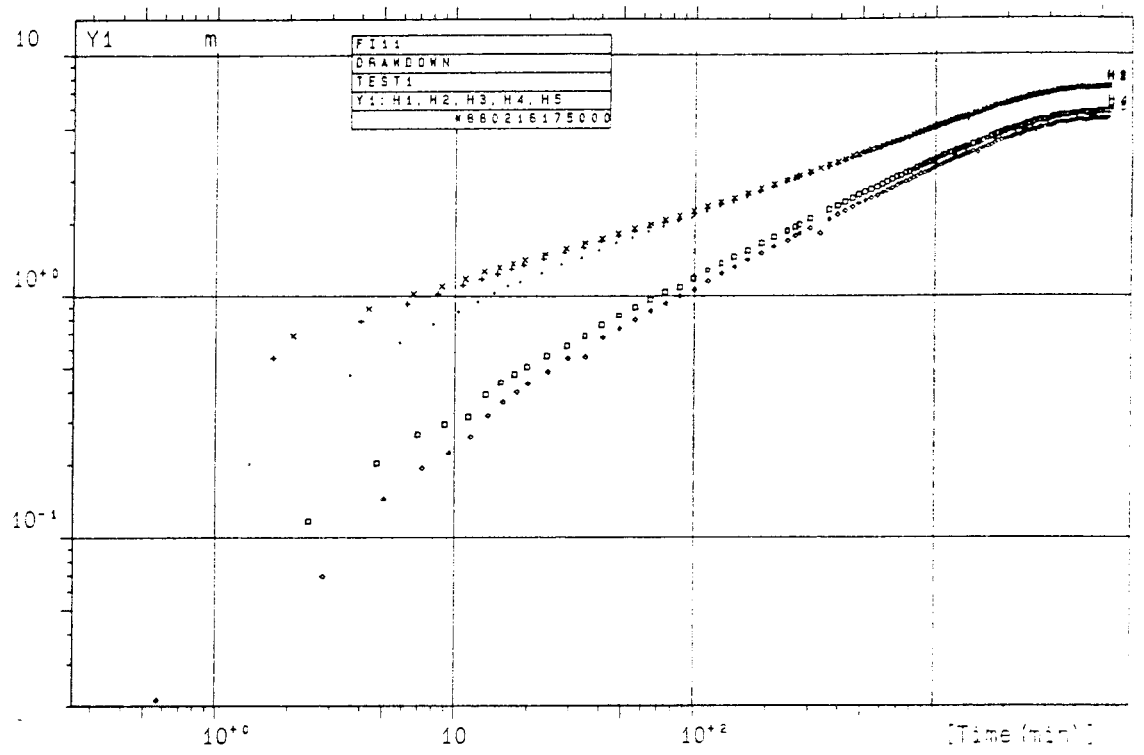

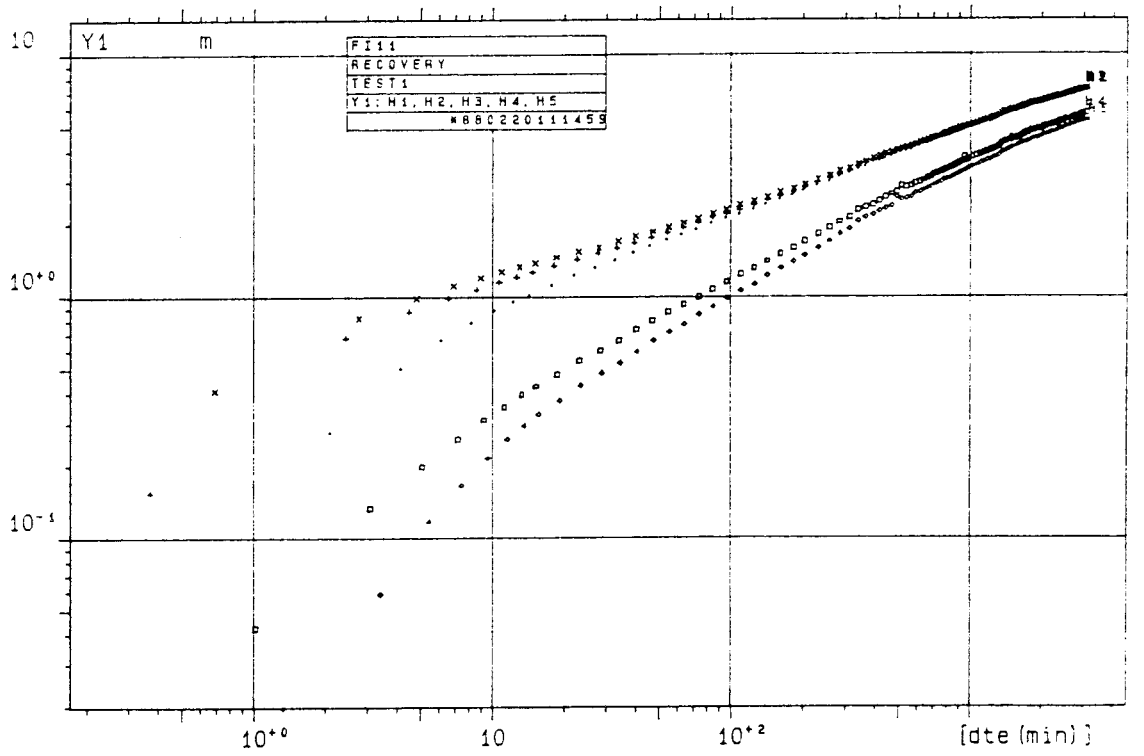

Appendix 2:8 Observed drawdown and recovery in borehole KFI11 during interference test 1.

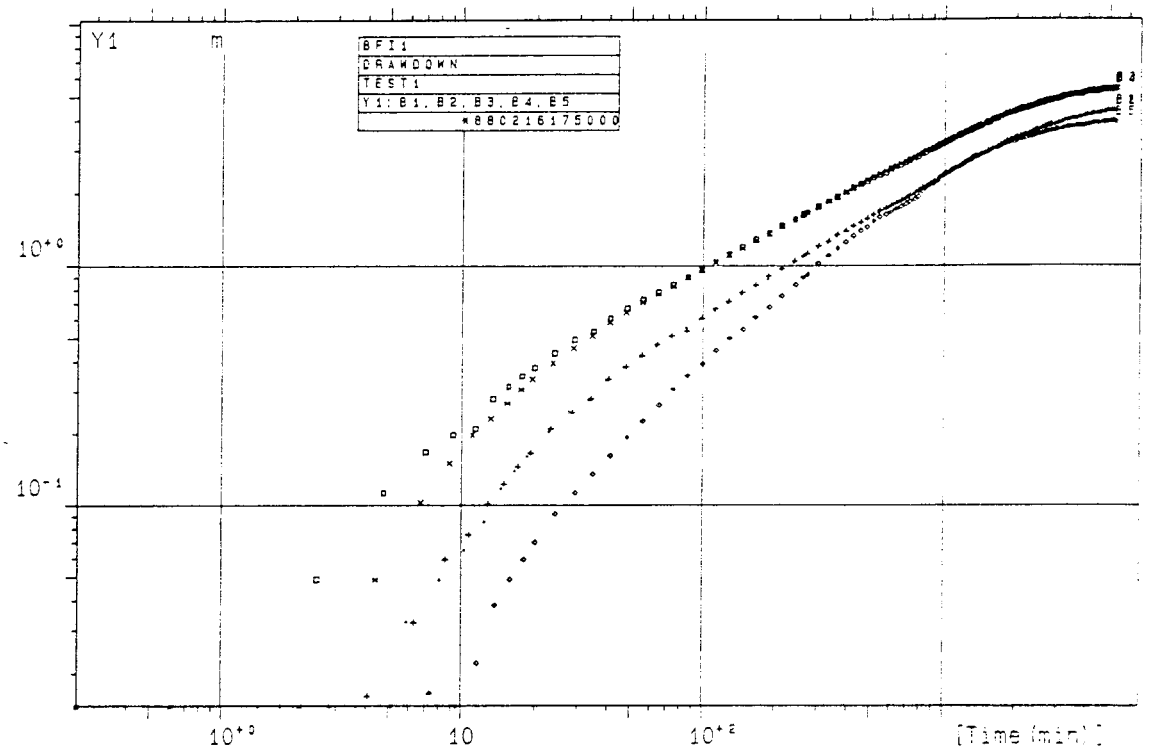

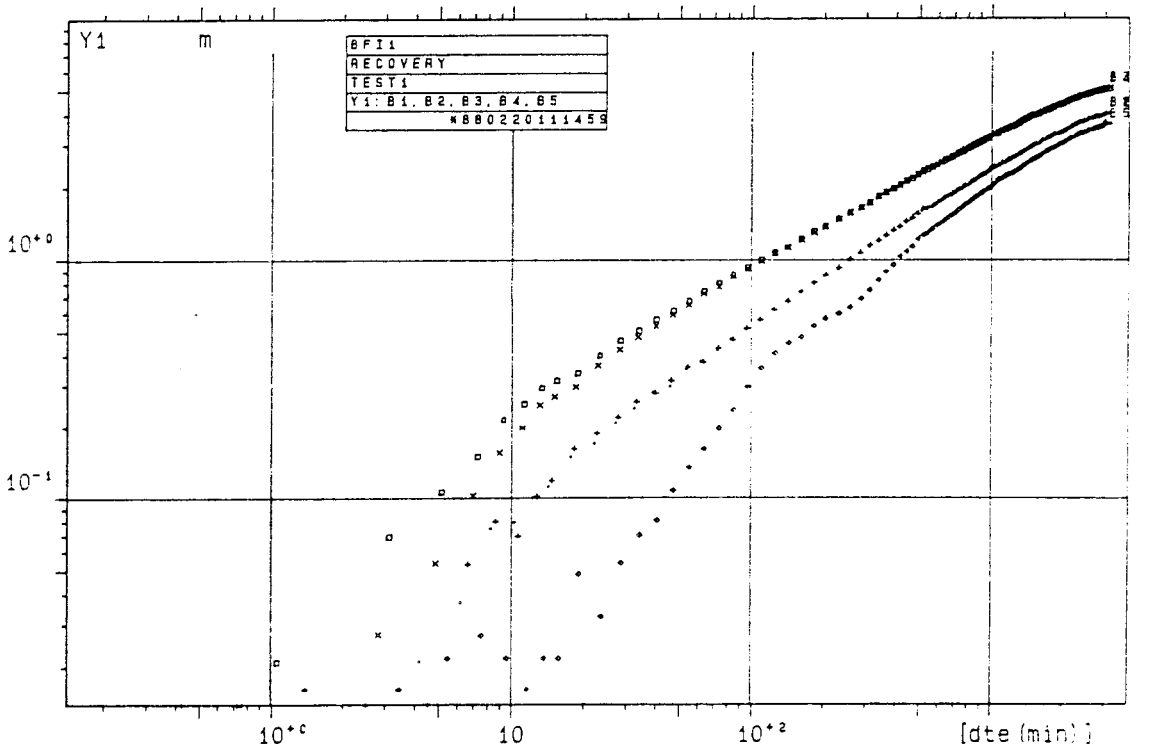

Appendix 2:9 Observed drawdown and recovery in borehole BFI01 during interference test 1.

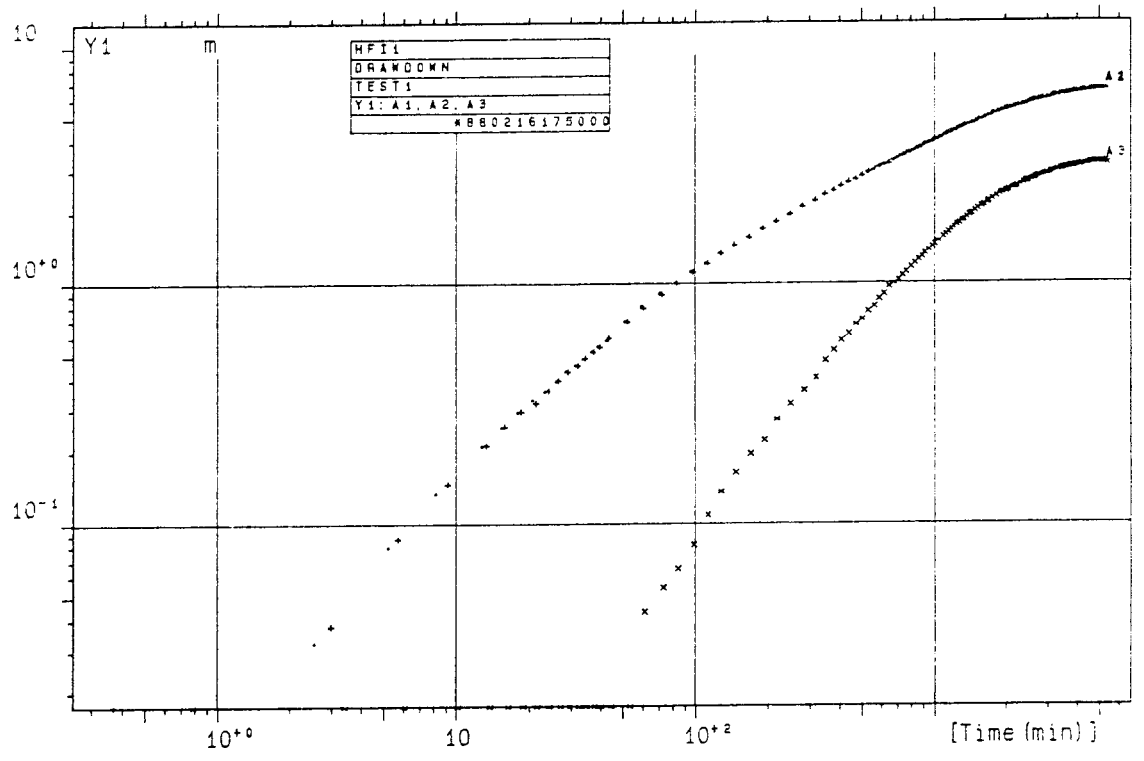

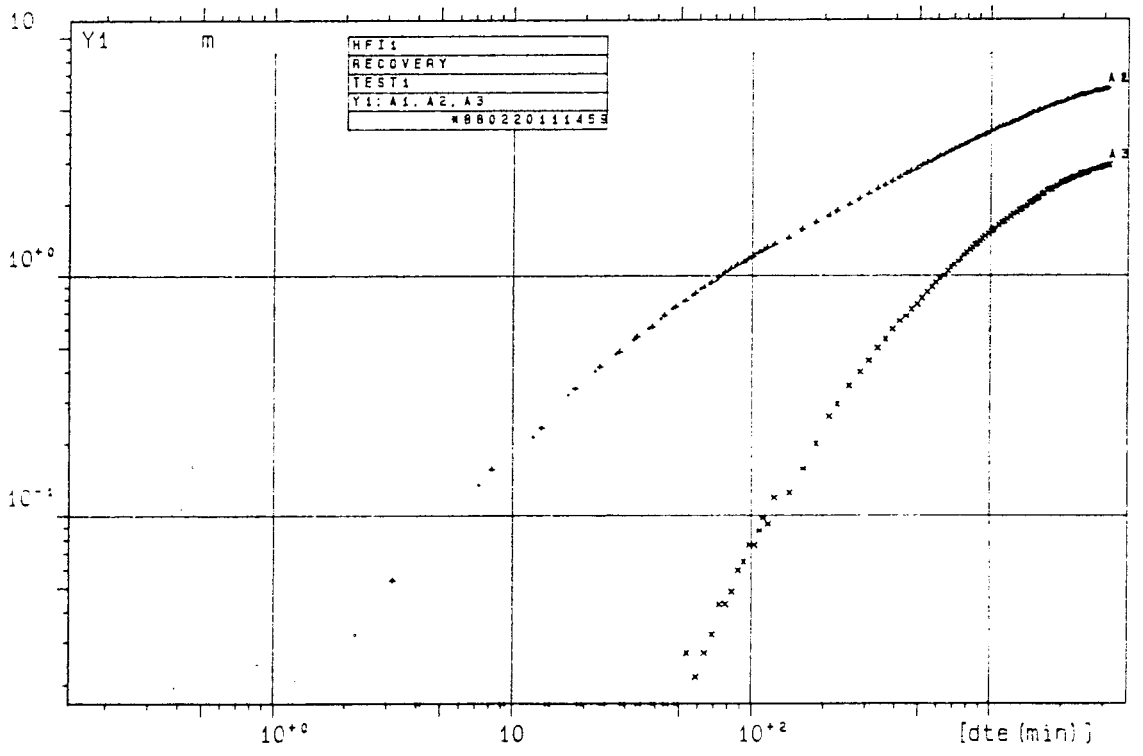

Appendix 2:10 Observed drawdown and recovery in borehole HFI01 during interference test 1.

APPENDIX 3

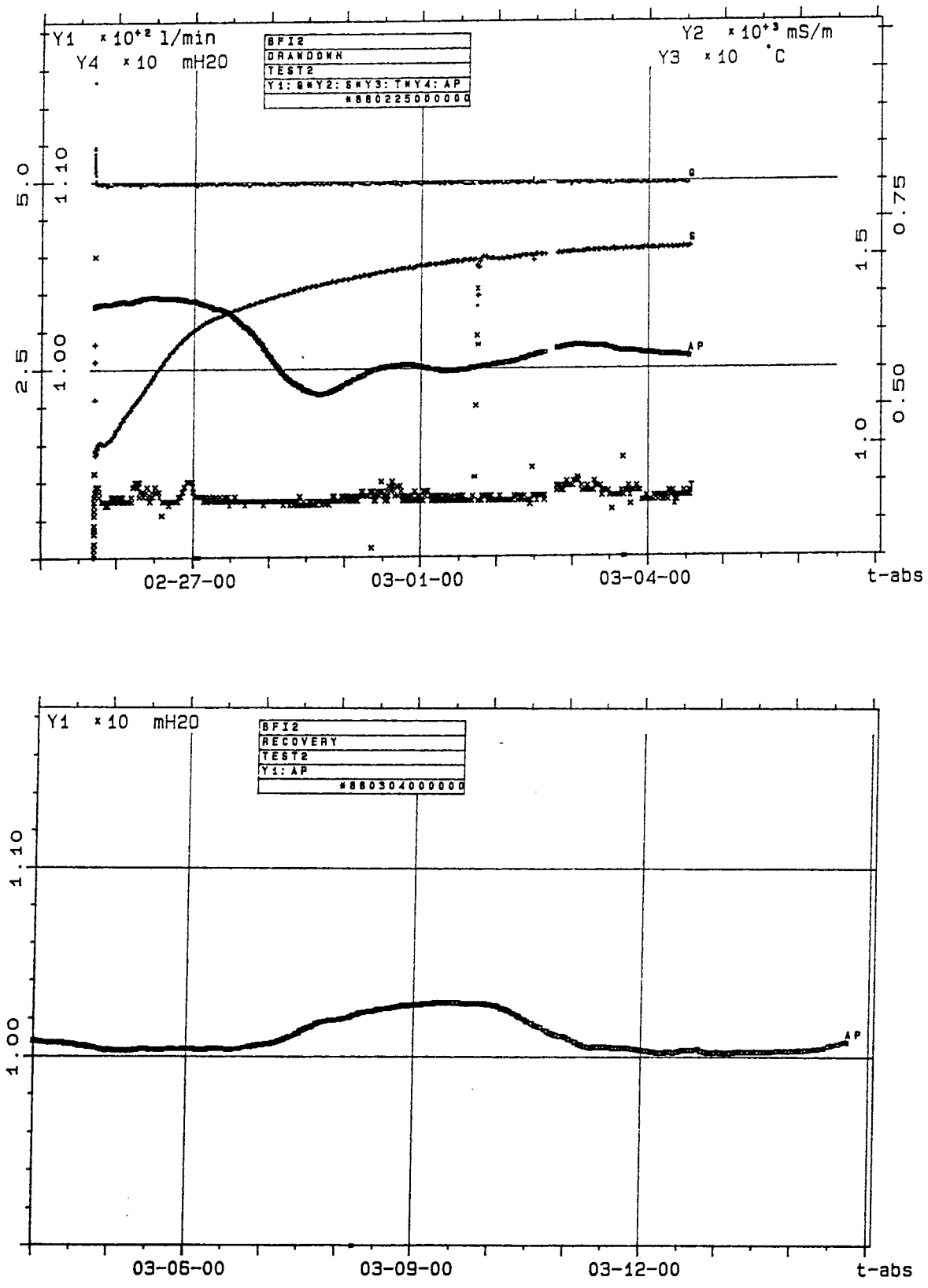

Appendix 3:1 Flow rate, electric conductivity, barometric pressure head and temperature during interference test 2 (linear time scale).

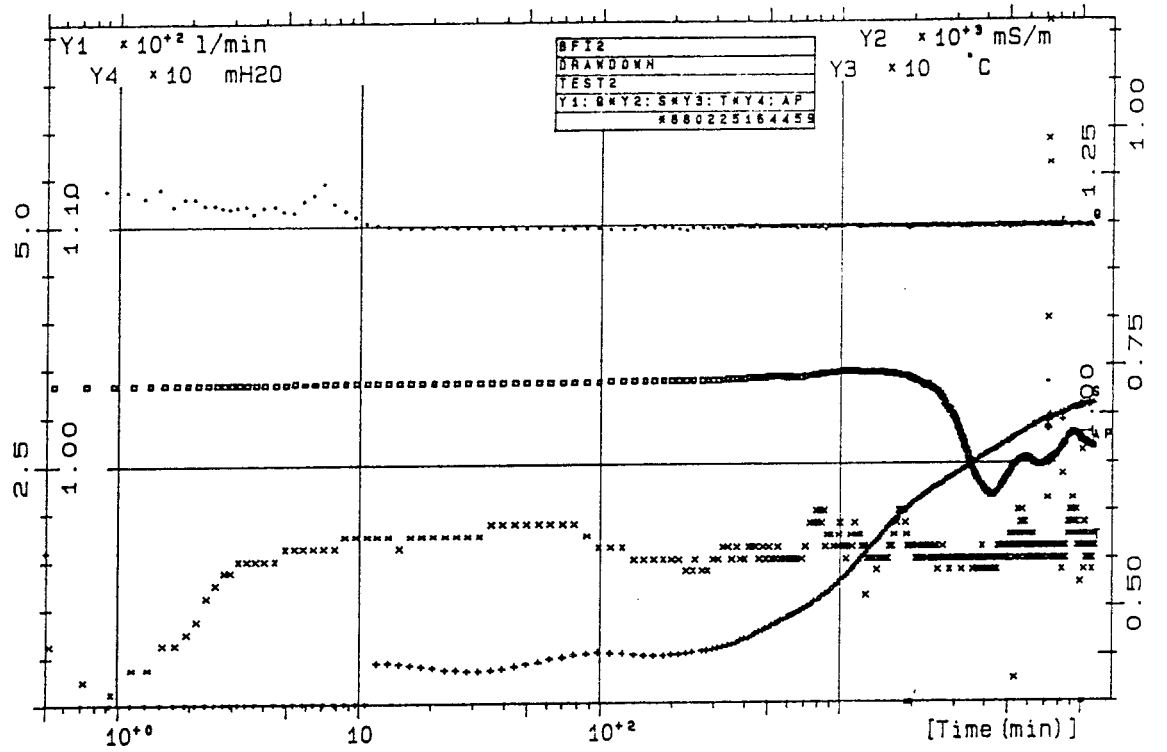

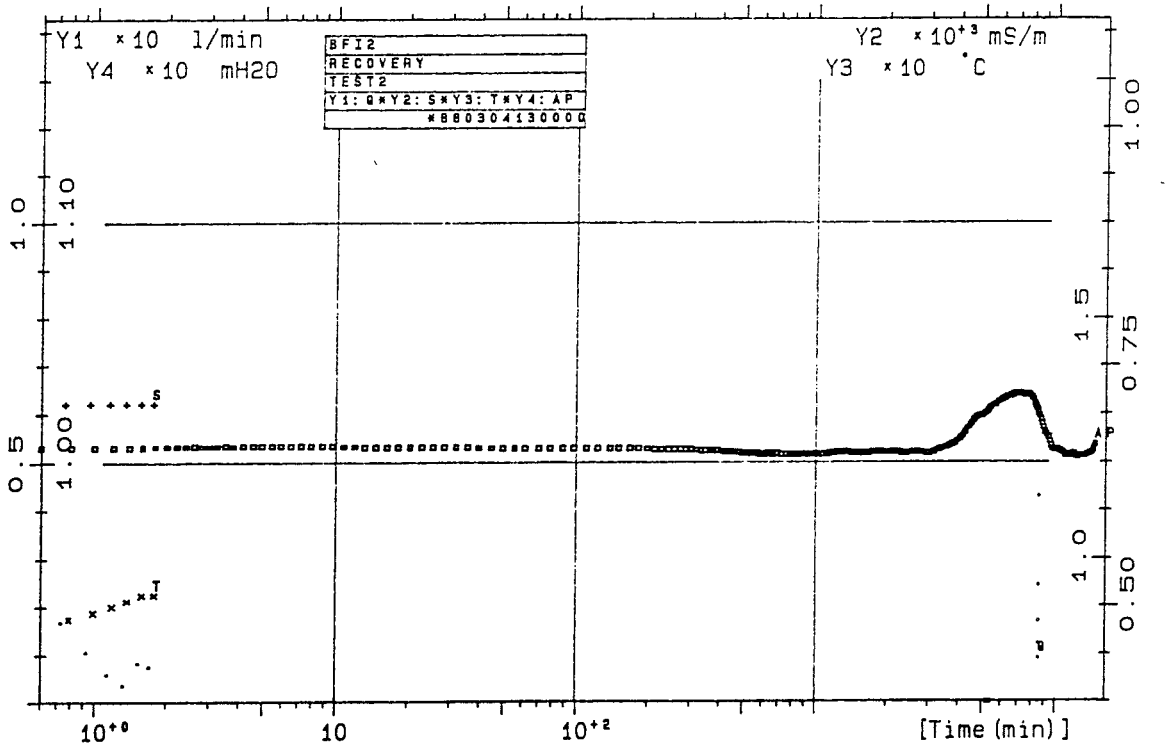

Appendix 3:2 Flow rate, electric conductivity, barometric pressure head and temperature during interference test 2 (logarithmic time scale).

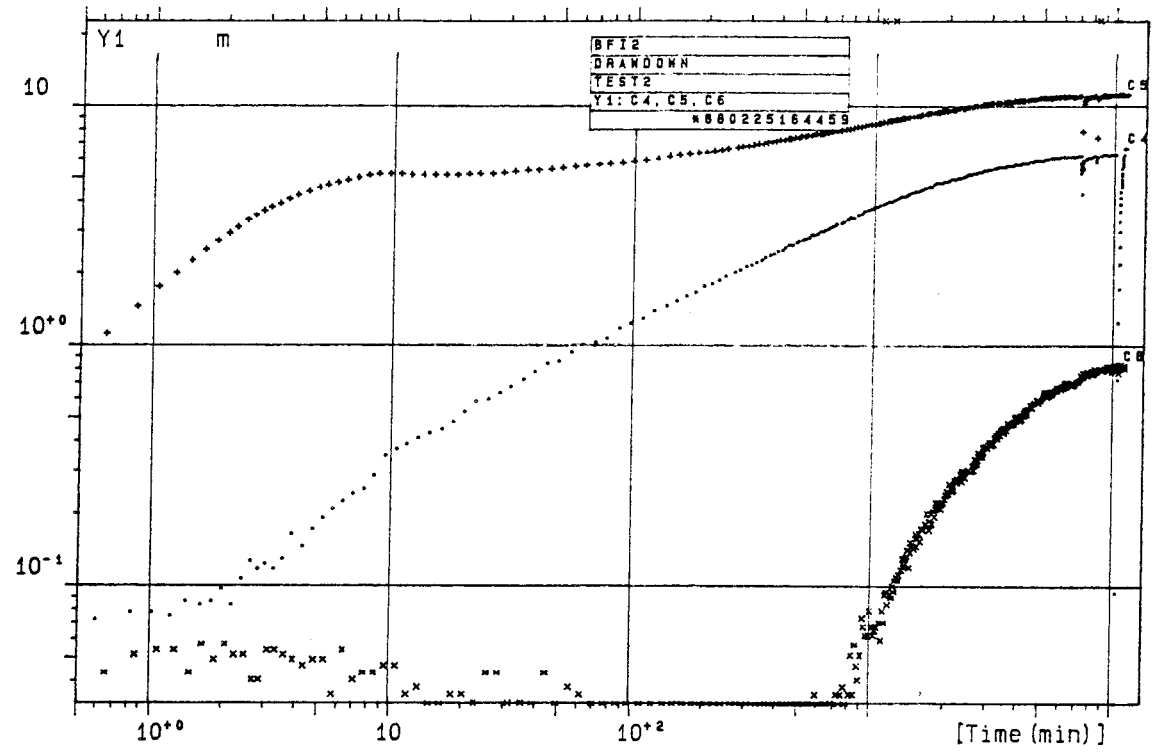

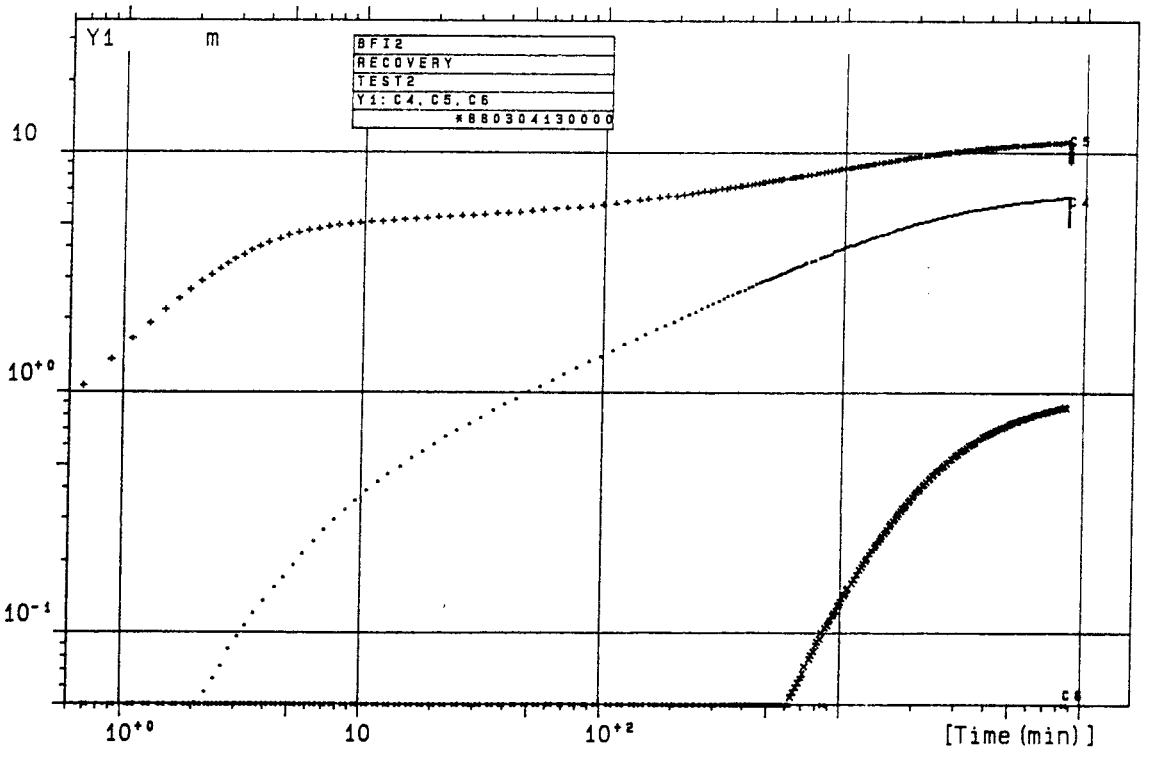

Appendix 3:3 Observed drawdown and recovery in borehole BFI02 during interference test 2.

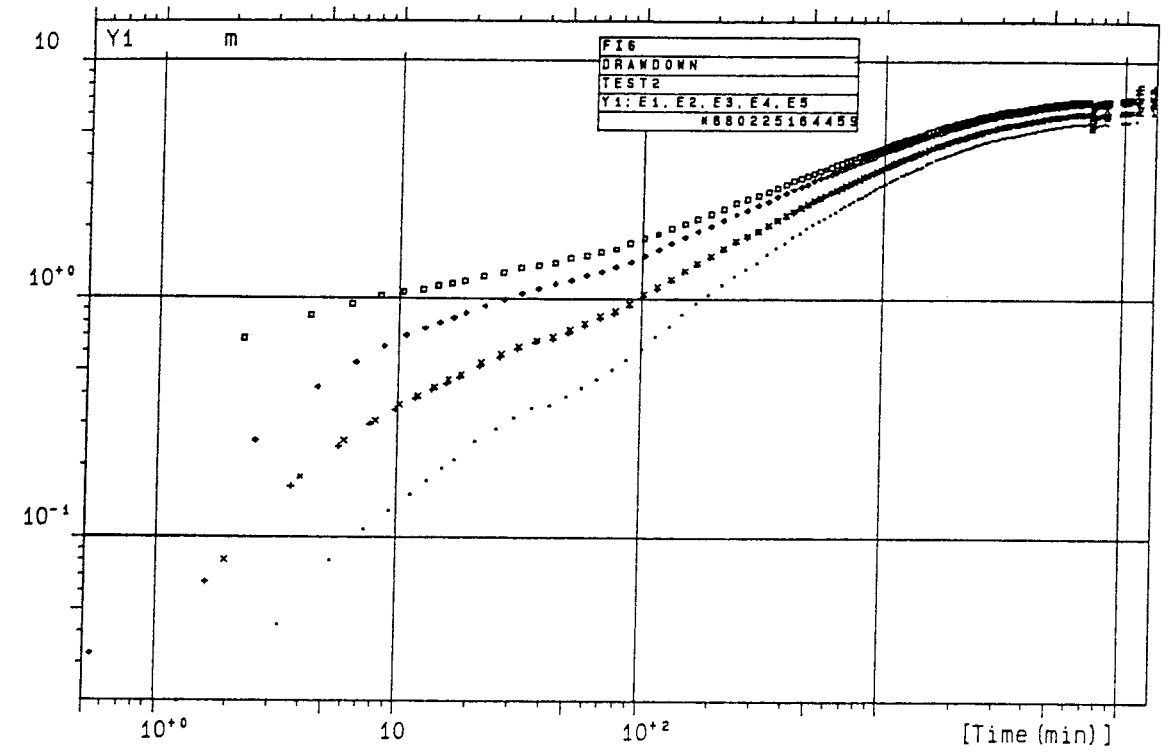

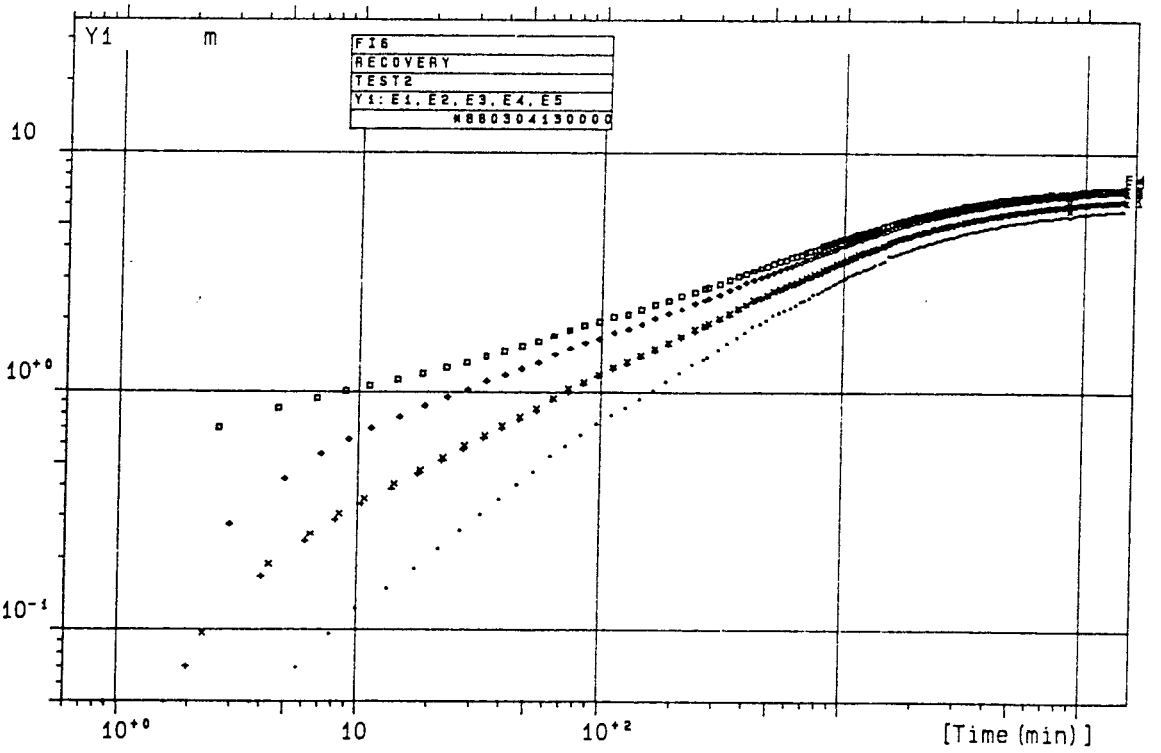

Appendix 3:4 Observed drawdown and recovery in borehole KFI06 during interference test 2.

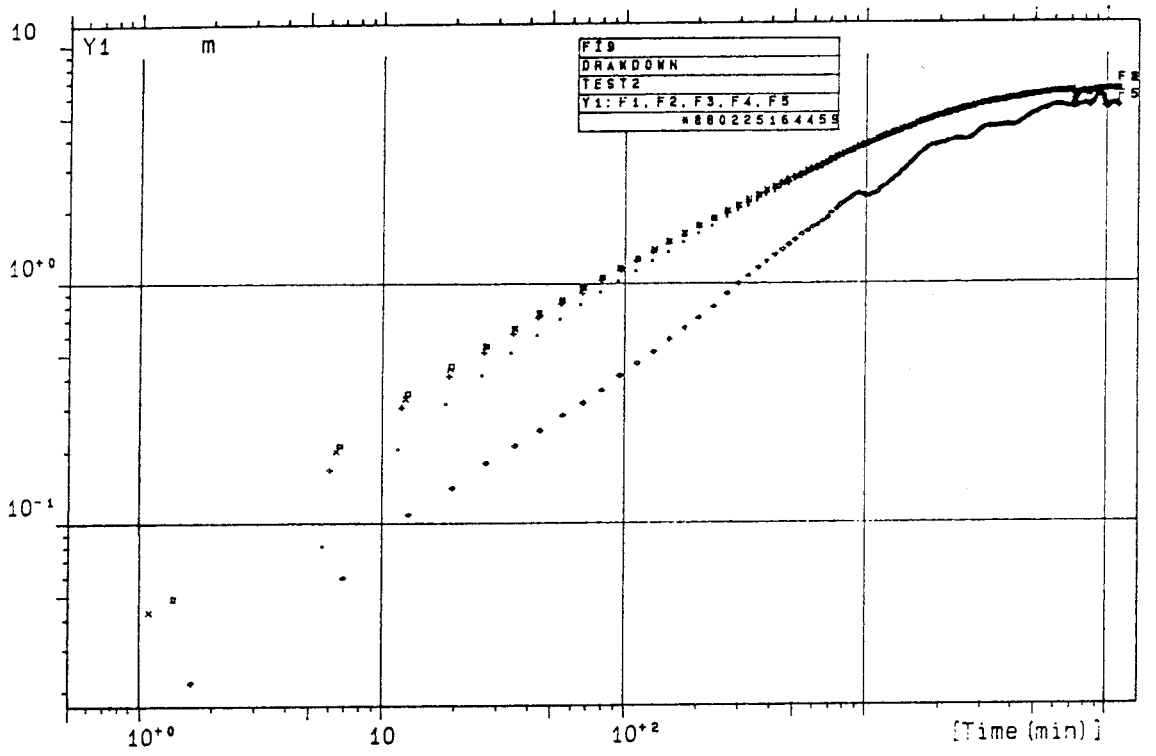

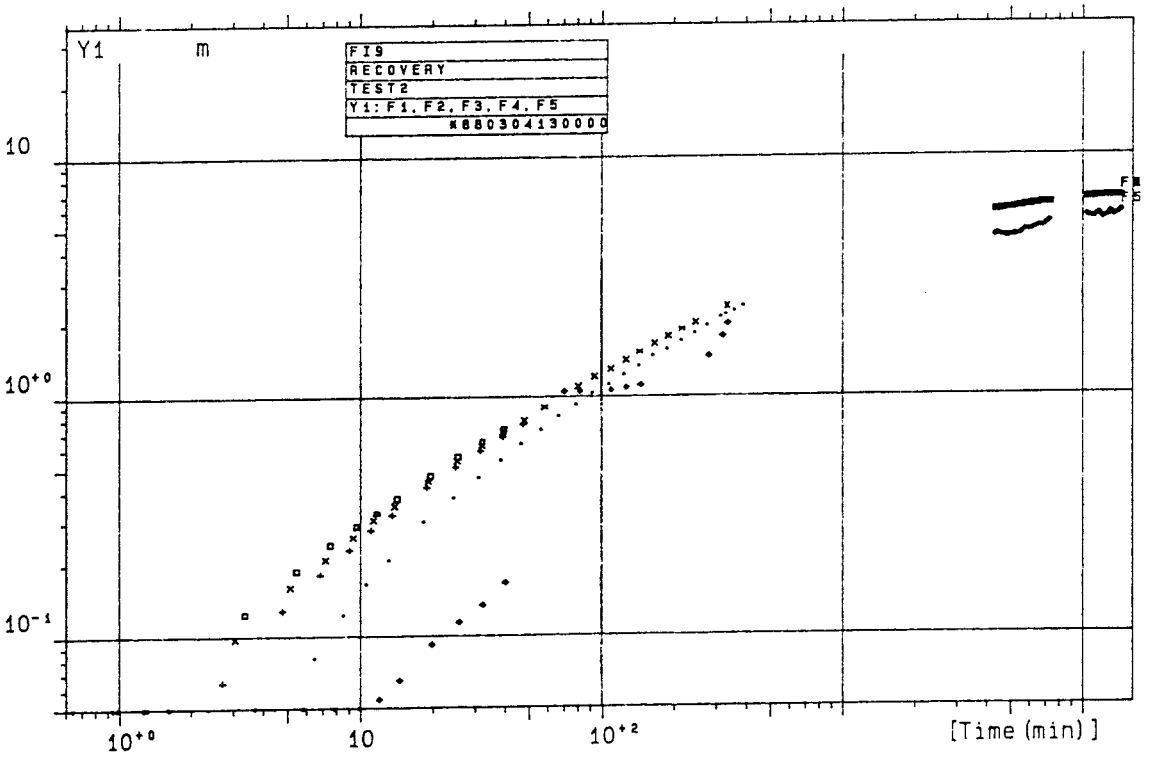

Appendix 3:5 Observed drawdown and recovery in borehole KFI09 during interference test 2.

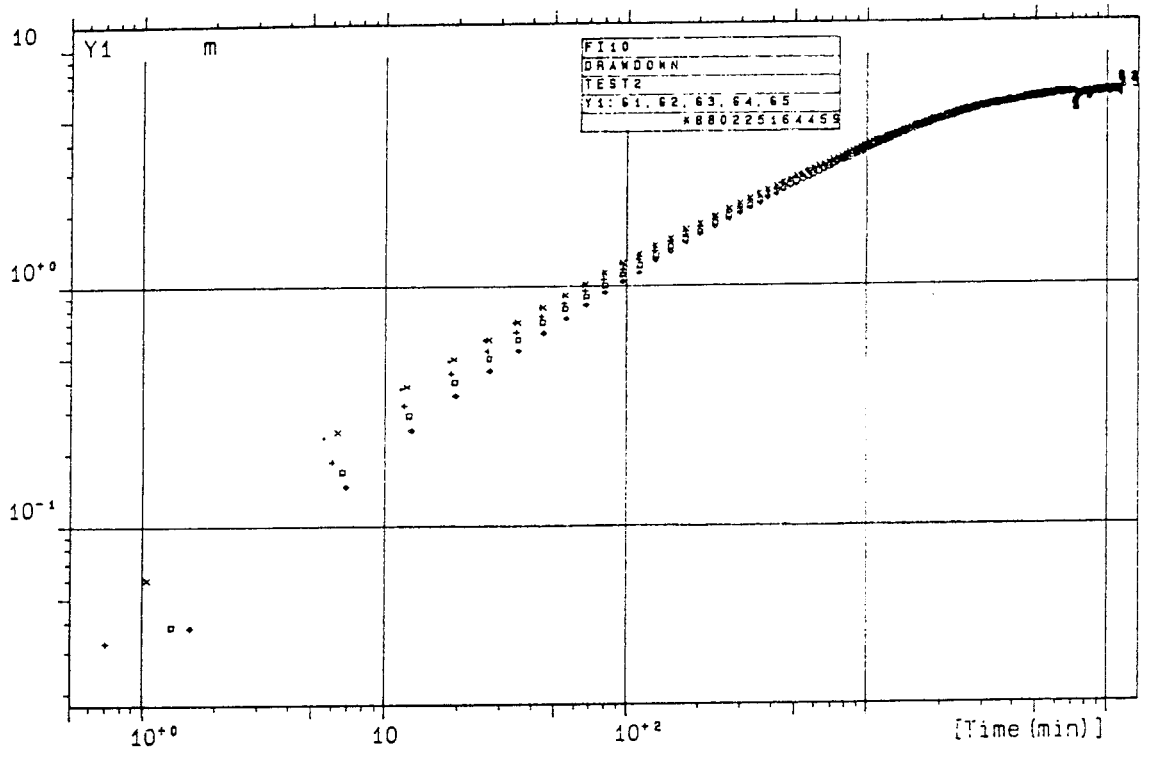

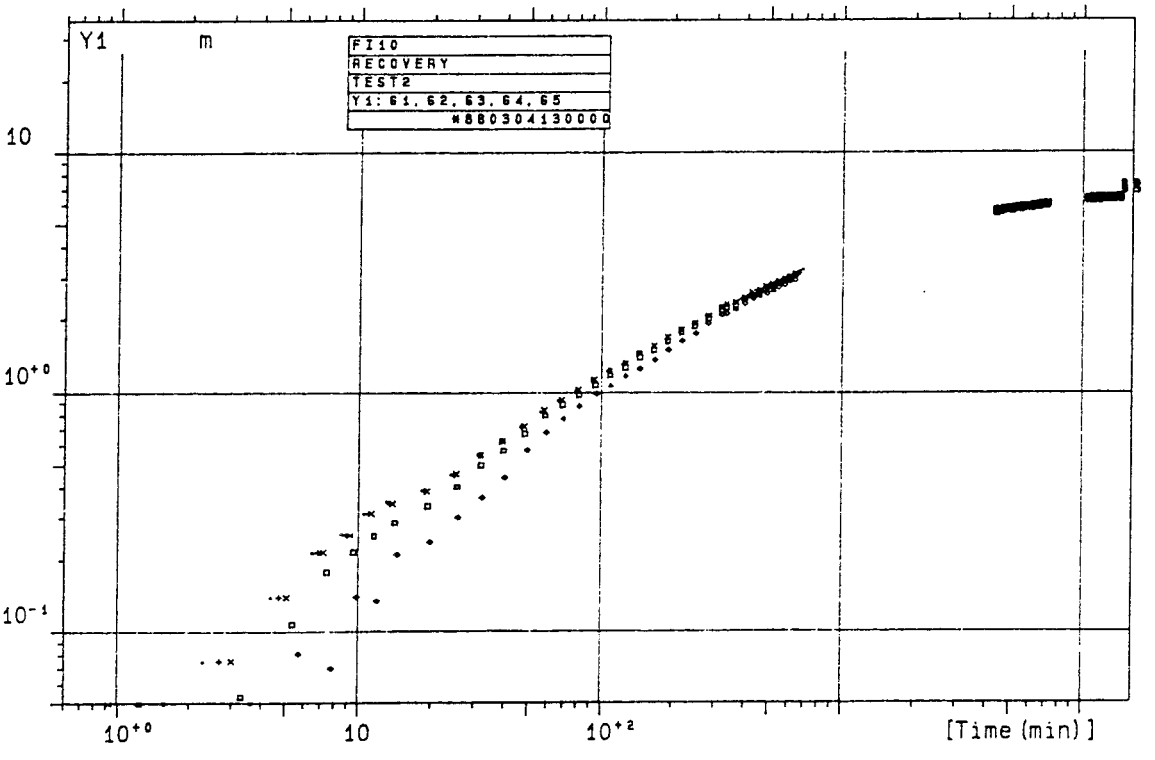

Appendix 3:6 Observed drawdown and recovery in borehole KFI10 during interference test 2.

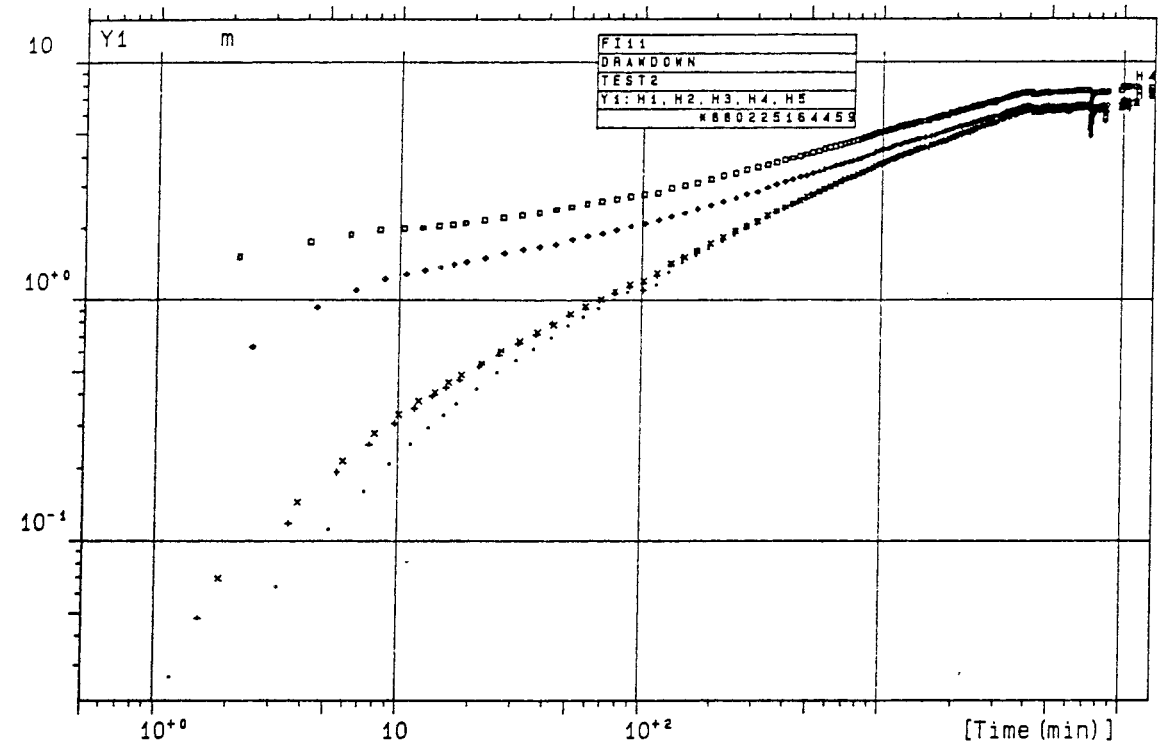

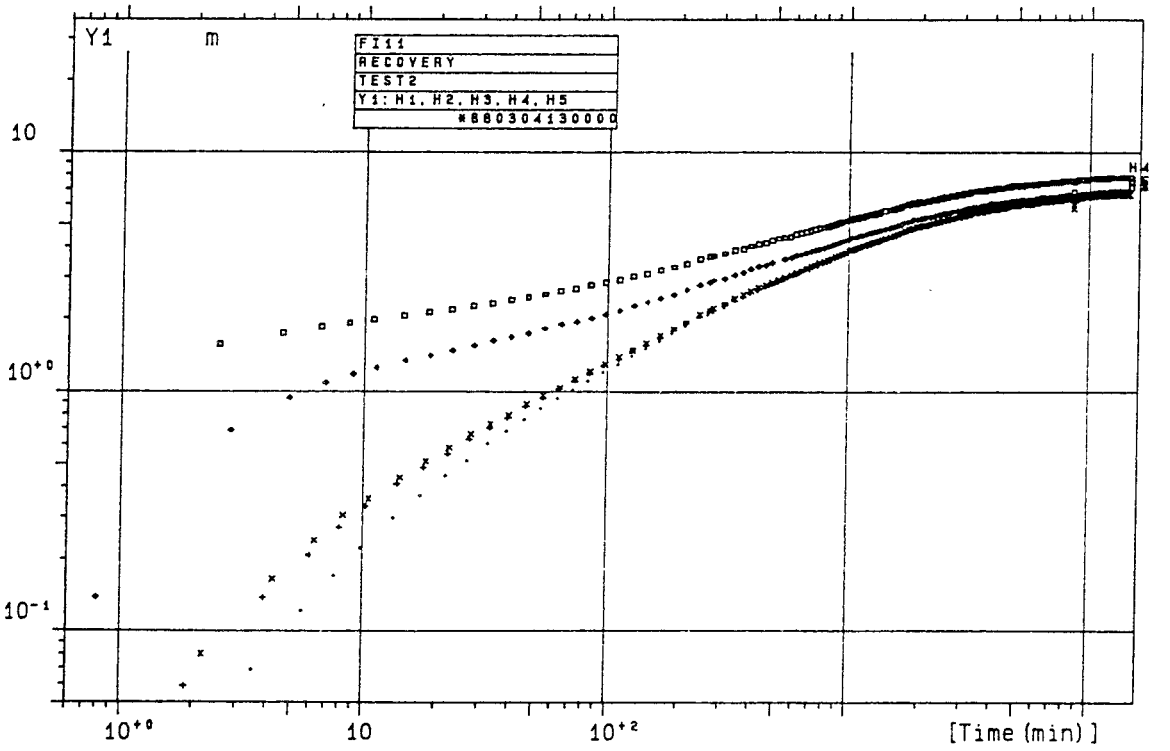

Appendix 3:7 Observed drawdown and recovery in borehole KFI11 during interference test 2.

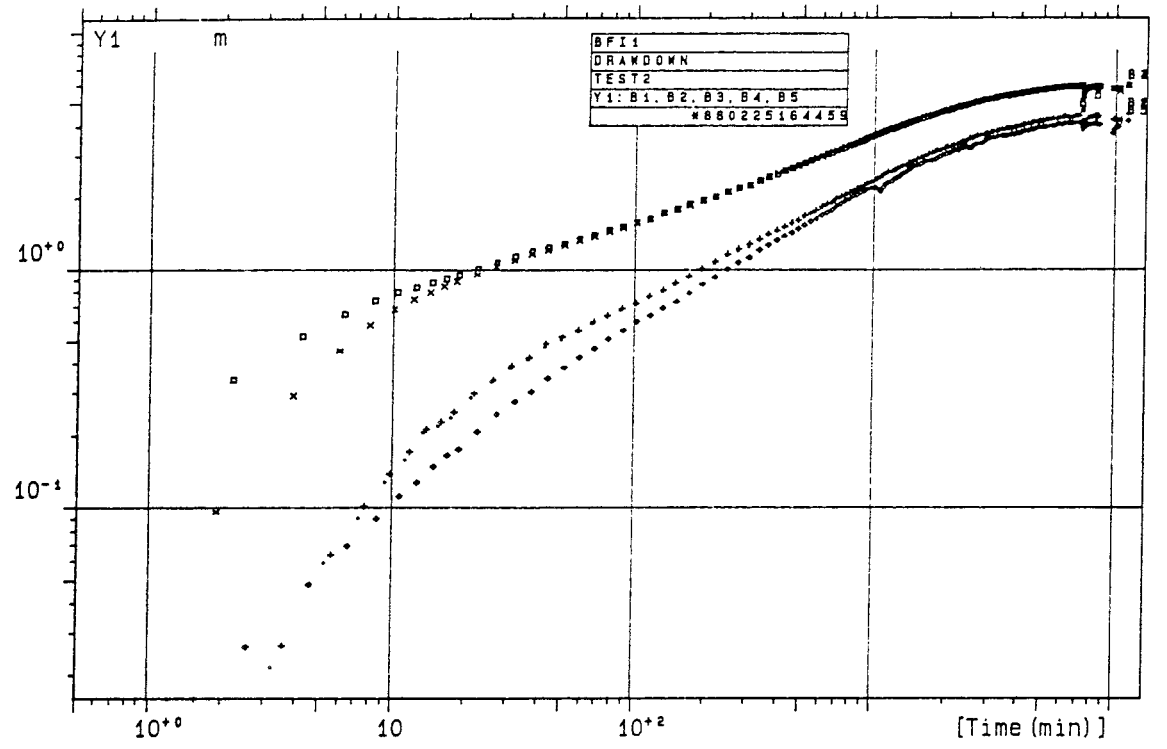

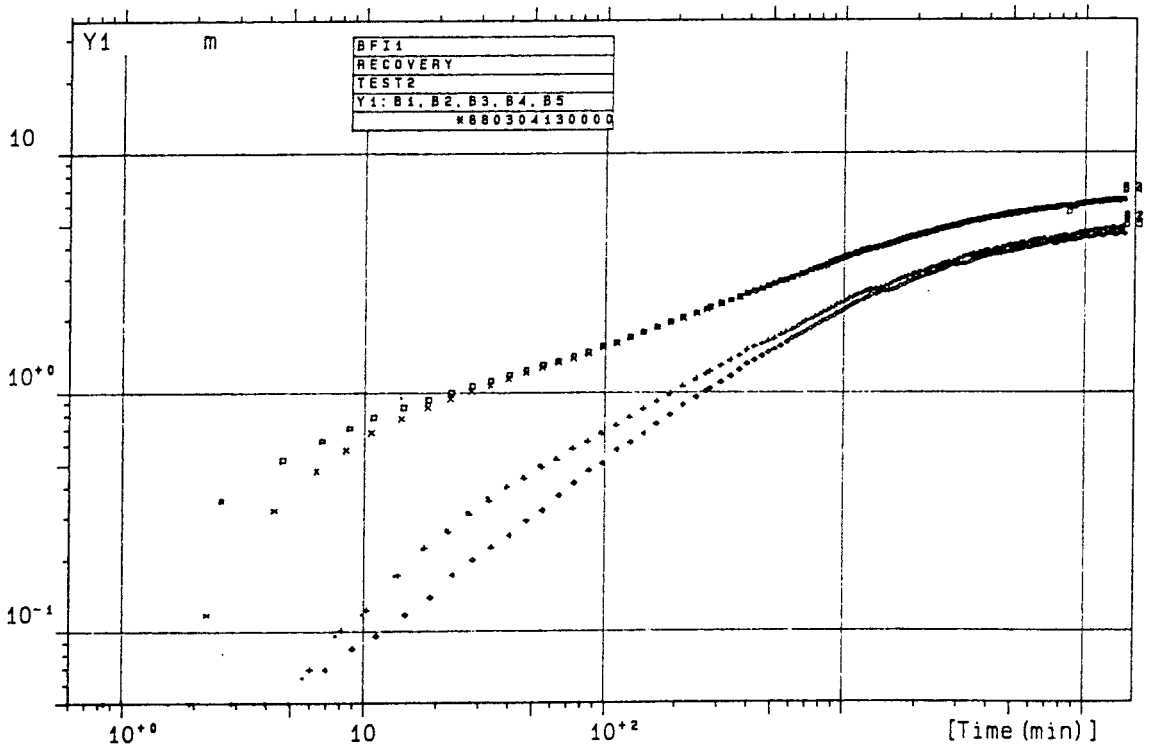

Appendix 3:8 Observed drawdown and recovery in borehole BFI01 during interference test 2.

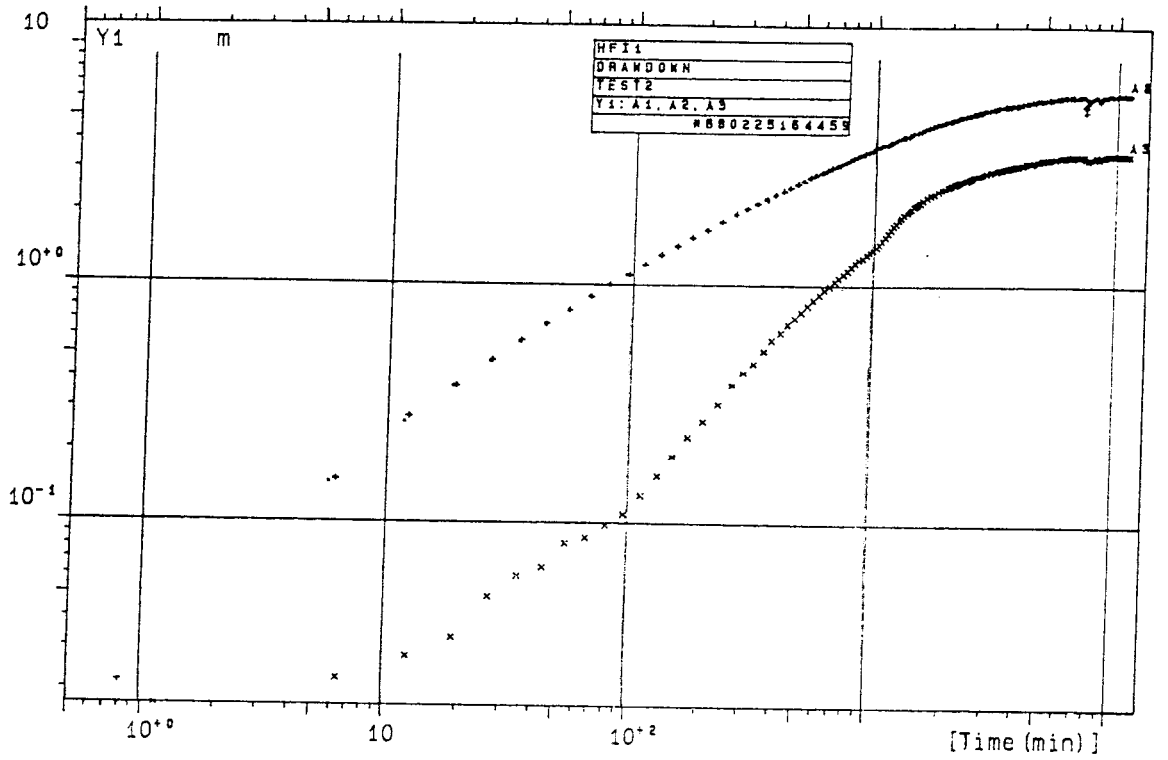

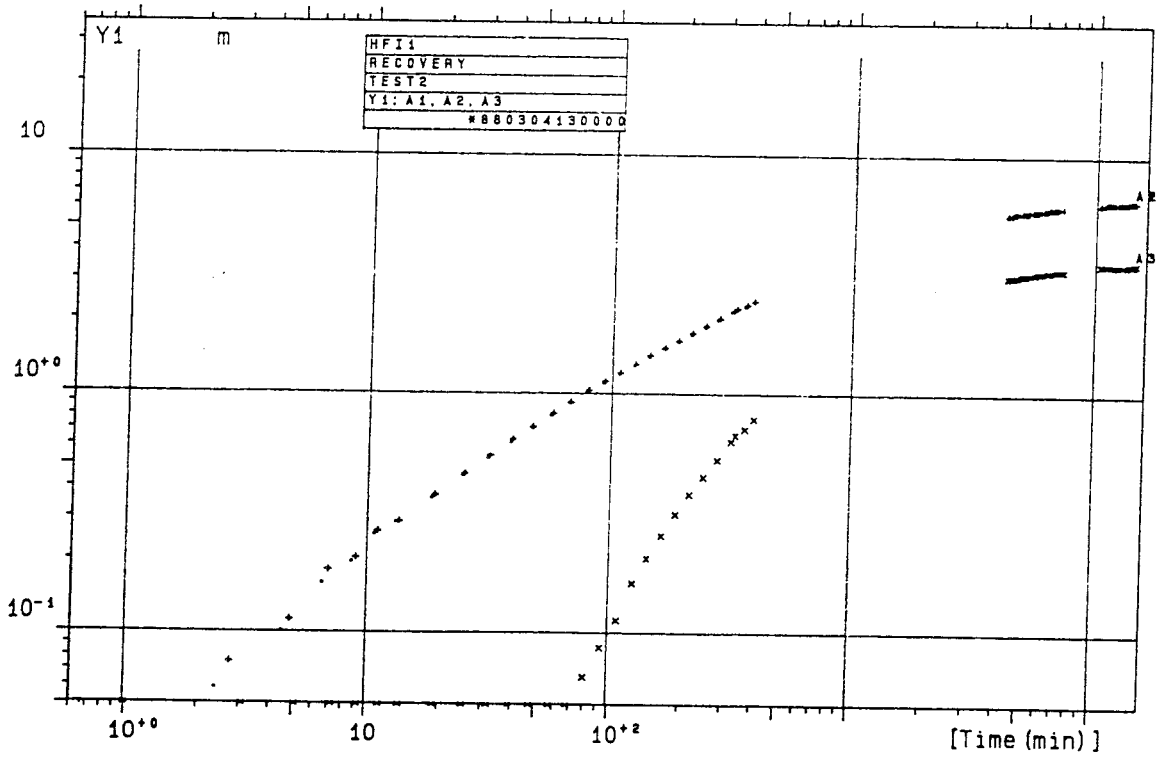

Appendix 3:9 Observed drawdown and recovery in borehole HFI01 during interference test 2.

APPENDIX 4

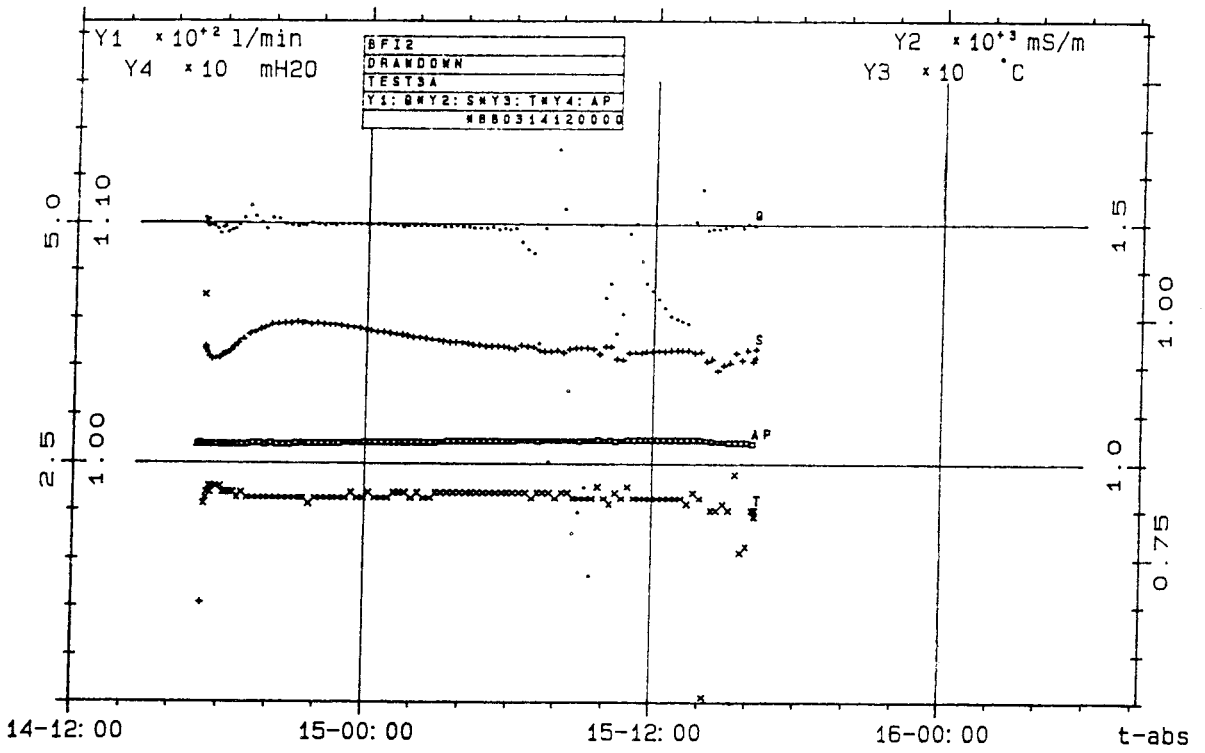

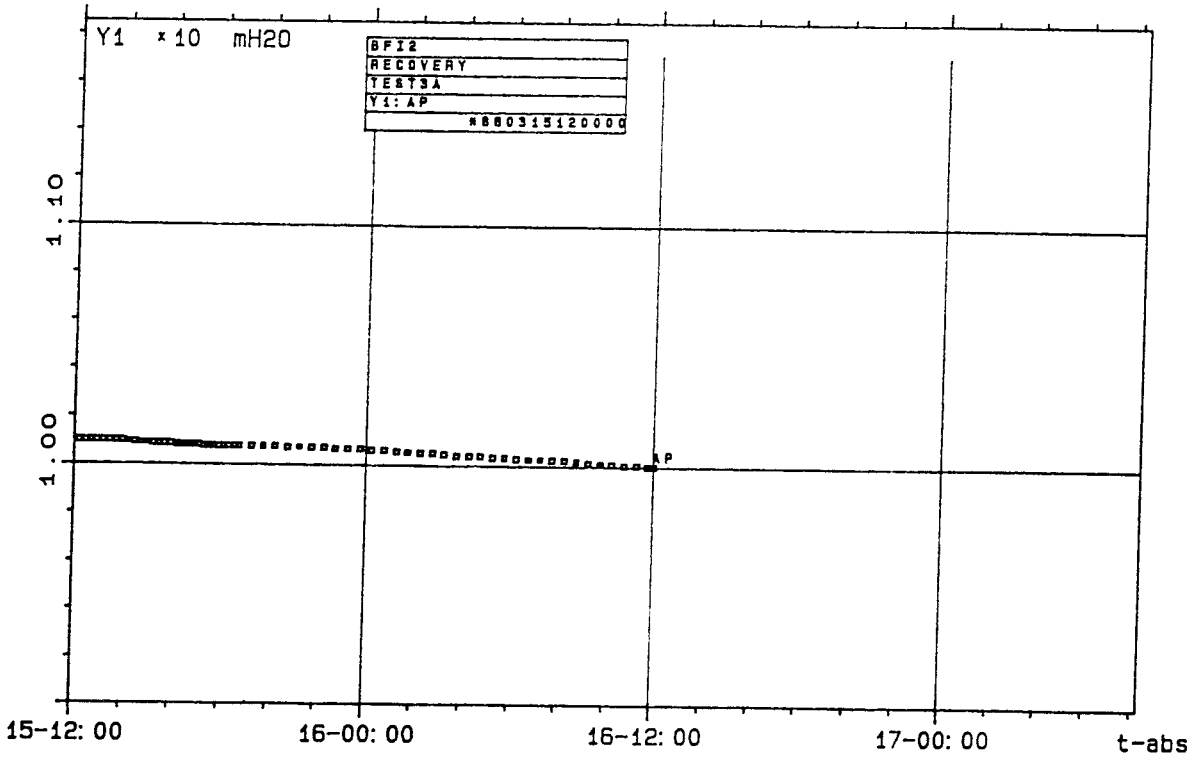

Appendix 4:1 Flow rate, electric conductivity, barometric pressure head and temperature during interference test 3A (linear time scale).

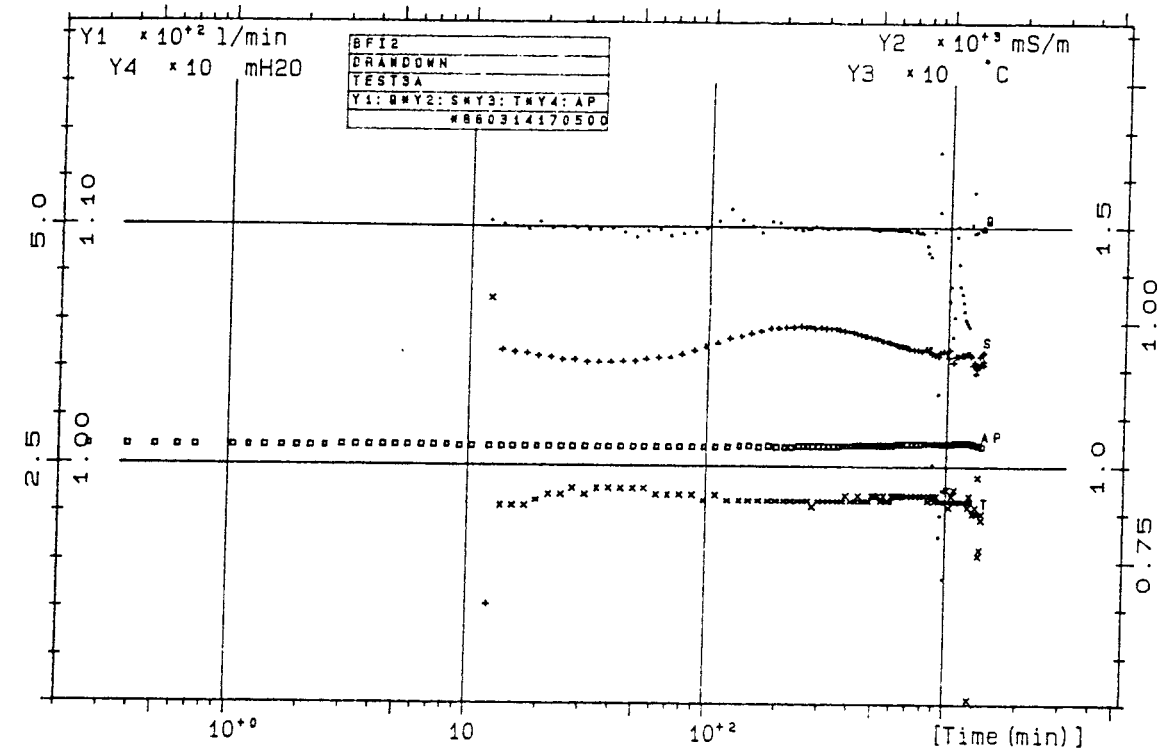

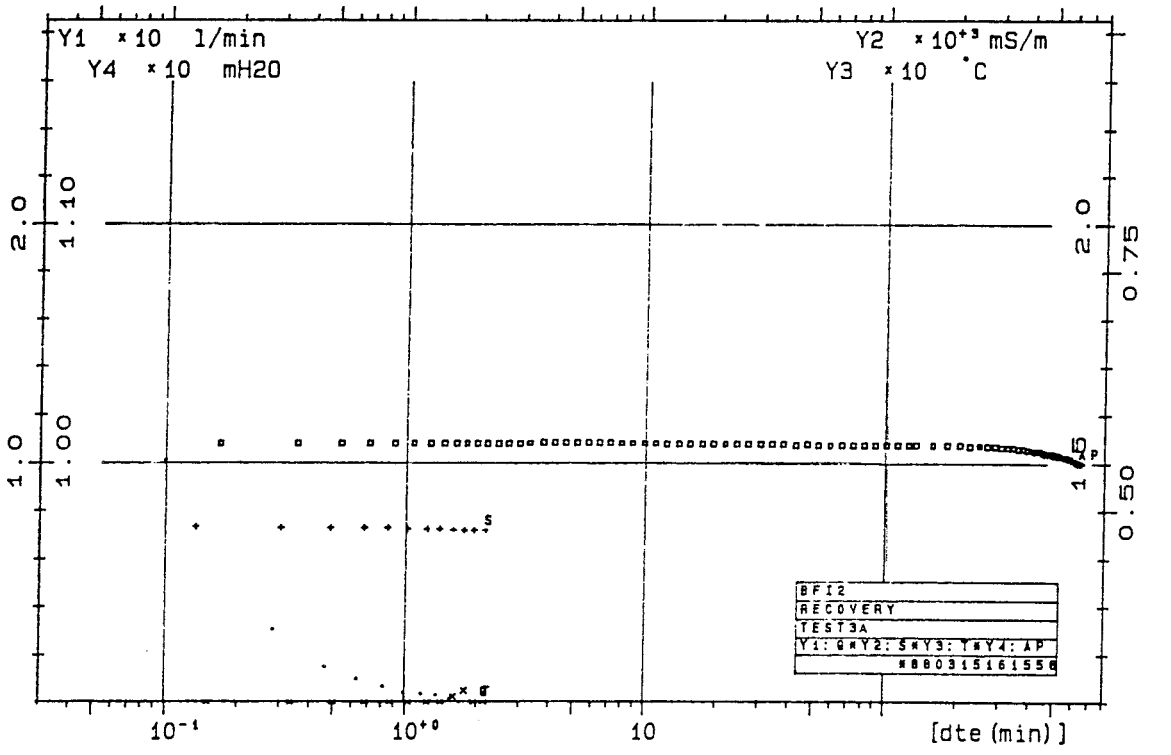

Appendix 4:2 Flow rate, electric conductivity, barometric pressure head and temperature during interference test 3B (logarithmic time scale).

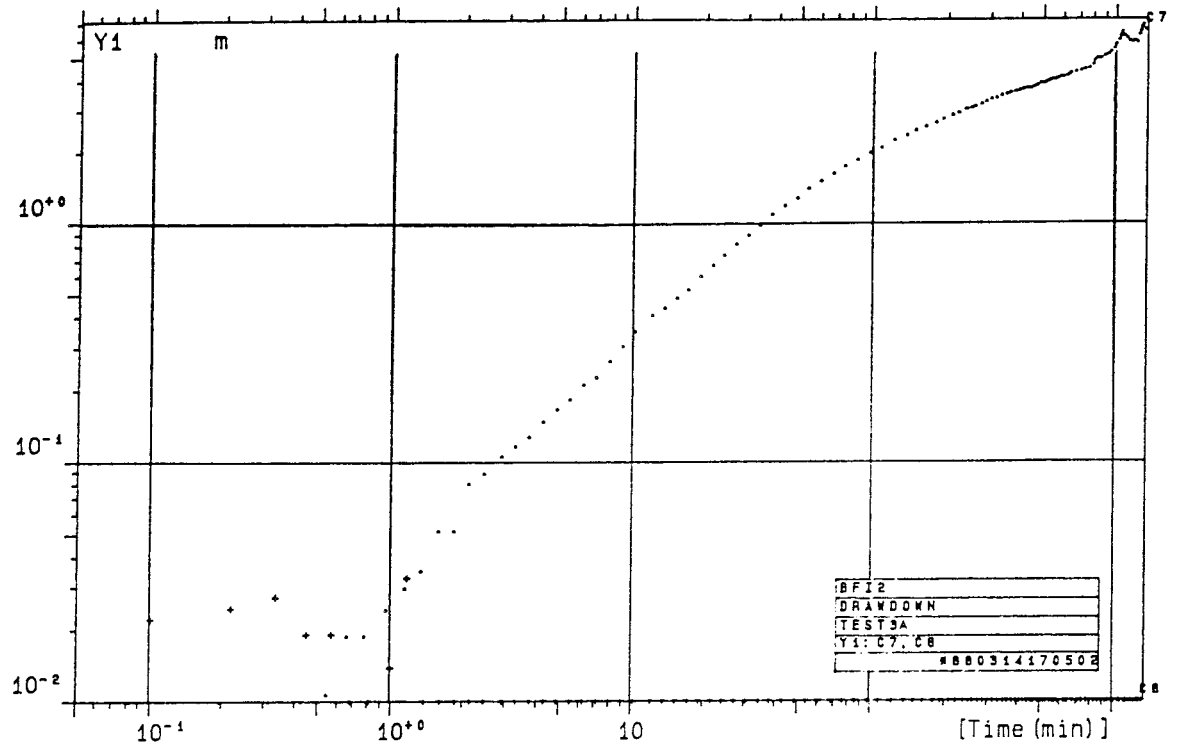

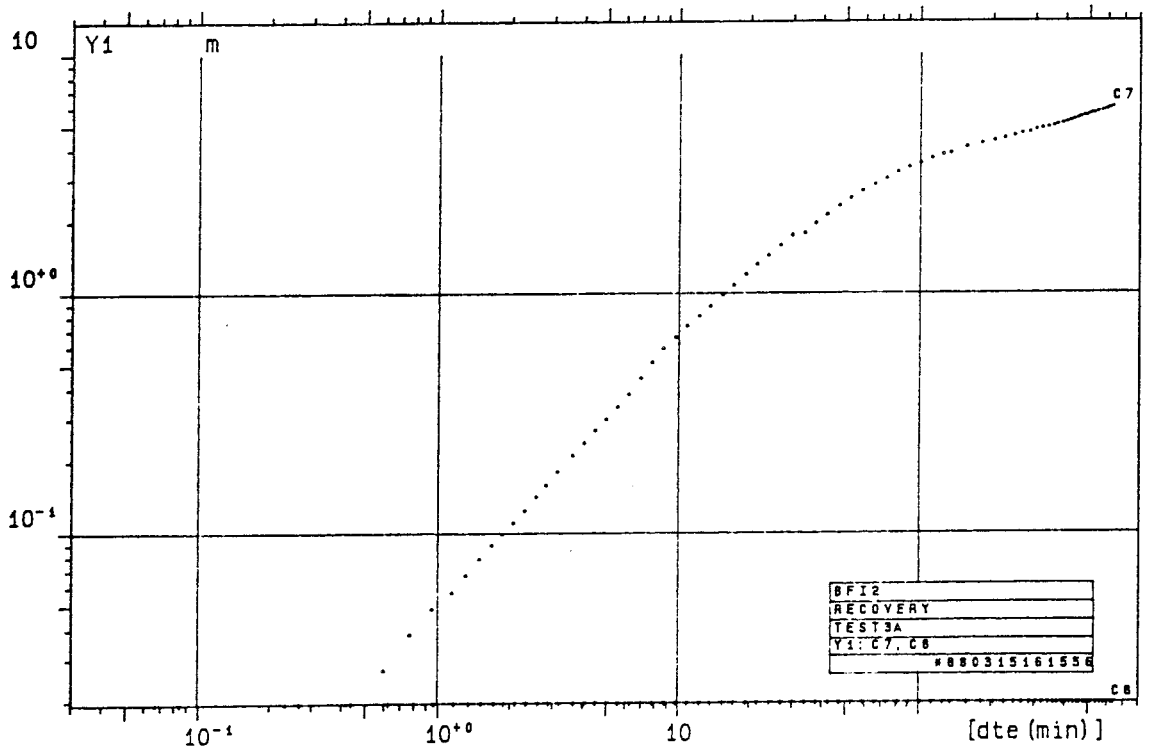

Appendix 4:3 Observed drawdown and recovery in borehole BFI02 during interference test 3A.

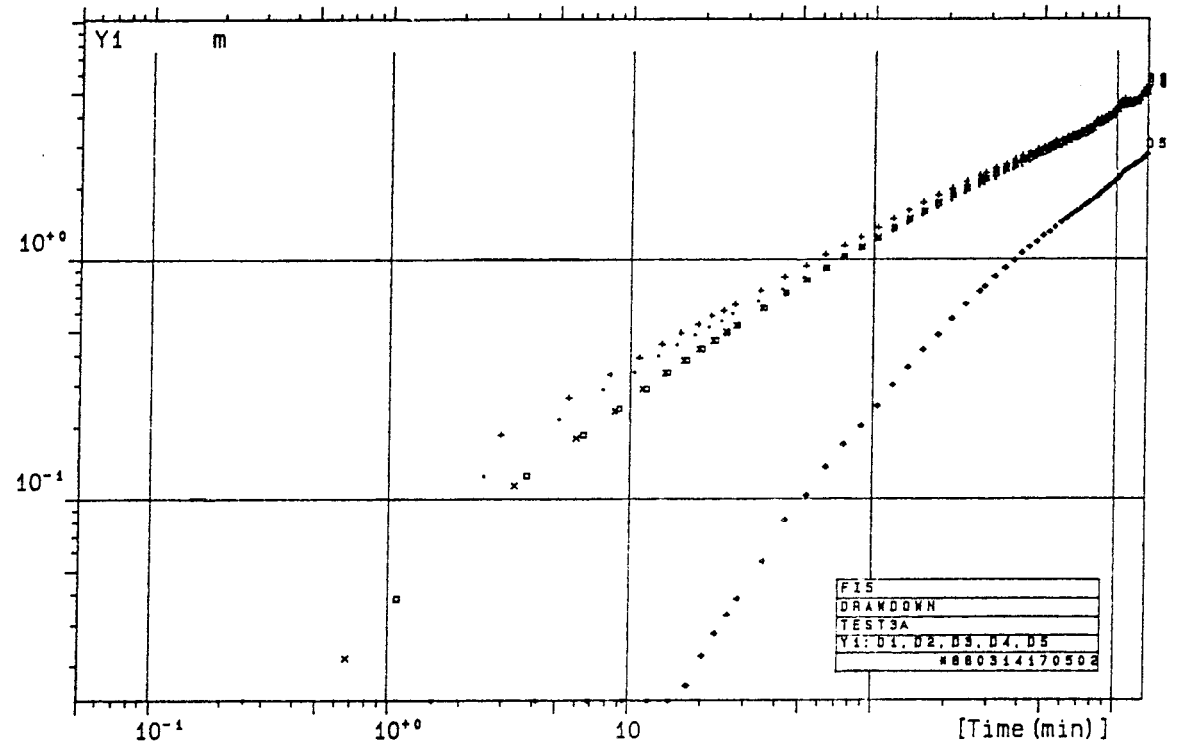

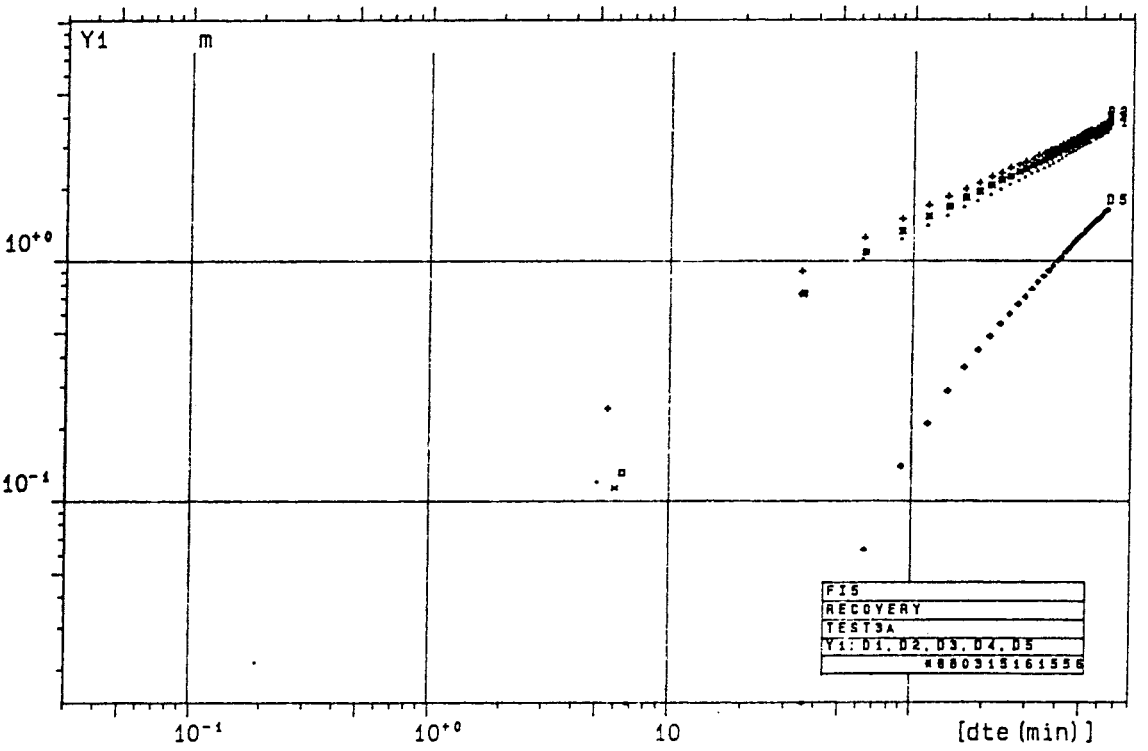

Appendix 4:4 Observed drawdown and recovery in borehole during interference test 3A.

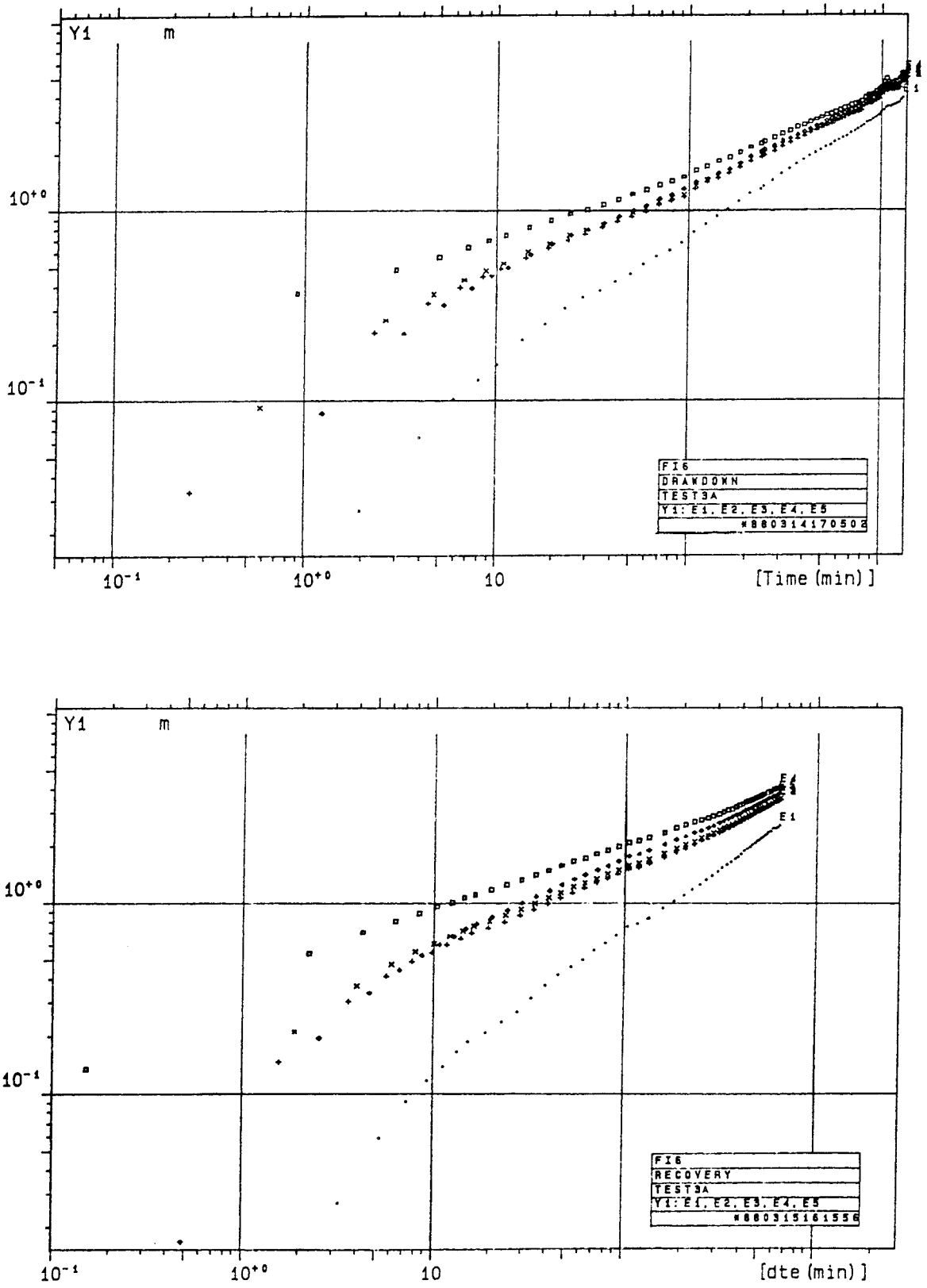

Appendix 4:5 Observed drawdown and recovery in borehole KFI06 during interference test 3A.

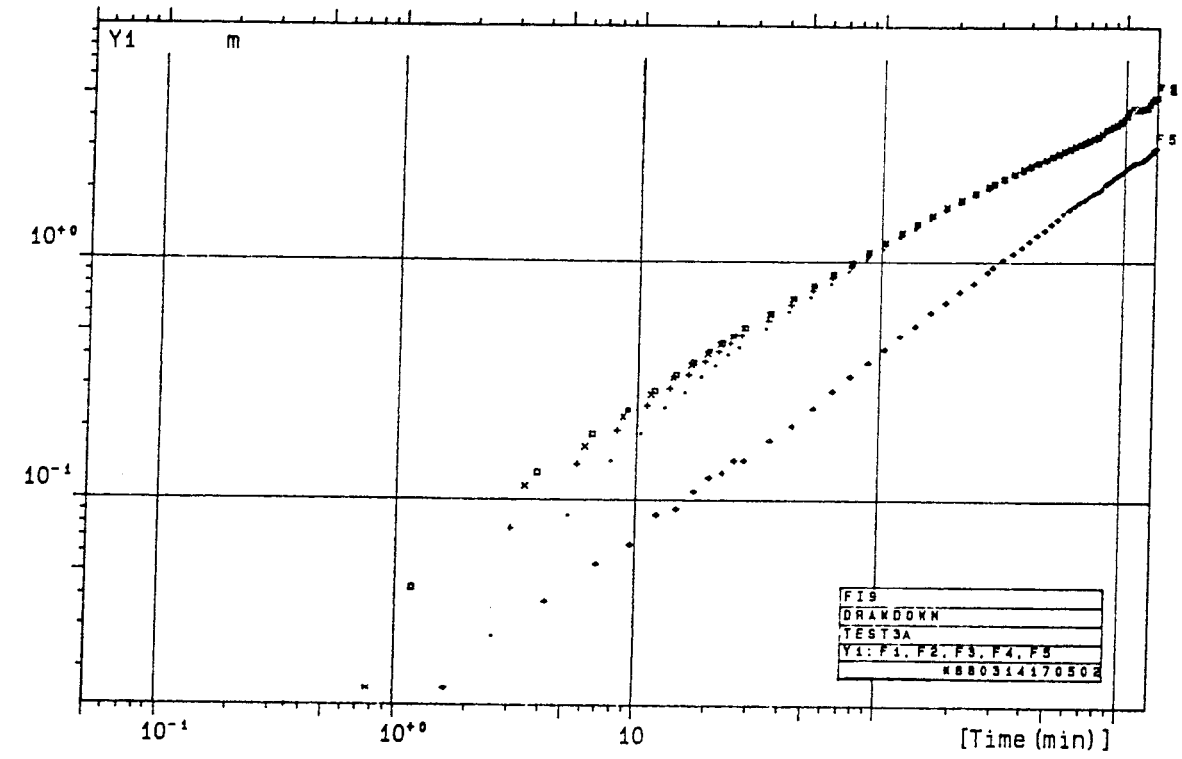

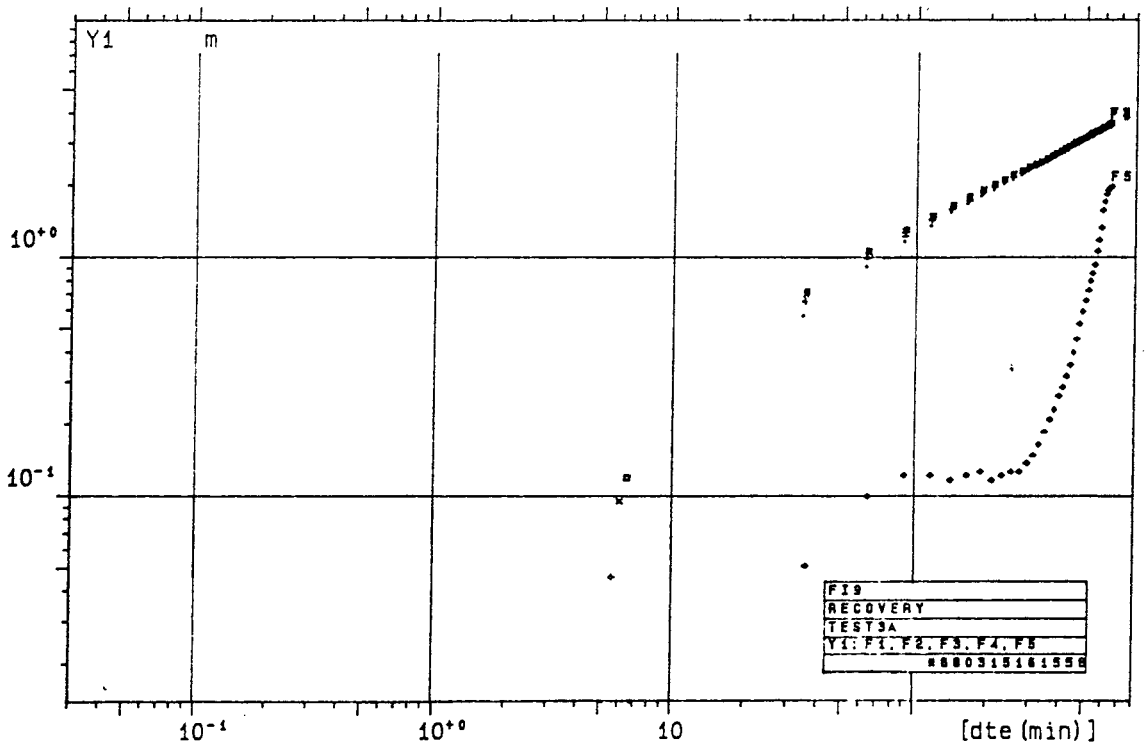

Appendix 4:6 Observed drawdown and recovery in borehole KFI09 during interference test 3A.

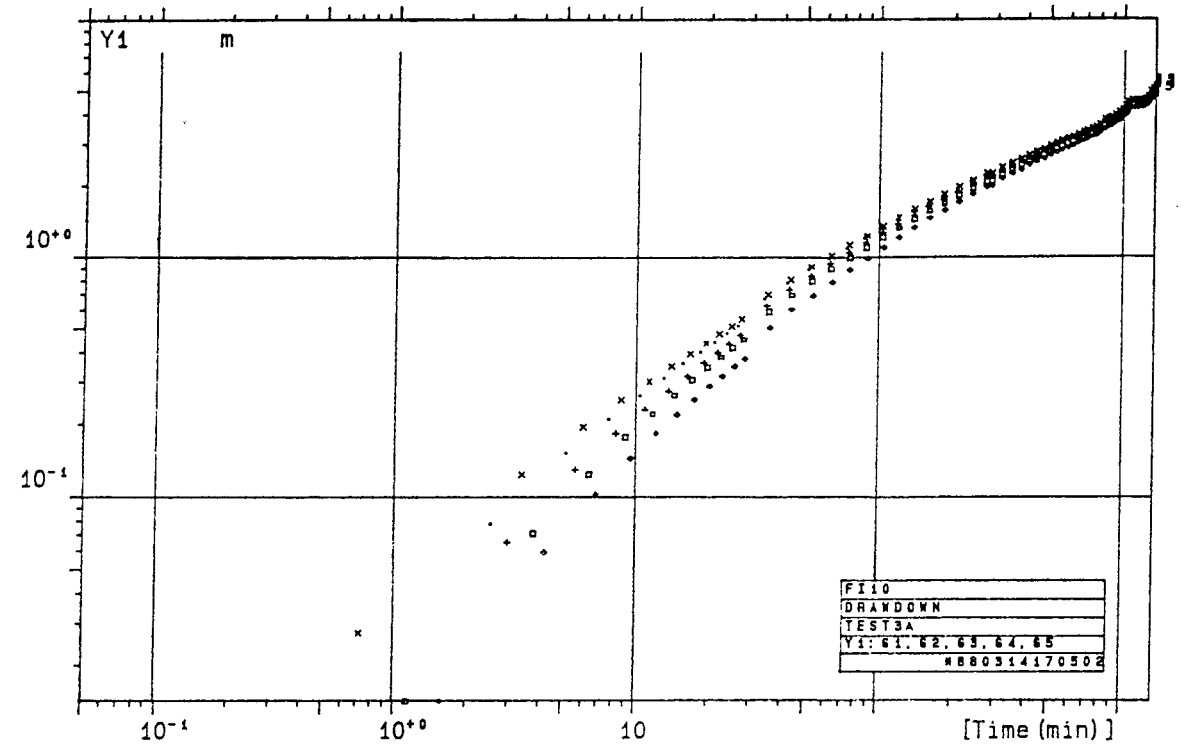

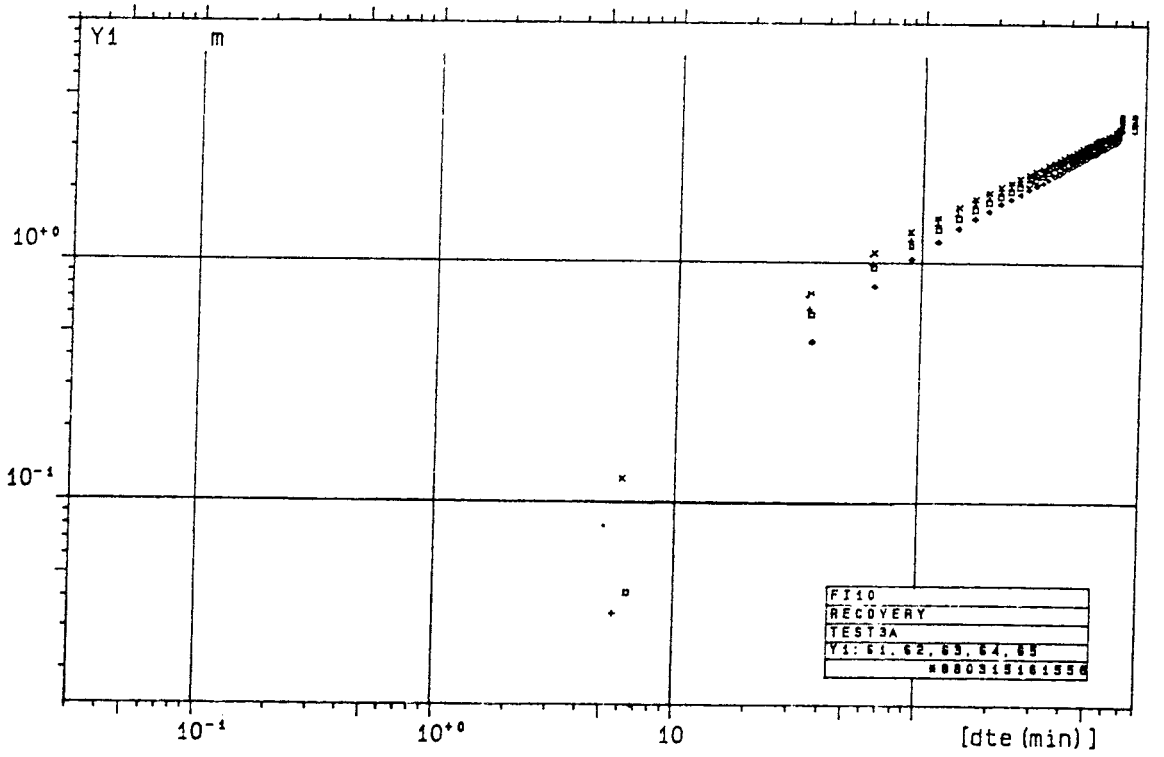

Appendix 4:7 Observed drawdown and recovery in borehole KFI10 during interference test 3A.

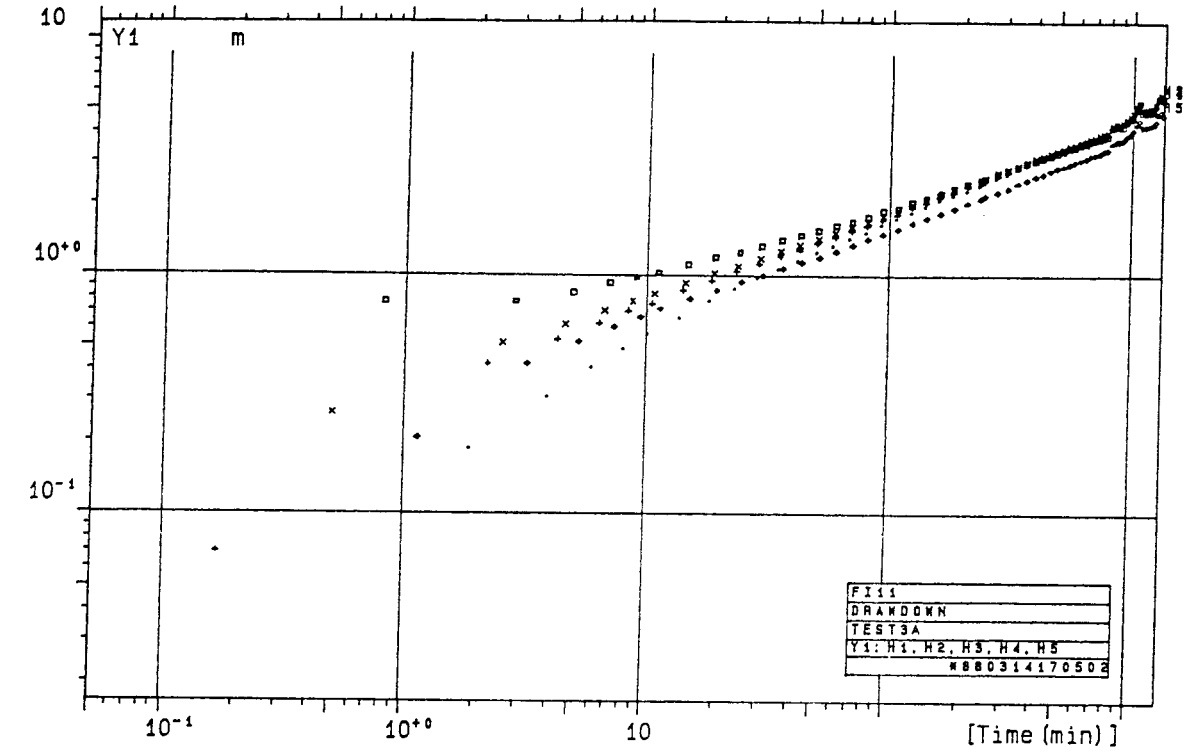

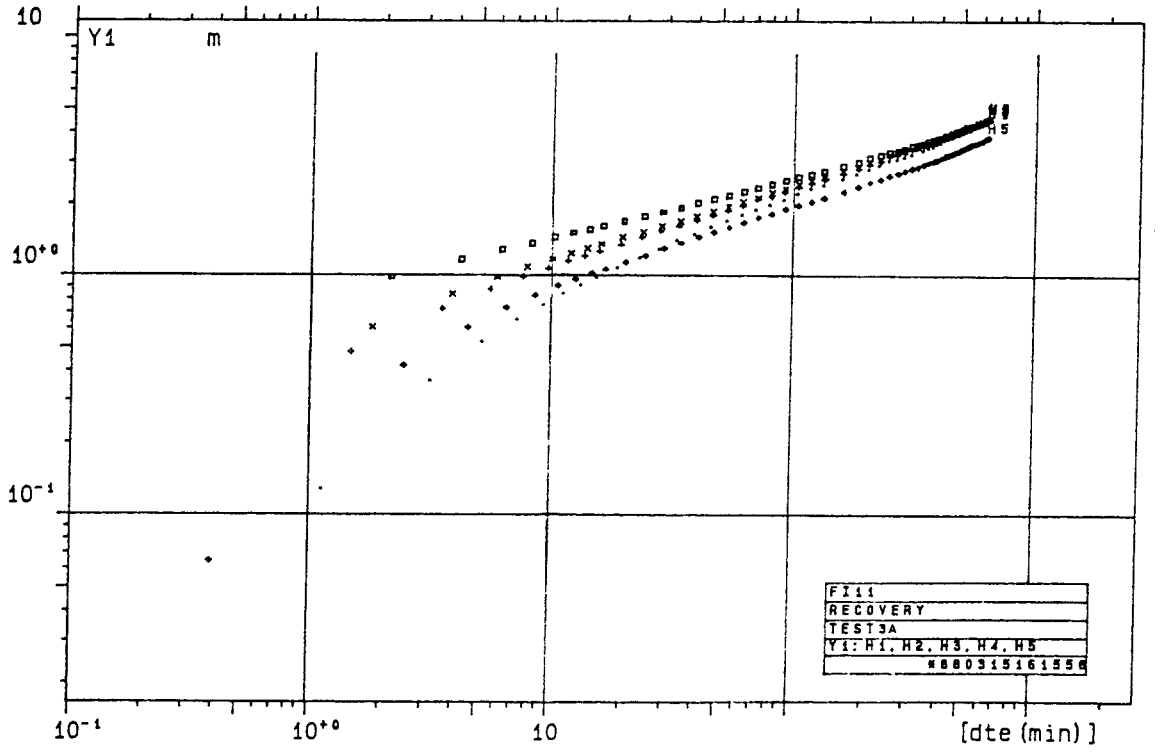

Appendix 4:8 Observed drawdown and recovery in borehole KFI11 during interference test 3A.

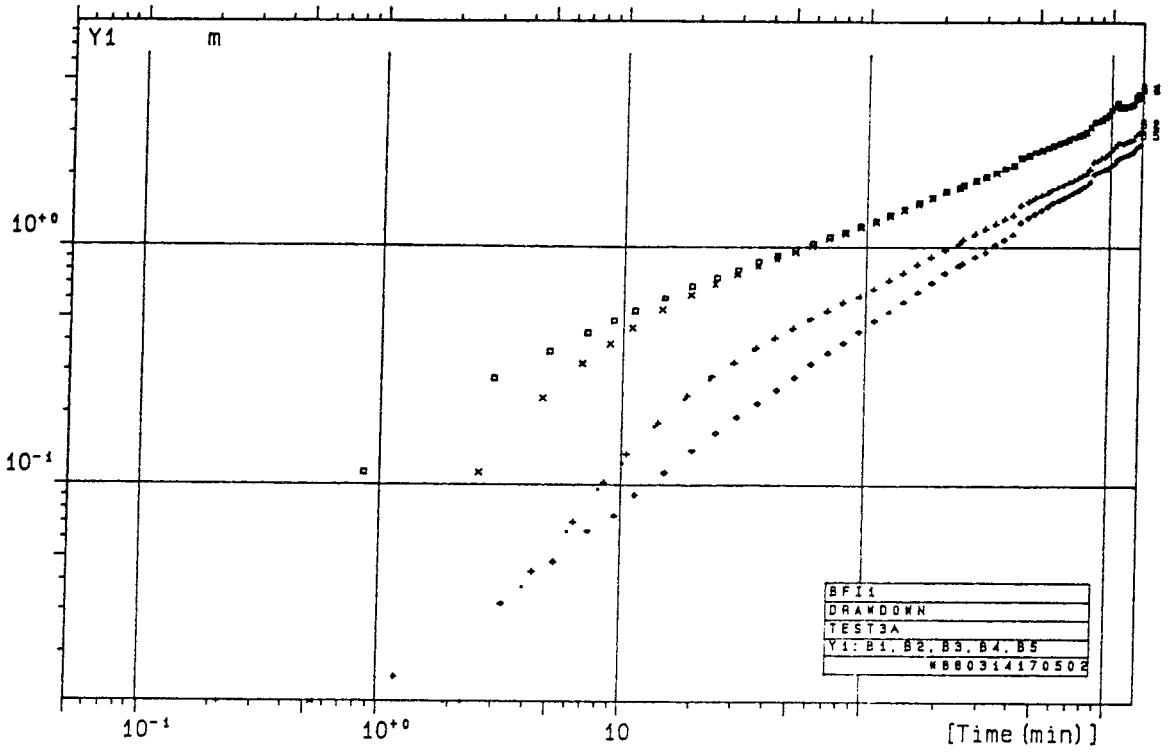

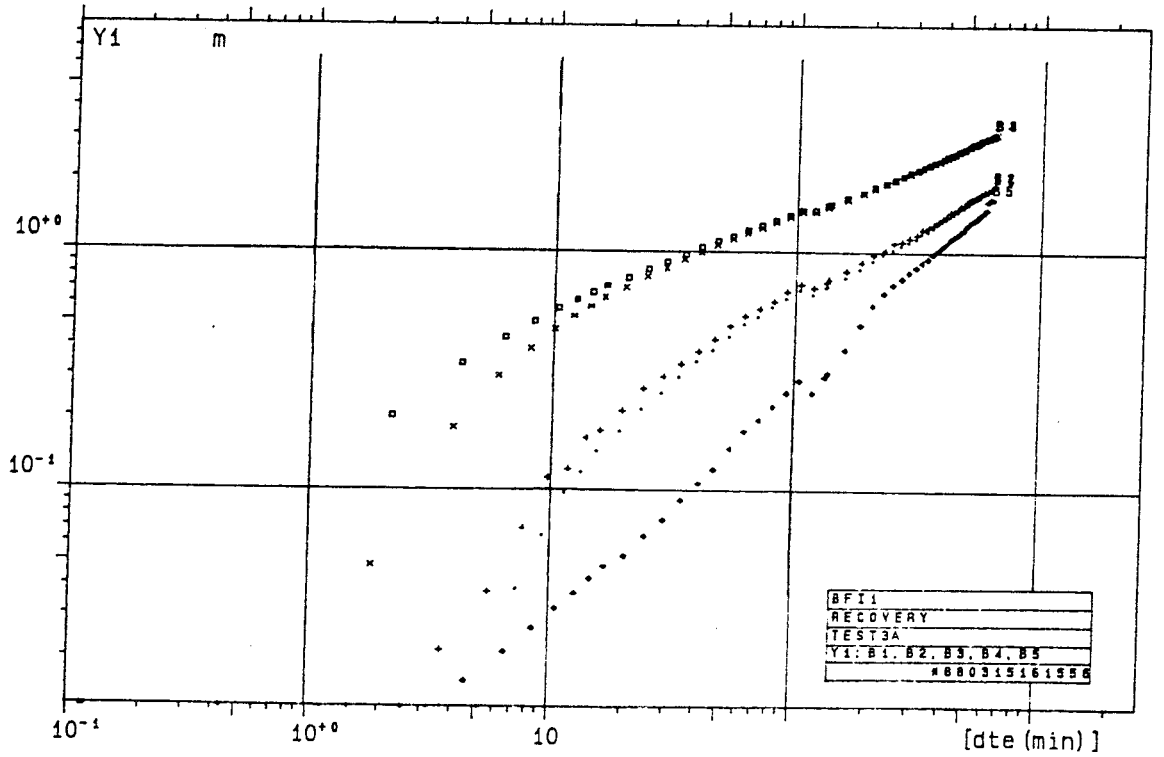

Appendix 4:9 Observed drawdown and recovery in borehole BFI01 during interference test 3A.

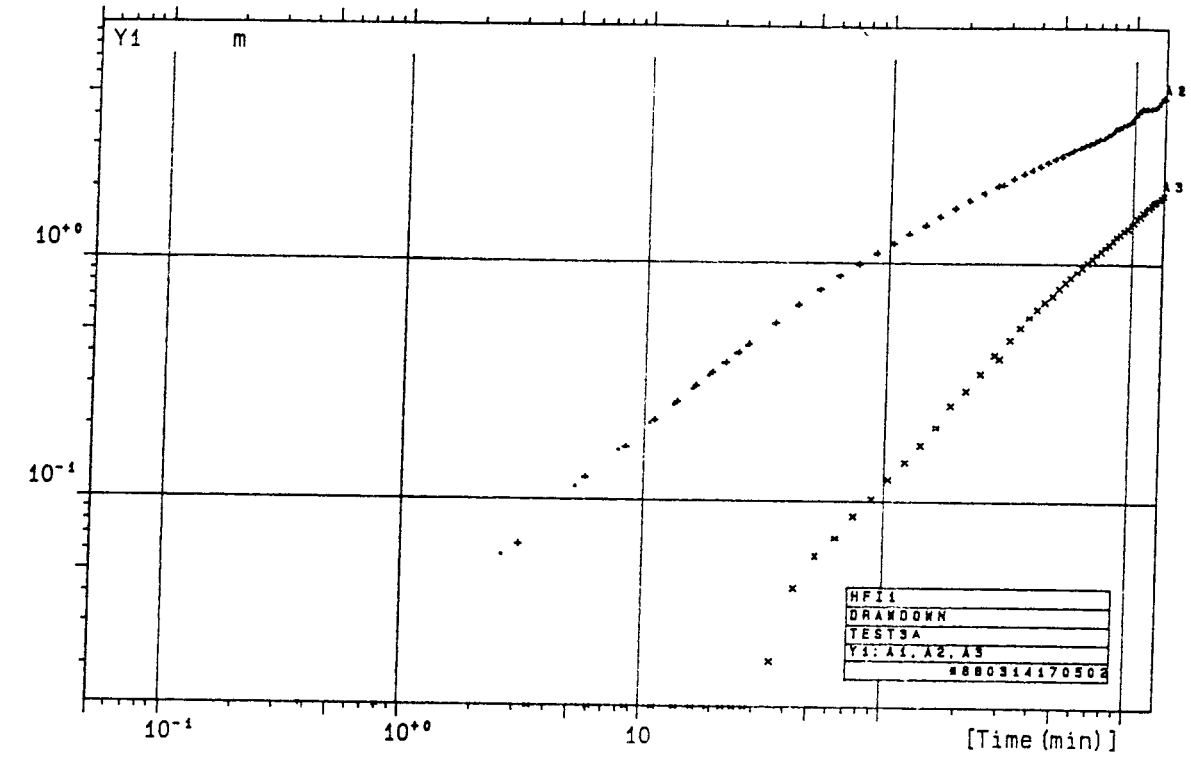

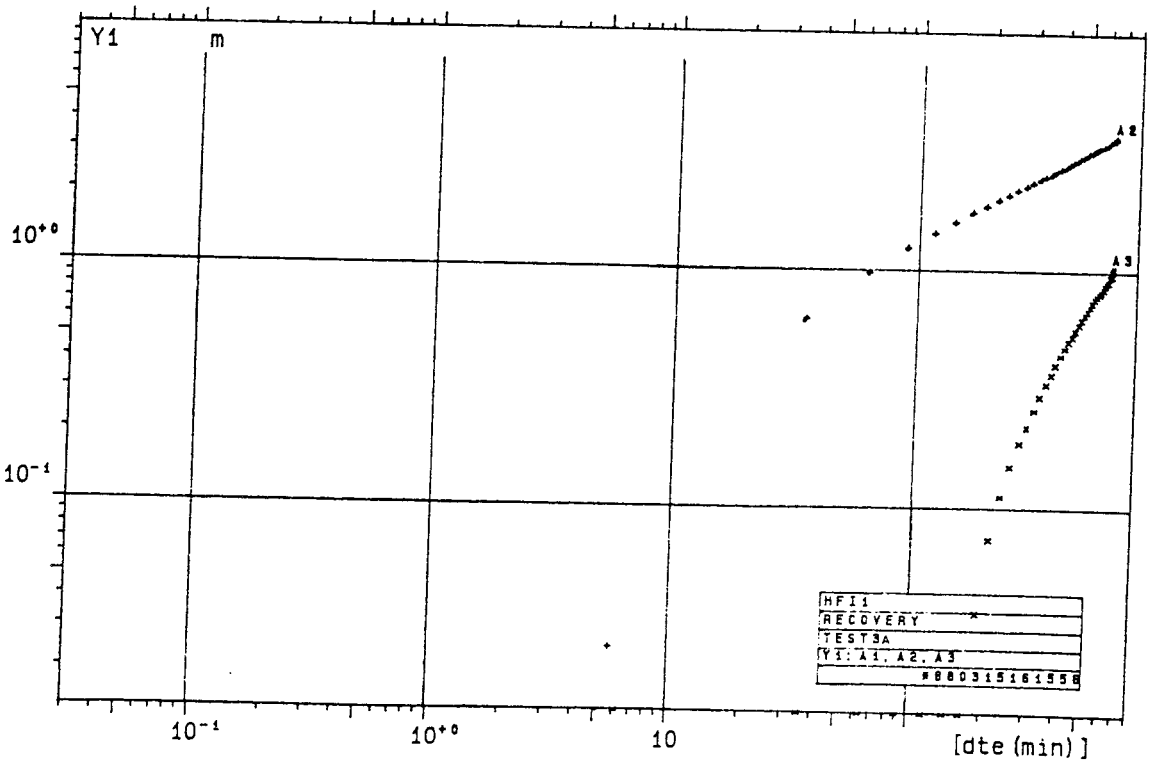

Appendix 4:10 Observed drawdown and recovery in borehole HFI01 during interference test 3A.

APPENDIX 5

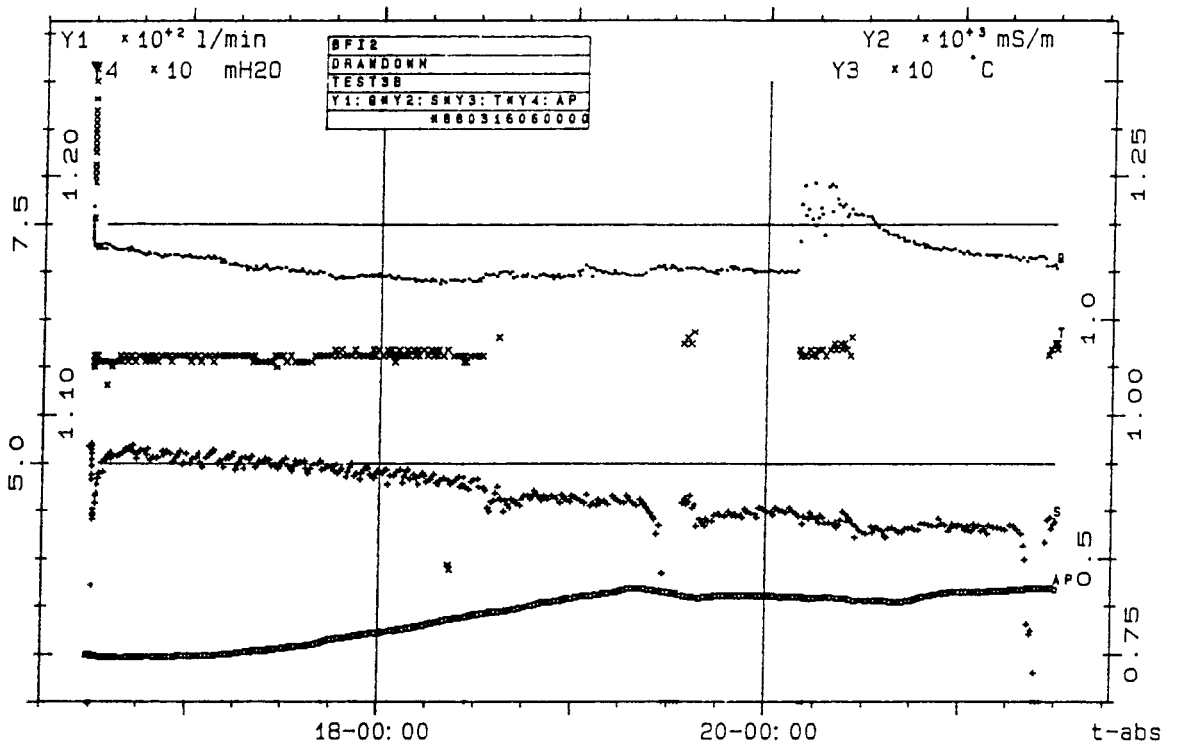

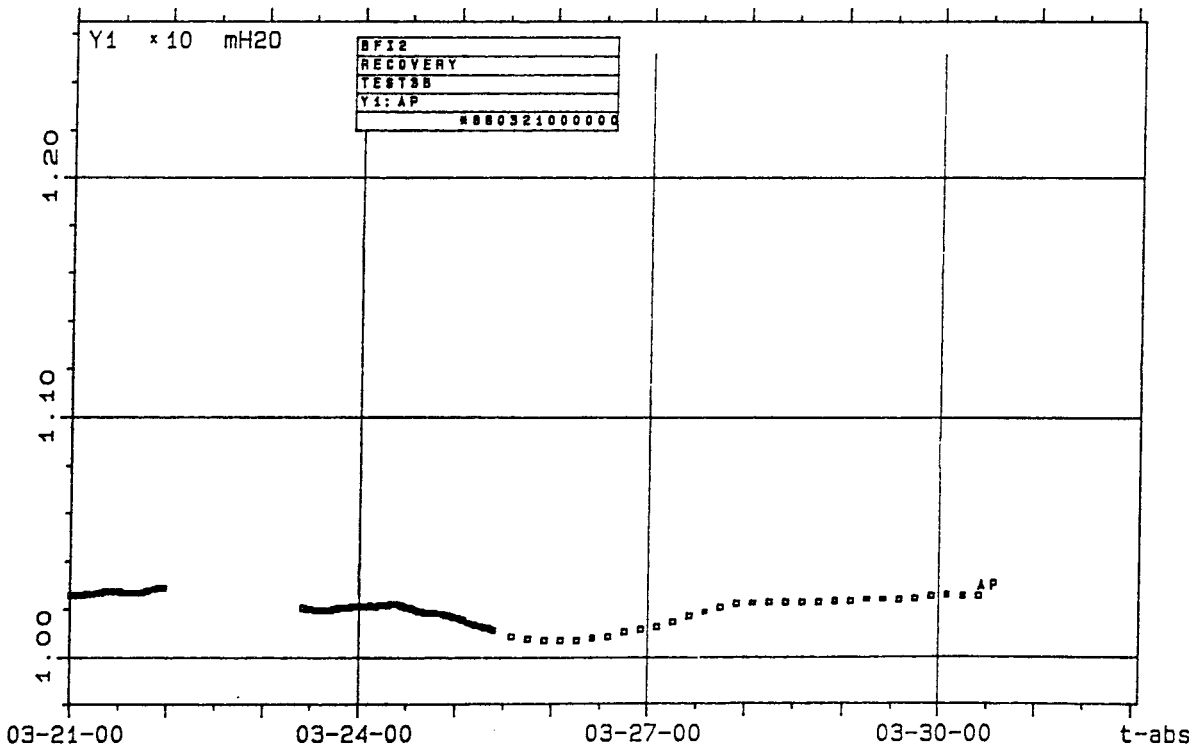

Appendix 5:1 Flow rate, electric conductivity, barometric pressure head and temperature during interference test 3B (linear time scale).

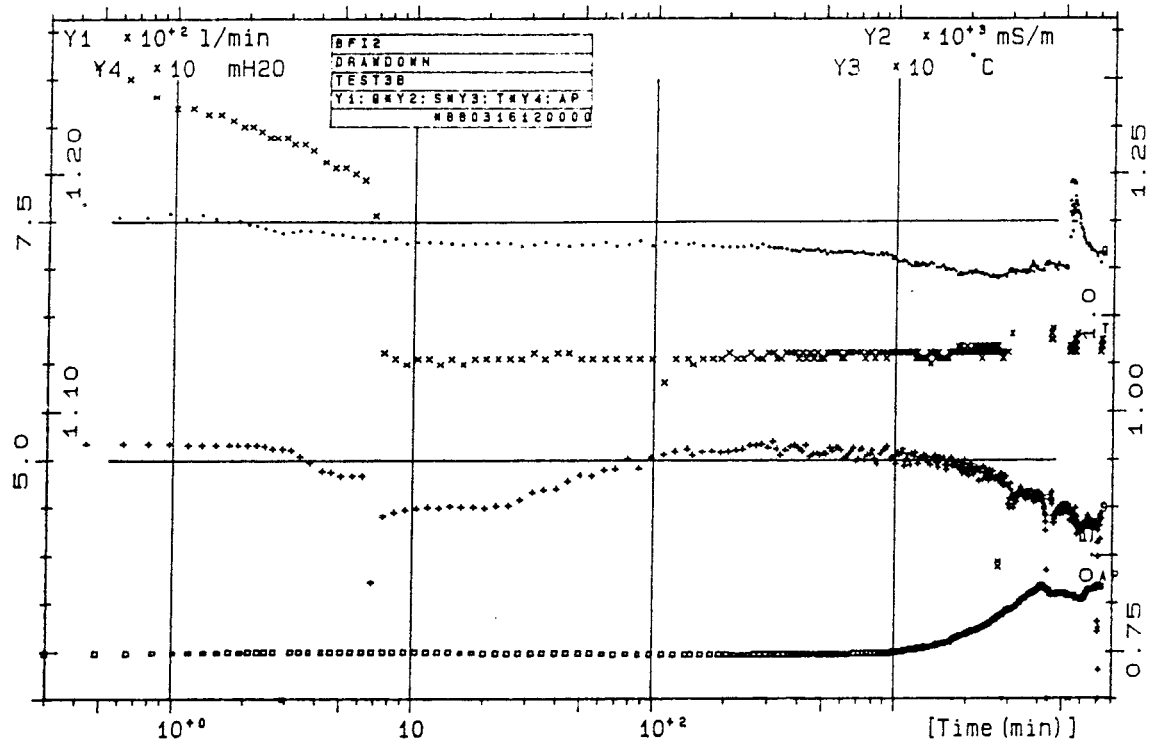

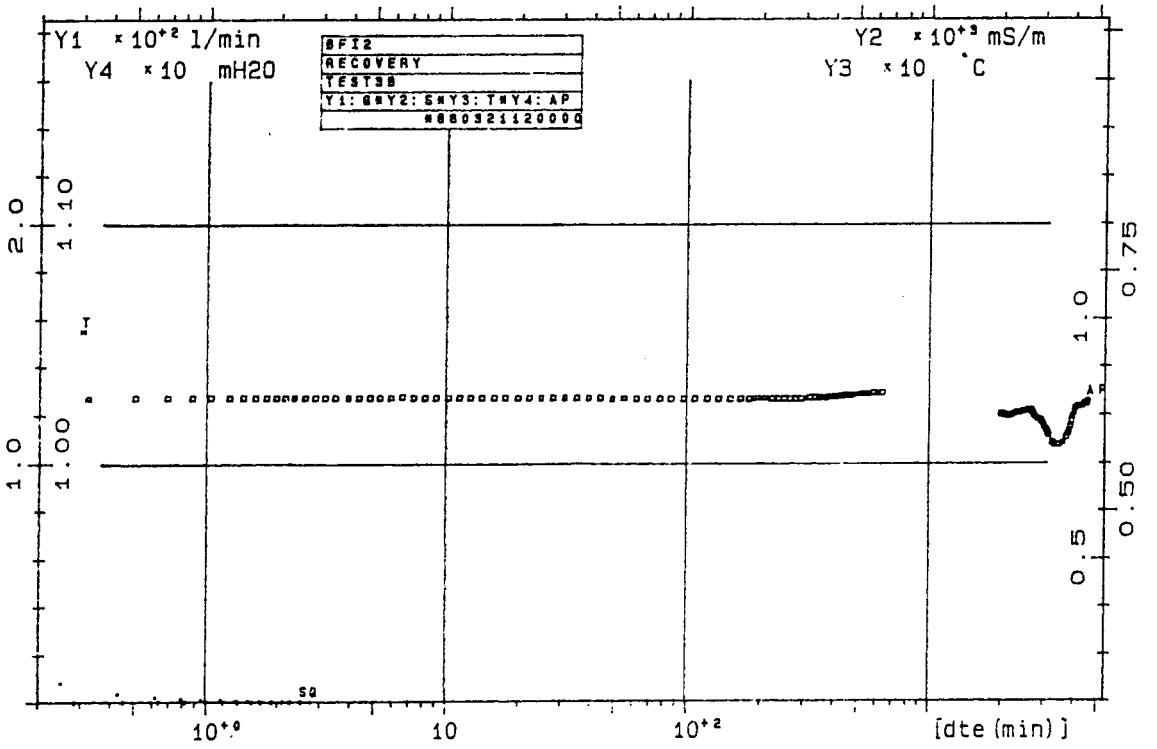

Appendix 5:2 Flow rate, electric conductivity, barometric pressure head and temperature during interference test 3B (logarithmic time scale).

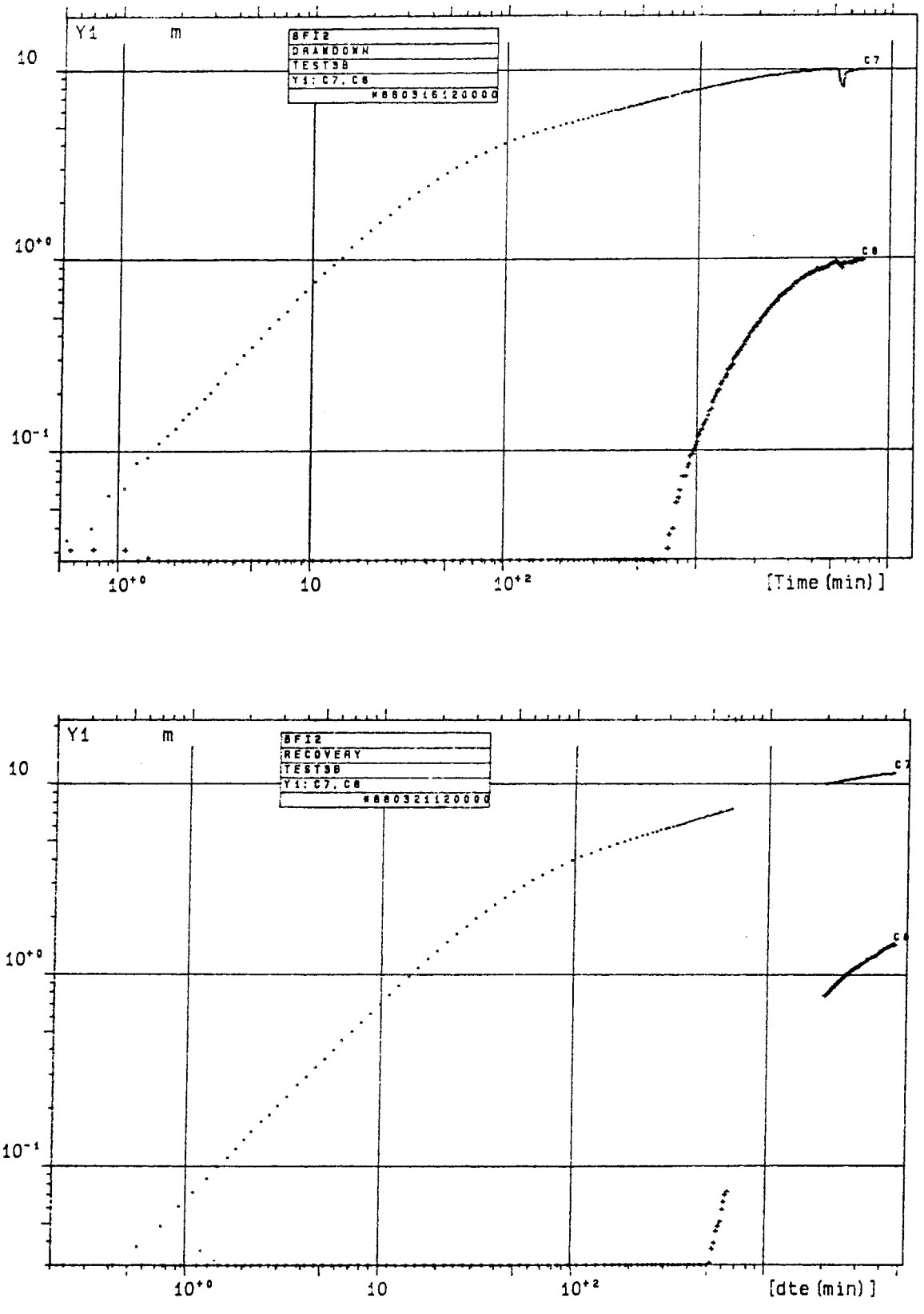

Appendix 5:3 Observed drawdown and recovery in borehole BFI02 during interference test 3B.

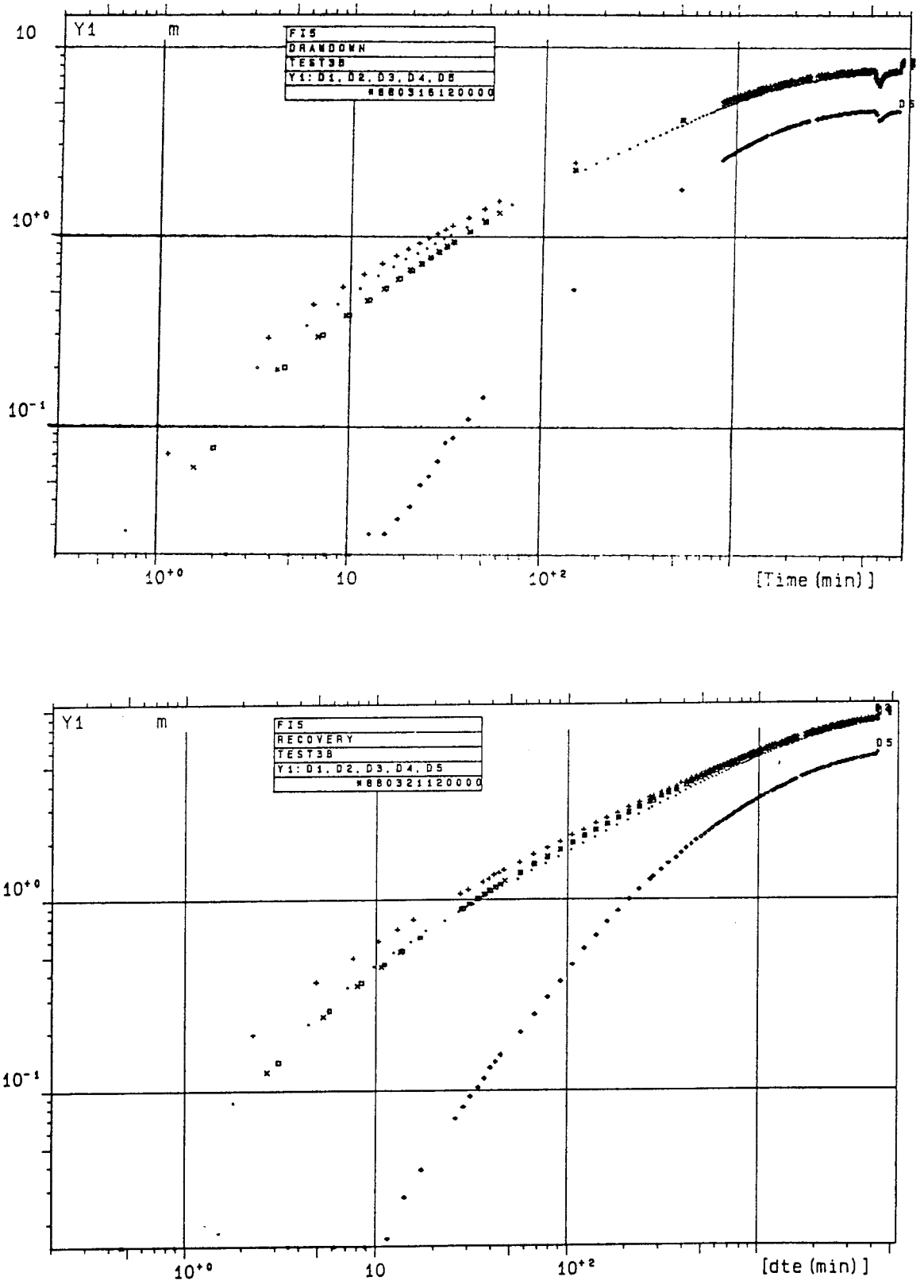

Appendix 5:4 Observed drawdown and recovery in borehole KFI05 during interference test 3B.

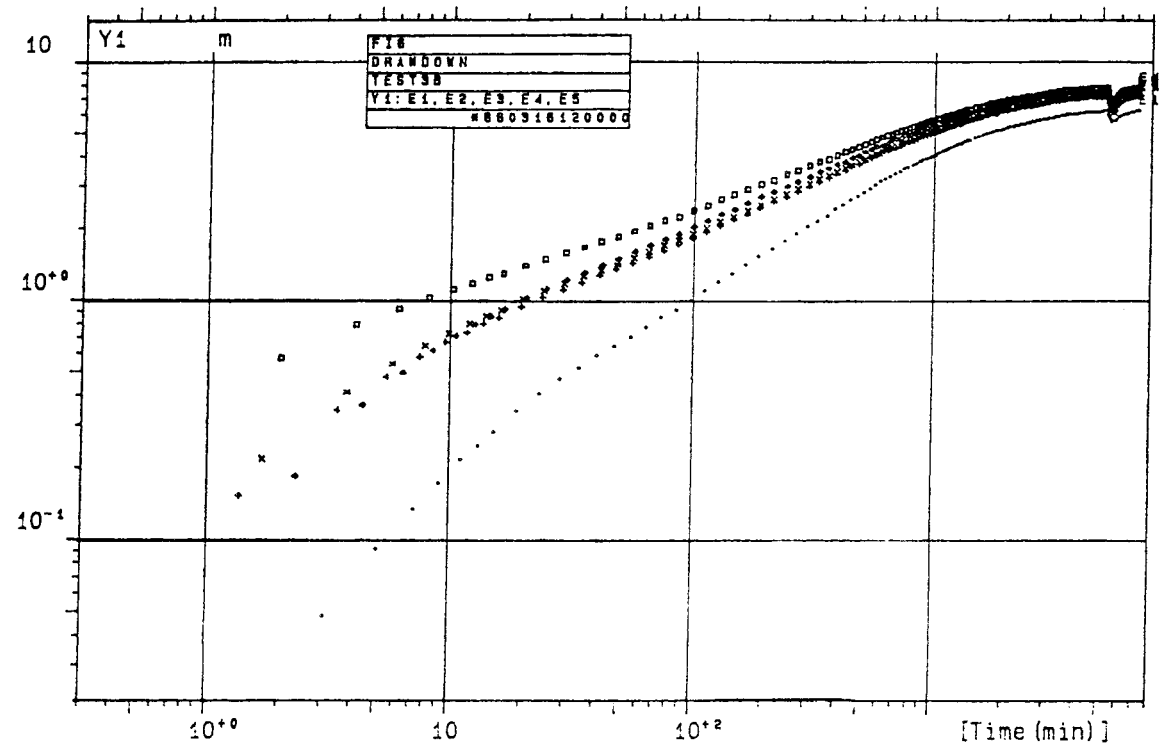

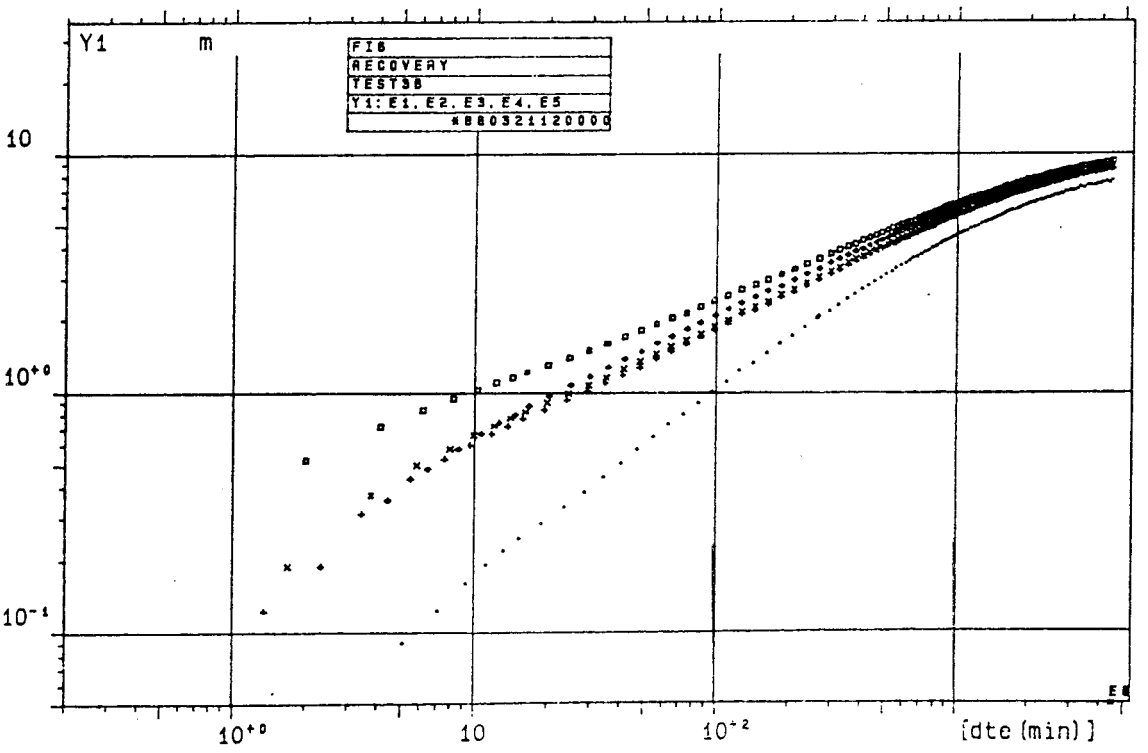

Appendix 5:5 Observed drawdown and recovery in borehole KFI06 during interference test 3B.

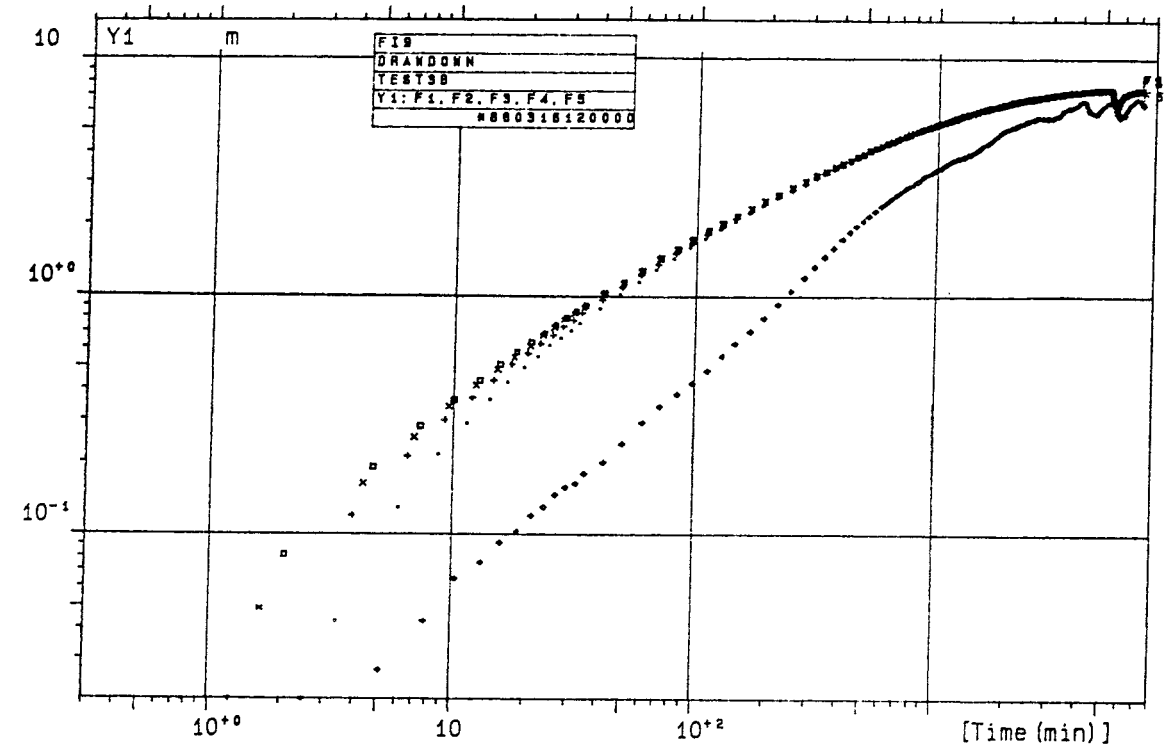

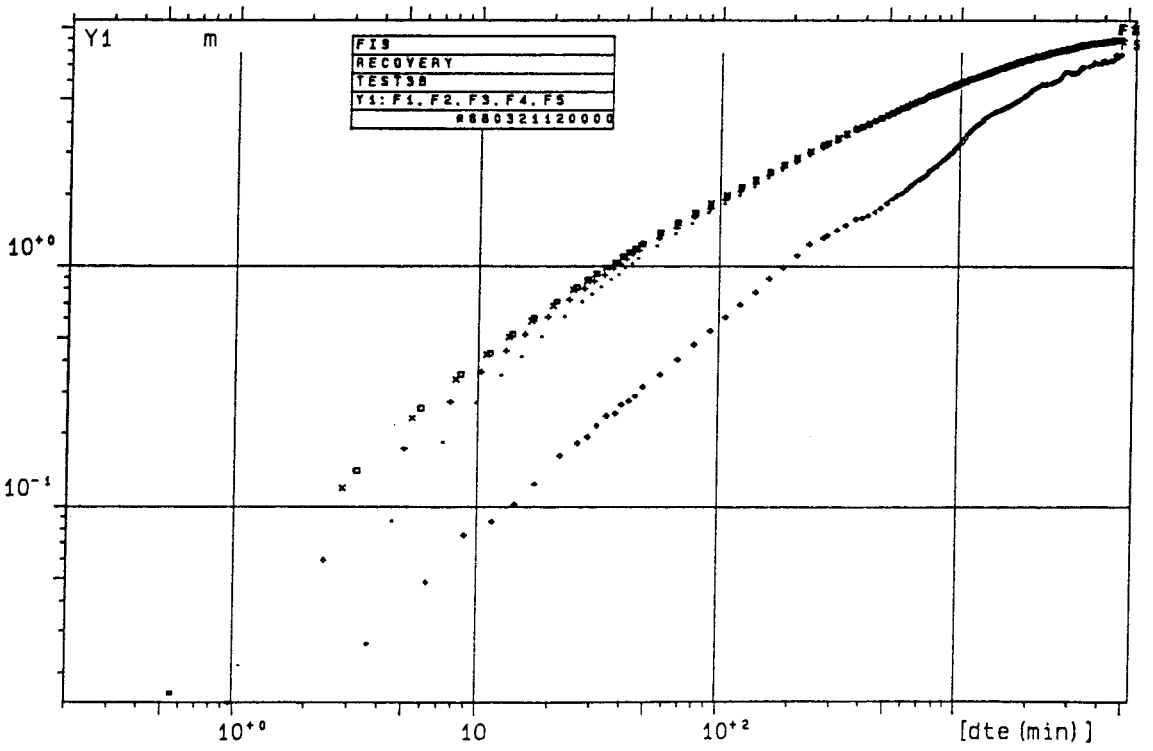

Appendix 5:6 Observed drawdown and recovery in borehole KFI09 during interference test 3B.

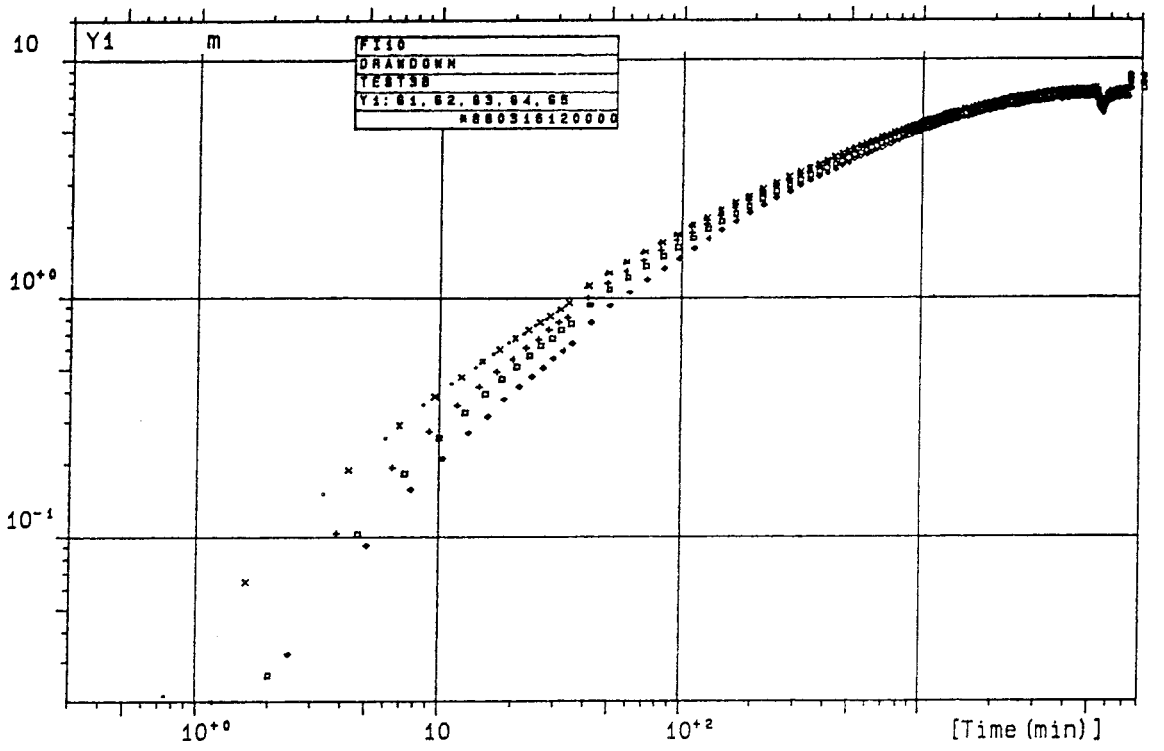

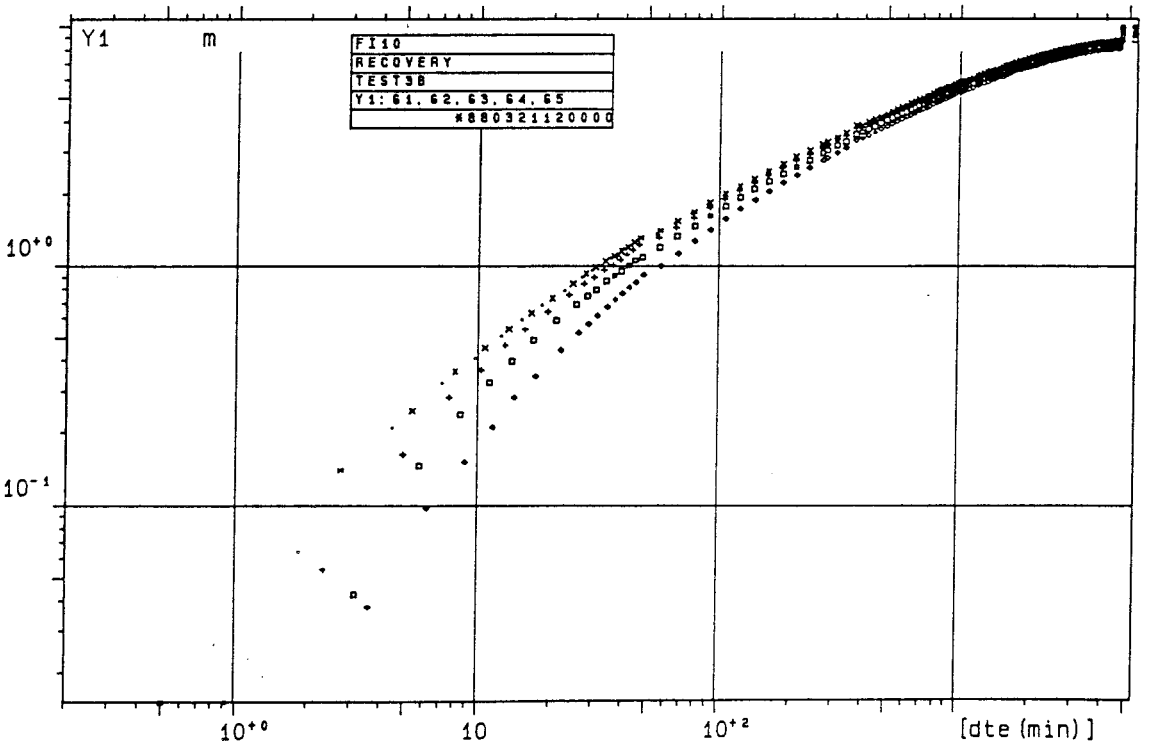

Appendix 5:7 Observed drawdown and recovery in borehole KFI10 during interference test 3B.

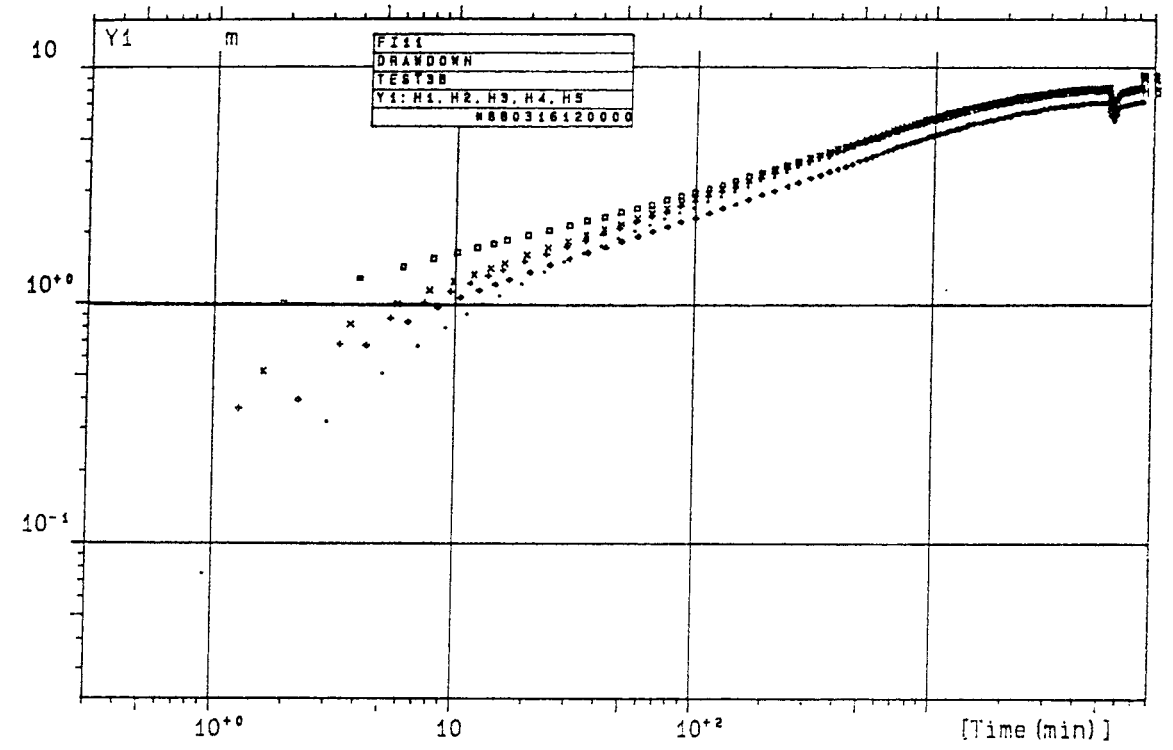

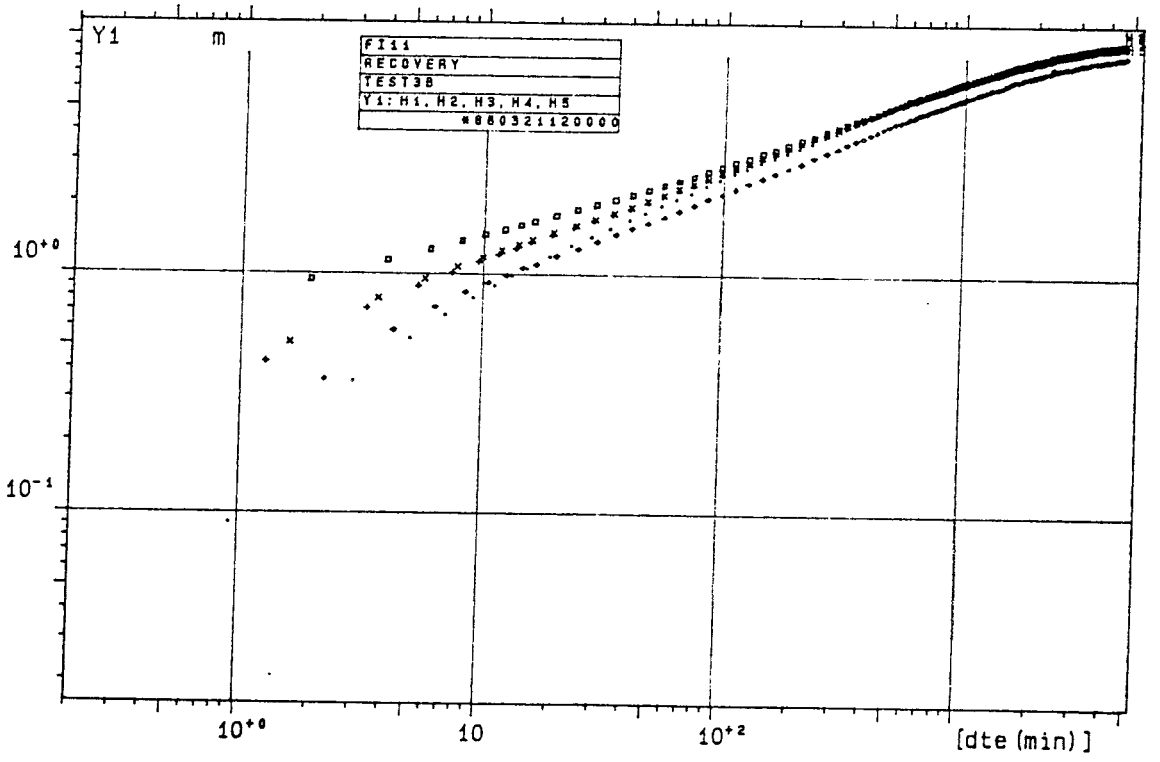

Appendix 5:8 Observed drawdown and recovery in borehole KFI11 during interference test 3B.

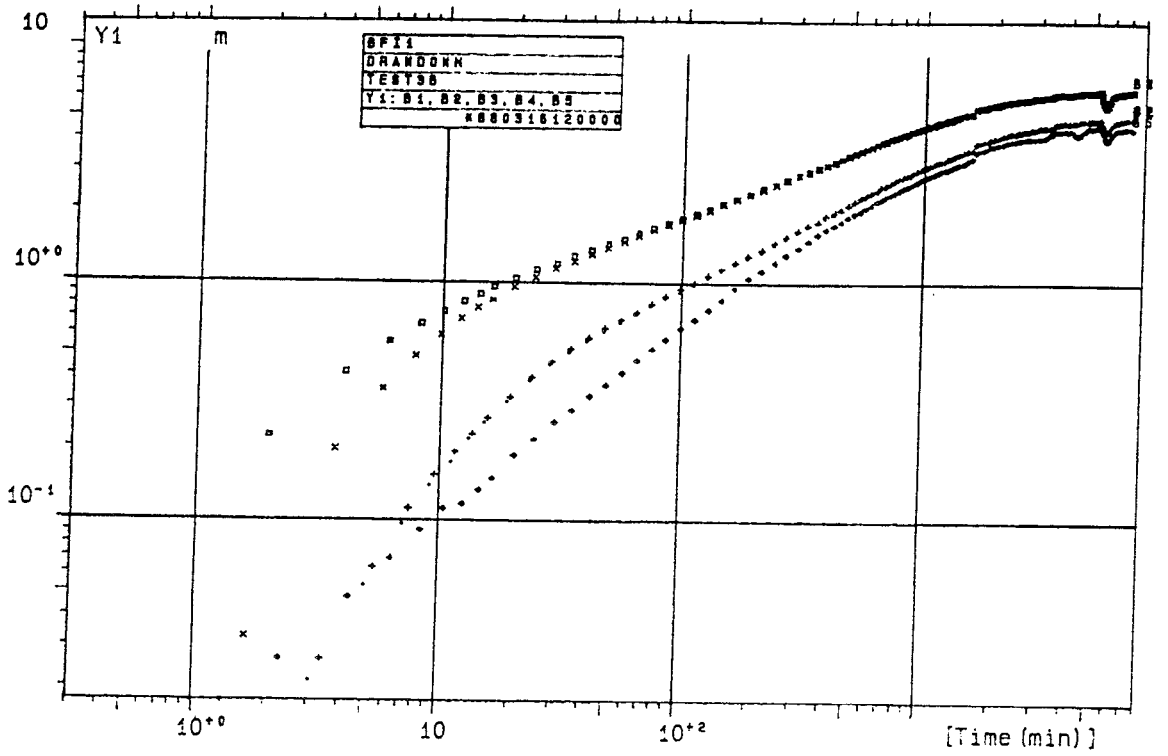

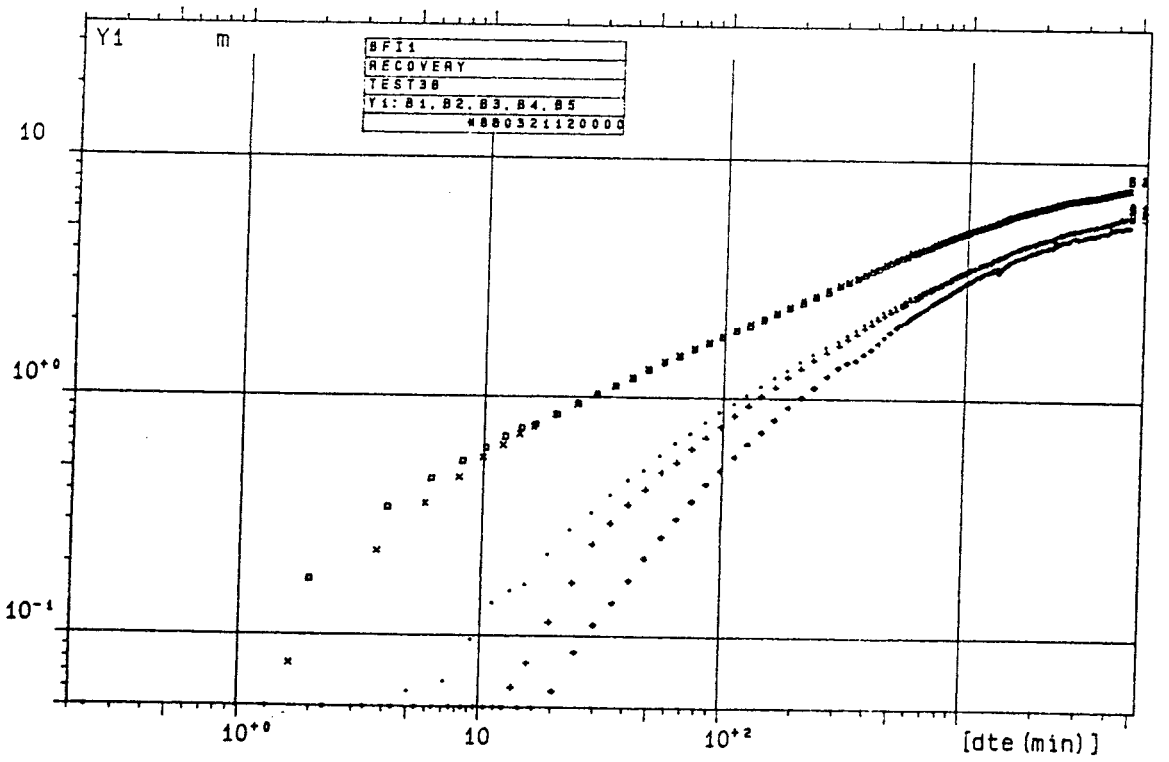

Appendix 5:9 Observed drawdown and recovery in borehole BFI01 during interference test 3B.

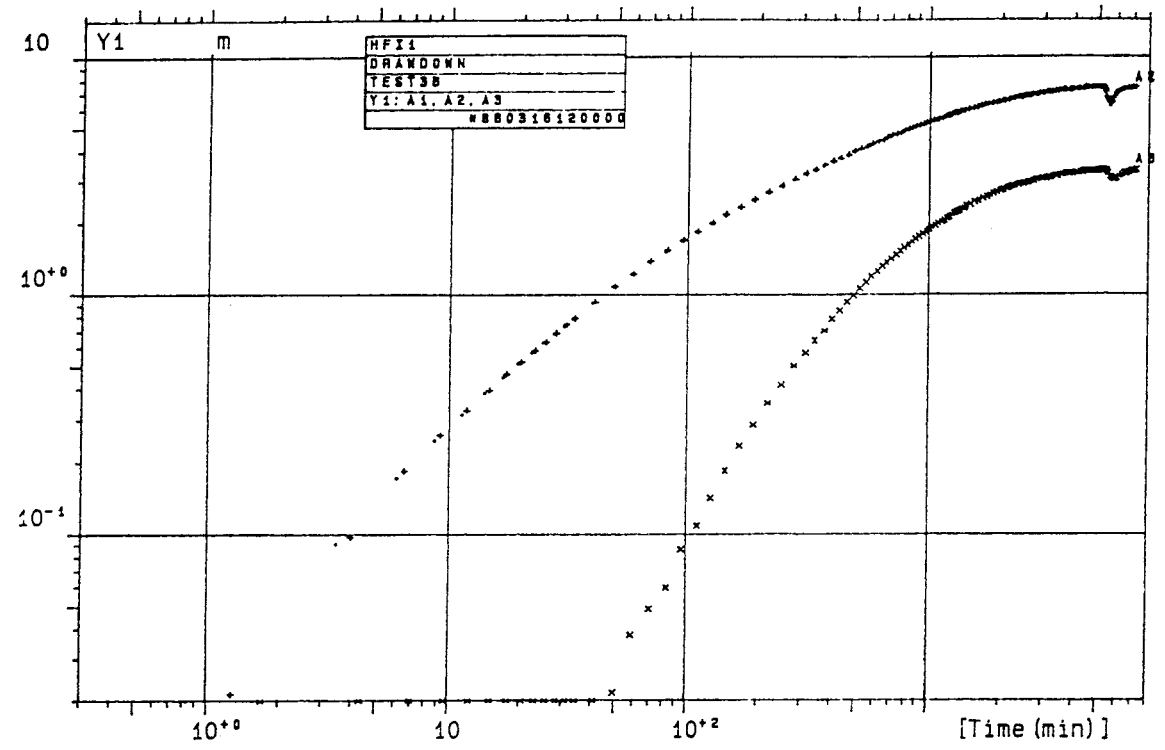

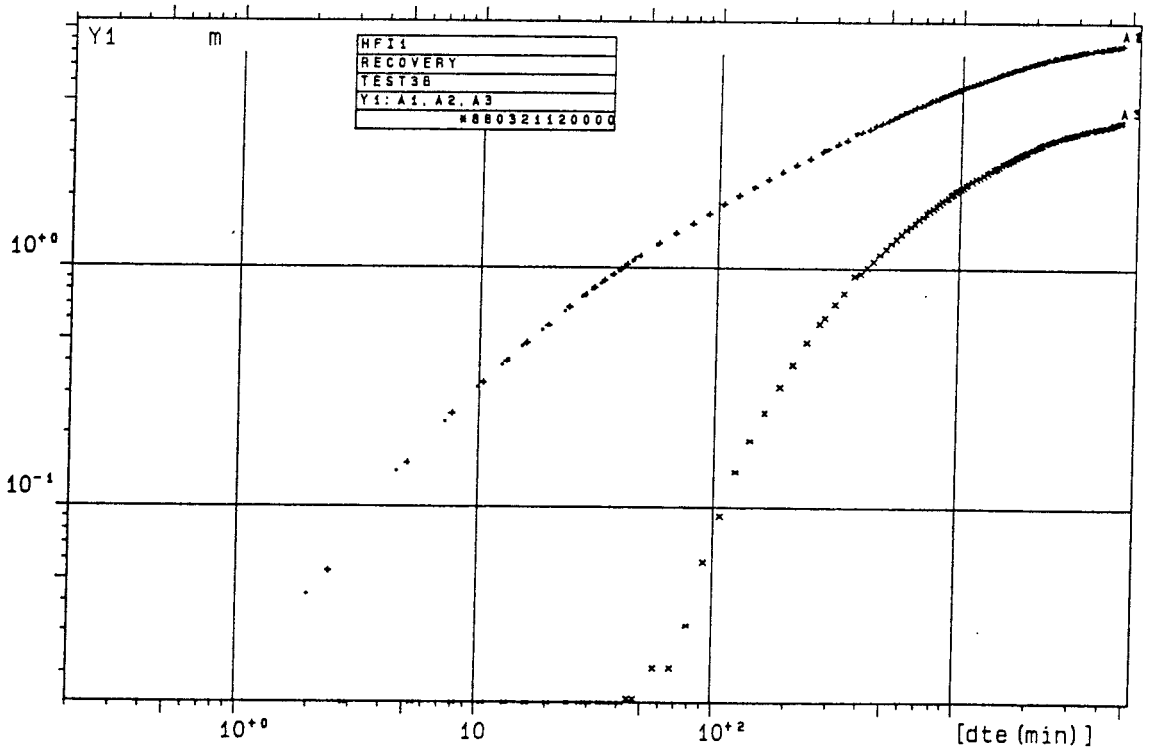

Appendix 5:10 Observed drawdown and recovery in borehole HFI01 during interference test 3B

APPENDIX 6

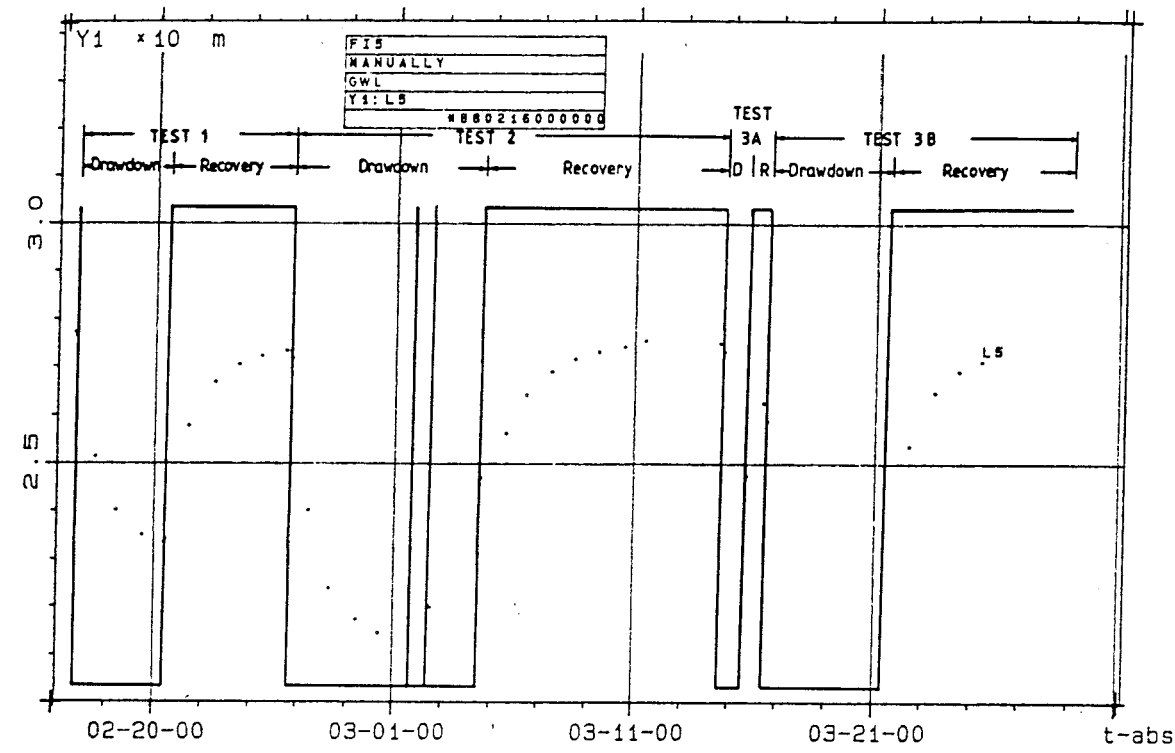

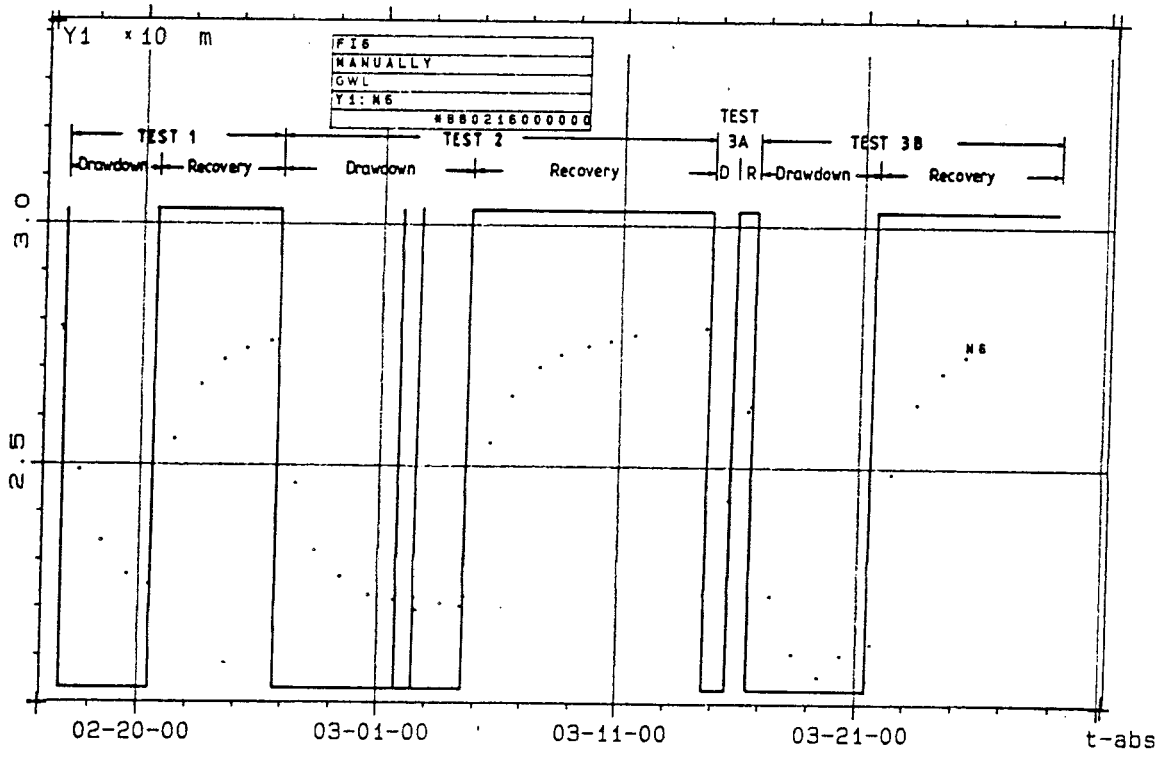

Appendix 6:1 Observed groundwater head in boreholes KFI05 and KFI06 during the interference tests.

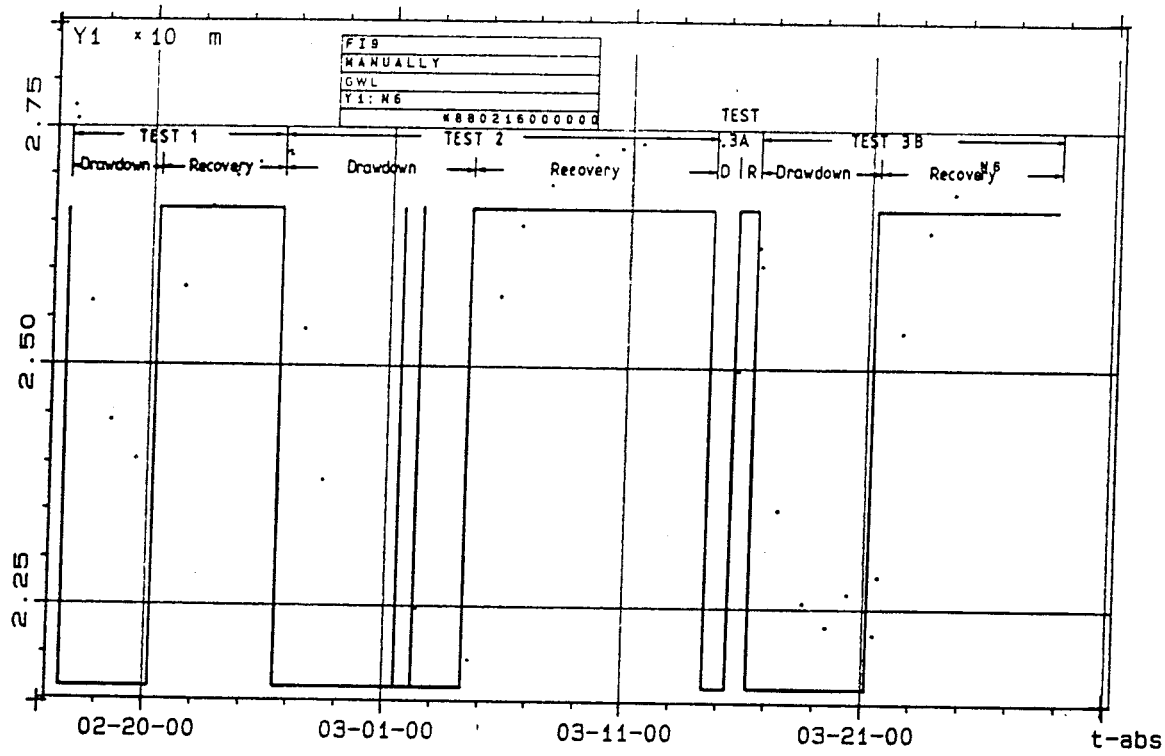

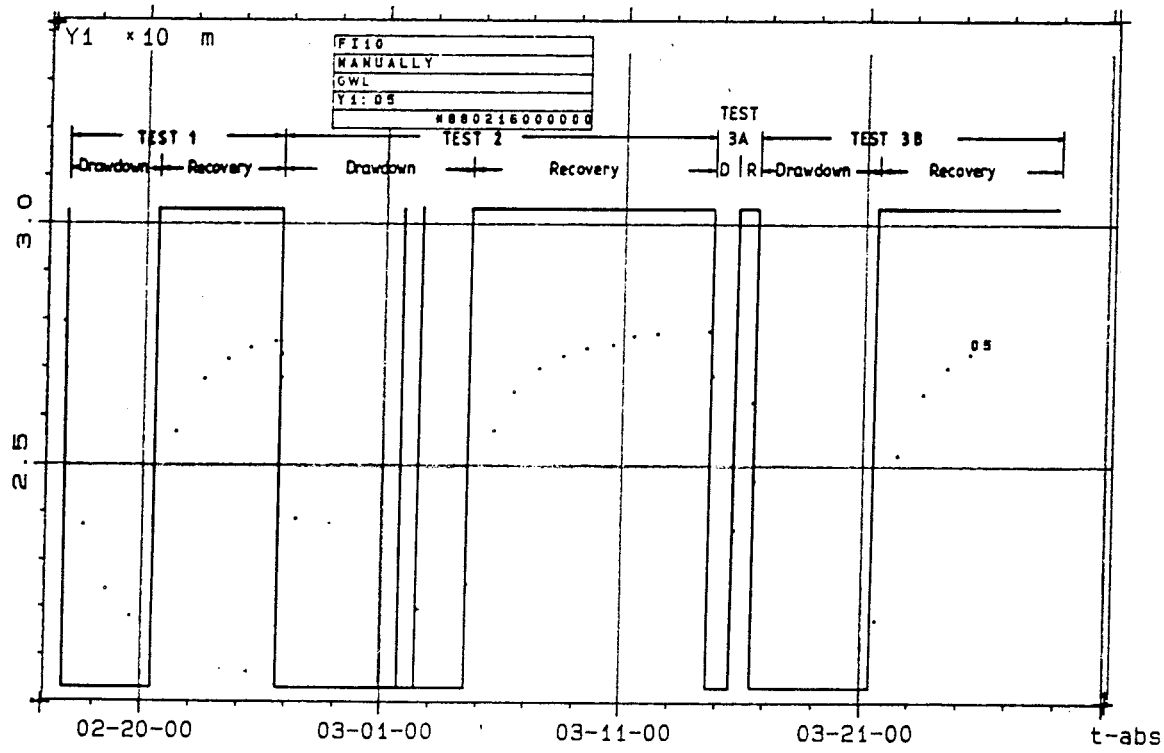

Appendix 6:2 Observed groundwater head in boreholes KFI09 and KFI10 during the interference tests.

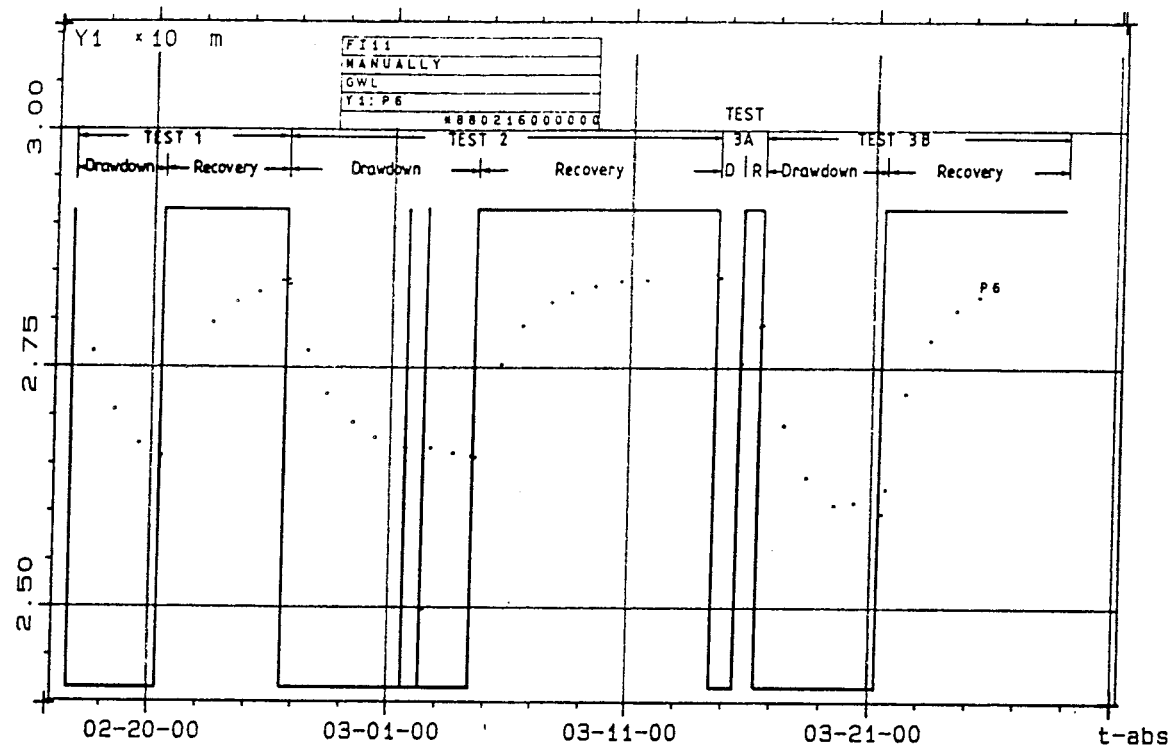

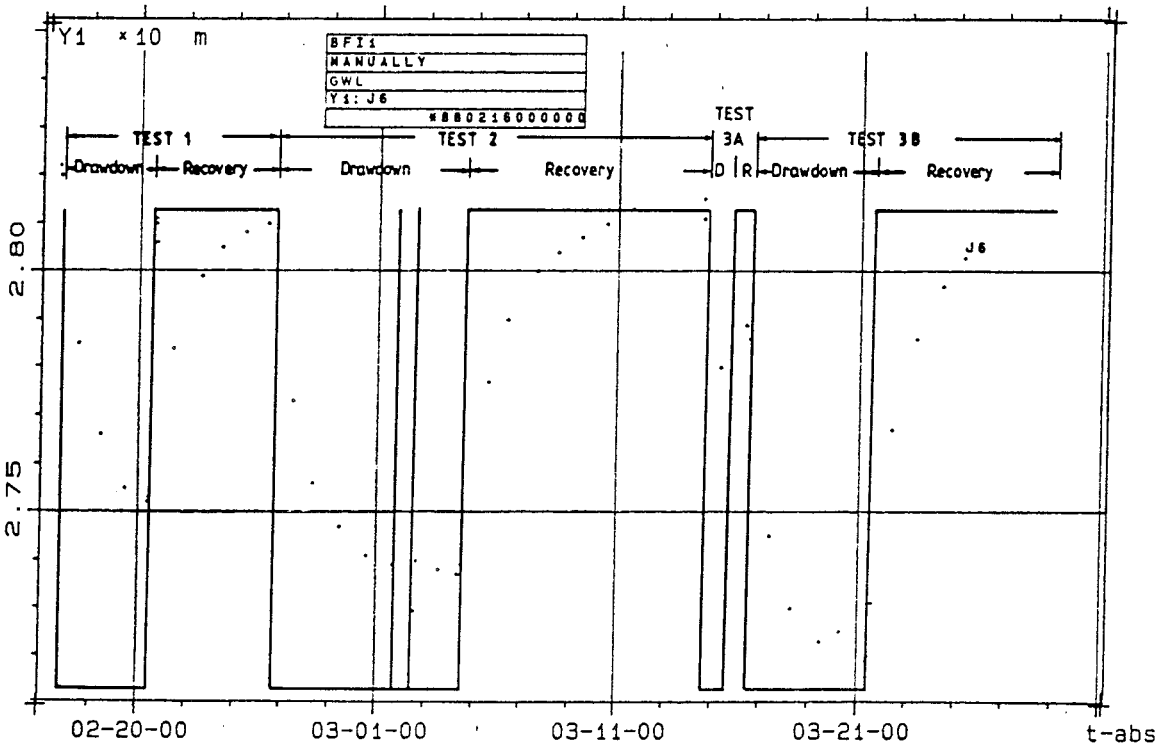

Appendix 6:3 Observed groundwater head in boreholes KFI11 and BFI01 during the interference tests.

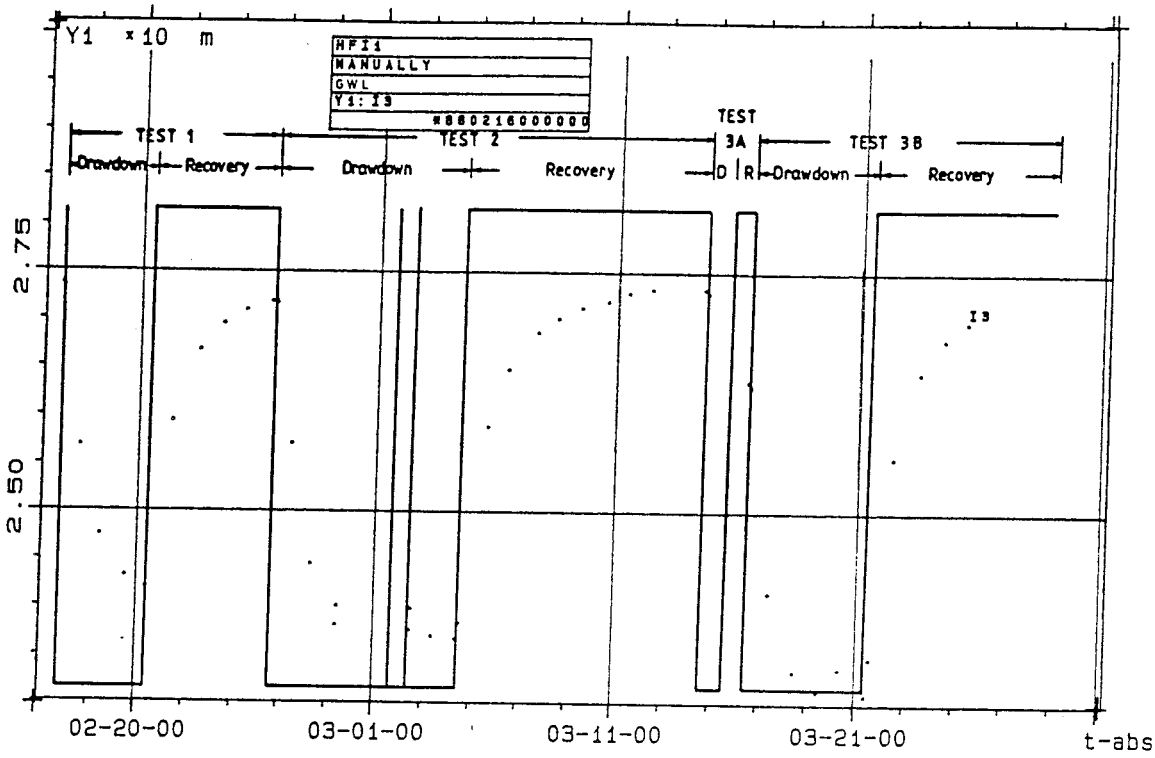

Appendix 6:4 Observed groundwater head in borehole HFI01 during the interference tests.

APPENDIX 7

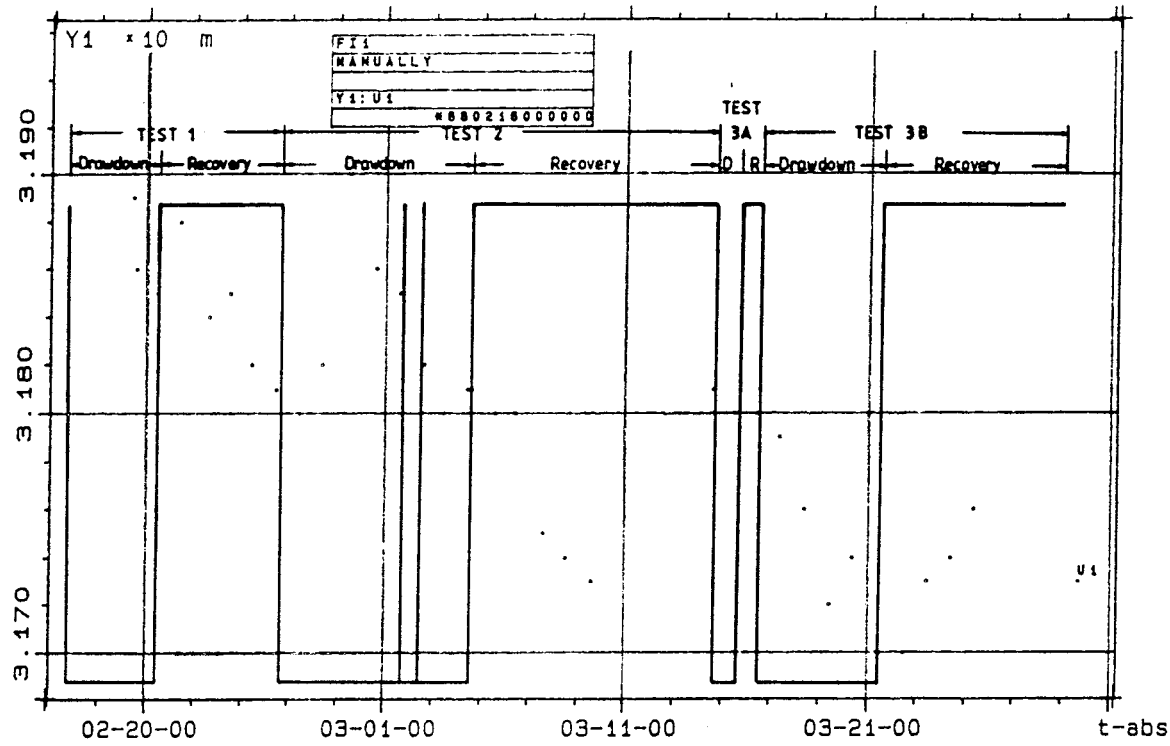

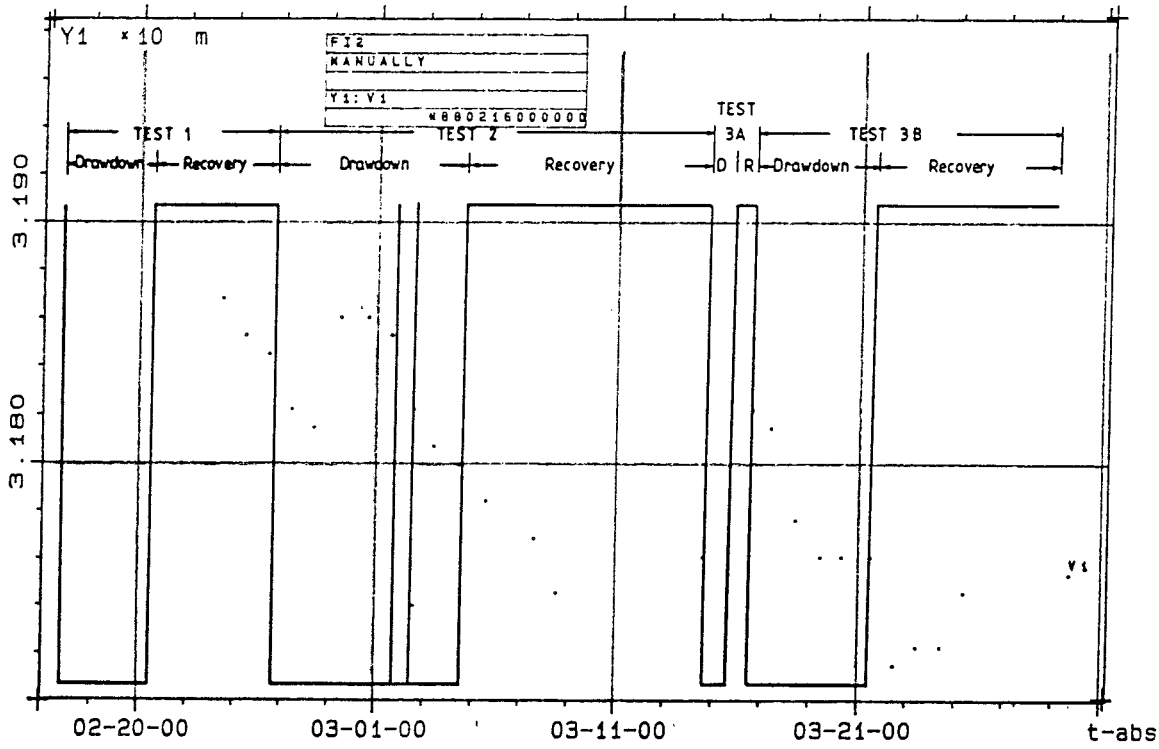

Appendix 7:1 Observed groundwater head in boreholes KFI01 and KFI02 during the interference tests.

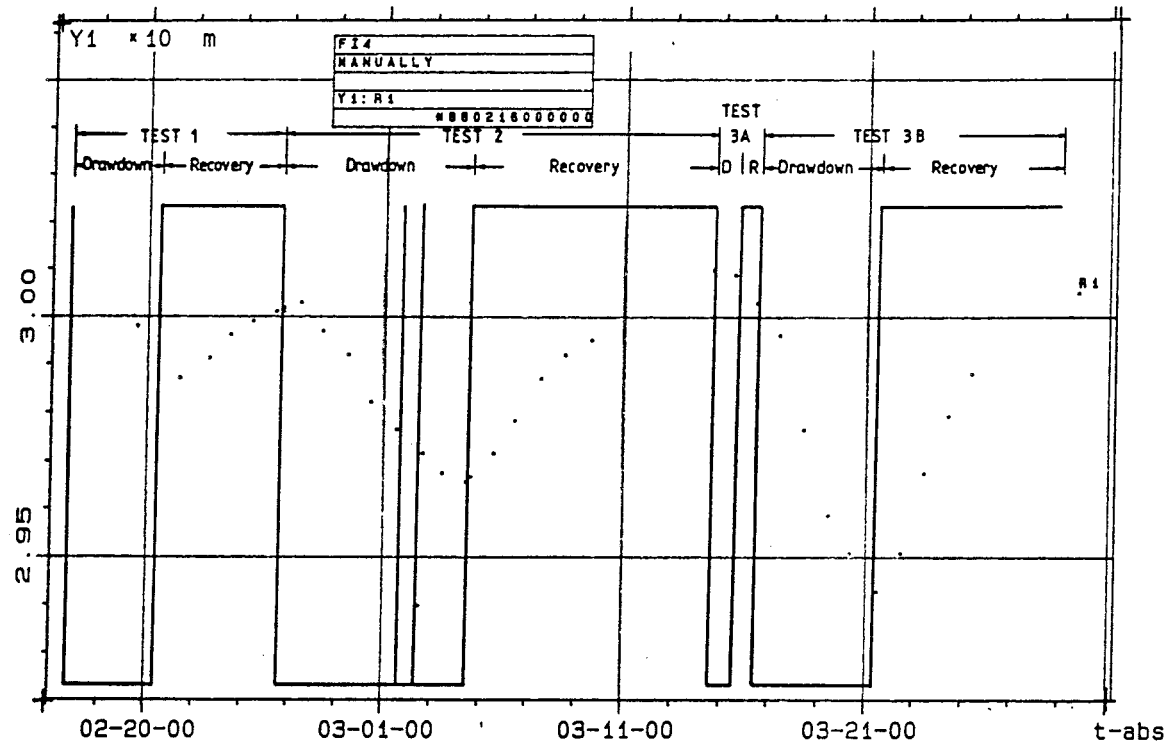

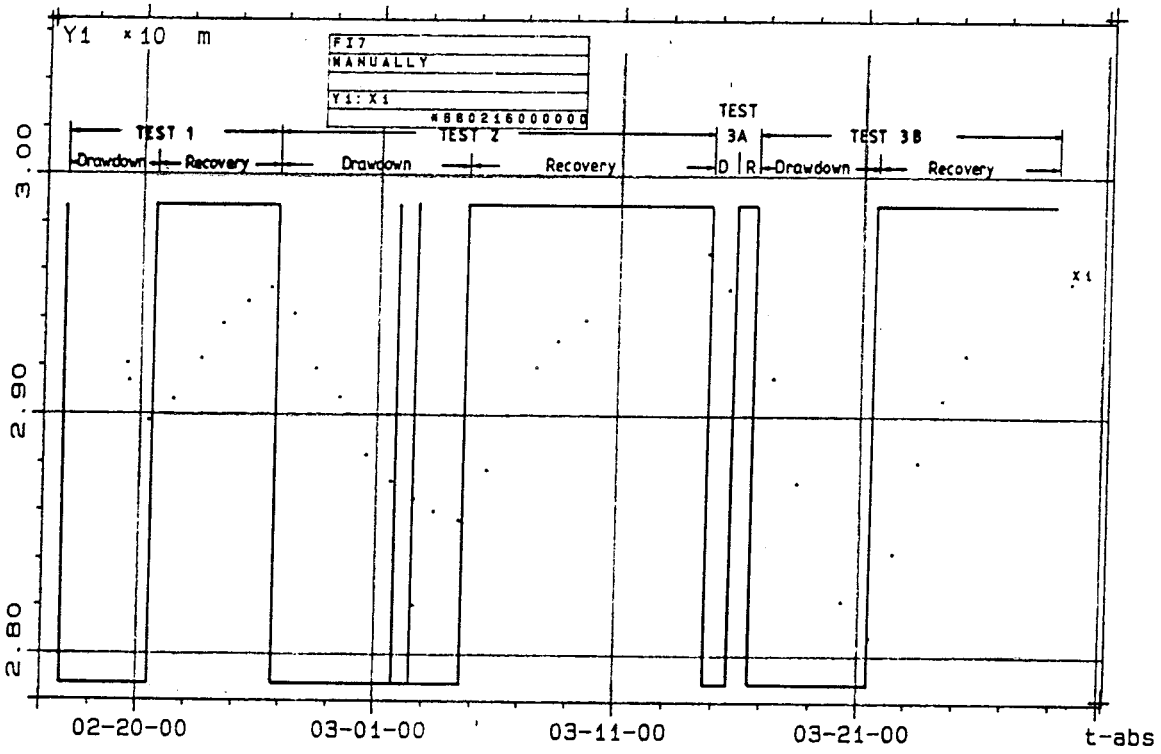

Appendix 7:2 Observed groundwater head in boreholes KFI04 and KFI07 during the interference tests.

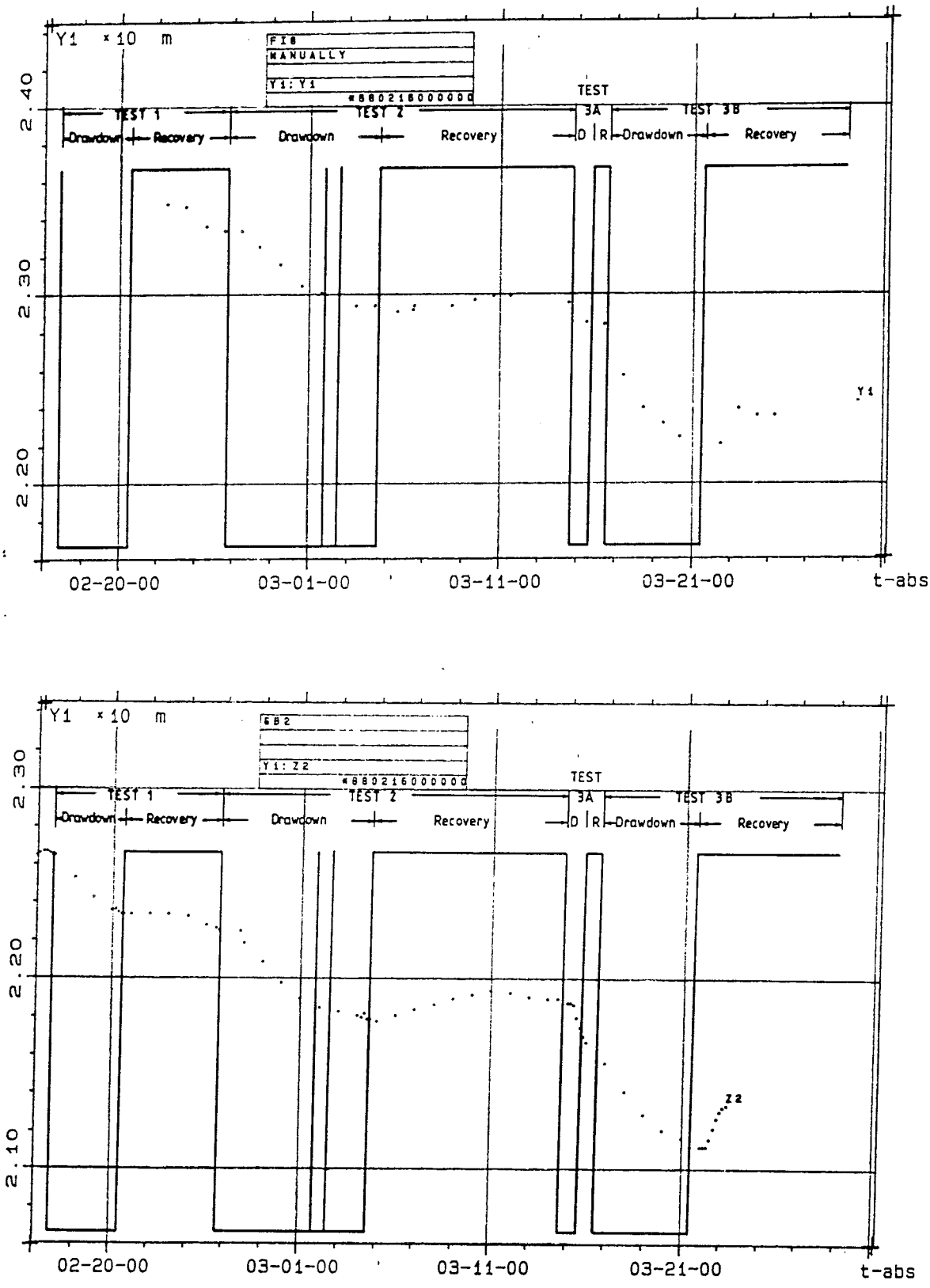

Appendix 7:3 Observed groundwater head in boreholes KFI06 and HGB02 during the interference tests.

APPENDIX 8

Appendix 8:1 Basic data about boreholes, sections and tracers used and pumping performed.

FINNSJÖN PULSE INJECTION 880225

PUMPING/SAMPLING SECTION : BFI02 , 193 - 217 m
INJECTION SECTIONS : KFI06 , 202 - 227 m
: KFI11 , 217 - 240 m
: BFI01 , 239 - 250 m

VOLUMES OF INJECTION SECTIONS AND TUBING:

KFI06: Section volume: 48.6 l
Tubing volume : 2.6 l
Total volume : 51.2 l

KFI11: Section volume: 43.4 l
Tubing volume : 2.8 l
Total volume : 46.2 l

BFI01: Section volume:234.5 l
Tubing volume : 11.3 l
Total volume :245.8 l

TRACERS, CONCENTRATIONS AND VOLUMES:

KFI11 AMINO G ACID, 20000 ppm, 50 l + 50 l unlabelled flushing water
KFI06 IODIDE, 1 M (127000 ppm), 50 l + 50 l unlabelled water
BFI01 URANINE, 10000 ppm, 125 l + 125 l unlabelled water

START AND STOP OF INJECTION OF TRACERS AND UNLABELLED WATER:

KFI06: 880225 11.00 - 880225 15.10
KFI11: 11.15 - 16.30
BFI01: 06.07 - 14.40

START AND STOP OF PUMPING:

880225 16.45 - 880304 12.00

PUMPING CAPACITY: 500 l/min

Appendix 8:2 Concentration of tracers versus time in borehole BFI02.

Tracer concentration (absolute) versus time (hours)
(T(0)= 880225 16.00)

TIME (h)	C (AG) (ppm)	C (I) (ppm)	C (U) (ppm)
0.75	0.122	0.059	0.001
1	0.111	0.063	0.001
2	0.109	0.064	0.001
3	0.104	0.063	0.004
4	0.100	0.064	0.001
5	0.117	0.063	0.001
6	0.510	0.063	0.001
7	1.989	0.063	0.001
8	2.951	0.081	0.001
9	2.833	0.49	0.001
10	2.425	1.52	0.001
11	1.969	2.96	0.001
12	1.699	4.74	0.001
13	1.450	5.93	0.001
14	1.180	6.60	0.001
15	1.000	7.03	0.001
16	0.841	6.94	0.001
17	0.748	6.86	0.002
18	0.657	6.77	0.001
20	0.517	5.59	0.007
22	0.434	4.74	0.051
24	0.345	3.81	0.169
26	0.284	3.22	0.352
28	0.234	2.79	0.535
30	0.192	2.46	0.606
32	0.170	2.20	0.698
34	0.149	1.86	0.706
36	0.141	1.61	0.682
38	0.131	1.44	0.677
40	0.122	1.36	0.640
42	0.116	1.19	0.668
44	0.114	1.10	0.619
46	0.111	1.02	0.595
48	0.104	0.89	0.540
50	0.099	0.85	0.522
52	0.097	0.71	0.480
54	0.094	0.68	0.425
56	0.097	0.63	0.406
58	0.090	0.59	0.364
60	0.099	0.56	0.343
62	0.097	0.53	0.310
64	0.099	0.53	0.264
66	0.089	0.49	0.237

Appendix 8:2 continued.

68	,	0.085,	0.46	,	0.215
70	,	0.084,	0.46	,	0.193
72	,	0.087,	0.46	,	0.178
74	,	0.087,	0.46	,	0.153
76	,	0.085,	0.44	,	0.142
78	,	0.085,	0.41	,	0.135
80	,	0.087,	0.38	,	0.125
82	,	0.087,	0.36	,	0.118
84	,	0.085,	0.33	,	0.110
86	,	0.092,	0.32	,	0.103
88	,	0.087,	0.31	,	0.089
90	,	0.080,	0.31	,	0.076
94	,	0.075,	0.29	,	0.061
98	,	0.082,	0.28	,	0.056
102	,	0.084,	0.26	,	0.054
106	,	0.070,	0.26	,	0.041
110	,	0.075,	0.25	,	0.040
114	,	0.073,	0.25	,	0.036
118	,	0.079,	0.24	,	0.035
122	,	0.079,	0.23	,	0.035
126	,	0.075,	0.21	,	0.030
130	,	0.080,	0.20	,	0.029
134	,	0.084,	0.20	,	0.027
138	,	0.072,	0.20	,	0.021
142	,	0.070,	0.20	,	0.020
146	,	0.077,	0.19	,	0.020
150	,	0.073,	0.19	,	0.019
154	,	0.075,	0.19	,	0.018
158	,	0.072,	0.19	,	0.018
162	,	0.082,	0.19	,	0.017
166	,	0.084,	0.18	,	0.017
168.7	,	0.077,	0.18	,	0.016
169	,	0.082,	0.18	,	0.016
169.3	,	0.077,	0.18	,	0.015
169.7	,	0.075,	0.18	,	0.017
170	,	0.075,	0.17	,	0.015
170.3	,	0.082,	0.17	,	0.015
170.7	,	0.072,	0.17	,	0.014
171	,	0.079,	0.17	,	0.015
171.3	,	0.079,	0.17	,	0.014
171.7	,	0.082,	0.17	,	0.015
172	,	0.077,	0.17	,	0.014
173	,	0.080,	0.17	,	0.014
174	,	0.079,	0.17	,	0.014
175	,	0.077,	0.17	,	0.014
176	,	0.079,	0.17	,	0.014
177	,	0.079,	0.17	,	0.014
178	,	0.077,	0.17	,	0.013
179	,	0.077,	0.17	,	0.013
180	,	0.079,	0.17	,	0.013

Appendix 8:2 continued.

181	,	0.079,	0.17	,	0.013
182	,	0.077,	0.17	,	0.013
183	,	0.084,	0.17	,	0.013
184	,	0.082,	0.17	,	0.013
186	,	0.084,	0.16	,	0.013
188	,	0.079,	0.16	,	0.012

APPENDIX 9

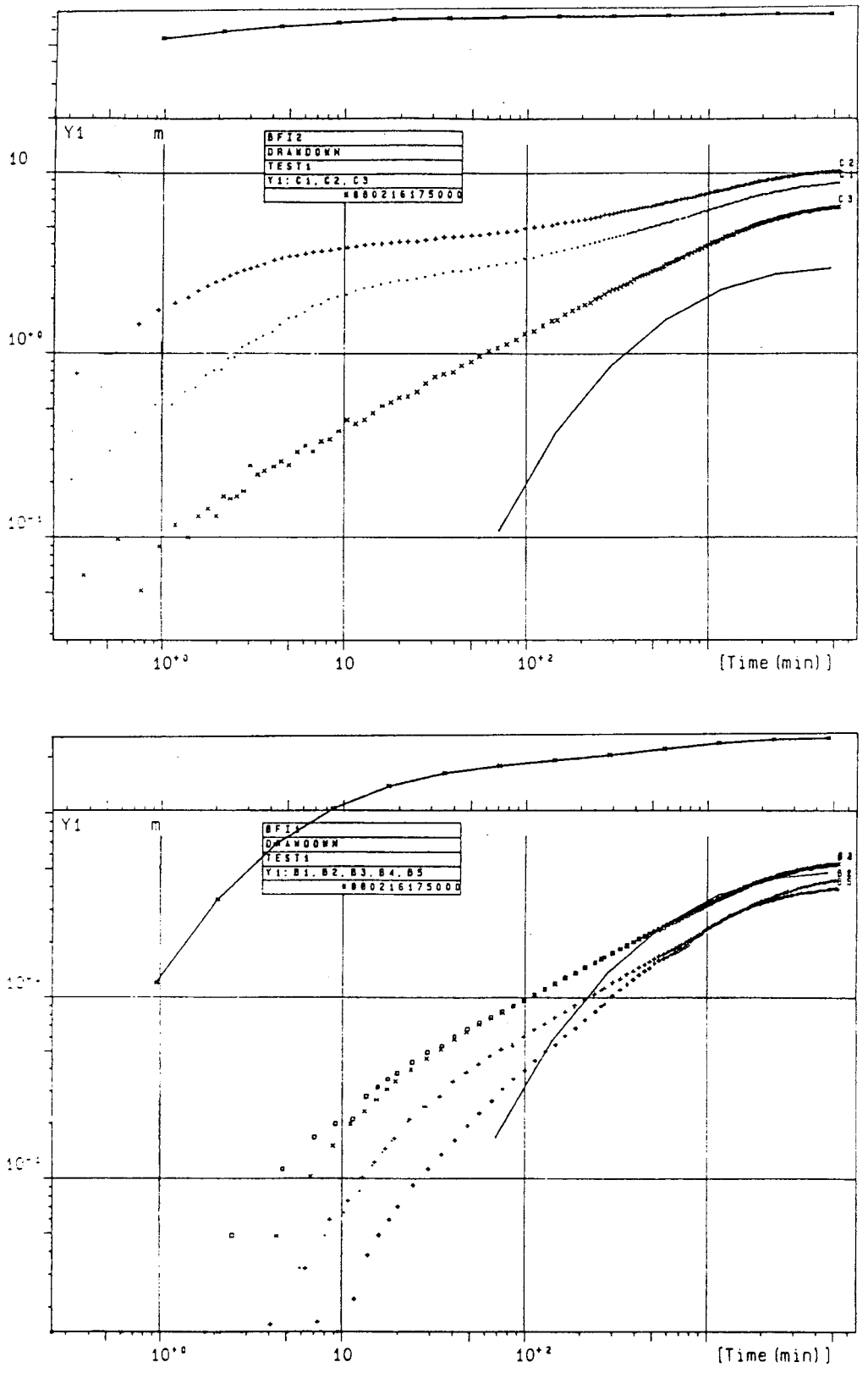

Appendix 9:1 Comparison of predicted and measured transient drawdown responses during test 1 from previous modelling for boreholes BFI02 and BFI01.

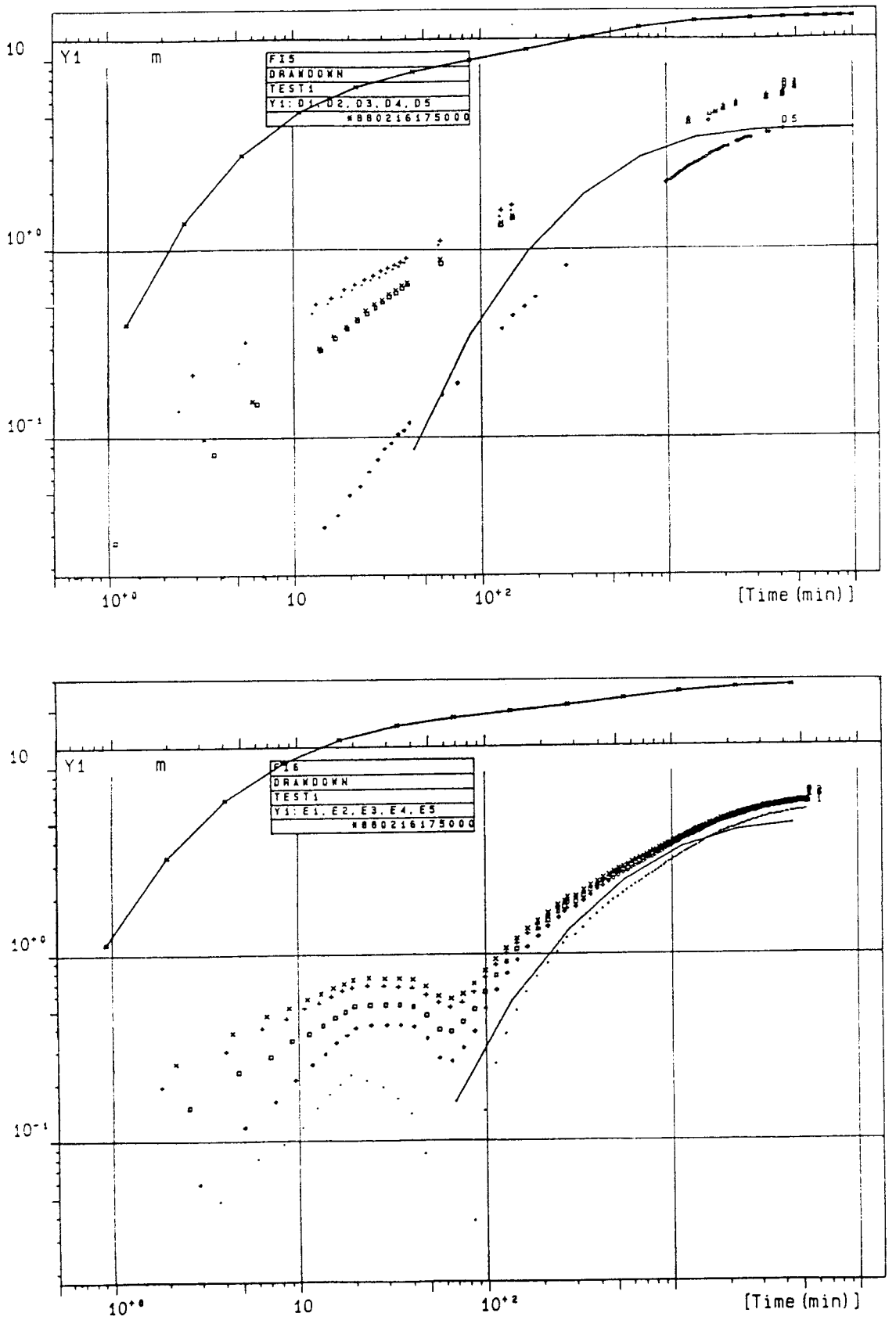

Appendix 9:2 Comparison of predicted and measured transient drawdown responses during test 1 from previous modelling for boreholes KFI05 and KFI06.

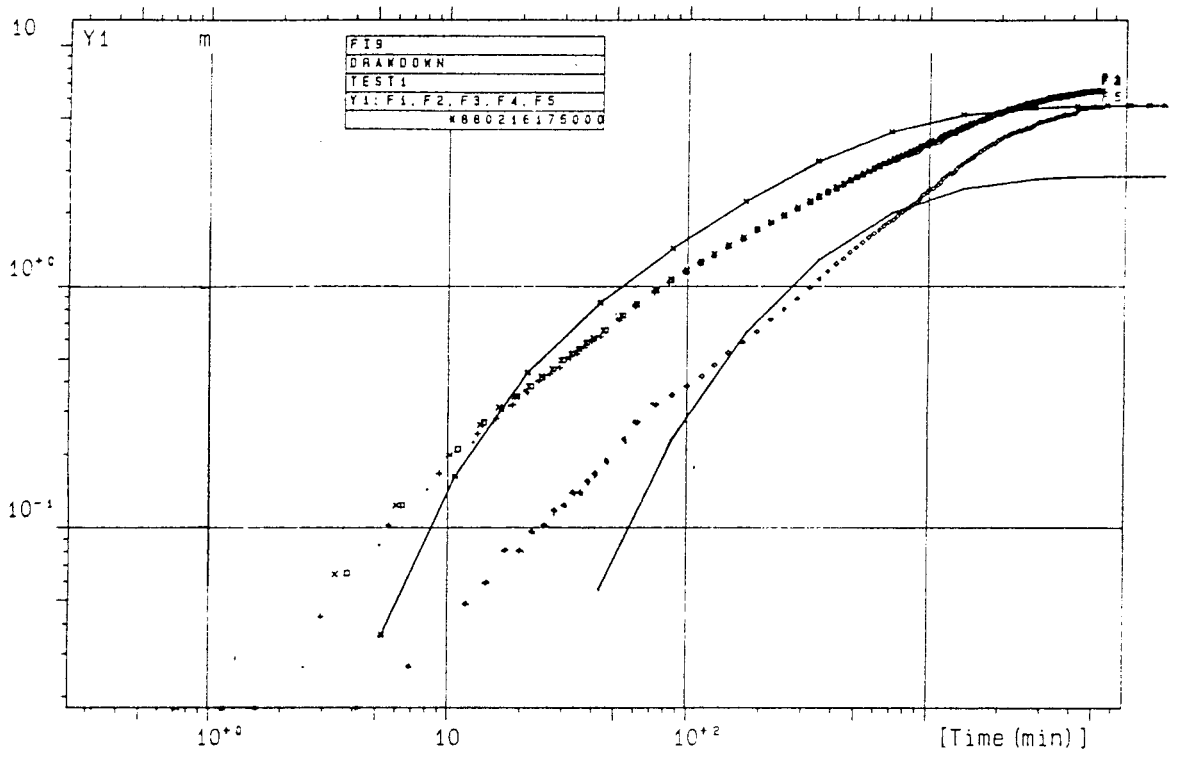

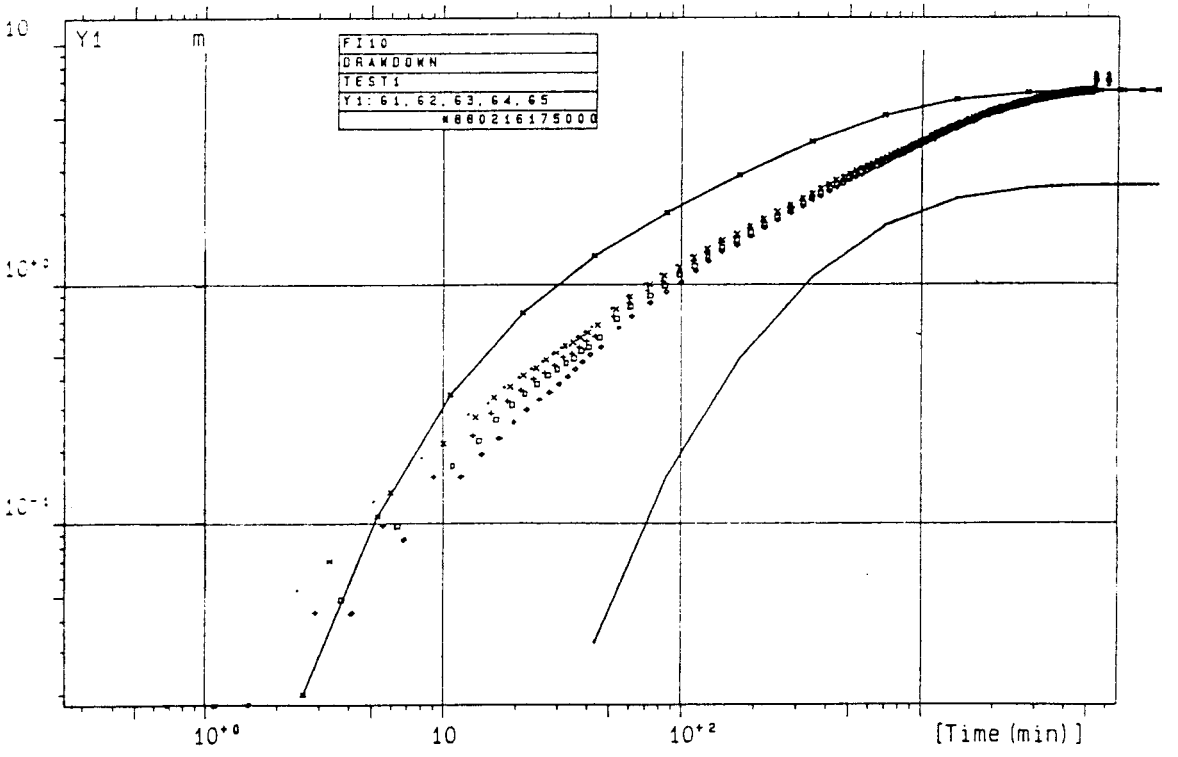

Appendix 9:3 Comparison of predicted and measured transient drawdown responses during test 1 from previous modelling for boreholes KFI09 and KFI10.

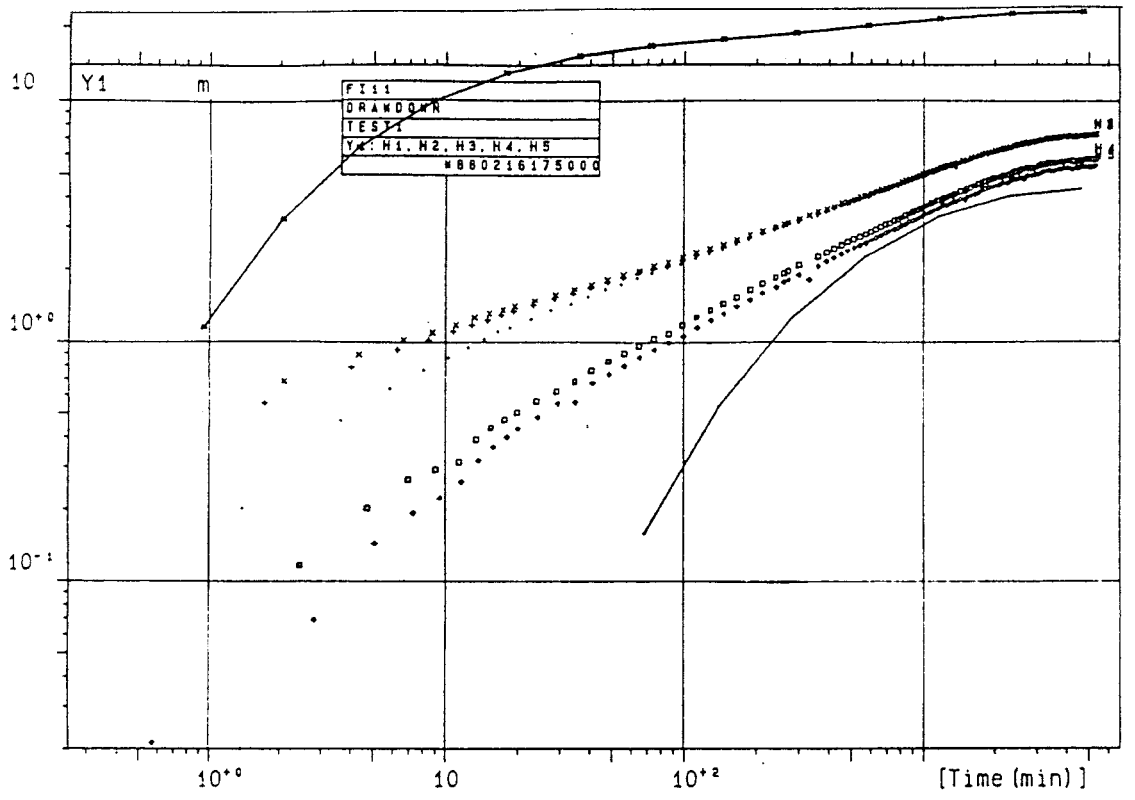

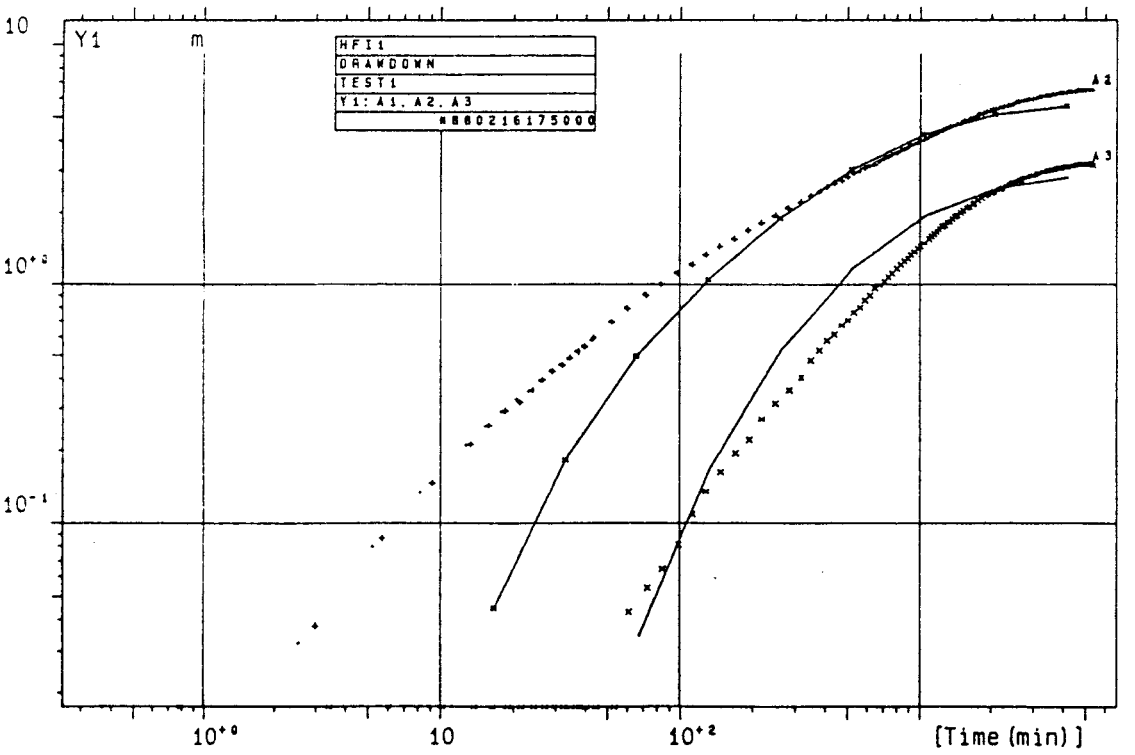

Appendix 9:4 Comparison of predicted and measured transient drawdown responses during test 1 from previous modelling for boreholes KFI11 and HFI01.

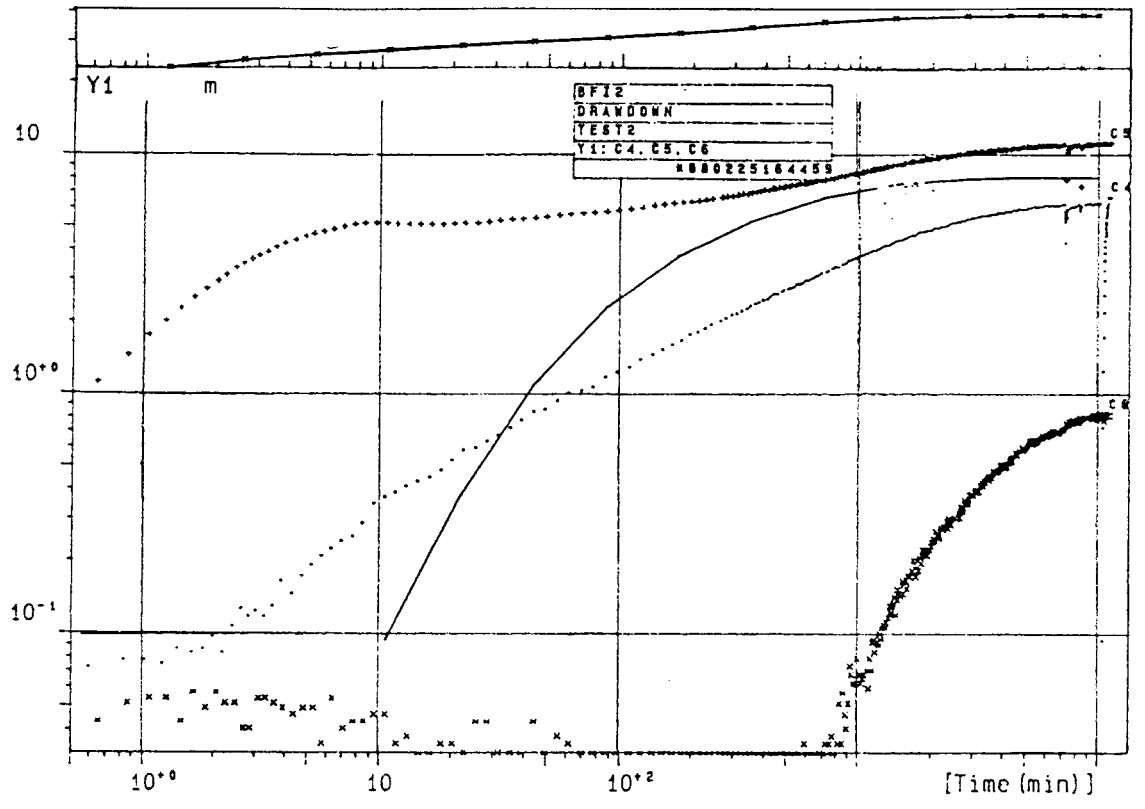

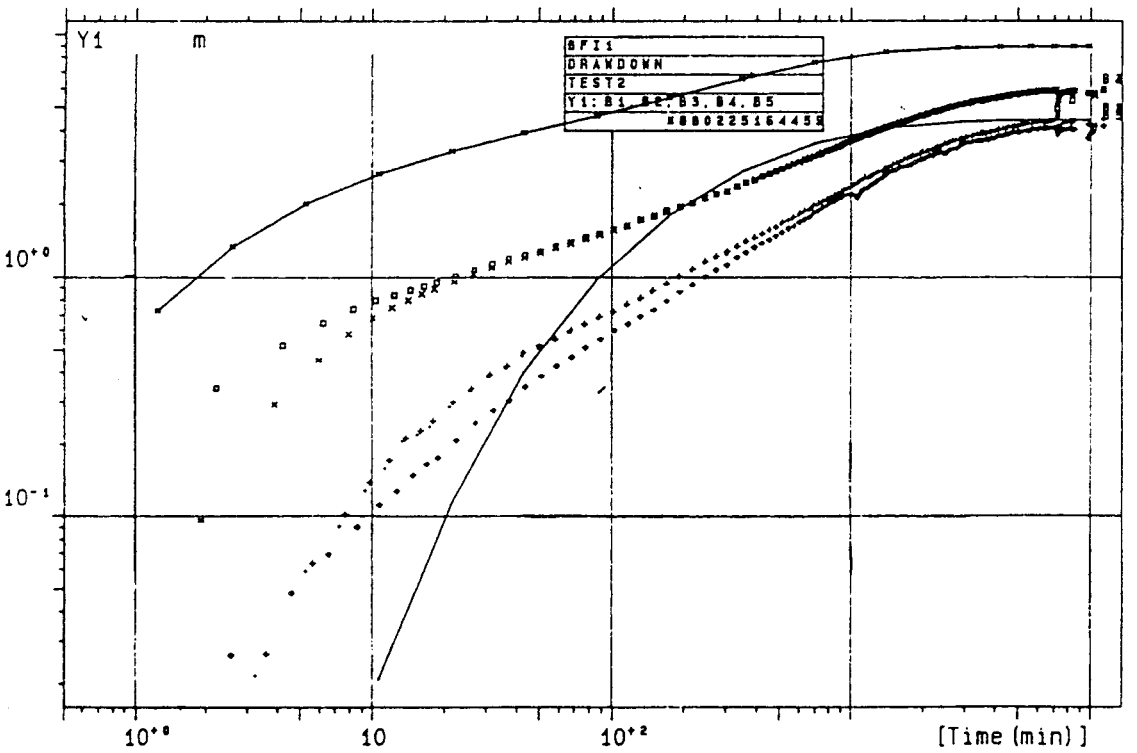

Appendix 9:5 Comparison of predicted and measured transient drawdown responses during test 2 from previous modelling for boreholes BFI02 and BFI01.

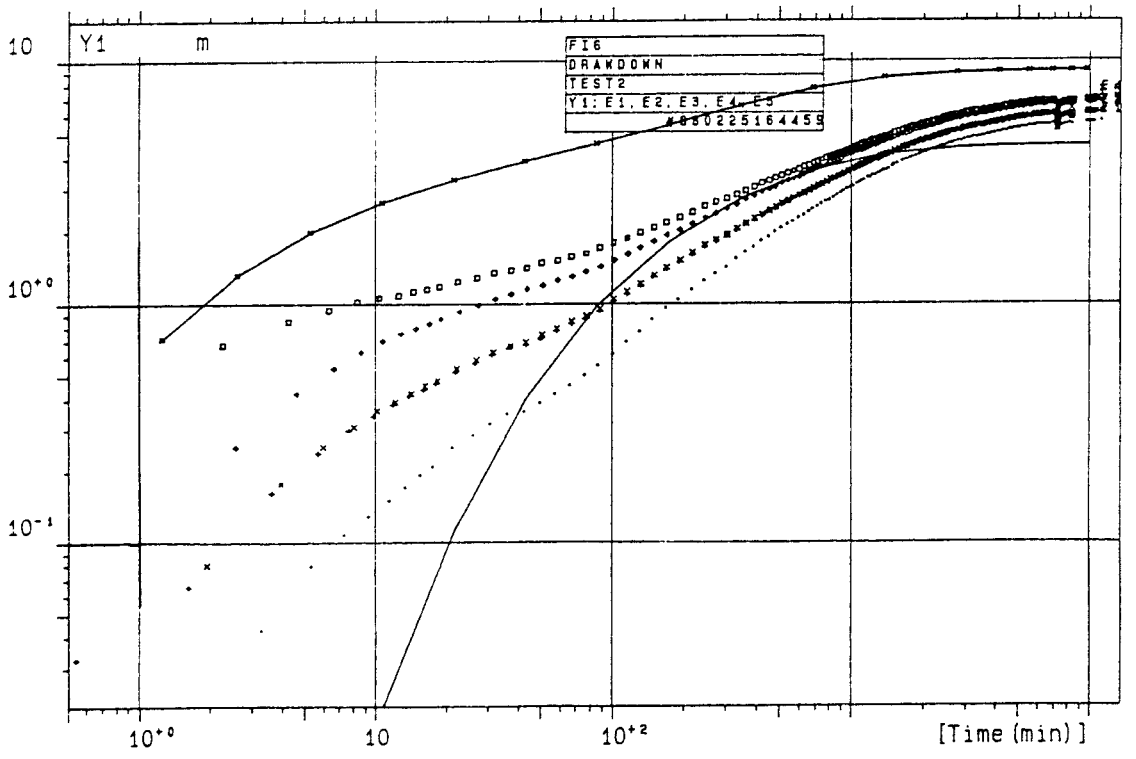

Appendix 9:6 Comparison of predicted and measured transient drawdown responses during test 2 from previous modelling for borehole KFI06.

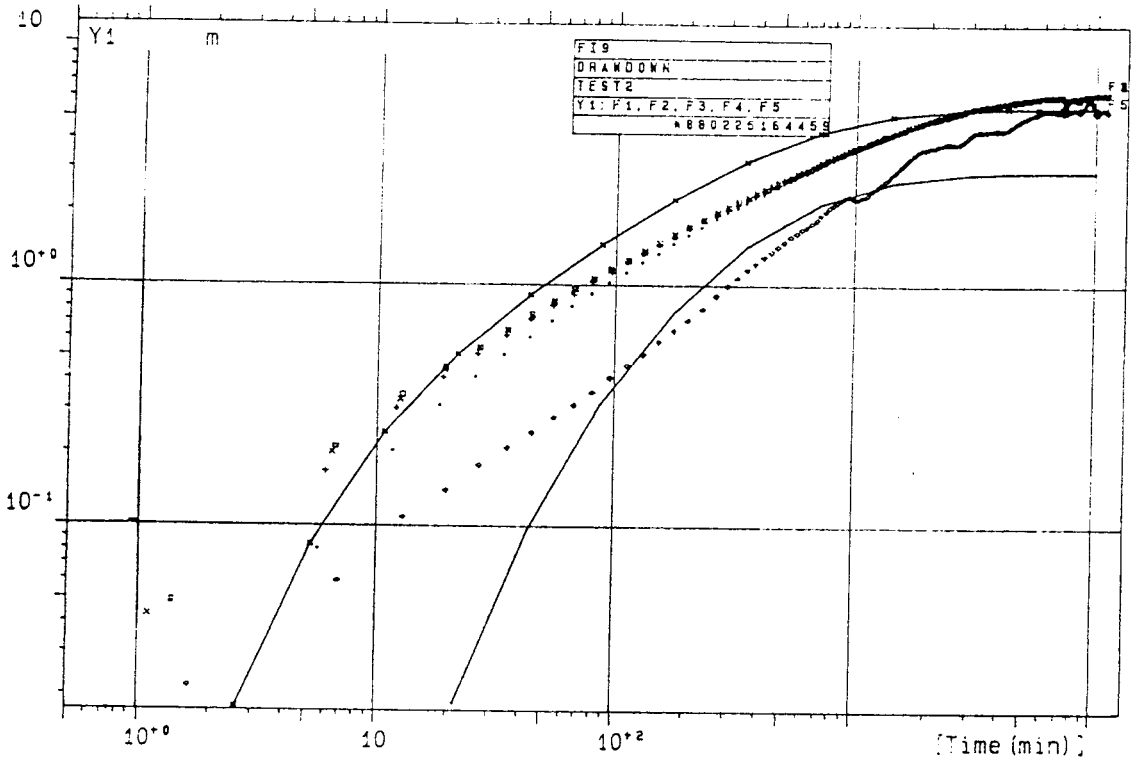

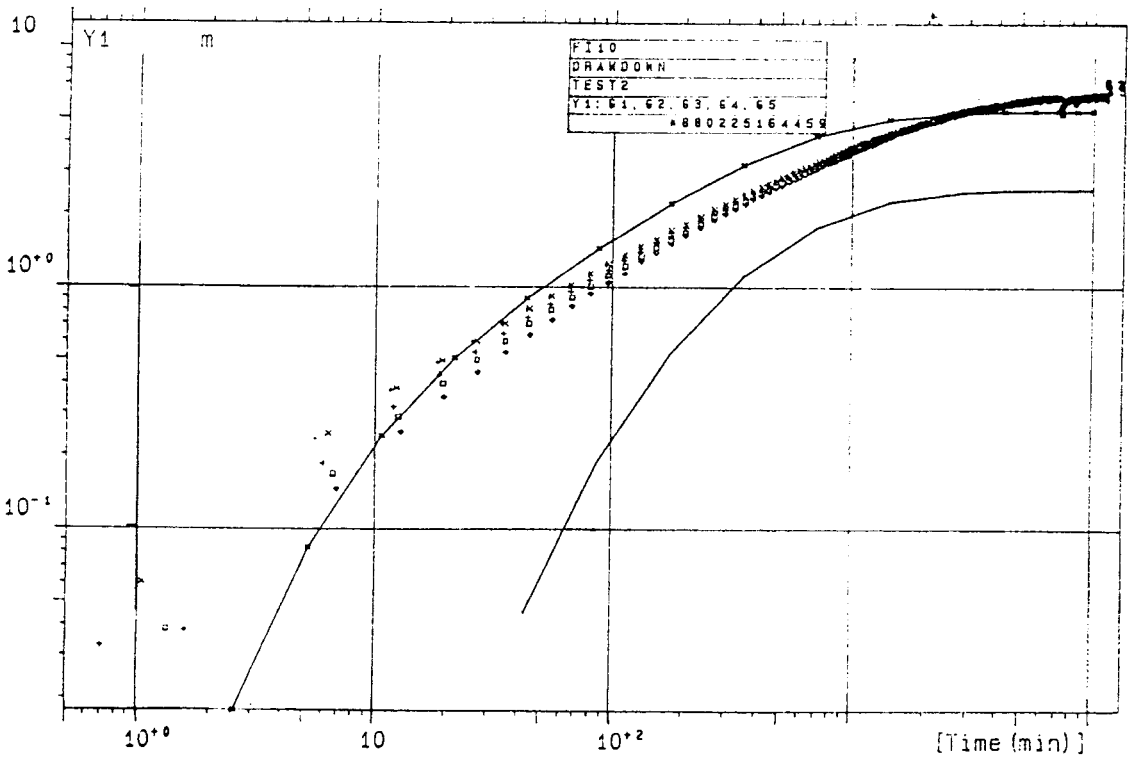

Appendix 9:7 Comparison of predicted and measured transient drawdown responses during test 2 from previous modelling for boreholes KFI09 and KFI10.

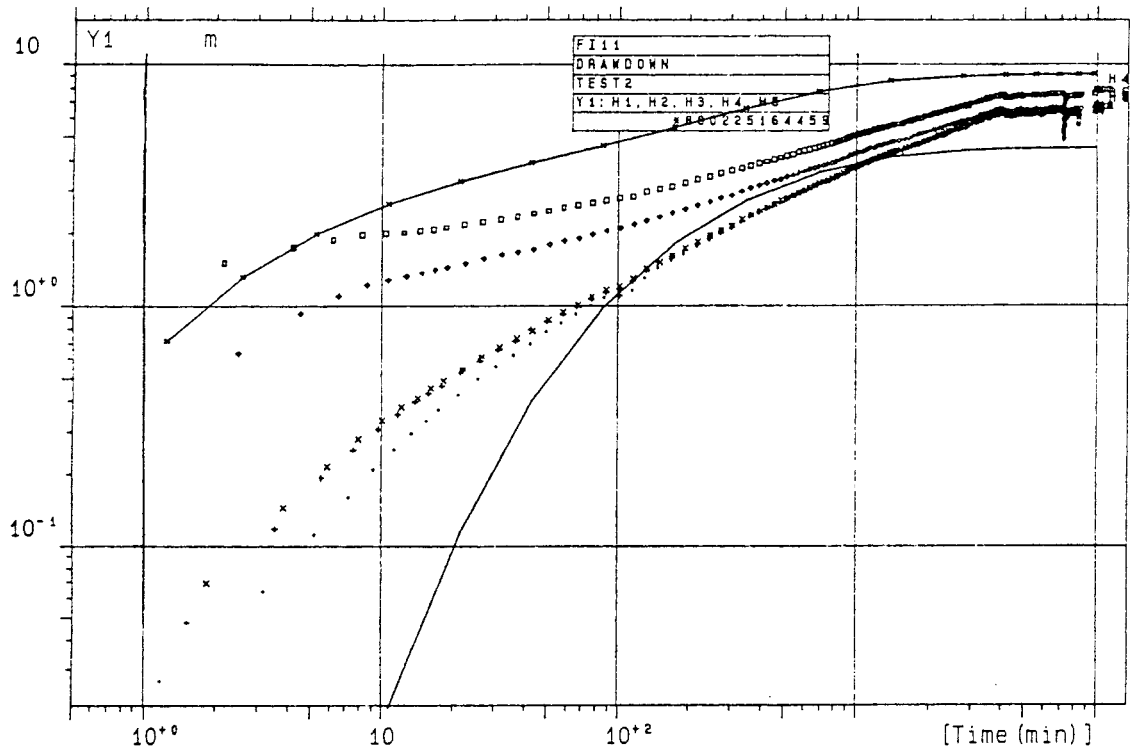

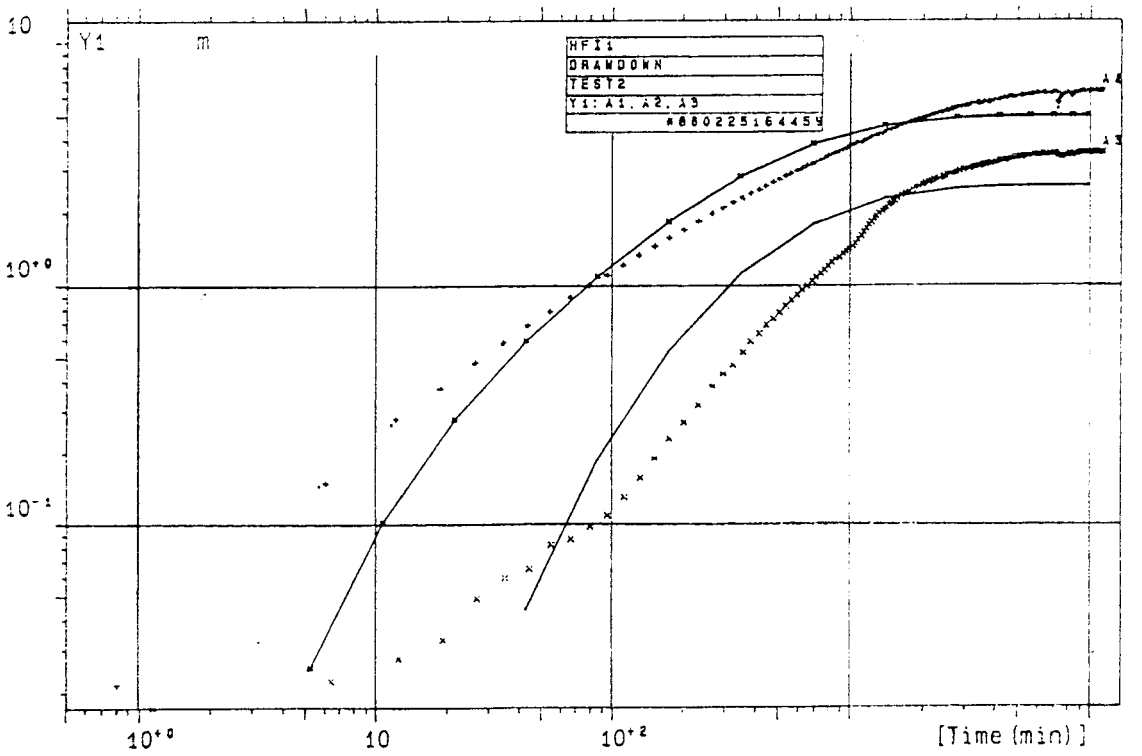

Appendix 9:8 Comparison of predicted and measured transient drawdown responses during test 2 from previous modelling for boreholes KFI11 and HFI01.

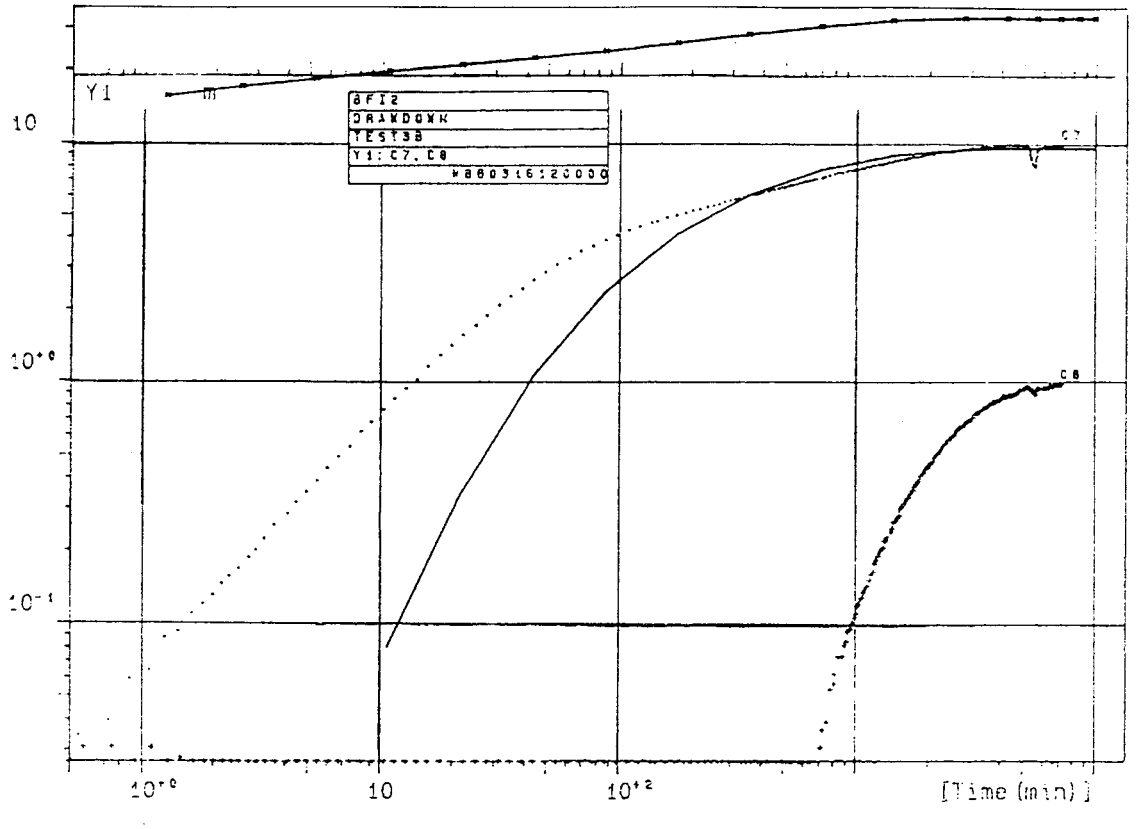

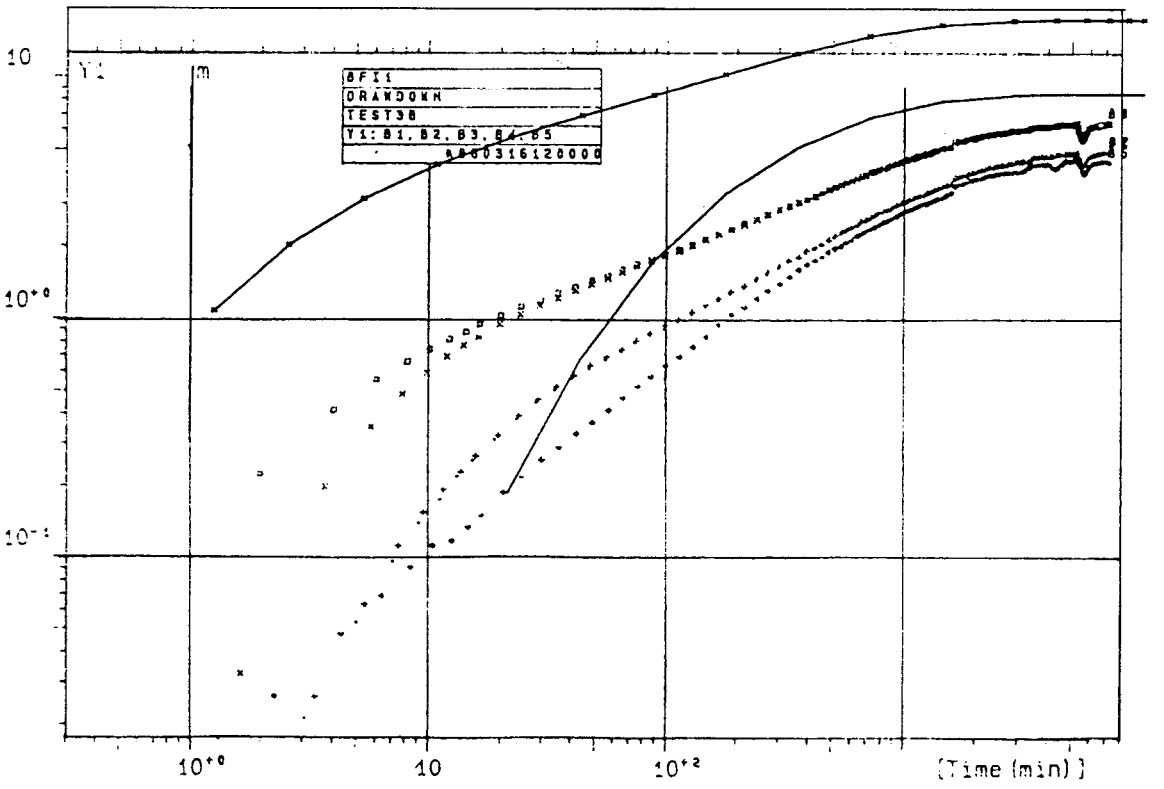

Appendix 9:9 Comparison of predicted and measured transient drawdown responses during test 3 from previous modelling for boreholes BFI02 and BFI01.

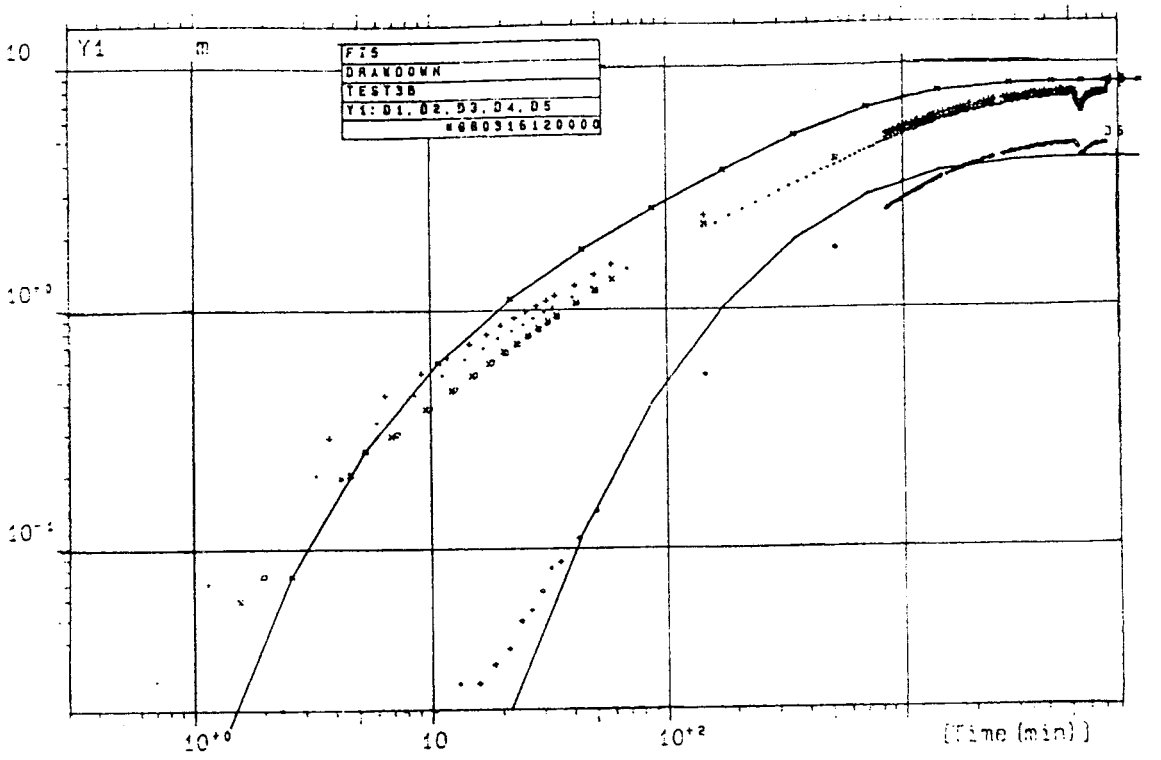

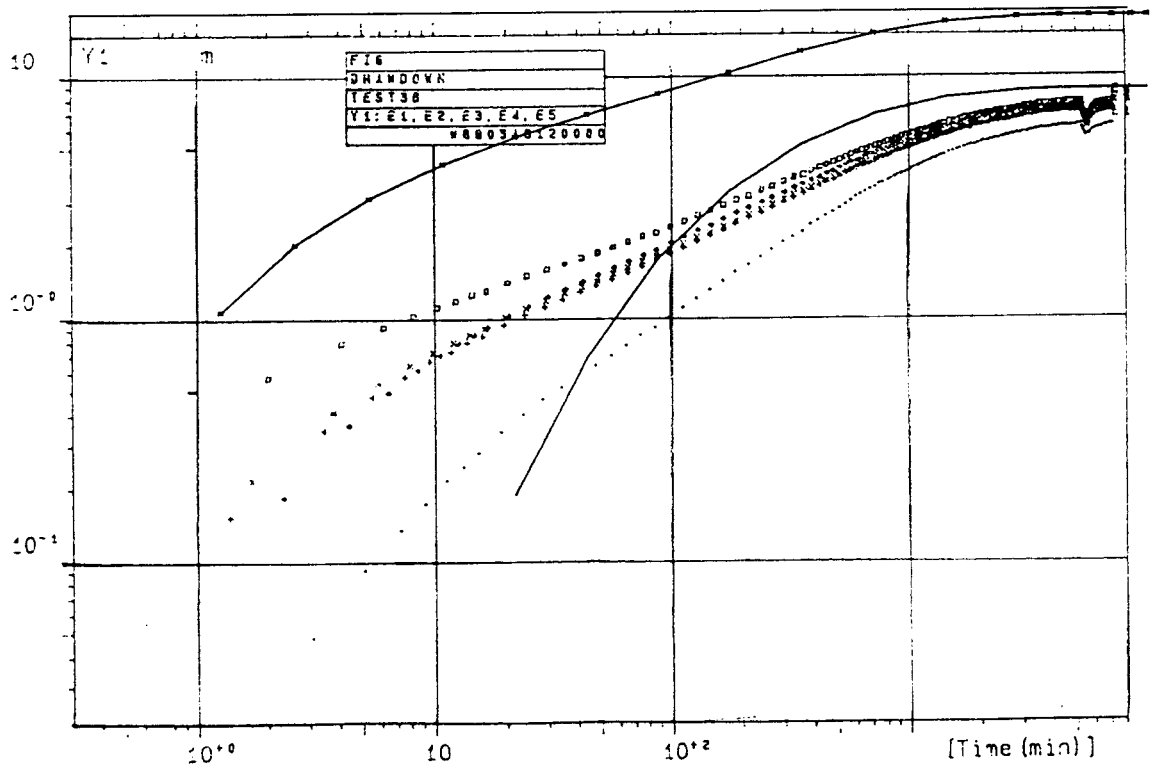

Appendix 9:10 Comparison of predicted and measured transient drawdown responses during test 3 from previous modelling for boreholes KFI05 and KFI06.

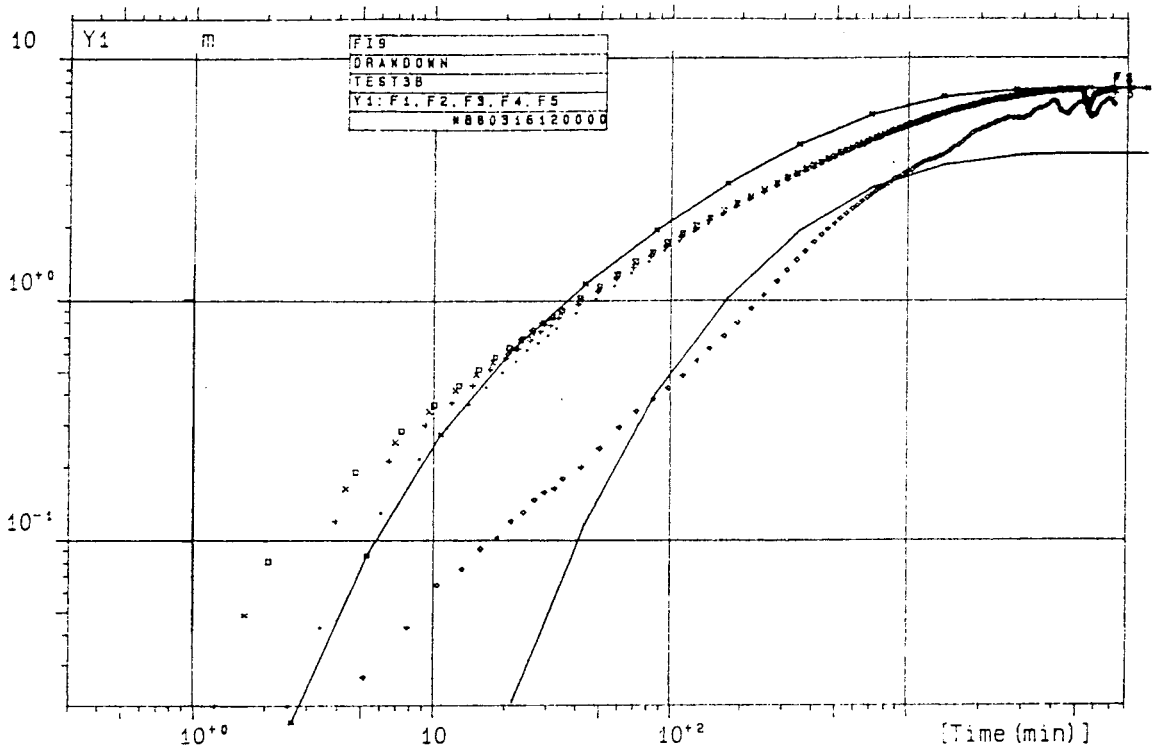

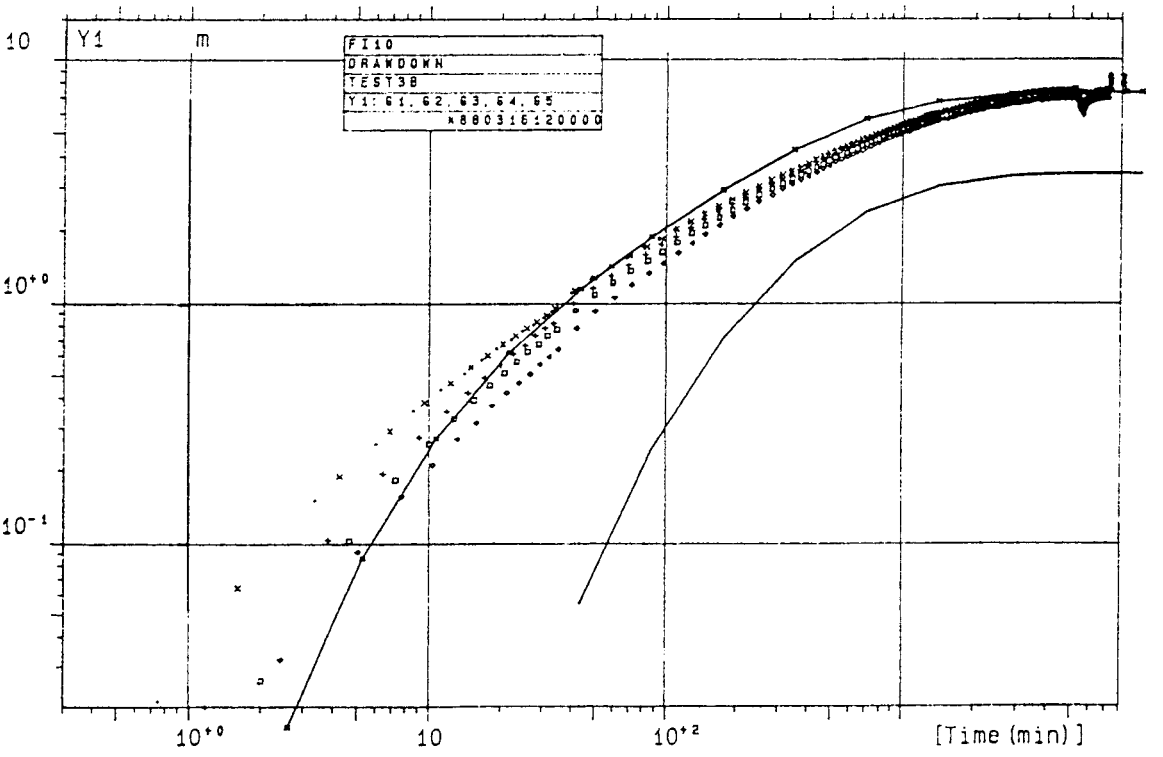

Appendix 9:11 Comparison of predicted and measured transient drawdown responses during test 3 from previous modelling for boreholes KFI09 and KFI10.

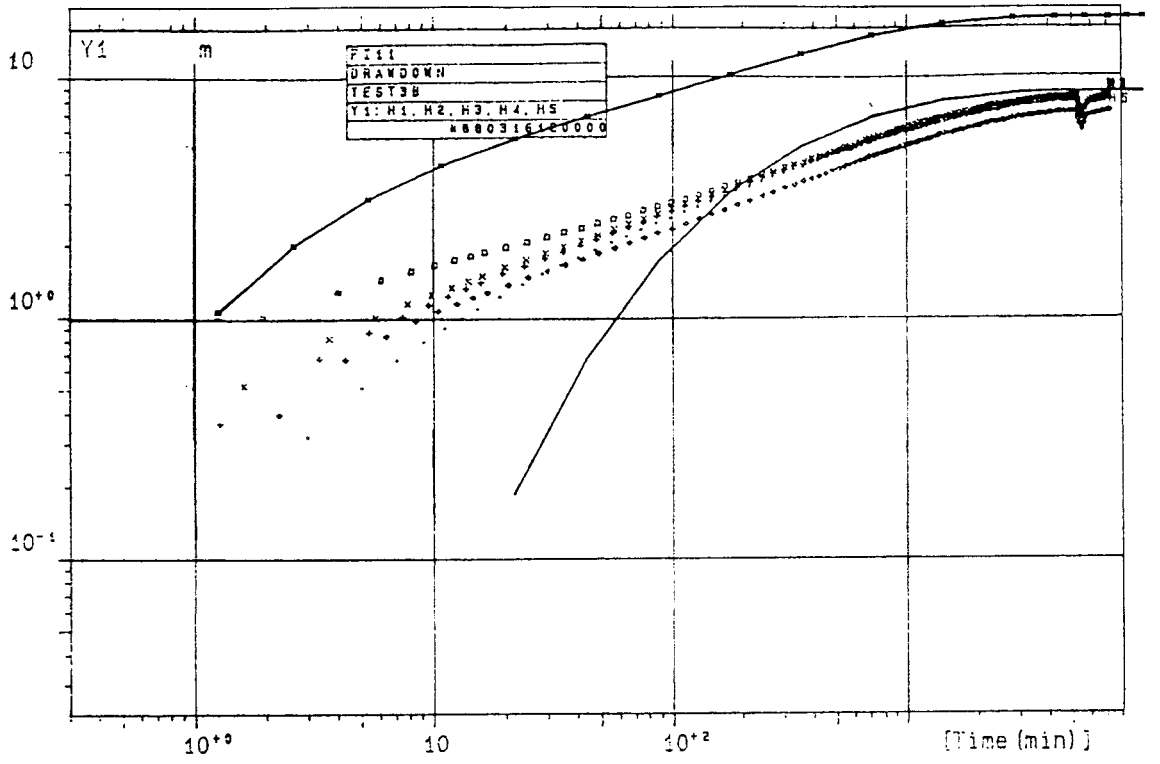

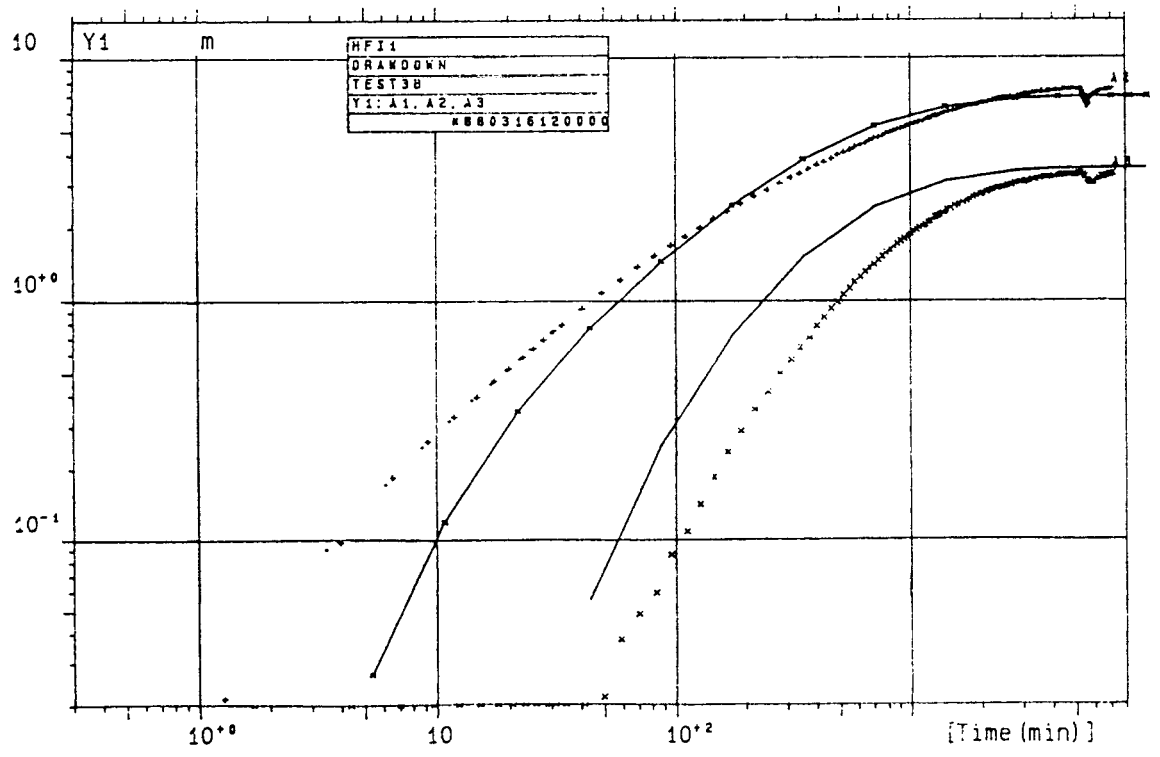

Appendix 9:12 Comparison of predicted and measured transient drawdown responses during test 3 from previous modelling for boreholes KFI11 and HFI01.

APPENDIX 10

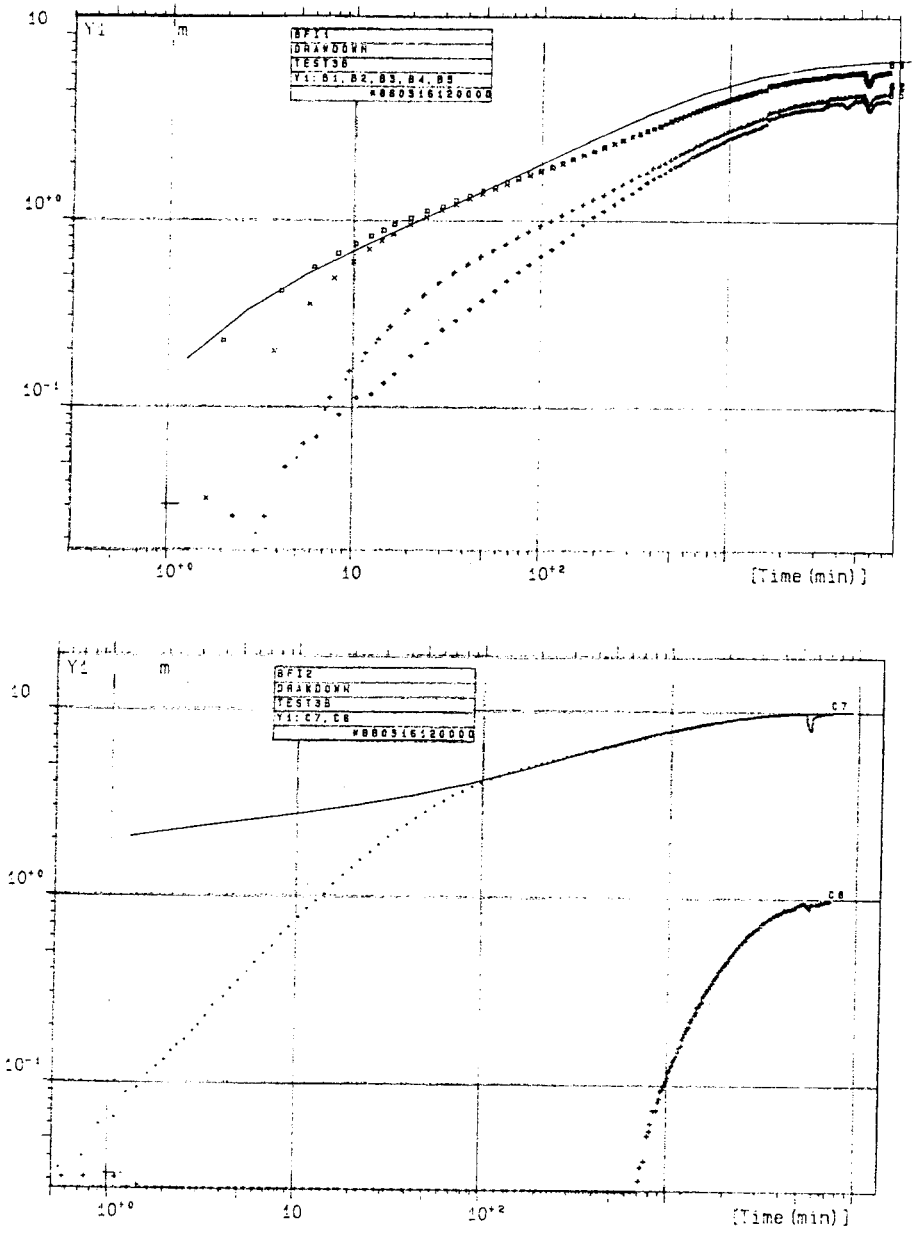

Appendix 10:1 Simulated (solid line) and observed drawdown responses in boreholes BFI01 and BFI02.

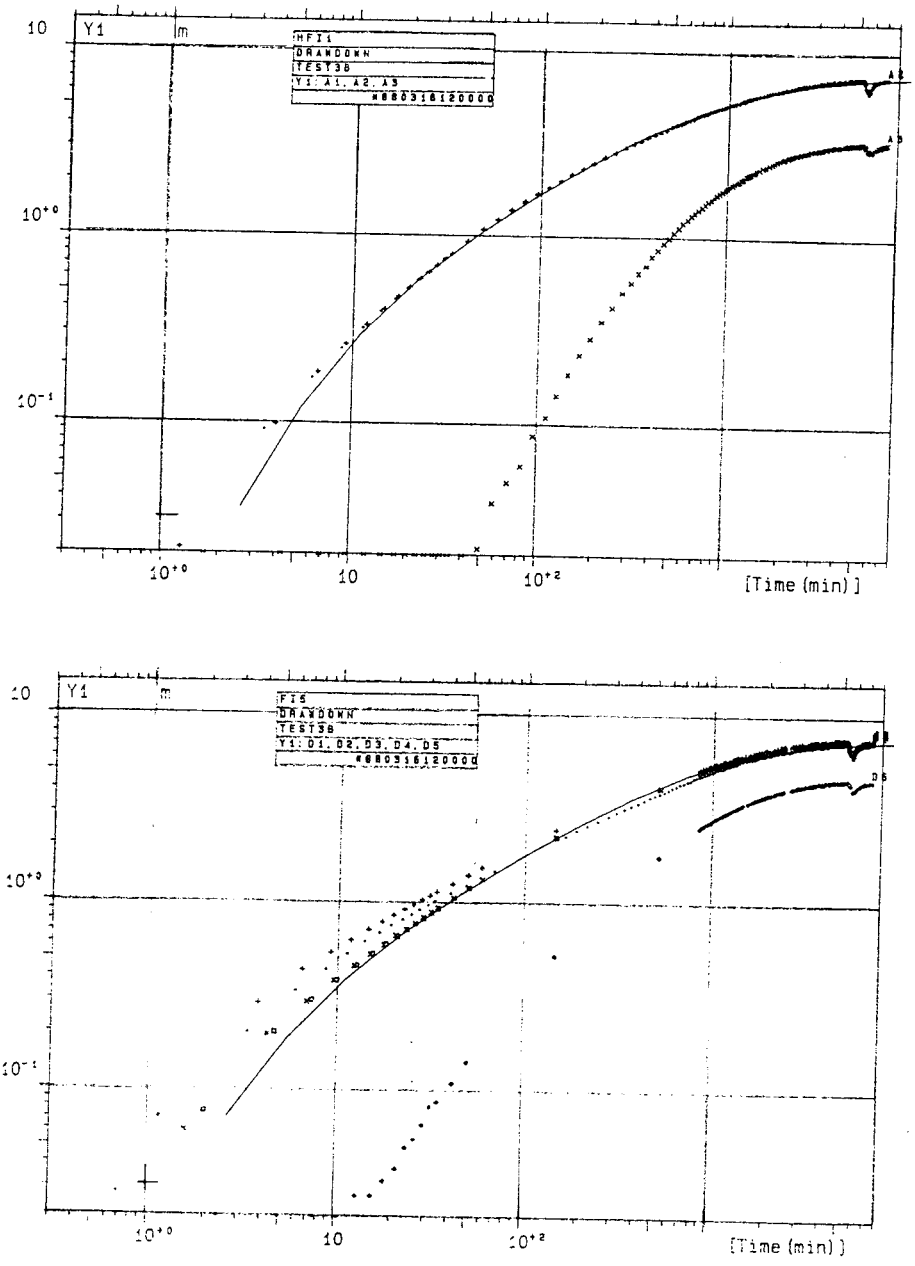

Appendix 10:2 Simulated (solid line) and observed drawdown responses in boreholes HFI01 and KFI05.

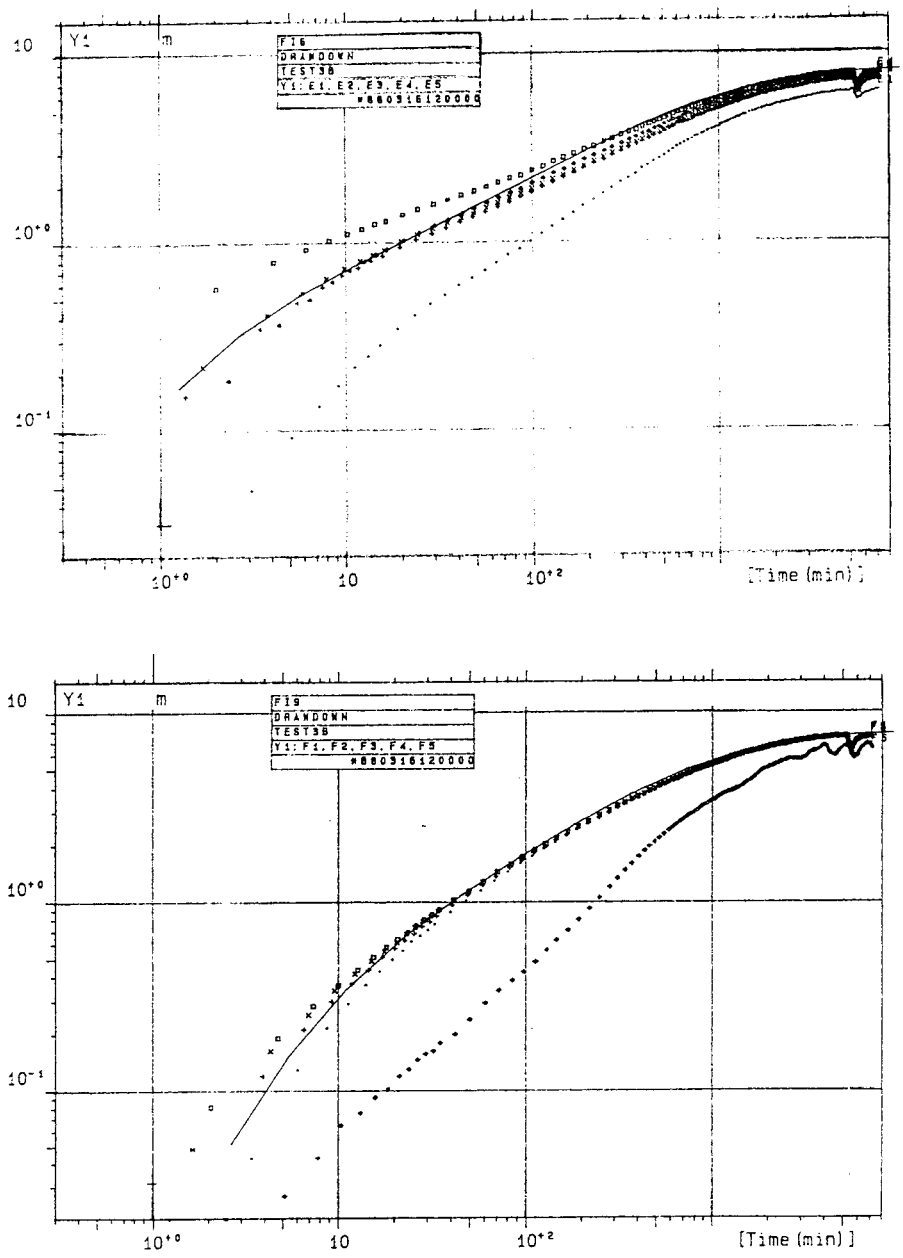

Appendix 10:3 Simulated (solid line) and observed drawdown responses in boreholes KFI06and KFI09.

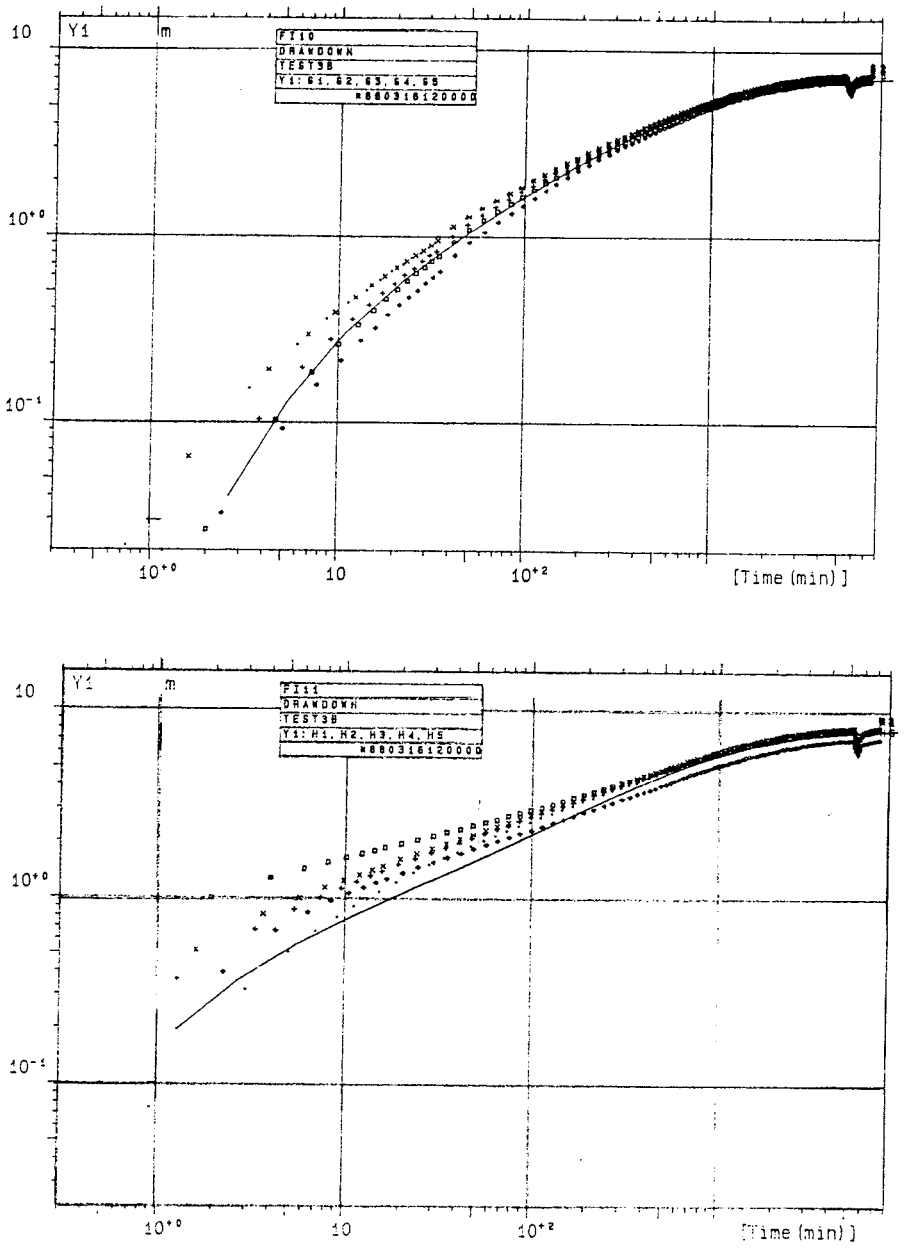

Appendix 10:4 Simulated (solid line) and observed drawdown responses in boreholes KFI10 and KFI11.

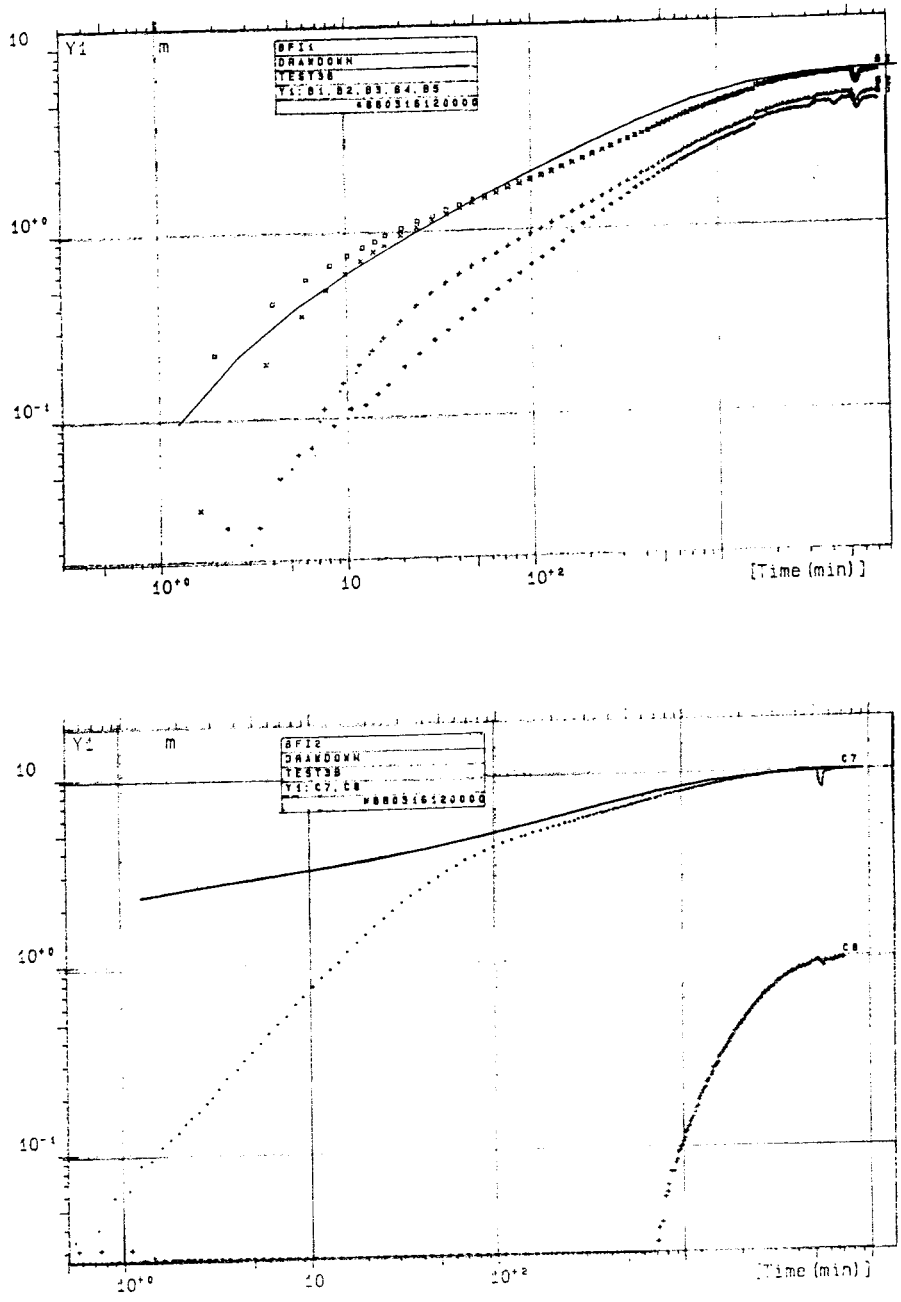

Appendix 10:5 Simulated (solid line) and observed drawdown responses in boreholes BFI01 and BFI02 for the anisotropic case.

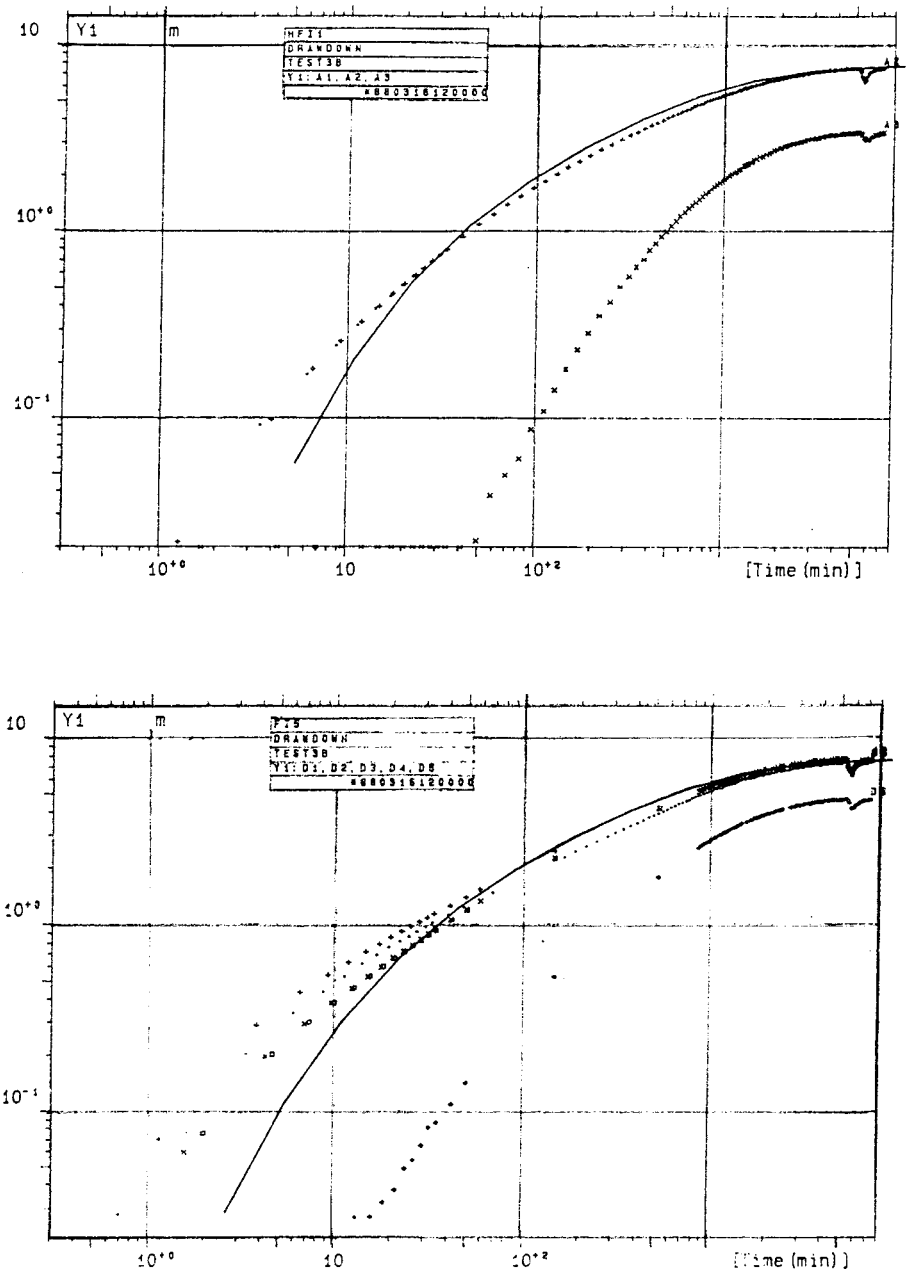

Appendix 10:6 Simulated (solid line) and observed drawdown responses in boreholes HFI01 and KFI05 for the anisotropic case.

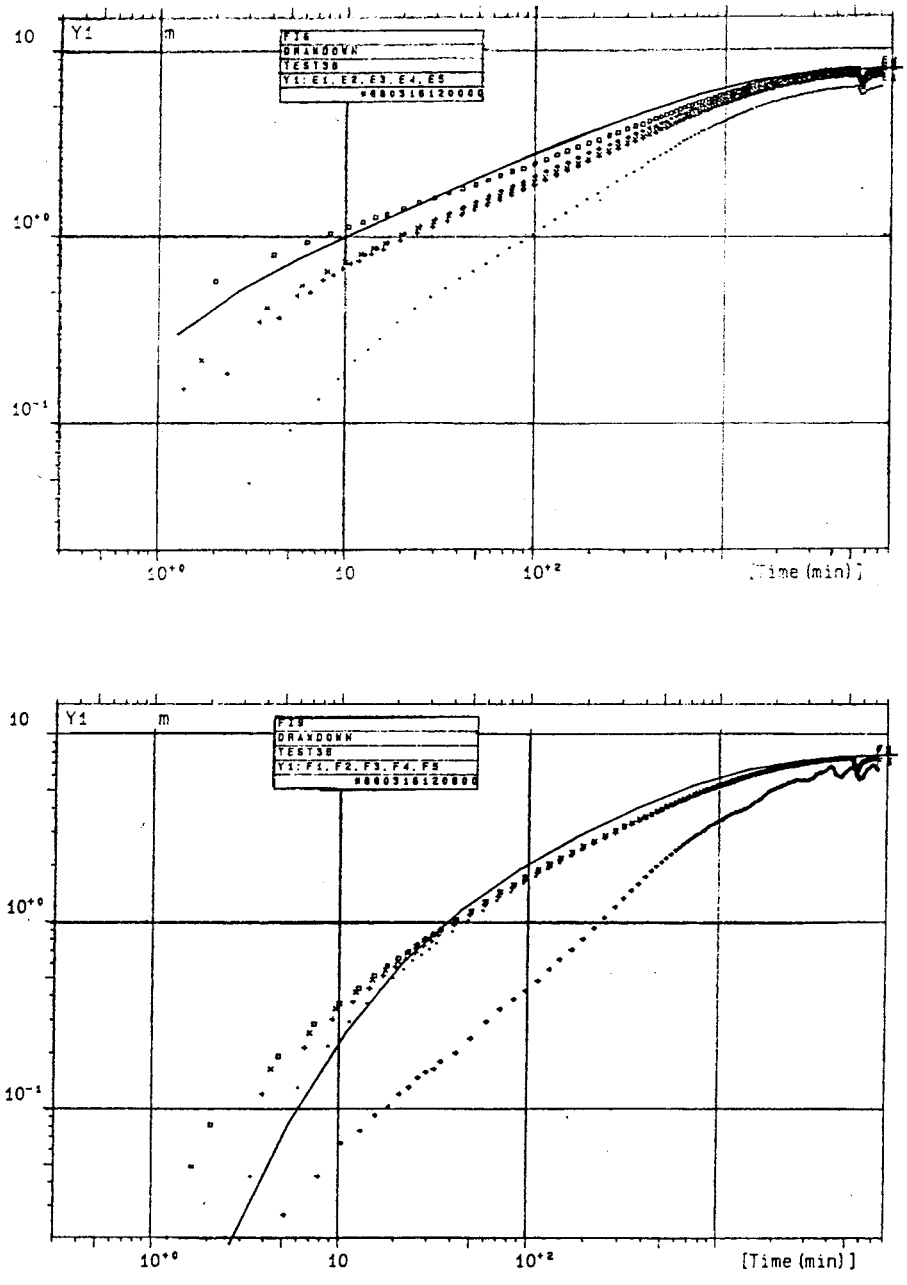

Appendix 10:7 Simulated (solid line) and observed drawdown responses in boreholes KFI06 and KFI09 for the anisotropic case.

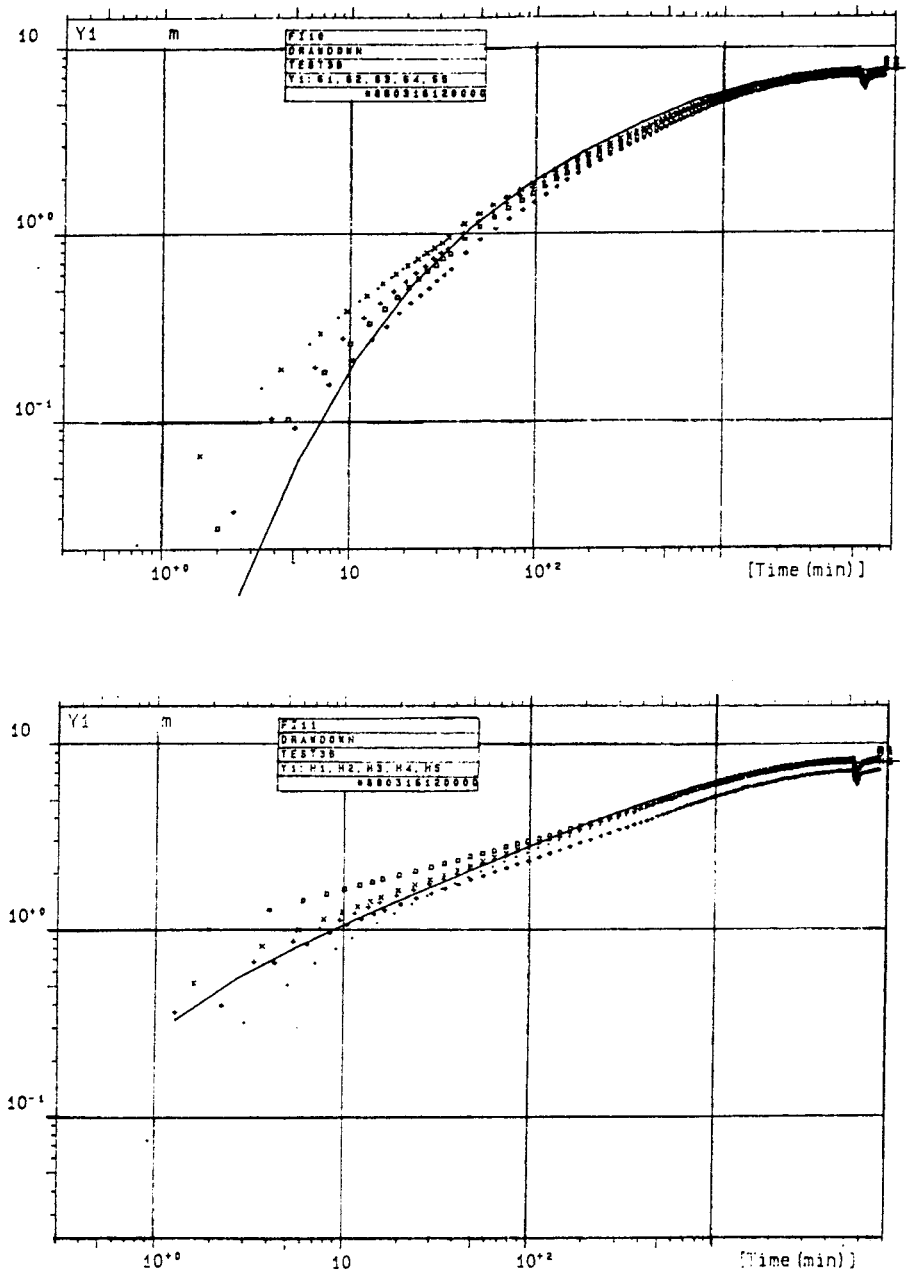

Appendix 10:8 Simulated (solid line) and observed drawdown responses in boreholes KFI10 and KFI11 for the anisotropic case.

List of SKB reports

Annual Reports

1977–78
TR 121
KBS Technical Reports 1 – 120.
Summaries. Stockholm, May 1979.

1979
TR 79–28
The KBS Annual Report 1979.
KBS Technical Reports 79-01 – 79-27.
Summaries. Stockholm, March 1980.

1980
TR 80–26
The KBS Annual Report 1980.
KBS Technical Reports 80-01 – 80-25.
Summaries. Stockholm, March 1981.

1981
TR 81–17
The KBS Annual Report 1981.
KBS Technical Reports 81-01 – 81-16.
Summaries. Stockholm, April 1982.

1982
TR 82–28
The KBS Annual Report 1982.
KBS Technical Reports 82-01 – 82-27.
Summaries. Stockholm, July 1983.

1983
TR 83–77
The KBS Annual Report 1983.
KBS Technical Reports 83-01 – 83-76
Summaries. Stockholm, June 1984.

1984
TR 85–01
Annual Research and Development Report 1984
Including Summaries of Technical Reports Issued during 1984. (Technical Reports 84-01– 84-19)
Stockholm June 1985.

1985
TR 85-20
Annual Research and Development Report 1985
Including Summaries of Technical Reports Issued during 1985. (Technical Reports 85-01-85-19)
Stockholm May 1986.

1986
TR 86-31
SKB Annual Report 1986
Including Summaries of Technical Reports Issued during 1986
Stockholm, May 1987

1987
TR 87-33
SKB Annual Report 1987
Including Summaries of Technical Reports Issued during 1987
Stockholm, May 1988

1988
TR 88-32
SKB Annual Report 1988
Including Summaries of Technical Reports Issued during 1988
Stockholm, May 1989

Technical Reports

1989
TR 89-01
Near-distance seismological monitoring of the Lansjärv neotectonic fault region Part II: 1988
Rutger Wahlström, Sven-Olof Linder, Conny Holmqvist, Hans-Edy Mårtensson
Seismological Department, Uppsala University, Uppsala
January 1989

TR 89-02
Description of background data in SKB database GEOTAB
Ebbe Eriksson, Stefan Sehlstedt
SGAB, Luleå
February 1989

TR 89-03
Characterization of the morphology, basement rock and tectonics in Sweden
Kennert Röshoff
August 1988

TR 89-04
SKB WP-Cave Project
Radionuclide release from the near-field in a WP-Cave repository
Maria Lindgren, Kristina Skagius
Kemakta Consultants Co, Stockholm
April 1989

TR 89-05
SKB WP-Cave Project
Transport of escaping radionuclides from the WP-Cave repository to the biosphere
Luis Moreno, Sue Arve, Ivars Neretnieks
Royal Institute of Technology, Stockholm
April 1989

TR 89-06
SKB WP-Cave Project
Individual radiation doses from nuclides contained in a WP-Cave repository for spend fuel
Sture Nordlinder, Ulla Bergström
Studsvik Nuclear, Studsvik
April 1989

TR 89-07
SKB WP-Cave Project
Some Notes on Technical Issues

TR 89-08
SKB WP-Cave Project
Thermally incuded convective motion in groundwater in the near field of the WP-Cave after filling and closure
Polydynamics Limited, Zürich
April 1989

TR 89-09
An evaluation of tracer tests performed at Studsvik
Luis Moreno[1], Ivars Neretnieks[1], Ove Landström[2]
[1] The Royal Institute of Technology, Department of Chemical Engineering, Stockholm
[2] Studsvik Nuclear, Nyköping
March 1989

TR 89-10
Copper produced from powder by HIP to encapsulate nuclear fuel elements
Lars B Ekbom, Sven Bogegård
Swedish National Defence Research Establishment
Materials department, Stockholm
February 1989

TR 89-11
Prediction of hydraulic conductivity and conductive fracture frequency by multivariate analysis of data from the Klipperås study site
Jan-Erik Andersson[1], Lennart Lindqvist[2]
[1] Swedish Geological Co, Uppsala
[2] EMX-system AB, Luleå
February 1988